Sources and fate of methylmercury in the Southern Ocean : use of model seabirds and mercury stable isotopes

Marina Renedo Elizalde

Thèse de Doctorat : Université de La Rochelle

Ecole doctorale : Sciences pour l'Environnement Gay Lussac
Spécialité : Chimie organique, minérale et industrielle

Marina RENEDO ELIZALDE

Pour obtenir le grade de Docteur de l'Université de La Rochelle

Sources et devenir du méthylmercure dans l'Océan Austral: utilisation des oiseaux marins modèles et des isotopes stables du mercure

Directeur: **Paco BUSTAMANTE**, Professeur, Université de La Rochelle
Codirecteur**: David AMOUROUX**, DR CNRS, Université de Pau et des Pays de l'Adour

Soutenue le 1er décembre 2017

Jury de thèse :

Aurélien DOMMERGUE – MCF HDR, Université Grenoble-Alpes (Rapporteur)
Krishna DAS – Senior Researcher FNRS, University of Liège (Rapporteur)
David POINT – CR IRD, Université Paul Sabatier (Examinateur)
Lars-Eric HEIMBURGER – CR CNRS, Aix Marseille Université (Examinateur)
Jérôme FORT- CR CNRS HDR, Université de La Rochelle (Examinateur)
Yves CHEREL – DR CNRS, Université de La Rochelle (Président)

Doctoral thesis: University of La Rochelle

Doctoral school: Sciences for the Environment Gay Lussac
Specialty: Organic, mineral, industrial chemistry

Marina RENEDO ELIZALDE

For the fulfilment of the degree of Doctor of the University of La Rochelle

Sources and fate of methylmercury in the Southern Ocean: use of model seabirds and mercury stable isotopes

Supervisor: **Paco BUSTAMANTE**, PR, University La Rochelle
Co-supervisor**: David AMOUROUX**, DR CNRS, University of Pau et Pays de l'Adour

Defended on December 1st, 2017

Jury composition:

Aurélien DOMMERGUE – MCF HDR, University Grenoble-Alpes (Reviewer)
Krishna DAS – Senior Researcher FNRS, University of Liège (Reviewer)
David POINT – CR IRD, University Paul Sabatier (Examiner)
Lars-Eric HEIMBURGER – CR CNRS, Aix Marseille University (Examiner)
Jérôme FORT- CR CNRS HDR, University La Rochelle (Examiner)
Yves CHEREL – DR CNRS, University La Rochelle (President)

Sources and fate of methylmercury in the Southern Ocean: use of model seabirds and mercury stable isotopes

This doctoral work was performed in collaboration of three laboratories:

Littoral, Environnement et Sociétés (LIENSs)
UMR 7266, CNRS-Université de La Rochelle

Institut des sciences analytiques et de physico-chimie pour l'environnement et les matériaux (IPREM)
UMR 5254, CNRS-Université de Pau et Pays de l'Adour

Centre d'Etudes Biologiques de Chizé (CEBC)
UMR 7372, CNRS-Université de La Rochelle

Thanks to the financial and logistical support of:

Région Poitou-Charentes (Nouvelle Aquitaine)
National program EC2CO Biohefect/Ecodyn//Dril/MicrobiEen (TIMOTAAF project)
Institut Polaire Français Paul Emile Victor (IPEV)

Abstract

Despite their distance from industrial pressure, marine southern and Antarctic environments are contaminated by worldwide distributed pollutants, such as mercury (Hg), through atmospheric transport and oceanic currents. So far, Hg contamination pathways in the Southern Ocean remains poorly understood, particularly in the Indian sector, and new studies are required to elucidate its fate and impact in these regions. Seabirds, as top predators of marine food webs, are exposed to elevated concentrations of biomagnified methylmercury (MeHg) via dietary intake and moreover, they forage in the different marine compartments both in spatial and depth terms. Therefore, they are considered as effective bioindicators of Hg environmental contamination and the good knowledge of their ecological characteristics permits their application for tracing Hg in such remote environments otherwise of difficult access. The **main objective** of this doctoral work is the **characterization of the exposure pathways of the MeHg accumulated in model seabirds and the identification of the processes involved in the Hg biogeochemical cycle in the Southern Ocean (from Antarctic to subtropical waters)**. The proposed methodological approach consisted on the combination of Hg isotopic composition and Hg speciation in tissues of a precise selection of seabirds of the Southern Ocean. In a first step, the **evaluation of tissue-specific Hg isotopic signatures** was accomplished notably in **blood and feathers**, as they can be non-lethally sampled. In chicks, both tissues can be effectively and indifferently used for biomonitoring of local contamination using Hg isotopes, whereas in adults each tissue provides access to different temporal exposure: blood at recent scale (i.e. exposure during the breeding period) and feathers at annual scale, thus providing complementary isotopic information at the different stages of seabird annual cycle. A **second** part was focused on the **exploration of MeHg sources** in four penguin species **within a same subantarctic location**, the Crozet Islands. Hg isotopes effectively discriminated the four populations and species-specific foraging habitats and latitudinal movements were found the main factors determining their exposure to distinct environmental MeHg sources. In a **third** part, **Hg isotopes** were investigated in two ubiquitous seabird models (skua chicks and penguins) **over a large a latitudinal scale from Antarctica to the subtropics**. Latitudinal variations of Hg isotopic values (δ^{202}Hg, Δ^{199}Hg) appeared to be influenced by different extent of photochemical processes and other biogeochemical pathways such as Hg reduction, and methylation/demethylation processes, as well as trophic or metabolic processes.

Keywords: mercury, seabirds, Southern Antarctic Territories, speciation, stable isotopes, ecology, trophic transfer, biogeochemistry

Résumé

Malgré leur distance de la pression industrielle, les milieux marins australs et antarctiques sont contaminés par des polluants globaux, tels que le mercure (Hg), par le transport atmosphérique et les courants océaniques. Jusqu'à présent, les voies de contamination du Hg dans l'Océan Austral restent peu connues, en particulier dans le secteur Indien, et de nouvelles études sont nécessaires pour élucider son devenir et son impact dans ces régions. Les oiseaux marins, en tant que prédateurs supérieurs des chaînes alimentaires marines, sont exposés à des concentrations élevées de méthylmercure (MeHg) via leur régime alimentaire. De plus, ils présentent des habitats de prédation contrastés dans les différents compartiments marins (en termes spatiaux et de profondeur). Par conséquent, ils sont considérés comme des bioindicateurs efficaces de la contamination par Hg et la bonne connaissance de leurs caractéristiques écologiques permet leur application comme traceurs du Hg dans des environnements éloignés, qui sont autrement difficiles à échantillonner. **L'objectif principal** de ce travail de doctorat **est la caractérisation des voies d'exposition des MeHg accumulé par les oiseaux marins et l'identification des processus impliqués dans le cycle biogéochimique du Hg dans l'Océan Austral (des eaux antarctiques aux eaux subtropicales).** L'approche méthodologique proposée consiste à combiner la composition isotopique du Hg et la spéciation du Hg dans les tissus d'espèces d'oiseaux marins de l'Océan Austral choisis précisément. Dans une **première étape**, une **évaluation des signatures isotopiques de Hg spécifique de chaque tissu** a été réalisée, notamment dans **le sang et les plumes**, car ceux-ci peuvent être échantillonnés de manière non létale. Chez les poussins, les deux tissus peuvent être utilisés efficacement et indifféremment comme bioindicateurs de la contamination locale en utilisant des isotopes du Hg, alors que chez les adultes, chaque tissu donne accès à une exposition temporelle différente: le sang à l'échelle récente (c'est-à-dire l'exposition pendant la période de reproduction) et les plumes à l'échelle annuelle, fournissant ainsi des informations isotopiques complémentaires aux différentes étapes du cycle annuel des oiseaux. Une **deuxième partie** a été axée sur **l'exploration des sources de MeHg dans quatre espèces de manchots d'une même zone subantarctique**, les îles de Crozet. Les populations ont été discriminées par leurs signatures isotopiques du Hg en fonction de leurs habitats de prédation et leurs mouvements latitudinaux, qui se trouvent être les facteurs principaux déterminant leur exposition à différentes sources de MeHg. Dans une **troisième partie**, les **isotopes du Hg ont été étudiés** dans deux modèles d'oiseaux (poussins de labbes et manchots adultes) **sur une grande échelle latitudinale de l'Antarctique à la zone subtropicale**. Les variations latitudinales des valeurs isotopiques du Hg (δ^{202}Hg, Δ^{199}Hg) semblent être influencées par une différente amplitude des processus photochimiques et d'autres voies biogéochimiques telles que la réduction du Hg, et les processus de méthylation / déméthylation, ainsi que les processus trophiques ou métaboliques.

Mots clés: mercure, oiseaux marins, Terres Australes et Antarctiques Françaises, spéciation, isotopes stables, écologie, transfert trophique, biogéochimie

Remerciements/Acknowledgements

Tout d'abord, je voudrais remercier mon directeur et co-directeur de thèse, Paco Bustamante et David Amouroux, d'avoir fait confiance à moi dans un premier temps et m'avoir soutenue au long de cette étape, pour vos conseils, vos lectures et relectures, votre patience… j'ai énormément appris de vous pendant ces trois années. Paco, merci beaucoup pour ton encadrement, ta disponibilité en tout moment, tes réponses et corrections super rapides et efficaces malgré la distance tu as été toujours là et tu as énormément facilité l'organisation et le bon déroulement de la thèse. David, mille merci pour tous tes conseils, réflexions et discutions enrichissantes, pour m'avoir communiqué tout ce savoir sur le mercure et les isotopes… et science appart, merci pour ton aide, ta compréhension et même pour m'avoir permis de faire des voyages incroyables pendant cette thèse !

Un énorme merci à Zoyne Pedrero pour la confiance que tu m'as faite du début, c'est avec toi que j'ai fait mes premiers pas dans le monde de la recherche et je suis très reconnaissante de m'avoir encouragé à faire cette thèse. Pour ton aide, ton amitié et tes conseils… mil gracias!

A Yves Cherel, merci beaucoup pour tes conseils, corrections et pour tout ce que tu m'as appris sur l'écologie et ce monde merveilleux des oiseaux.

Merci aussi à Aurélien Dommergue et Krishna Das d'avoir accepté d'être rapporteurs de cette thèse et merci à David Point, Lars-Eric Heimbürger et Jérôme Fort d'être les examinateurs.

Merci beaucoup à toutes les personnes qui ont fait partie de ce projet, à tous les fieldworkers qui ont contribué à la collection des échantillons dans le cadre du programme no. 109 (H. Weimerskirch) soutenu par l'Institut Polaire Français Paul Emile Victor (IPEV) et Terres Australes et Antarctiques Françaises (TAAF) et par l'Agence Nationale de la Recherche (program POLARTOP, O. Chastel). Merci également à Alice Carravieri, pour l'organisation des échantillons, les fichiers de données et les réponses super rapides.

Un grand merci à Emmanuel Tessier et Sylvain Bérail pour vos conseils techniques, votre attention en tout moment, les coups de main dans les grosses sessions d'analyses et surtout votre patience ! J'ai beaucoup appris à votre côté et ça a été un vrai plaisir de travailler avec vous.

Merci beaucoup à Julien Barre qui m'a supporté au labo mais aussi au bureau pendant ces presque quatre ans, pour m'aider et solutionner toutes les doutes et m'accompagner pendant les longues semaines d'analyse. A Sylvain Boucher, pour les coups de main avec la machine et les conseils. A Bastien, pour ton aide lors de la deuxième année, grâce à ta bonne humeur les grosses étapes de travail ont été un plaisir avec les rockeurs, les punks et les métalleurs. Thanks to Joana and Caiyan for being my guides and for all your help and encouragement inside and outside the lab.

Merci aussi à toutes les autres personnes du LCABIE pour la bonne ambiance de travail, à mes collègues de bureau, les anciens et les nouveaux: Nagore, Ariane, Alice, Marine A., Tiago, Alyssa, Wahid. Un super merci à tous mes collègues et amis, qui ont été un grand soutien pour moi, à Sara, Javi, Maxime, Marine, Manue, Mathieu, Andy, Jota … pour tous les repas, pauses cafés, rires, sorties et soirées ensemble.

Un millón de gracias a los colegas de la Universidad de Valparaíso, a Gaby Lobos y su equipo, Paty, Dani, Felipe por su acogida, su buen humor y toda su ayuda durante mi estancia y mis viajes por Chile, fue una experiencia inolvidable en gran parte gracias a vosotros.

Y por último muchas gracias a todas esas personas increíbles que tengo la buenísima suerte de tener a mi lado. A mi pequeña familia paloise, Iris, Izar, Amaia, Jesús, Clément, Aralar, Jérôme, Leire, Iñigo, Dani…porque os adoro a pesar de las infinitas anchoas y traquenards. A Sara, mi compi de aventuras, por estos cuatro años (y todos los que quedan) siendo también protagonista de mi vida. A Diego, por todos los ánimos y también por cuidarme y alimentarme estas últimas semanas. A Sofi y Quike, mi inspiración y referentes allá donde vayan, gracias por ser tan geniales. A Krikri, mein Wunderprofessor, thank you so much for your inspiring words, your humour and all the laughs together. A Christian, Luci y Ana por ser capaces de hacerme soltar una carcajada y apoyarme desde cualquier parte del mundo. A Claupi, Moni y a mi gente de Somo y Loredo por ayudarme a desconectar y por todos los ánimos sobre todo este último verano. Y un millón de gracias a mi familia, por todo el cariño, apoyo y todos los empujoncitos hacia arriba… ¡gracias!

.

Table of content

List of abbreviations and acronyms

AMAP- Arctic Monitoring and Assessment Programme

AMDEs: Atmospheric Mercury Depletion Events

ASGM- Artisanal and Small-Scale Gold Mining.

BAF- Bioaccumulation factor

CRM- Certified Reference Material

DDT- Dichlorodiphenyltrichloroethane

DOC/DOM- Dissolved organic carbon/matter

Fe- iron

GC-ICPMS- Gas Chromatography-Inductively Coupled Plasma Mass Spectrometry

HB- Hotblock

HNO_3- Nitric acid

IAEA- International Atomic Energy Agency

ID- Isotope Dilution

IDA- Isotope Dilution Analyses

iHg- Inorganic mercury

IPD- Isotope Pattern Deconvolution

IRB- Iron reducing bacteria

IRM- Internal Reference Material

IRMM- Institute for Reference Materials and Measurements

IUPAC- International Union of Pure and Applied Chemistry

LMWOC- low-molecular-weight organic compounds

LOD- Limit of detection

LOQ- Limit of quantification

MC-ICPMS-Multicollector-Inductively Coupled Plasma Mass Spectrometry

MDF- Mass dependent fractionation

MeCo- methylcobalamin

MeHg- Methylmercury

merA- mercuric reductase

MIE- Magnetic Isotope Effect

MIF- Mass independent fractionation

MW- Microwave

$NaBEt_4$- Sodium tetraethylborate

NFS- Nuclear Field Shield Effect

NIES- National Institute for Environmental Studies

NRCC- National Research Council of Canada

POC- Particulate organic carbon

$SnCl_2$- Stannous chloride (II)

SRB- sulphate reducing bacteria

SSE- Self-shielding effect

THg- Total mercury

TMAH- Tetramethylammonium hydroxide

TMS- Trophic magnification slope

UNEP- United Nations Environment Programme

WHO- World Health Organization

Chapter 1.

General introduction

Chapter 1. General introduction

Part 1: Mercury: a global pollutant of major concern

1.1 Properties

Mercury is a chemical element represented by the symbol Hg from the Greek “hydrargyros”, meaning silver water. It is a transition metal which appears under its liquid form at normal conditions of temperature and pressure. Hg atomic number is 80, its atomic mass 200.59 $g \cdot mol^{-1}$. Regarding its electronic configuration, Hg is classified as a transition metal IIB presenting an unsaturated "d" layer, hence it is easily polarizable. Hg presents three oxidation states: Hg^0 (metallic), Hg_2^{2+} and Hg^{2+}. It tends to form stable complexes with similar ligands such as thiols (-SH) and cyanides (-CN).

Due to its physicochemical properties, Hg naturally occurs in all types of environmental compartments, is easily transported over long distances and accumulated in the environment. One important characteristic of Hg is its volatility (due to its relatively high vapour pressure for being a metal) (Stein et al., 1996), which facilitates its release in the air and, consequently, the direct discharges into the sea via rainfall and river runoff. The global Hg cycle is therefore dominated by exchanges between the atmosphere and the aquatic environment. Hg can appear under different chemical forms: elemental mercury (Hg^0), divalent inorganic form (Hg^{2+} or iHg), and organic forms including monomethylmercury (CH_3Hg or MeHg), dimethylmercury ($(CH_3)_2Hg$ o DMHg) and ethylmercury (C_2H_5Hg).

1.2 Toxicity and effects of Hg in health

Hg is nowadays considered as a priority and global pollutant especially due to its accumulation and biomagnification in aquatic food webs. Hg causes severe toxic effects on animal and human health and its degree of toxicity strongly depends on its speciation (Tan et al., 2009). Its organometallic form, MeHg, is recognized by its capacity to bioaccumulate in the tissues of the organisms and biomagnificate during trophic transfer. Indeed, seafood consumption remains the major contributor to Hg contamination in humans and is generally used as a reliable criteria for the risk assessment associated to Hg exposition. Moreover, MeHg is a potent neurotoxin and causes irreversible damages to the nervous system and brain. This problematic has positioned Hg (and especially MeHg) as pollutants of major concern and have been widely investigated in the last decades for better understanding of the mechanisms of MeHg generation, transformations and

occurrence in the environment and led to the agreement of the Minamata Convention with the objective of reducing the utilisation and emission of Hg. Exposure of Hg in humans

Despite its utilisation in the past as a cure of syphilis and various infections, it has been established that Hg can produce serious and irreversible damages on reproduction, behaviour, endocrinology and development (Grandjean et al. 2010). Although the main route of human exposure to Hg compounds is related to fish consumption (mainly in form of MeHg), it can also occur by inhalation or skin contact. Indeed, Hg poisoning by inhalation of Hg^0 is the most fatal intoxication since around 80% penetrates easily into the blood where it is retained by oxidation. This can produce harmful effects on the nervous, digestive, and immune systems and the lungs and kidneys (WHO 2007). The negative effect of Hg is aggravated by its capacity of binding proteins and biomolecules. Indeed, the intoxication by Hg in humans results in the inhibition of the biological functions of certain enzymes that contain thiol groups (-SH).

As a consequence of Hg neurotoxicity, brain is considered a primary target organ and, at sufficient concentrations, Hg may disrupt neurological processes due to this high affinity for protein thiols (Clarkson and Magos 2006). In the 19th century, the use of liquid Hg by English hat manufacturers caused them severe neurological symptoms (depression, tremors and slurred speech), a grave disease illustrated by the widely known character of the “mad hatter” in Lewis Carroll writing “Alice’s adventures in wonderland”.

1.2.1 Intoxications by Hg in the History

The first known large scale Hg poisoning occurred in Minamata Bay, Japan, in 1956 by the release of Hg in the wastewater of a factory where Hg was used as a catalyst for the production of acetaldehyde. Following the subsequent methylation of the released Hg by microorganisms in the sediment, MeHg enters the food chain and contaminated the local fishermen and their families. This disaster caused more than 1000 deaths during 36 years and nearly 2 million people suffered from a neurological syndrome, so called Minamata disease, due to the consumption of intensely contaminated fish and seafood. Hg concentrations in fish ranged between 5.61 and 37.5 $\mu g.g^{-1}$ (Harada 1995). Analyses of hair samples from contaminated people displayed concentrations that could reach 705 $\mu g.g^{-1}$ (threshold considered "at risk" 30 $\mu g.g^{-1}$ (Legrand et al. 2010)). Between 1964 and 1965, a similar same tragedy took place in Niigata, Japan (Tsubaki and Irukayama 1977), known as “Second Minamata”, where victims experienced the first symptoms up to 5 years after MeHg intake. The agent was identified earlier than in Minamata and several studies demonstrated the neurotoxic effects of Hg, which were particularly severe among children exposed during their prenatal period (Harada 1995). Several sequences of poisonings from seed flours coated with fungicide containing MeHg occurred in Iraq in 1956, 1960 and 1971 (Bakir et al. 1973); as well as in New Mexico in 1969 (Snyder 1971).

Nowadays, Hg is already largely used for gold extraction by the artisanal and small-scale gold mining (ASGM) community. Gold is extracted with Hg by the formation of an amalgam which is later heated so that Hg is evaporated from the mixture leaving gold. This method is the cheapest alternative for gold extraction and it is quick, easy and can be performed by one single person (UNEP 2013; AMAP 2011). Hence, ASGM industry has rapidly expanded over the last two decades in developing countries (Hagan et al. 2015); principally in South America, Africa, and Asia; but also in North America and Australia (UNEP 2013). It has been estimated that approximately 15 million people participate in the ASGM industry in 70 countries (UNEP 2012). Although most uses of Hg are diminishing, ASGM represents the most significant source of global Hg emissions (UNEP 2013) and is expected to increase even more. Indeed, between 2005 and 2010, Hg emissions produced by ASGM doubled (UNEP 2013).

Figure 1.1 Artisanal and small-scale gold mining in San Juanito mine, Bolivia. Photo from Laffont et al., 2009.

1.2.2 Regulation/ implications

In 2009, the Governing Council of the United Nations Environment Programme (UNEP) initiated the development of a legally necessary global implementation to protect the human health and the environment from anthropogenic emissions and releases of Hg. In 2013, governments from 127 countries signed for this agreement which was called the Minamata Convention on Mercury. This convention was principally addressed to the development of national plans for public health, application of controlled measurements on Hg releases to the environmental compartments and regulation of ASGM and exposure to its communities, including strategies for compilation of health data, training for health-care workers and educating for consciousness.

Many governments control legal limits on maximum levels of MeHg in fish for consumption. World Health Organization (WHO) actually give their recommendations in terms of daily oral intake of MeHg and estimated that the normal concentration for a non-contaminated population should be comprised between 5 et 10 μg L^{-1} in blood (WHO 2008). Consumption of long-lived predatory species such as shark and swordfish have been especially disapproved. Hg^0 air concentrations in areas surrounding ASGM burning sites have been found to exceed the WHO limit for public exposure of 1.0 μg m^{-3} (WHO 2008). It was reported that workers exposed to 30 μg m^{-3} Hg experienced tremble, but renal diseases and changes in plasma enzymes are expected at 15 μg m^{-3} (WHO 2000). Furthermore, Hg exposure by ASGM affects not only the health of workers but also the people from adjacent communities (UNEP, 2012). Given this problematic situation, the continuous application of studies on Hg contamination is necessary to assemble health data and levels of exposure in order to favour the implementation of control policy to regulate and prevent Hg pollution.

1.3 Main sources of Hg in the environment

Although Hg natural sources such as soils, rocks, volcanoes or biomass can be involved in the remobilization of Hg at a global scale, the main source of this metal comes from the anthropogenic activities. Its high electrical conductivity and its ability to form amalgams with other metals like gold and silver, have potentiated the heavy exploitation of Hg in mining, in metallurgical field and in the process of fossil fuels combustion.

1.3.1 Natural sources

Natural sources represent all the direct emissions of Hg coming from processes such as volcanic eruptions, geothermal activities or soil erosion or minerals that contain Hg naturally, mainly as cinnabar (HgS). Globally, it is estimated that about 30% of Hg emissions derive from natural sources (Amos et al., 2013). Volcanoes, geothermal and terrestrial sources are considered primary natural sources of Hg, whereas the re-emission of previously deposited Hg on surface waters, vegetation or land are related to biomass burning, meteorological conditions and exchange of Hg^0 at air-water, air-land or snow-ice interfaces (Mason and Pirrone 2009). Oceans (which represent 70% of the planetary surface) are considered a substantial natural input of Hg into the atmosphere (Morel et al., 1998) estimated as 52% of Hg natural sources (Pirrone et al., 2010).

Table 1.1. Global Hg emissions by natural sources estimated for 2008 (Pirrone et al. 2010).

Natural source	Hg (Mg·year $^{-1}$)	Contribution (%)
Oceans	2682	52
Lakes	96	2
Forests	342	7
Tundra/grassland/savannah/prairie/chaparral	448	9
Desert/metalliferous/non-vegetated zones	546	10
Agricultural areas	128	2
Evasion after AMDEs	200	4
Biomass burning	675	13
Volcanoes and geothermal areas	90	2
Total	5207	100

1.3.2 Anthropogenic sources

The anthropogenic activity is considered the main source of Hg in the environment and is the result of its exploitation in mining, electrolytic industries using Hg electrodes, the fumes of fossil fuels, pesticide based on Hg compounds and alkaline batteries (Somer 1978). Current anthropogenic emissions correspond approximately to 2000 Mg·year^{-1} (Streets et al. 2011). Mineral exploitation and fuel fossil combustion are nowadays the major contributors of human Hg emissions (UNEP 2013). Actually, coal combustion critically enhanced the natural cycle of Hg in environmental compartments during the Industrial Revolution and, at the present time, it continues to be the most expanded source of anthropogenic Hg as a result of its widespread use for electricity and heat production around the world. Emissions from fuel fossil combustion have been estimated around 35-45 % of the total Hg input (Pacyna et al., 2006). In South America, ASGM is today responsible for the largest proportion of the emissions (about 60%) (UNEP 2013). Since the Ancient times, the exploitation of Hg natural reservoirs has been extensively accomplished for precious metal recovery in South America, predominantly at the time of Spanish colonization (the release of nearly $2 \cdot 10^5$ Mg of Hg was estimated from 1550 to 1850). Hg mineral exploitation achieved its apogee from 1860 to 1920, during which emissions achieved 2500 Mg·year^{-1} (Streets et al., 2011). Indeed, it has been suggested that the remarkable Hg concentrations exiting nowadays could be likely the heritage of the significant exploitation of Hg for gold extraction at this time. Today, the main Hg extraction mines all around the world are located in the periphery of the Pacific Ocean (principally in Peru and Mexico).

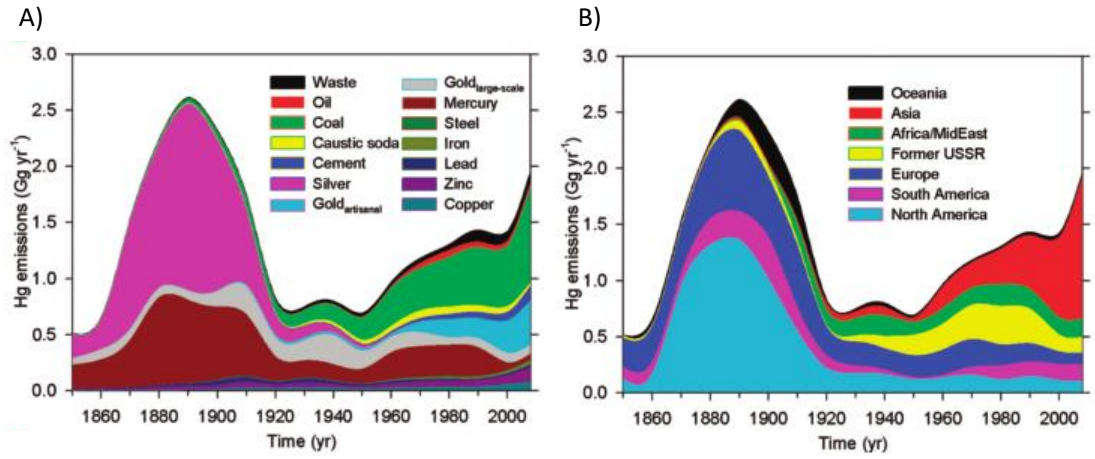

Figure 1.2. Temporal trends in Hg anthropogenic emissions by (a) source type and (b) geographical region. Figure from Streets et al., 2011.

Emission inventories showed that Asian countries accounted for more than 50% of the global anthropogenic Hg, especially China which is now responsible of 25% of worldwide Hg emissions (Tang et al., 2007). Coal burning and power plants are responsible of the total combustion emissions of Hg in China. However the global situation is nowadays more encouraging since emission control policies have been restructured in order to reduce the environmental impact of air pollutants from the Chinese sector in recent years (AMAP 2011).

In the marine environment, anthropogenic emissions have produced an extreme impact, involving the substantial increase of Hg levels in the ocean (concentrations have duplicated in the first 100 meters of the world's oceans in the last 100 years) (UNEP 2013). As a consequence, Hg content in several species of marine top predators have amplified by 12 times, implying that over 90% of their accumulated Hg comes from anthropogenic sources.

Hg atmospheric concentration is determined by the combination of primary direct sources (natural and anthropogenic) and the continuous re-emission from environmental compartments. Actually, it is believed that, before the industrialisation, Hg levels in the environment were in equilibrium, with a balance between mobilization from long-term geological reservoirs and removal from the different reservoir compartments (atmosphere, soils, and oceans) (AMAP 2011). The extreme amplification of anthropogenic emissions since the beginning of the industrial period has perturbed this natural balance so that Hg became a contaminant of major concern through global atmospheric, oceanic circulation and biological turnover.

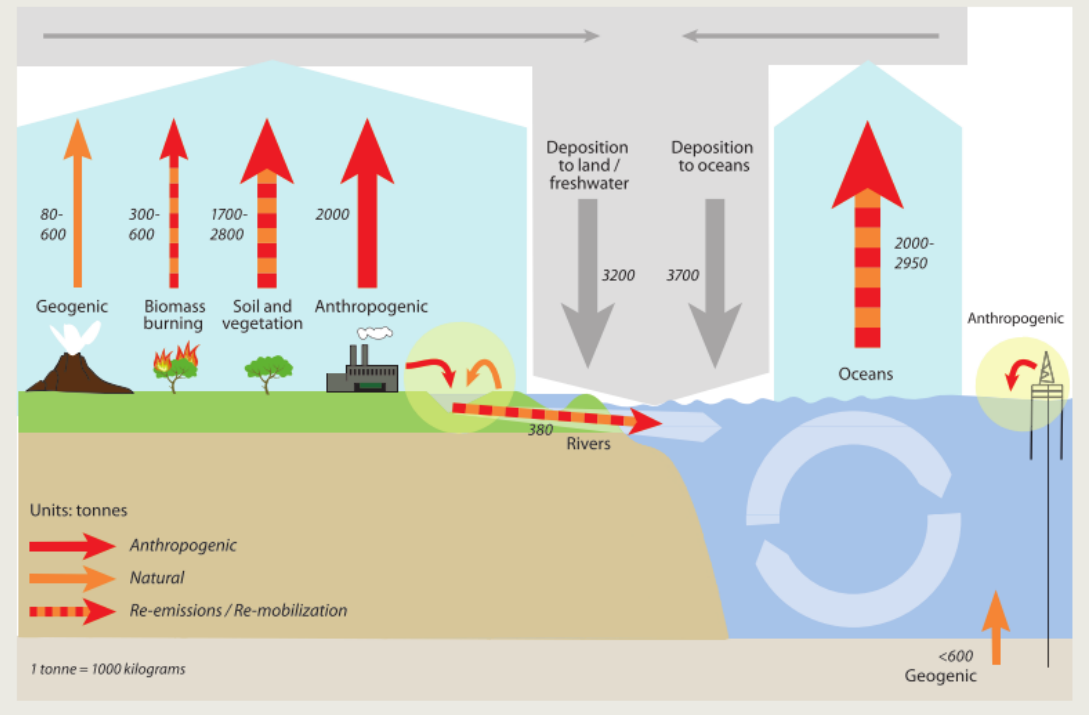

Tonnes = Mg = 1000 Kg

Figure 1.3 Global Hg budgets in the main environmental compartments and pathways that are of importance in the global Hg cycle. Estimations of natural and anthropogenic releases to air land and water are based in models. Figure from UNEP 2013.

1.4 Biogeochemical cycle of Hg in the marine environment

1.4.1 Which are the potential sources of Hg in remote marine areas such as the Southern Ocean?

In the Ocean, the primary source of Hg is direct atmospheric input, however, it is known that mobilisation from sediments and submarine hydrothermal inputs also contribute to Hg amounts in the marine compartment (Mason et al., 2012). Despite the distance from industrial focus, the Southern Ocean is affected by the anthropogenic stress mainly via atmospheric circulation of contaminants and ocean currents (Pacyna et al., 2010). The relatively long residence time of Hg in the atmosphere favours its redistribution at a global scale (Schroeder and Munthe, 1998) and therefore, significant amounts of Hg arrive to remote zones mainly due to long-range transport from human sources at lower latitudes.

Other potential source of Hg in the Ocean is sediment erosion and mobilization (Mason et al., 2012; Lamborg et al. 2014). Due to its affinity to organic matter, Hg can be released from the water column and deposited on sediments. Different iHg species are distributed among the dissolved, colloidal and particulate phases, bound to different ligands that form a variety of

complexes. In anoxic environments, sulphurs (S^{2-}) are the most abundant species but when they are absent, Hg forms complexes preferentially with the organic matter. Chlorinated complexes ($HgCl_{x2-x}$) and hydroxides ($Hg(OH)_{x2-x}$) are predominant in oxygenated and slightly eutrophic environments. This fact involves a different Hg speciation distribution between marine and freshwater systems. Coastal areas are thus under considerably higher Hg pressure (Lamborg et al., 2014) so that Hg export to the open ocean areas is not negligible (Amos et al., 2012). In the Southern Ocean, Hg release to the opened areas may be thus more significant in water masses surrounding Antarctic continent or coastal zones in the vicinity of subantarctic islands whereas open waters are mainly between 4000 and 5000 meters deep.

An important Hg input into polar oceanic zones is melting ice, snow and permafrost (AMAP 2011; Sheppard et al., 1997). Additionally, oxidation of Hg in the atmosphere has been found to be an important source into polar oceans with meaningful inputs occurring during springtime as a result of atmospheric Hg depletion events (AMDEs), when halogen radicals oxidize Hg^0 of the air (Ebinghaus et al., 2002). Thus, sea ice represents an important Hg reservoir derived from freeze rejection, scavenging of atmospheric Hg and discharge from sea ice cover (Chaulk et al., 2011). Because Hg is deposited under inorganic forms, its rate of methylation (and demethylation) in the physical environment, prior its transfer within food webs, is crucial for Hg accumulation in Antarctic biota, in which high levels of MeHg have been detected (Bargagli et al., 1998).

1.4.2 Main processes involved in Hg biogeochemical cycle in the marine system

Marine systems constitute an important part of the Hg biogeochemical cycle. Actually, the presence of Hg in oceanic compartments can represent an important source of contamination for the atmosphere due to volatilization of the gaseous form Hg^0, for sediments as iHg and for trophic webs through the MeHg accumulation. This last process is of major concern since it is the main way of Hg exposure for humans and animals by the consumption of seafood. Since Hg is highly reactive in aqueous medium, it undergoes different transformations (oxidation, reduction, methylation and demethylation) which are carried out by biological and abiotic processes. Abiotic reactions are mainly induced by photochemistry so that they take place in the photic zone of the water column (Hammerschmidt et al., 2007; Monperrus et al., 2007; Lehnherr et al., 2009). The bio-physicochemical characteristics of a given ecosystem will define Hg speciation, and consequently, its mobility and toxicity.

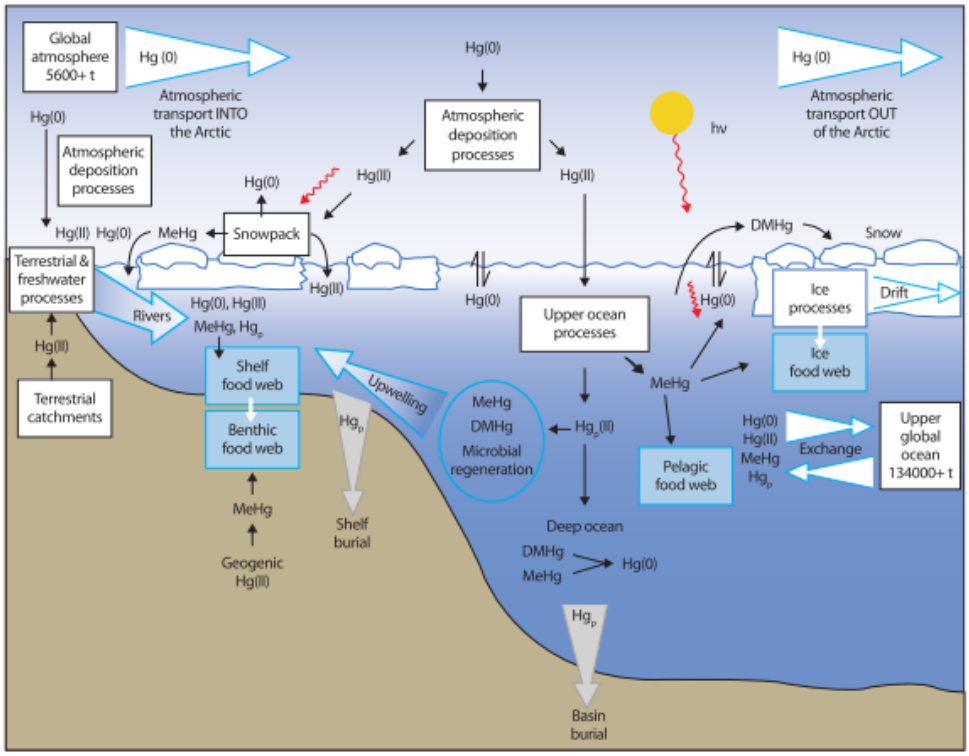

Figure 1.4 Schematic diagram of the Hg cycle in the Arctic Ocean. Figure from AMAP 2011.

1.4.2.1 Redox cycling and air-sea exchange in marine and polar systems

Hg is emitted into the atmosphere in the form of elemental vapour (Hg^0) which passes into its Hg divalent form (Hg^{2+}). This oxidized form of Hg is very soluble, then it can react rapidly with rainwater or snow, or can even be adsorbed by small particles, and subsequently deposited in the environment. Therefore, it is widely recognized that Hg^0 constitutes the largest component of the total gaseous Hg concentration in the troposphere and it is transported on a hemispheric scale (Slemr et al., 1985). The residence time of the Hg^0 in the troposphere is around 0.8 to 1.6 years (Selin et al., 2007), while the soluble forms remain only few weeks. Divalent Hg species can be introduced on the soil (in the form of dry or wet deposit) where they can be methylated into more toxic organic forms by biological processes.

In marine systems, two main processes control the atmospheric-water compartment interactions: iHg reduction and Hg^0 oxidation. Since iHg is the substrate for methylation, its reduction into Hg^0 and sea to air exchanges are also important processes regulating MeHg levels in surface waters. The reduction of iHg will produce volatile Hg^0 reducing the Hg amount in the water system, whereas the opposite Hg^0 oxidation reaction will decrease the volatile Hg^0 pool and the water-air Hg transfer contributing to the increase of iHg concentrations in the aquatic compartment and its later methylation.

Biotic reduction mechanisms can be mediated by Hg-resistant bacteria found in oceans and estuarine areas (Mason and Fitzgerald 1990; Mason et al., 1995), including in the Arctic (Barkay et al., 2003; Møller et al. 2014) and Antarctic sea ice (Gionfriddo et al., 2016). These microorganisms are able to reduce Hg^{2+} into Hg^0 by the mercuric reductase (merA), which is a part of the *mer* operon that encodes a group of proteins involved in the detection, transport and reduction of Hg. Phototrophic organisms, such as phytoplankton has also been found to reduce iHg (Poulain et al, 2004).

Although biological Hg reduction occurs in the Ocean, Hg photochemical reduction is the main mechanism occurring in surface waters and is responsible of the re-emission of Hg^0 to the atmosphere. The production of dissolved gaseous Hg is mostly photomediated and involves the reduction of iHg species by solar irradiation in the presence of dissolved organic carbon (DOC), which is assumed to be crucial in the production of dissolved Hg^0 (Amyot et al., 1997). DOC plays a complex role in the Hg aquatic chemistry since it creates strong bounds with Hg controlling its distribution and availability, but also provides highly redox active radicals that may serve as reductants or oxidants during photochemical reactions (Zhang and Lindberg, 2001). Different factors can also potentiate Hg^0 photo-oxidation, such as the presence of –OH, $-O_2^-$ and chloride ions (Lalonde et al., 2002). Direct photolysis of NO_3^-, NO_2^- and H_2O_2 can potentiate the release of active halogens and OH radicals in seawater (Mopper and Zhou, 1990) and in snow (Poulain et al., 2004). The $-O_2^-$ radical also presents the capability to oxidize Hg^0 and can be produced by photochemistry in natural surface waters. Both processes have been found to occur in snow packs and are induced by photochemistry (Lalonde et al., 2002; Poulain et al., 2004) after the formation of initial radicals.

Polar zones present a unique Hg cycle, mainly characterized by the occurrence of atmospheric phenomena (AMDEs) and the presence of sea ice cover, which both contribute to particularly different processes at the air-ocean interface. AMDEs consist in the rapid oxidation of atmospheric Hg^0 into gaseous Hg^{2+} (also known as reactive gaseous Hg) during the spring season through reactions with halogens such as bromine (Lindberg et al., 2002; Ariya et al., 2002), which is released from sea-salt to the atmosphere during sea ice formation (Schroeder and Munthe 1998; Lindberg et al., 2002). These events involve the transfer of oxidized iHg into particles which are deposited on the snow pack, involving Hg depletion from atmosphere (Temme et al., 2003) and its potential transfer to the ocean during melting (Lindberg et al., 2002). AMDEs have been shown to concur with an abrupt simultaneous decrease in atmospheric ozone concentrations (Lindberg et al., 2002, Schroeder and Munthe, 1998). Although the exact mechanism is still undefined, previous studies have proposed the occurrence of reactions involving ozone and certain halogenated compounds (including BrO_x, Br, BrO) that lead to ozone depletion events (Simpson et al., 2007).

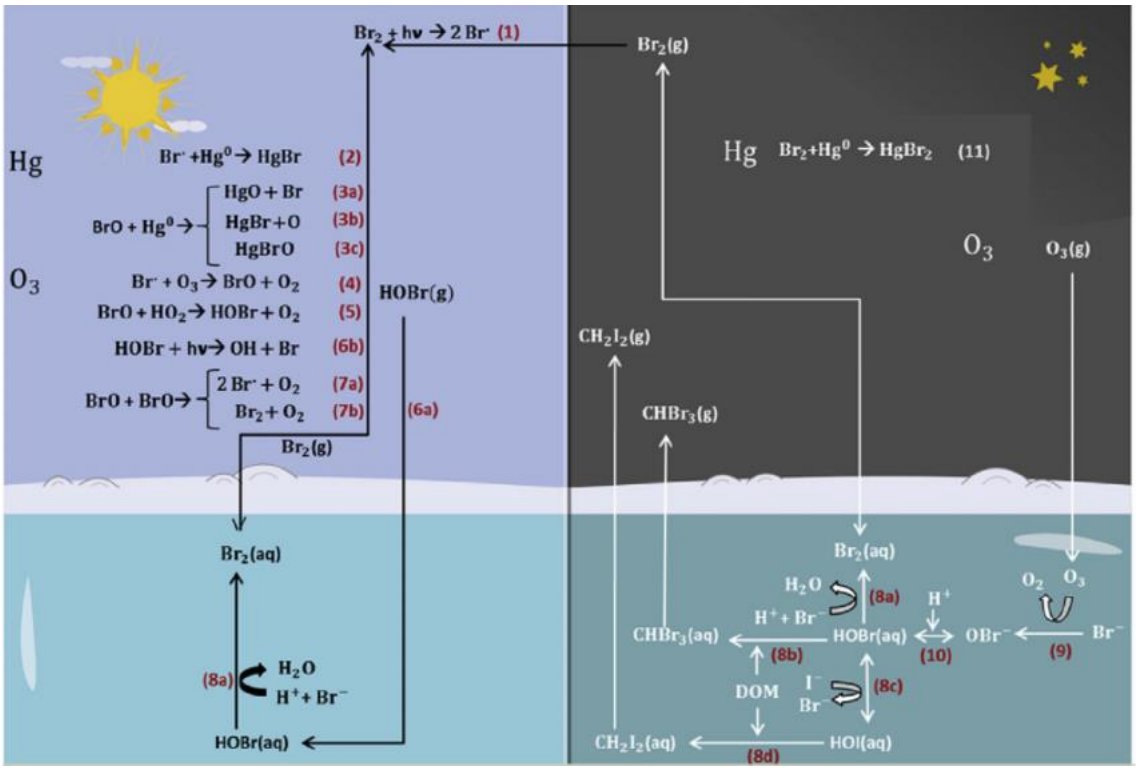

Figure 1.5. Schematic diagram of proposed reactions of bromine, Hg species and ozone involved in depletion events during light and dark conditions. Figure from Nerentorp Mastromonaco et al., 2016.

The existence of this phenomenon was first discovered in the Arctic (Schroeder and Munthe, 1998) and later observed in coastal Antarctica (Ebinghaus et al., 2002; Bargagli et al., 2005). Indeed, AMDEs have been detected all along the fringes of Antarctic sea ice, in polynyas and between pack ice and fast ice (Dommergue et al., 2009). These events are assumed to have been occurring in coastal Antarctica over long periods, becoming especially important during the last glacial period, when sea ice recorded much higher concentrations of sea salt and dust (Jitaru et al., 2009). Hg^0 in coastal Antarctic marine boundary layer is known to be present in lower concentrations than further north ecosystems (Soerensen et al., 2010). Nevertheless, much higher concentrations of Hg^{2+} have been documented comparing to northern latitudes (Soerensen et al., 2010), which could lead to greater Hg deposition on coastal snow packs enhancing Hg concentrations in the surface snow and, consequently, into the ocean during sea ice melting (Brooks et al., 2008). The observation of a constant increase of oxidized Hg in the Antarctic environment during the sunlight period could suggest the existence of more elevated Hg^0 oxidation rates comparing to the Arctic sea ice (Dommergue et al., 2009). Moreover, the fast reactivity of Hg^0 and the presence of Hg^{2+} from late winter to summer are proposed as substantial contributors of net input of atmospheric Hg on Antarctic surfaces (Dommergue et al., 2009). After the deposition of Hg^{2+} on snow, the most part of this Hg^{2+} (50-80%, Dommergue et al., 2003) is

believed to be photoreduced and re-emitted to the atmosphere as Hg^0 in a few days (Steffen et al., 2014; Poulain et al., 2004; Lalonde et al., 2002).

The presence of sea ice cover in Polar Regions has been demonstrated to influence Hg cycling in marine systems, due to inhibition of aquatic photochemistry. Antarctica is an ice-covered continent isolated from the other continents by marine currents that favour the accumulation of ice in the continent. However, the decline of sea ice in the Antarctic ecosystems is accelerated by currents of warmer waters from lower latitudes and the action of large ocean waves that also involve ice fragmentations (Comiso, 2003). Sea ice is composed of frozen seawater, brine, gases, minerals, particles, and biota (Beattie et al., 2014). Annually, sea ice around East Antarctica melts releasing nutrients (Arrigo and Thomas, 2004) and also Hg (Cossa et al. 2011). The sequestration of atmospheric Hg in sea ice compartment is indeed responsible of an additional input of Hg in the ocean. It is believed that Antarctic sea ice melting contributes over 9.6 Mg of Hg to seawater each year (Gionfriddo et al., 2016), which is more considerable than some Arctic Ocean estimations (Beattie et al., 2014). Recent measurements in the east coast of Antarctica indicated elevated concentrations of total Hg in surface snow samples and evidenced that Hg atmospheric deposition processes are enhanced comparing to the Arctic ecosystem (Angot et al., 2016a). Furthermore, coastal Antarctic ecosystems are affected by intense katabatic winds that transport Hg from Antarctic inland atmospheric reservoir towards the coast (Angot et al., 2016a), which can strongly influence the cycle of atmospheric Hg at a continental scale (Temme et al., 2003; Angot et al., 2016a; Angot et al., 2016b; Sprovieri et al., 2016).

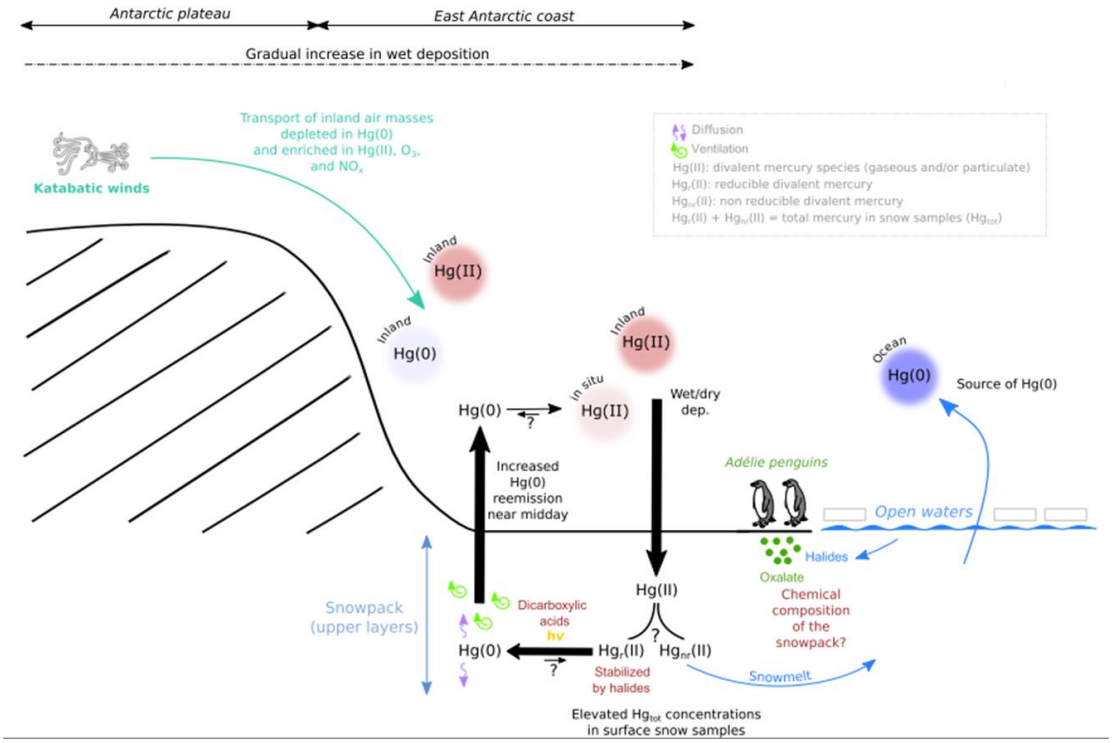

Figure 1.6. Illustration of the processes of transport and transformations of Hg occurring in coastal Antarctica (Dumont d'Urville, Adélie Land) during summer. Figure from Angot et al., 2016a

1.4.2.2 Methylation and demethylation of Hg in marine and polar systems

Hg methylation and demethylation are two key processes regulating the Hg cycle in marine environments because they determine the fate of MeHg in the water column, contributing in a major way to its bioaccumulation in food webs. Methylation and demethylation in the marine environment can be driven by both biological activities and abiotic mechanisms (Cossa et al., 2009). Biological reactions pathways have been proposed to be of major importance for Hg species transformations in seawater (Barkay et al., 2003) and anoxic lake waters (Eckley and Hintelmann, 2006). Nevertheless, most studies highlighted the requirement of anaerobic metabolism or reducing conditions to achieve a substantial production of MeHg, taking into account the reversible demethylation pathways (Rodríguez Martín-Doimeadios et al., 2004). DMHg is considered the main product of biotic methylation (Mason and Sullivan, 1999) and its production is closely linked to primary productivity in marine polar regions (Pongratz and Heumann, 1999; Lehnherr et al., 2011)

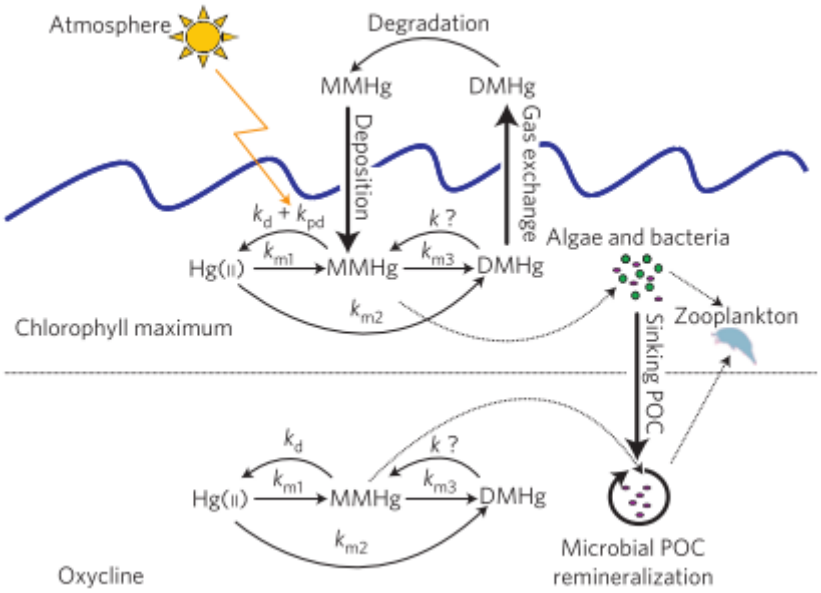

Figure 1.7. Conceptual model of Hg methylation/demethylation in marine waters. Figure from Lehnherr et al., 2011

1.4.2.2.1 Abiotic/biotic methylation

Natural abiotic methylation requires the availability of methyl-donor compounds that have been observed both in sediments and in the water column (Krishnamurthy, 1992; Cossa et al., 2009). This process is strongly affected by numerous environmental factors such as pH, temperature, salinity, organic matter, redox conditions, among others (Ullrich and Abdrashitova, 2001). These methyl-donor compounds can be small organic molecules such as methylcobalamin (MeCo), methyl-iodide or methyltin; or larger molecules belonging to dissolved organic matter (DOM), such as fulvic and/or humic acids (Thayer, 1989; Celo et al., 2006). MeCo is a naturally occurring coenzyme of vitamin B12 considered the main potential environmental agent of Hg abiotic methylation in aquatic environments (Thayer, 1989; Chen et al., 2007). This reaction is carried out by transfer of methyl groups in the form of methylcarbanion (CH_3^-), radical ($-CH_3$) or carbonium ion (CH_3^+) (Ridley et al., 1977; Krishnamurthy, 1992). In the environment, abiotic methylation may occur in the atmosphere (Gårdfeldt et al., 2003) resulting from the presence of acetate as methyl-donor and Hg^{2+} in the atmospheric aqueous phase.

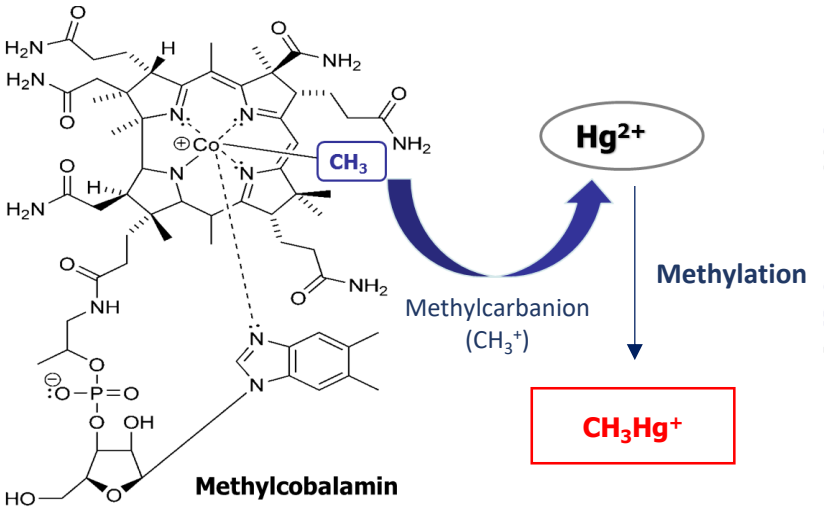

Figure 1.8. Transfer of a methyl group via the MeCo (or CH_3CoB12) in form of methylcarbanion for methylation of iHg.

Biotic methylation is considered to be significantly faster than abiotic methylation (Choi et al., 1994) and includes the transfer of methyl groups from MeCo to Hg^{2+} mediated by bacteria. In marine systems, it is mainly carried out by sulphate and iron reducing bacteria (SRB and IRB, respectively) (Gilmour et al., 1992; Fleming et al., 2006). SRB (representative of the genus *Desulfovibrio*) are recognized as the principal Hg organisms methylating iHg in aquatic anoxic environments (Compeau and Bartha, 1985). Experiments in microcosms have demonstrated that

the absence of SRB involves a significant decrease of the methylation rates (Avramescu et al. 2011). Numerous studies have focused in the investigation of *Desulfovibrio desulfuricans* ND132 as a model organism (Gilmour et al., 2011). One recent study (Parks et al., 2013) identified the two gene clusters associated to bacterial methylation (*hgcA* and *hgcB*), which has supposed an important advance for the application of genomics to investigate microbial Hg methylation pathways in the environment. Hg metabolic methylation processes are not completely understood and it has been suggested as a protective mechanism against Hg toxicity in some microorganisms (Pedrero et al., 2012a). However, not all SRB present Hg methylation capacities and the methylation yields are variable between strains (Bridou et al., 2011). In the case of complete oxidizers, Hg methylation seems to require the activation of acetyl coenzyme A synthetase in the cytoplasm (Choi et al., 1994), whereas incomplete oxidizers can methylate independently of the acetyl coenzyme A (Ekstrom et al., 2003).

SRB are anaerobic bacteria that oxidize organic substances using sulphate as the terminal electron acceptor (Harmon et al., 2007), then total sulphur is believed to play an important role in Hg^{2+} availability and is also an indicator of the presence of SRB (Schartup, Balcom, and Mason 2014). The rate of Hg methylation is therefore dependent on many environmental parameters, including pH, temperature, sulphate and DOM concentrations and redox potential in sediments (Choi, Chase, and Bartha 1994). All these conditions will influence the speciation and availability of mobile Hg^{2+} and the abundance and activity of microorganisms. MeHg can also apparently be produced during detrital remineralization in oxic marine waters, associated with nutrient maxima and oxygen utilization (Sunderland et al. 2009; Cossa, Averty, and Pirrone 2009).

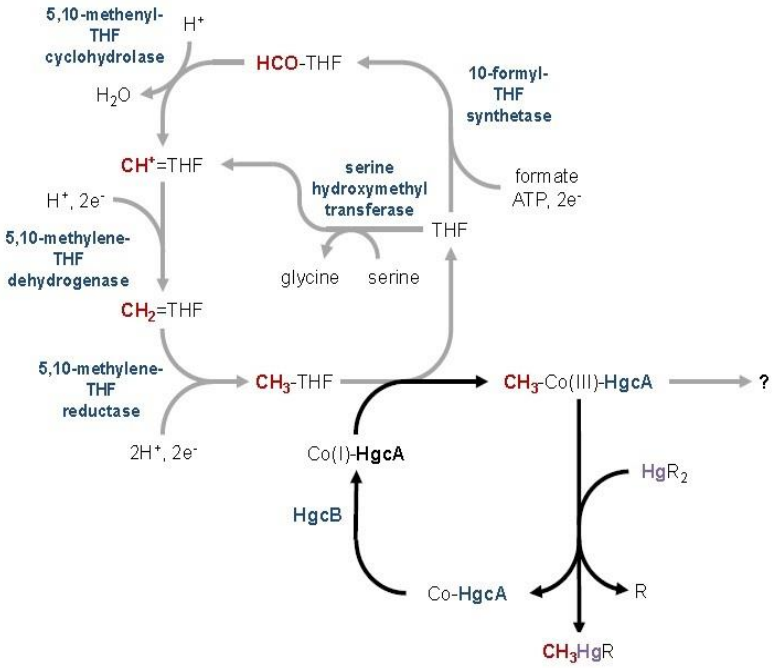

Figure 1.9. Hypothetical explanatory model at the molecular scale of the Hg methylation process by encoded protein by genes hgcA and hgcB. Figure from Parks et al., 2013.

Some studies in the Arctic region have proposed the presence of occurring bacterial Hg methylation in the lower parts of sea ice (Beattie et al., 2014), sea ice brine (Douglas et al., 2008), snow packs (Larose et al., 2011) and frost flowers (Bowman et al. 2014), although this has not been proved by the identification of Hg-methylating microbes (i.e, containing functional hgc genes) in sea ice or polar surface waters. However, in a recent study in Antarctic sea ice (Gionfriddo et al., 2016), potential Hg methylation genes from a marine nitrite-oxidizing bacterium (Nitrospina) and *mer* operons from Proteobacteria have been identified, providing a considerable advance for understanding Hg methylation in polar regions. Furthermore,

Nitrospina-like microorganisms have been found to be present across the sea ice–brine–sea water interface (Ngugi et al., 2015; Delmont et al., 2014).

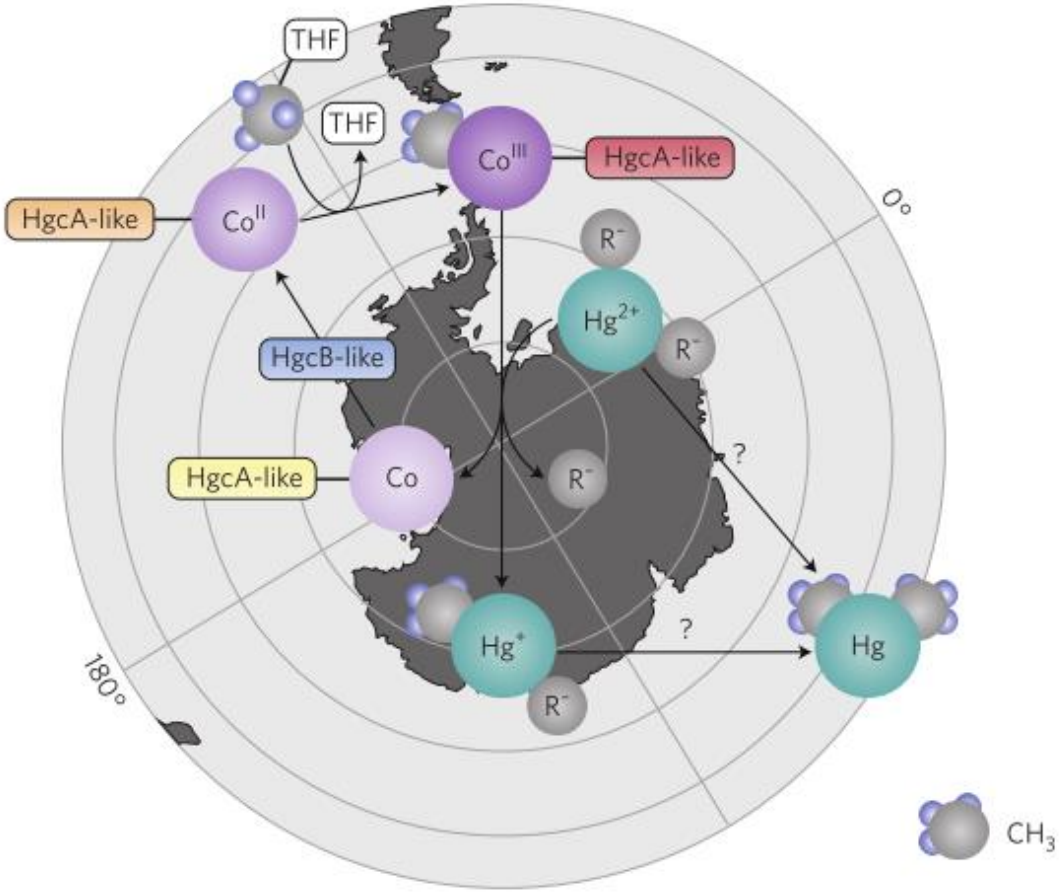

Figure 1.10. Proposed mechanism by Gionfriddo et al., 2016 for methylation of iHg mediated by a microaerophilic nitrite-oxidizing bacterium, Nitrospina, in Southern Ocean sea ice containing an hgcA-like protein. Figure from Sunderland and Schartup, 2016.

Despite the large amount of anaerobic Hg-methylating bacteria (Gilmour et al., 2011), methylation has also been observed in well-oxygenated polar surface waters (Heimbürger et al., 2015; Lehnherr et al., 2011; Schartup et al., 2015). Hg methylation by anaerobic bacteria is known to be partially dependent on the activity of phytoplankton, as it has been confirmed in freshwater biofilms (Desrosiers et al., 2006; Hamelin et al., 2011) and in sea ice interface (Gionfriddo et al., 2016). This has been reasoned from the observation of higher MeHg concentrations observed in Antarctic sea ice enriched in phytoplankton comparing to the water column. During this process, the release of metabolites (such as extracellular thiols) could influence iHg bioavailability (Leclerc et al., 2015) or the interaction of iHg or Hg^0 with methylating ligands such as haloalkanes (Yin et al., 2014; Celo et al., 2006; Larose et al., 2010). However, the exact role of phytoplankton with respect to the marine production of MeHg remains unknown (Grégoire and Poulain, 2014).

Another study in the Arctic (Pućko et al., 2014) proposed that iHg could be methylated by intestinal microbial communities in a zooplankton species (*Calanus hyperboreus*), however further studies are needed to confirm this hypothesis.

1.4.2.2.2 Abiotic/biotic demethylation

Photoinduced MeHg demethylation is the main abiotic process of MeHg degradation in aquatic environments (Barkay et al., 2003; Lehnherr et al., 2009). The extent of MeHg photodegradation is strongly dependent on the type of MeHg-binding ligands (Zhang and Hsu-Kim, 2010). Greater and faster photodemethylation rates have been observed in freshwater comparing to the oceans, where this process is much slower particularly when compared to MeHg degradation processes mediated by microorganisms (Whalin et al., 2007). These differences are the result of different MeHg complexes in both ecosystems, in freshwater MeHg is mainly bound to sulphur-containing ligands whereas in seawater it is mainly associated with DOM and Hg−chloride complexes (Zhang and Hsu-Kim, 2010). The high stability of chloride compounds such as methyl-chloride (CH_3HgCl) makes MeHg degradation much difficult (Whalin et al., 2007). Different radicals have been evidenced as reactive intermediates responsible for photodegradation: hydroxyl radicals (-OH) (Chen et al., 2003), singlet oxygen (O_2) from DOM (Chen et al., 2003; Zhang and Hsu-Kim, 2010).

Regarding biotic demethylation, two principal types of processes have been observed: reductive demethylation and oxidative demethylation. Reductive demethylation is carried out by bacteria possessing the mer operon, occurring mostly in the aerobic zone (Barkay et al., 2003). Briefly, this process consists on a first demethylation of MeHg by an enzyme (merB, organomercurial lyase) resulting in iHg that is then degraded inside the bacterial cell by another enzyme (merA) and then evacuated from the cell as Hg^0 (Barkay et al., 2003; Kritee et al., 2009). Oxidative demethylation by anaeorobic bacteria is still poorly understood but it possibly occurs as a by-product of metabolism by SRB (Marvin-DiPasquale et al., 2000). MeHg is thus degraded to CO_2 and a small amount of CH_4, involving the release of iHg that would be available again for methylation (Marvin-DiPasquale et al., 2000; Barkay et al., 2003). It has been suggested by several environmental studies that oxidative demethylation mechanisms are predominant at lower Hg concentrations (<100 $ng \cdot g^{-1}$) in anaerobic conditions, whereas reductive *mer*-operon mediated demethylation seems to dominate at high Hg concentrations in more aerobic medium (Marvin-DiPasquale et al., 2000; Oremland et al., 1991; Hines et al., 2000). In contrast to reductive demethylation, catalyzed by the enzymatic system encoded by the operon *mer*, oxidative demethylation does not appear to be a process for MeHg detoxification (Marvin-DiPasquale et al., 2000). Experimental studies in laboratory have indicated that most part of methylating SRB are also capable of demethylating MeHg, however not all the bacteria that demethylate do necessarily methylate (Bridou et al., 2011). As well as for methylation, demethylation rates appear

to be largely influenced by environmental parameters such as pH, redox conditions and salinity (Compeau and Bartha, 1985). However, biological methylation has been supposed to be slower and controlled by the assimilation of iHg, whereas demethylation is faster and does not depend on the MeHg concentration (Bridou et al., 2011). Biotic demethylation has been suggested to constitute a regulator process of the MeHg accumulation in contaminated environments (Barkay et al., 2003).

1.4.3 Bioaccumulation and biomagnification in marine food webs

1.4.3.1 Incorporation of Hg in the food web

Microorganisms such as bacteria, phytoplankton and protozoan are considered the primary entrance access of Hg in marine food webs (Pickhardt et al., 2002; Chen et al., 2008). Phytoplankton is known to concentrate 10^4-10^5 higher Hg levels than ambient water concentrations and this accumulation represents the largest relative increase in MeHg levels at any point in a food web (Mason et al., 1995). The specific bioaccumulation of the different Hg compounds is controlled by biological processes, being MeHg the preferentially bioaccumulated due to a better efficiency in the trophic transfer (Morel et al., 1998). Hg^0 and DMHg are not reactive and diffuse both inside and outside unicellular microorganisms (Mason et al., 1996). The difference in bioaccumulation between MeHg and iHg is more delicate and depends on the concentrations of MeHg and iHg in the studied compartment, the proportion of each species under its lipophilic form ($HgCl_2$, CH_3HgCl or organic complexes in the water) and their ability to be assimilated by organisms (Mason et al., 1996). In an aquatic system, and more specifically in an oceanic environment, iHg concentration is ~20 times higher than MeHg, however, the ability to form lipophilic complexes with chloride ions is greater for MeHg (100%) than for iHg (45%) (Morel et al., 1998). Although the two lipophilic compounds are assimilated equally, MeHg is concentrated in the cytoplasm and associated with the soluble fraction of phytoplankton whereas iHg mainly remains adsorbed on the cell membrane (Morel et al., 1998). This different distribution in the unicellular organisms involves that the efficiency of MeHg assimilation is four times greater than iHg, even if $HgCl_2$ complexes are more lipophilic (Kow = 3.3) than CH_3HgCl (Kow = 1.7) (Morel et al., 1998).

Once in the organism, the complexation of MeHg with aminoacids containing thiol groups (e.g. cysteine and methionine) or non-sulphured aminoacids (e.g., histidine), will determined the bioavailability for the microorganisms predators and this complexation appears therefore essential to regulate Hg solubility in the gastrointestinal tract and its subsequent assimilation.

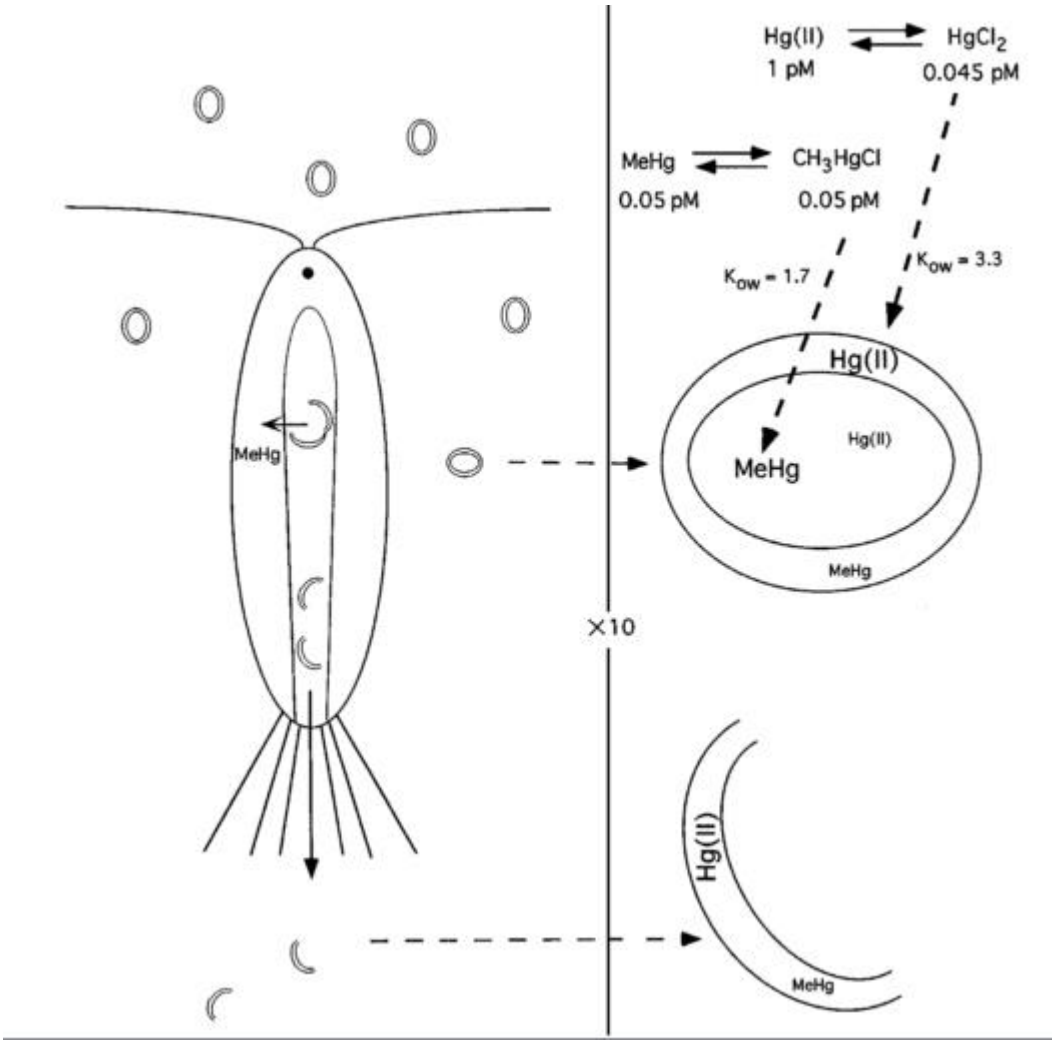

Figure 1.11. Specific assimilation of Hg species at the first trophic levels of the food web. Figure from Morel et al., 1998.

1.4.3.2 Bioaccumulation and bioamplification of MeHg

Since MeHg accumulates mainly in the cytoplasm of the cell and iHg is mainly sequestered by membrane thiols (Mason et al., 1996), the transfer to the upper trophic level is enhanced for MeHg while iHg is mainly excreted, especially when digestive process are fast. Moreover, the assimilation efficiency is much high for MeHg compare to iHg (Wang and Wong, 2003). This specific selectivity of Hg compounds explains the exponential increase of MeHg fractions (and decrease of iHg) with trophic levels observed along food webs (Watras et al., 1998), with 20 and 50% of MeHg accumulated in the phytoplankton and more than 75% in the second trophic level (zooplankton), reaching values close to 90-100% in muscles of predators such as fish.

Physiological factors also determine Hg accumulation since concentrations are known to increase with size, weight and age of the species considered (Hammerschmidt and Fitzgerald,

2006). In general, an increase in Hg concentrations is observed in an individual's tissues during its life span. However Hg exposure strongly depends on foraging strategies (i.e. benthic or pelagic) within a same trophic level. Hg bioaccumulation in aquatic food webs is thus controlled by many parameters, some of them still not verified or completely understood, involving some incertitude about this phenomenon particularly in cases where predators belonging to low-contaminated ecosystems accumulate elevated Hg concentrations (e.g., Carravieri et al., 2017).

The processes of Hg accumulation in the top predators of marine food webs (i.e. large fish, seabirds or marine mammals) appears to be relatively complex due to the developed metabolic strategies face to Hg contamination. Diet represent the main pathway of exposure for these predators, it is absorbed in the intestine and transported by the blood stream towards the main storage tissues (muscle, liver) and target organs (kidney and brain). Specific Hg complexes (with ligands containing thiols, e.g. cysteine, or with Se) appear to regulate the accumulation and elimination in the different organs (Wagemann et al., 1998; Bridges and Zalups, 2010; Kim et al., 1996). Subsequently, Hg can be stored definitely or temporarily, metabolized or remobilized to be eliminated through excreta, skin appendages (nails, claws, feathers, hairs, etc.) and to the offspring (fetuses or eggs) (Thompson et al., 1998b).

MeHg is mainly accumulated in muscles (storage tissue) and also in brain tissue (target organ), associated to the potent neurotoxic effects of MeHg (AMAP 2011). Marine mammals and seabirds can remobilise MeHg stored in the muscles and excrete it through replacement of hair and feathers, which constitutes an effective excretory pathway (Honda et al., 1986; Braune, 1987). During feather moult in birds, Hg is transferred from the internal tissues and organs into the growing feathers, leading to a decrease of Hg concentrations in storage tissues (Furness et al., 1986). Avian Hg dynamics are thus highly influenced by this sequential moult and the rates of excretion, whereas in mammals Hg is excreted by hair or fur continuously with the notable exception of cetaceans. Indeed, baleen and toothed whales, have no fur and are thus deprived of this route of Hg excretion (Dietz et al., 2013). A key detoxification mechanism of Hg is its co-precipitation with Se to form HgSe granules or tiemanite, process that appears to be particularly developed in the case of hairless mammals or in top predators strongly exposed to Hg such as albatrosses (Palmisano et al., 1995; Nakazawa et al., 2011; Arai et al., 2004; Ikemoto et al., 2004; Wagemann et al., 1998). This efficient detoxification process allows to reduce Hg bioavailability and thus its toxicity (Cuvin-Aralar and Furness, 1991).

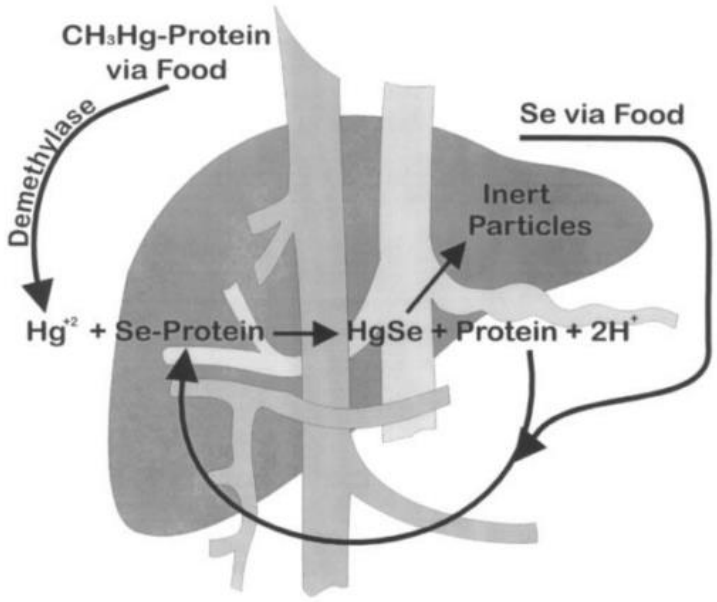

Figure 1.12. Hypothetical demethylation mechanism with consequent formation of inert HgSe granules (tiemanite) in the liver. Figure from Wagemann et al., 1998.

As a consequence of the complexity of Hg dynamics in the organism, MeHg demethylation mechanisms are still relatively poorly understood and it is still not clear if Hg demethylation exclusively takes place in liver or also in other organs and tissues. Due to the high fractions of iHg in livers of marine mammals and seabirds (Kehrig et al., 2015; Wagemann et al., 1998), liver is considered the main organ responsible of MeHg demethylation. However, it is still not completely understood whether the fraction of iHg found in different organs depends on the specific capacity of each organ to demethylate MeHg, or if it is the result of Hg species-specific storage after transport from a key organ. Demethylation of MeHg have been observed in kidney and brain (Dock et al., 1994; Vahter et al., 1995), by anaerobic microbes of the intestinal tract (Clarkson et al., 2007; Dock et al., 1994; Rowland, 1988), red and white blood cells (Berglund et al., 2005; Clarkson, 2002) and hair follicles (Berglund et al., 2005). After *in vivo* demethylation, the produced iHg can be eliminated from the body in faeces or is transported to the kidney and excreted by urine (Smith et al. 1994). Blood, which is responsible of transporting Hg by thiol-conjugate ligands (Bridges and Zalups, 2010; Clarkson et al., 2007), is an equilibrium vector between Hg uptake, tissue storage and remobilisation due to the continuous inter-organ circulation of Hg.

Part 2. Mercury stable isotopes: tracing sources and transformations in the environment

2.1 Introduction to stable isotopic fractionation

An isotope of a given element is an atom whose nucleus has the same number of protons (Z) but a different number of neutrons (N), and thus occupy the same position in the periodic table. Therefore, two isotopes of a same element have a similar atomic number (number of protons in the nucleus), but different mass number (sum of the number of neutrons and the number of protons in the nucleus). Each isotope is then identified by its mass number. Most elements have several natural isotopes which can be stable or unstable (also called radioactive because they can decay into more stable isotopes emitting radiation).

The interest of using stable isotopes started at the mid-20th century (Urey, 1947), where differences in physicochemical behaviour between isotopes of the same element were explained by their mass difference. The first studies on the isotopic fractionation of the elements was focused on light isotopes (C, H, O, N, S) because their relative mass differences ($\Delta m / m$) are higher compared to heavier elements, and consequently the expected fractionation between their isotopes is greater (and easily measured). The isotopic fractionation of these elements has made it possible to investigate numerous geochemical processes and to study paleoclimates. At the end of the 20th century, the development of high-performance analytical devices (MC-ICPMS) allowed to measure with high precision and accuracy the slight variations of isotopic ratios and thus to extend the application of isotopic fractionation studies also to heavier stable isotopes, such as iron (Fe), calcium (Ca), copper (Cu), zinc (Zn), selenium (Se), thallium (Th), lead (Pb) or mercury (Hg).

Hg has seven stable isotopes with the following masses and relative abundances: ^{196}Hg (0.15%); ^{198}Hg (9.97%); ^{199}Hg (16.87%); ^{200}Hg (23.10%); ^{201}Hg (13.18%); ^{202}Hg (29.86%) and ^{204}Hg (6.87%). During the last decades, In the last decades, the measurement of Hg isotopic fractionation has become an essential tool in identifying sources of Hg and biogeochemical processes within the different compartments of the environment (Blum et al., 2014).

2.2 Hg isotopic fractionation: theories and mechanisms

Isotopic fractionation is defined as the enrichment of one isotope relative to another due to physical or chemical processes. In a chemical reaction, molecules containing lighter isotopes will react more easily than those containing heavy isotopes due to the less dissociation energy of light

isotopes (Hoefs, 1997). Thus, the isotopic fractionation of an element is the distribution of its isotopes between two substances or between two phases of the same substance and can be defined by the alpha fractionation factor (α) which is given by the ratio of two isotopes in one compound A (R_A) divided by the ratio of these same two isotopes in a compound B (R_B), as represented in this equation:

$$\alpha_{A-B} = \frac{R_A}{R_B} = \frac{\frac{isotope1}{isotope2}A}{\frac{isotope1}{isotope2}B}$$

In the case of Hg this equation is defined as:

$$\alpha^{xxx} = \frac{(^{xxx}Hg/^{198}Hg)_A}{(^{xxx}Hg/^{198}Hg)_B}$$

Hg isotopes show mass dependent fractionation and mass independent fractionation depending on the chemical reaction or environmental compartment studied.

2.2.1 Mass dependent fractionation (MDF)

MDF involves an enrichment of products in lighter isotopes whereas heavier isotopes will remain in the reactant during a given process. Hg isotopic signatures are normalized with a reference standard iHg solution (NIST 3133) that is used by the international community to facilitate inter-laboratory comparisons. Isotope composition is reported using delta notation (δ) which is the per mil (‰) deviation with respect to this standard (Bergquist and Blum, 2007).

$$\delta^{xxx} = \left(\frac{\frac{xxx}{198}Hg_{\ sample}}{\frac{xxx}{198}Hg_{\ NIST\ 3133}} - 1 \right) \times 1000 \quad (‰)$$

where xxx is the mass of each Hg isotope between (196, 199, 200, 201, 202, or 204), the isotope 198 is used as the reference isotope since it is the lightest and most abundant isotope (isotope 196 represents only 0.15%). Generally, Hg isotopic studies focus on the 5 most abundant isotopes 198, 199, 200, 201 and 202.

Two main processes induce isotopic fractionation of an element: equilibrium fractionation and kinetic fractionation.

- Equilibrium fractionation

The equilibrium fractionation corresponds to the isotope exchange reactions between two equilibrium substances. This fractionation is induced by the difference of vibrational energy between two isotopes of one element bound to another atom. Heavy isotopes require a greater

vibrational energy than the light ones to be dissociated from a chemical bond, and consequently, they are more stable in a molecule with the strongest chemical bonds.

- Kinetic fractionation

The kinetic isotopic fractionation is involved by the difference in reaction rates between two isotopically distinct molecules. This fractionation is associated with unidirectional and incomplete processes such as evaporation, dissociation, diffusion, oxidation or reduction reactions, as well as during biological transformations (Hoefs, 1997). Since light isotopes have higher translation rates and higher diffusion coefficients, and form weaker bonds that are more easily breakable, they will react faster involving an enrichment of heavy isotopes in the residue of the reaction.

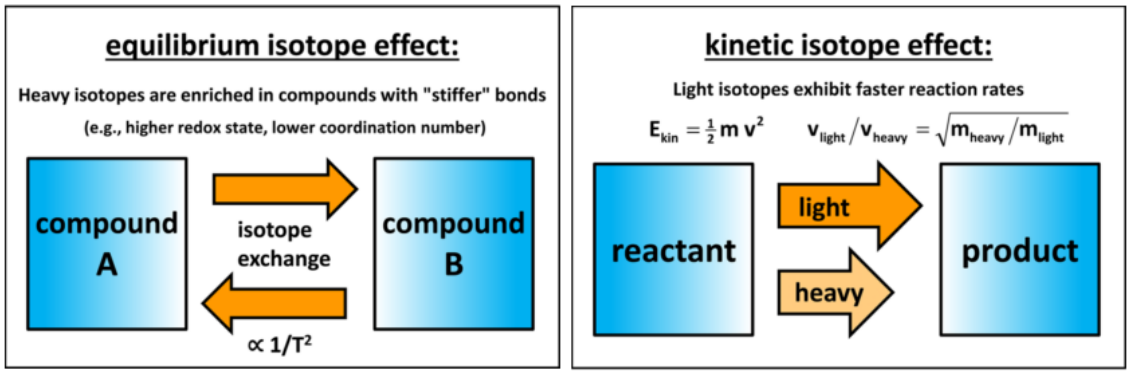

Figure 1.13 Schematic diagram of kinetic and equilibrium stable isotope fractionation. Figure from Wiederhold, 2015.

2.2.2 Mass independent fractionation (MIF)

Hg MIF is reported using Δ which is the deviation of the measured isotope ratio from the theoretical ratio predicted by MDF.

$$\Delta^{xxx}Hg = \delta^{xxx}Hg - (\beta_{xxx} \cdot \delta^{202}Hg)$$

where xxx is the mass of the Hg isotope and βxxx is the kinetic or equilibrium fractionation factor appropriate for each isotope relative to the more abundant isotope (202) and is defined by the following equation, slightly different if considering equilibrium or kinetical fractionation (Young et al., 2002):

$$\beta_{xxx}^{equilibrium} = \frac{\ln\left(\frac{1}{198}\right) - \ln\left(\frac{1}{xxx}\right)}{\ln\left(\frac{1}{198}\right) - \ln\left(\frac{1}{202}\right)}$$

$$\beta_{xxx}^{kinetic} = \frac{\ln\left(\frac{198}{xxx}\right)}{\ln\left(\frac{198}{202}\right)}$$

The differentiation of these two processes (equilibrium vs kinetic) in Hg isotopes would require accurate measurements (in the order of 0.01 ‰) that is rarely observed, and therefore, will not have impact in the measurement of the observed isotopic ratios. Values for factor β were recommended by Bergquist and Blum (Bergquist and Blum 2007) for each Hg isotope:

$$\Delta^{204}Hg = \delta^{204}Hg - (1.493 \cdot \delta^{202}Hg)$$

$$\Delta^{201}Hg = \delta^{201}Hg - (0.752 \cdot \delta^{202}Hg)$$

$$\Delta^{200}Hg = \delta^{200}Hg - (0.502 \cdot \delta^{202}Hg)$$

$$\Delta^{199}Hg = \delta^{199}Hg - (0.252 \cdot \delta^{202}Hg)$$

Two mass-independent mechanisms are responsible of isotope fractionation: the nuclear field shift effect (NFS) and the magnetic isotope effect (MIE). A third minor mechanism has been recently observed: self-shielding effect (SSE).

- Nuclear field shift effect (NFS)

NFS depends on the nuclear volume and nuclear charge radius (Schauble, 2007). Since the nucleus of isotopes differ on the number of neutrons, they will have different masses and size, however, nuclear volume does not increase linearly. Odd isotopes are often smaller than expected based on linear relationship relative to even isotopes (Figure 1.14). This relative difference in size leads to a higher nuclear charge density so that the electrons will be more strongly linked to the nucleus and consequently, it will influence the ground-state energies of atoms and their efficiency and participation in chemical reactions. If all the isotopes are in the form of elemental Hg, the odd isotopes will form weak covalent bonds and will be more volatile (Bigeleisen, 1996; Schauble, 2007).

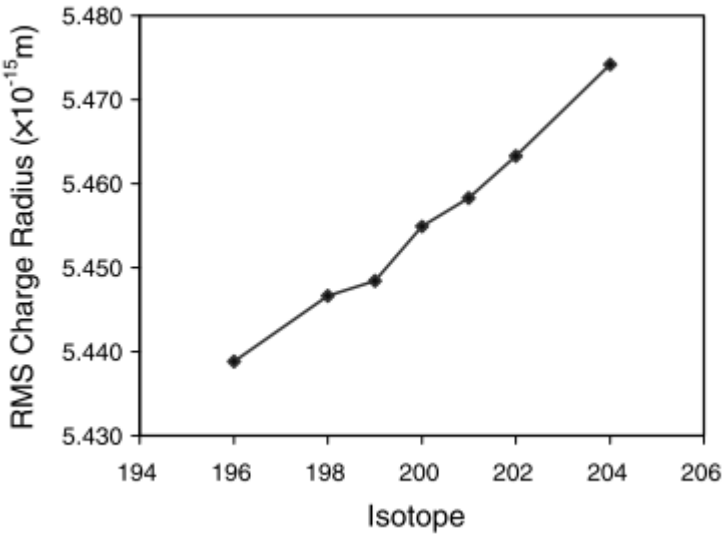

Figure 1.14. Root mean squared charge radii of Hg stable isotopes showing that odd isotopes (^{199}Hg and ^{201}Hg) tend to be smaller than a trend line through even isotopes. Figure from Schauble, 2007.

- Magnetic isotope effect (MIE)

MIE only occurs during kinetic reactions in which reactants absorb the photonic or thermal energy to produce a pair of R radicals, involving spin conversion. Nuclides with an odd number of protons or neutrons are characterized by a non-zero nuclear spin that induces a magnetic moment in the nuclei (isotopes ^{199}Hg and ^{201}Hg present a nuclear +1/2 and +3/2 and a magnetic moment of +0.5029 and -0.5602 μB, respectively). Since radical pairs with magnetic nuclei can undergo spin conversion more rapidly than radical pairs without magnetic nuclei, odd isotopes are more likely to recombine whereas even isotopes are more likely to become products (Buchachenko et al., 2007). MIE is an effect of light exposure and is considered the more probable responsible of the large MIF observed in photochemical reactions (Bergquist and Blum, 2007).

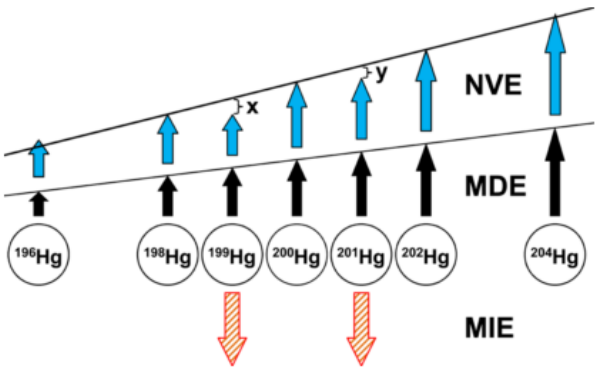

Figure 1.15. Schematic illustration of fractionation mechanisms for Hg isotope system. NVE represents fractionation due to NFS. MDE means mass difference effect. Figure from Wiederhold, 2015.

- Self- shielding effect (SSE)

SSE has been observed in one experimental study compact fluorescent lamps during which they found significant unusual fractionation of even Hg isotopes (Δ^{200}Hg =-10.69‰) (Mead et al., 2013). In these lamps, the light is generated by excitation of vapour Hg^0. Due to different nuclear spin and mass of the seven Hg isotopes, Hg absorption line at 254 nm is divided into distinct lines due to thermal and collisional increase and the specific transfers at each line is not identical and will be related to the isotopic abundance (Mead et al., 2013). Therefore, this mechanism induces an unusual isotopic fractionation that does not change linearly with mass but it favours the photoexcitation of Hg isotopes with low abundance (e.g., ^{196}Hg) rather than those with high abundance (e.g., ^{202}Hg). Since only odd isotopes ^{199}Hg and ^{201}Hg have non-zero nuclear spins and magnetic moments, and the NFS is assumed to generate negligible MIF of the even Hg isotopes (Bergquist and Blum, 2007), SSE is the most possible mechanism creating even-MIF.

MIF of even Hg isotopes had been determined in natural samples mainly related to the atmosphere (Gratz et al., 2010; Sherman et al., 2012b; Chen et al., 2012; Demers et al., 2013; Rolison et al., 2013; Štrok et al., 2015; Wang et al., 2015; Yuan et al., 2015). Nevertheless, the different conditions existing in nature (low concentration of Hg^0 in the atmosphere and the different spectrum of sunlight) indicate that SSE mechanisms must not be representative in nature and therefore, more information is needed to confirm the appropriate cause of even-MIF in the environment.

2.3 Experimental determination of Hg isotopic fractionation

2.3.1 Processes inducing MDF and MIF of Hg

In the last decades, the measurement of Hg isotopic MDF and MIF has become an essential tool in identifying sources of Hg and biogeochemical processes within the different compartments of the environment. The area of research on Hg isotopes in the environment is continuously growing and is permitting to better elucidate fractionation mechanisms and to apply Hg isotopes as useful tracers of Hg sources and pathways in the environment. Also, numerous experimental studies have been carried out to provide a basic outline for better understanding of Hg isotopic fractionation mechanisms during biotic and abiotic processes.

Briefly, all chemical reactions have been documented to induce Hg MDF, which is known to affect all Hg isotopes during equilibrium or chemical reactions. MDF reactions follow the conventional kinetic fractionation law and favour the reduction of light isotopes leaving a residual pool of Hg enriched in heavy isotopes. Biotic and dark abiotic reactions do not produce significant MIF. Only photochemical reactions have been established to involve the production of large MIF

(Bergquist and Blum, 2007; Estrade et al., 2009) and are consequently of primary importance in the field of Hg isotopes.

Since Hg isotopic fractionation (especially MDF) can be caused by such numerous processes, the discrimination of Hg processes involved in the fate of Hg from its emission to its accumulation in the environment remains a great challenge. In order to better determine these processes, several studies focused on the characterization of the magnitude of isotopic fractionation in kinetic or equilibrium reactions during physical, chemical and biological processes. The measurement of fractionation factors is based in a Rayleigh-distillation system in which the product of a kinetic or equilibrium process will be enriched in lighter isotopes compared to the remaining fraction. In the case of Hg, the fractionation factors are usually reported as $\alpha^{198/202}$ corresponding to the variation in the isotope ratio 202/198 ($^{202}\Delta Hg_{\text{ product-reactant}}$). For the anomalous fractionation of the isotope ratio 199/198 the fractionation is reported as $^{(\Delta 199Hg)}\Delta Hg_{\text{ product-reactant.}}$

The first experimental study about Hg isotopic fractionation demonstrated that iHg photoreduction and MeHg photodemethylation induced at the same time Hg MDF and MIF in aquatic systems (Bergquist and Blum, 2007). These authors confirmed that only Hg odd isotopes (199 and 201) showed a significant MIF signature (Δ^{199}Hg and Δ^{201}Hg), whereas even isotopes followed a MDF law. A latter study about iHg photoreduction in natural waters confirmed both types of fractionation between Hg^0 product and the remaining iHg (Zheng and Hintelmann, 2009a). Since only odd isotopes present a non-zero nuclear spin and a nuclear magnetic moment that can interact with the magnetic moments of electrons, some authors proposed that MIF on odd isotopes was caused by the isotopic MIE (Malinovsky et al., 2010). However, the NFS appears to be more pronounced for the isotope 199 than for the isotope 201 and thus occurs mainly during equilibrium processes (Schauble, 2007).

Significant MDF of Hg isotopes has been shown to be produced during microbial reduction of iHg and microbial demethylation of MeHg (Kritee et al. 2007; Kritee et al., 2009) as well as methylation of iHg by SRB (Rodriguez Gonzalez et al., 2009). Hg isotopic fractionation induced by microorganisms was first investigated during biological reduction in Hg-resistant bacteria containing the enzyme merA, which involved a $\alpha^{198/202}$ ranging from 1.0013 to 1.0020, meaning an enrichment of δ^{202}Hg between -1.3 and -2.0‰ (Kritee et al., 2007). One year later, Kritee et al., (2008) measured isotopic fractionation during reduction by two Hg-resistant strains and a Hg-sensitive strain without the enzyme merA and obtained in both cases similar results as their previous study ($\alpha^{202/198}$ =1.0016±0.0004). Kritee et al., (2009) measured a lower MDF for degradation of MeHg to Hg^0 ($\alpha^{202/198}$ =1.0004±0.0002). On the contrary, no MIF is induced during these processes, which is coherent with the absence of MIE in biological transformations. MDF in reactions mediated by bacteria was demonstrated to be dependent of both cell-specific

physiological factors (e.g., enzyme catalysis rate, gene expression, cell transport) and external environmental factors determining Hg bioavailability (Kritee et al., 2009). Hg isotopic fractionation during bacterial methylation under dark conditions and in anoxia indicated a higher extent of the MDF was than biotic or abiotic reduction reactions ($\alpha^{202/198}$ = 1.0026 ± 0.0004) (Rodriguez-Gonzalez et al., 2009). Under these conditions, since some methylator bacterial strains are also able to demethylate (Bridou et al., 2011), the simultaneous bacterial demethylation may affect the Hg kinetic fractionation effect of the methylation, since the iHg in the medium would constitute a mixed pool of residual isotopically heavier iHg from methylation and isotopically lighter iHg from demethylation (Rodriguez Gonzalez et al. 2009). Indeed, the impact in Hg isotopic compositions of the bacterial demethylation process was demonstrated in SRB cultures (Perrot et al., 2015), in which a steady-state between iHg and MeHg isotopic composition was observed after 24h of experiment. During microbial demethylation, the lighter Hg isotopes of the MeHg molecules are preferentially transformed and have been found to influence the Hg species isotope composition when significant amounts of MeHg are accumulated (Pedrero et al., 2012a). It has also been demonstrated that a lower MeHg bacterial production yield is obtained under sulphate respiration comparing to fumarate conditions because of the formation of insoluble Hg sulphide complexes which reduce the bioavailability of iHg for the cells (Benoit et al., 2001; Gilmour et al., 2011). Perrot et al., (2015) investigated Hg isotopic fractionation during bacterial methylation under sulphate and fumarate respiration conditions, reporting similar "apparent" kinetic fractionation factors. The authors referred to the term "apparent" fractionation because methylation and demethylation were occurring simultaneously so that the product of the reaction (MeHg) would be converted back to the product of the reaction, leading to uncertainty in the modelled fractionation factor.

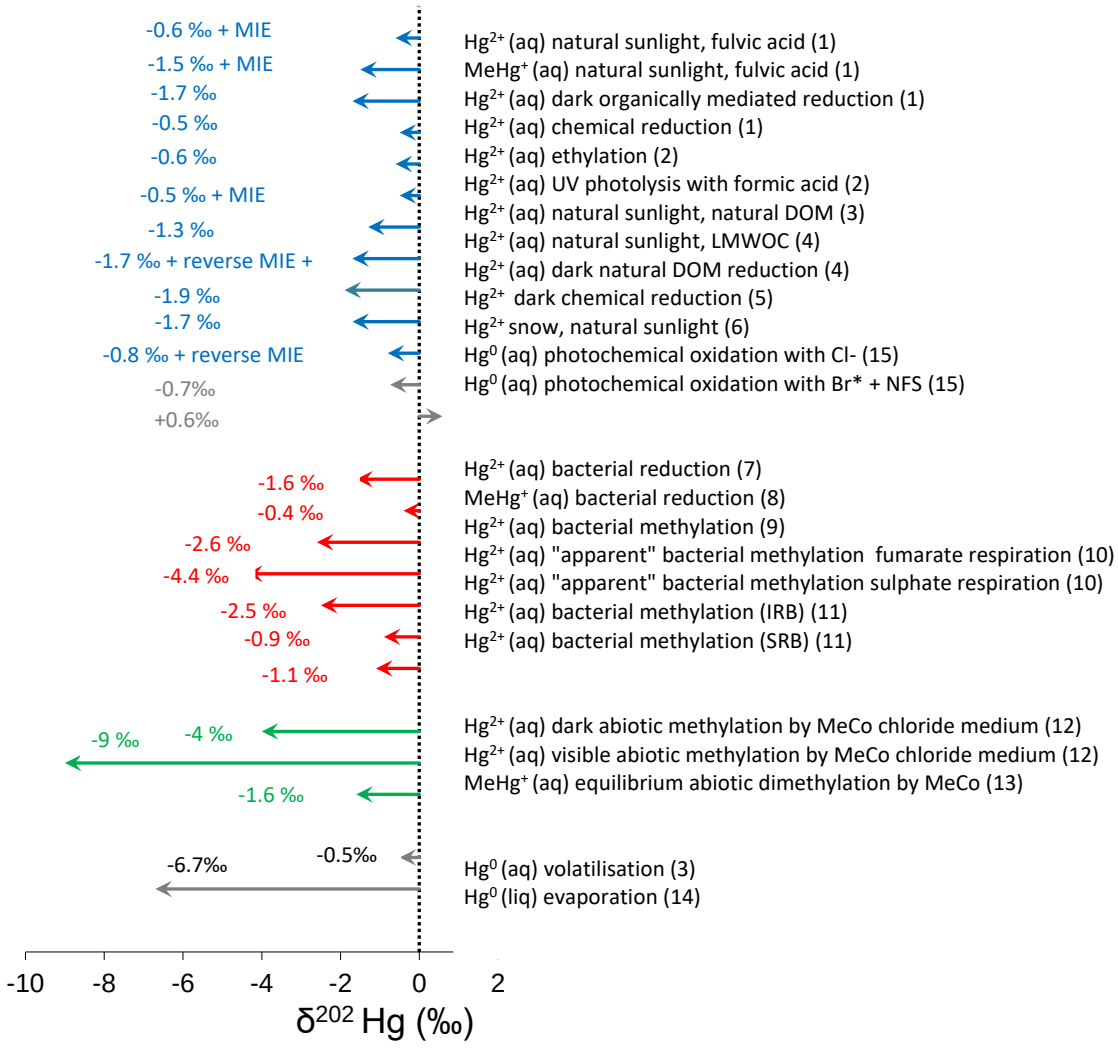

Figure 1.16. Variation of amplitude of the isotopic fractionation factor in the isotope ratio 202/198 ($^{202}\Delta Hg_{\ product\text{-}reactant}$) measured in experimental studies for kinetic and equilibrium reactions. References correspond to (1) Bergquist and Blum, 2007, (2) Yang and Sturgeon, 2009 (3) Zheng et al., 2007, (4) Zheng and Hintelmann, 2010a, (5) Zheng and Hintelmann, 2010b, (6) Sherman et al., 2010, (7) Kritee et al., 2007, (8) Kritee et al., 2009 (9) Rodriguez Gonzalez et al., 2009, (10) Perrot et al., 2015, (11) Janssen et al., 2016, (12) Perrot et al., 2013, (13) Jiménez-Moreno et al., 2013, (14) Estrade et al., 2009, (15) Sun et al., 2016. In the case where MIF has been demonstrated, the MIE or NFS type is reported. Updated from Bergquist and Blum, 2009.

MDF has also been identified during experimental abiotic methylation of iHg by MeCo with slightly lower amplitude ($\alpha^{202/198}$ ranging from 1.0005 to 1.0015) (Malinovsky and Vanhaecke, 2011). During kinetic experiments with MeCo with the presence of chloride, a decrease of the methylation extent was observed especially significant under visible light conditions due to the enhancement of MeHg photodemethylation (Jiménez-Moreno et al., 2013). However, these experiments did not produce MIF, probably due to the complexation by chloride and/or the lack of higher energy UV radiation.

2.3.2 Determination of $\Delta^{199}Hg/\Delta^{201}Hg$ ratio for identifying photochemical processes

MIF signatures can provide supplementary information on Hg sources and biogeochemical cycle. For samples that display $\Delta^{199}Hg$ values greater than ±0.30‰, it is useful to consider $\Delta^{199}Hg/\Delta^{201}Hg$ ratios (Blum et al., 2014) because Hg pathways have the particularity to lead to a different $\Delta^{199}Hg/\Delta^{201}Hg$ ratio, that is therefore used as indicator of MIF mechanisms. Experimental studies on aqueous solutions with DOC demonstrated that photochemical reduction of iHg into Hg^0 resulted in a $\Delta^{199}Hg/\Delta^{201}Hg$ ratio of 1.02±0.02 (Bergquist and Blum, 2007). A similar ratio was later obtained in Arctic snow samples during iHg photoreduction (Sherman et al., 2010). Photochemical demethylation of MeHg displayed a $\Delta^{199}Hg/\Delta^{201}Hg$ ratio of 1.36±0.03 (Bergquist and Blum, 2007). Malinovsky et al., (2010) reported a lower ratio (1.28±0.03) during experimental MeHg photodemethylation under UV-C radiation. Recently, other studies have focused in the influence of the type of solar radiation and DOC ligands in MeHg photodemethylation processes in aquatic systems. Chandan et al., (2015) documented variable $\Delta^{199}Hg/\Delta^{201}Hg$ ratios for MeHg photodemethylation under different types and concentrations of DOC (with different content of reduced sulphur). Under low MeHg/S-red-DOC ratios $\Delta^{199}Hg/\Delta^{201}Hg$ slopes were consistent and less variable (1.38±0.02); whereas high MeHg/S-red-DOC ratios presented lower slopes varying from 1.17±0.04 to 1.30±0.02. Rose et al., (2015) investigated the effect of solar radiation (different intensities and frequencies) on Hg MIF during MeHg aquatic photodemethylation and obtained a ratio similar to Bergquist and Blum (2007).

MIF slopes have also been determined during equilibrium and dark processes thus corresponding to NFS. Dark iHg reduction exhibited a $\Delta^{199}Hg/\Delta^{201}Hg$ ratio near to 1.6 in presence of DOC and $SnCl_2$ (Zheng and Hintelmann 2010b), similar to equilibrium fractionation between dissolved iHg and thiol-binding Hg (Wiederhold et al., 2010) and during liquid Hg^0 evaporation (Estrade et al., 2009; Ghosh et al., 2013).

Table 1.2. . $\Delta^{199}Hg/\Delta^{201}Hg$ slopes calculated during experimental or environmental processes.

Reference	Process	Conditions	Slope $\Delta^{199}Hg/\Delta^{201}Hg$
Bergquist and Blum, 2007	Aqueous MeHg photodemethylation	Natural sunlight, high Hg/DOC ratio	1.36±0.03
Malivnosky et al., 2010	Aqueous MeHg photodemethylation	UVC radiation, alkaline and acid solutions	1.28±0.03
Chandan et al., 2015	Aqueous MeHg photodemethylation	Artificial light, low MeHg/DOC ratio	1.38±0.02
Chandan et al., 2015	Aqueous MeHg photodemethylation	Artificial light, high MeHg/DOC ratio	1.17±0.04 to 1.30±0.02
Rose et al., 2015	Aqueous MeHg photodemethylation	UVA and UVB radiation	1.35±0.16
Bergquist and Blum, 2007	Aqueous iHg photoreduction	Natural sunlight, high Hg/DOC ratio	1.02±0.02
Zheng and Hintelmann, 2009	Aqueous iHg photoreduction	Increasing Hg/DOC ratios	1.19±0.01 to 1.31±0.07
Sherman et al., 2010	iHg photoreduction from snow	Natural sunlight, snow	1.07±0.04
Sun et al., 2016	Hg^0 photoxidation (NFS)	Presence of Br-	1.64±0.30
Sun et al., 2017	Hg^0 photoxidation	Presence of Cl-	1.89±0.18
Zheng and Hintelmann, 2009	Dark iHg reduction (NFS)	Presence of DOC	1.53±0.17/ 1.54±0.06
Zheng and Hintelmann, 2010b	Dark iHg reduction (NFS)	Presence of $SnCl_2$	1.59±0.11 / 1.62±0.08
Wiederhold et al., 2010	Equilibrium fractionation (NFS)	Dissolved iHg-thiol binding	1.54±0.22
Estrade et al., 2009	Evaporation liquid Hg^0		2.00±0.60
Ghosh et al., 2013	Evaporation liquid Hg^0		1.59±0.05

2.3.3 Determination of $\Delta^{199}Hg/\delta^{202}Hg$ ratio in experimental processes

A useful parameter used for determining sources and processes in environmental samples is the $\Delta^{199}Hg/\delta^{202}Hg$ ratio. Photochemical reduction of iHg from an aqueous solution in the presence of DOC has been observed to produce a $\Delta^{199}Hg/\delta^{202}Hg$ slope of 1.15 ± 0.07 (Bergquist and Blum, 2007) whereas photochemical reduction of MeHg into Hg^0 induced a $\Delta^{199}Hg / \delta^{202}Hg$ ratio of 2.43 ± 0.10 (Bergquist and Blum, 2007). Other photochemical reactions such as iHg reduction from snow crystals (Sherman et al., 2010) and artificial light–induced iHg reduction via thiol ligands (Zheng and Hintelmann 2010b) have also reported significant MIF, which is mainly attributed to the MIE. Contrastingly, equilibrium evaporation with liquid Hg^0 is fractionated to a small extent (MIF due to the NFS) and presented a $\Delta^{199}Hg/\delta^{202}Hg$ slope of ~0.1 (Estrade et al., 2009; Ghosh et al., 2013). Non-photochemical abiotic reductions can be easily distinguished from photochemical reductions because without MIE they generate a significantly lower MIF (Zheng and Hintelmann 2010b). Also, photochemical reduction of Hg is often accompanied by a

concurrent non-photochemical reduction (Zheng and Hintelmann 2010b). Therefore, all photochemical reactions that have been studied produce changes in both MDF and MIF and their ratio of Δ^{199}Hg to δ^{202}Hg appears to be indicative of the type of reaction. An overview of the some of the fractionation slopes (Δ^{199}Hg vs δ^{202}Hg) that have been observed experimentally is presented in Figure 1.17.

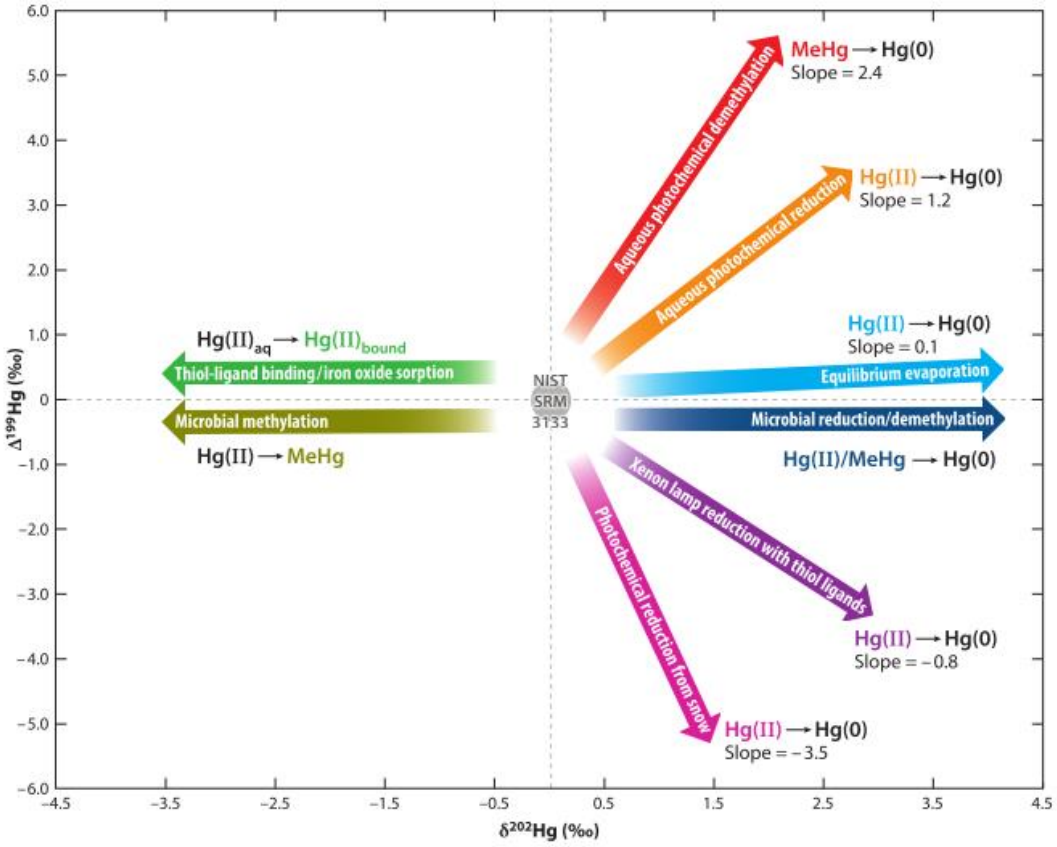

Figure 1.17. Summary of Δ^{199}Hg vs δ^{202}Hg slopes of Hg isotopic fractionation observed in experimental studies. References: Bergquist and Blum, 2007, Zheng et al., 2007, Zheng and Hintelmann, 2010b, Sherman et al., 2010, Kritee et al., 2007, Kritee et al., 2009, Rodriguez Gonzalez et al., 2009, Estrade et al., 2009, Jiskra et al., 2012, Wiederhold et al., 2010, Ghosh et al., 2013. In the case where MIF has been demonstrated, the MIE or NFS type is reported. Figure from the review of Blum et al., 2014.

The approach of experimental studies is very helpful to estimate the different reactions originating Hg isotopic fractionation in nature. The degree of fractionation (δ^{202}Hg, Δ^{199}Hg) as well as certain parameters such as the Δ^{199}Hg/Δ^{201}Hg and Δ^{199}Hg/δ^{202}Hg ratios observed in the different environmental samples are diagnostic of the sources and undergone reactions since the initial Hg isotopic signature is later modified by intermediate reactions inducing Hg isotopic fractionation.

2.4 Hg isotopic composition in environmental studies

2.4.1 Variation of Hg isotopic composition in environmental samples

Hg isotopic fractionation enables the characterisation of different processes but also the determination of Hg sources and mechanisms in the environment. However, Hg isotopic variations occurring in natural samples result from multiple transformations and strongly depend on environmental conditions, thus it is very probable that they are slightly modified from modelled experimental studies. A total δ^{202}Hg variation of 10 ‰ was observed in nature so far, varying from -4.5 ‰ to +3.4 ‰ (Blum et al., 2014). The variationsin Δ^{199}Hg values was greater and ranged from -5 ‰ to +6.5‰.

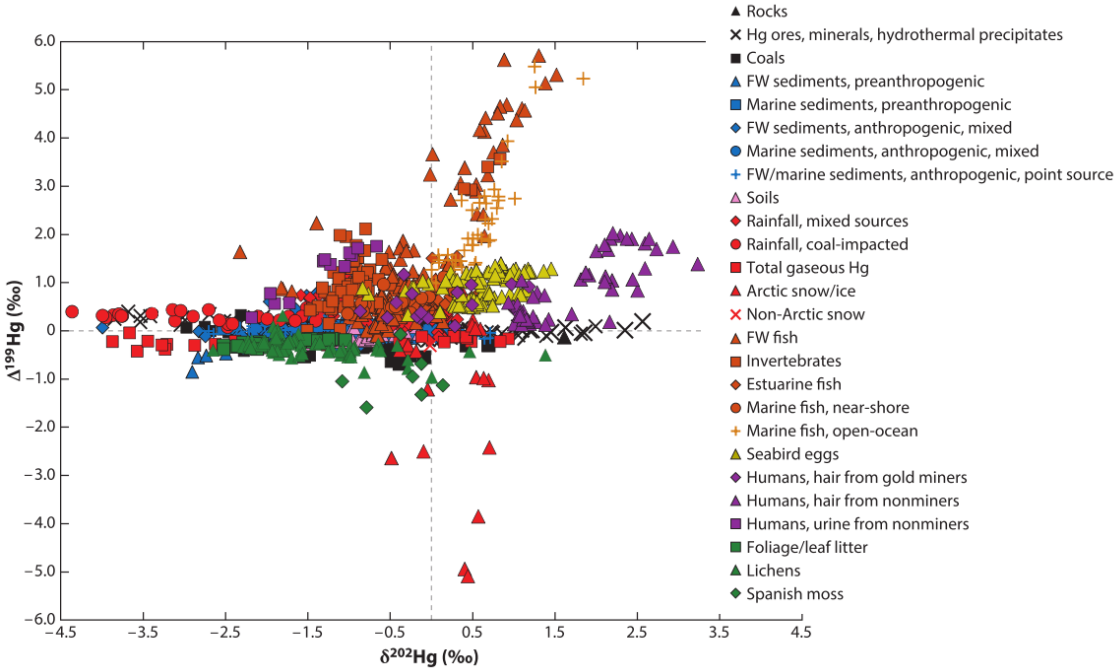

Figure 1.18. Compilation of MDF (δ^{202}Hg) and MIF (Δ^{199}Hg) values reported in several natural and environmental samples in literature. Figure from Blum et al., 2014.

Environmental samples such as soils, snow, lichens and peat bogs have been found to be good Hg tracers of natural and anthropogenic inputs since they incorporate atmospheric Hg deposition (Estrade et a 2011; Sherman et al., 2010; Estrade et al., 2010; Enrico et al., 2016). One characteristic of these samples is their generally negative MIF values that seem to represent the signature of Hg^0 evaporated to the atmosphere after photoreduction in aquatic systems (Bergquist and Blum, 2009; Estrade et al., 2009; Sherman et al., 2010). A preferential sequestration of isotopically light iHg (lower δ^{202}Hg) has been demonstrated when binding to mineral phases and organic matter, leading to a residual pool of heavier isotopes in soils and sediments (Jiskra et al.,

2012; Wiederhold et al., 2010). In natural organic matter, Hg dominantly bounds to reduced sulphur groups (thiols, -SH) (Skyllberg et al., 2006) as a result of their exceptionally high affinity for Hg.

Hg isotopic compositions in precipitation and gaseous Hg over North America great lakes first reported an enrichment in heavier isotopes the vapour phase compared to precipitation, while Δ^{199}Hg values were positive in precipitation and negative in the vapour phase (Gratz et al., 2010). In addition, these authors first documented even isotope anomalies (reported as Δ^{200}Hg) of up to 0.25‰ in atmospheric precipitation samples over North America. Later, Chen et al., (2012) confirmed the occurrence of significant even-MIF by determination of Δ^{200}Hg up to 1.2‰ in rain and snowfall samples in Canada, also observing seasonal variation of Δ^{200}Hg, with greater values in winter than in summer. Since then, numerous studies have observed even-MIF in atmospheric samples and therefore, it is thought to be associated to mechanisms occurring in the atmosphere, such as photo-oxidation in the tropopause and/or neutron capture in space (Gratz et al., 2010; Sherman et al., 2012b; Chen et al., 2012; Demers et al., 2013; Rolison et al., 2013; Štrok et al., 2015; Wang et al., 2015; Yuan et al., 2015). However, the exact process inducing significant even Hg isotopes-MIF remains still unclear and the understanding of even-MIF could provide useful information about the biogeochemical cycle of Hg, mainly about atmospheric processes, such as air-surface exchanges, and the influence of climate changes (Cai and Chen, 2015).

Due to the complex Hg cycle in aquatic systems, characterized by numerous biogeochemical transformations, numerous studies have focused on Hg isotopic composition of aquatic organisms to help elucidating Hg pathways in these ecosystems (e.g. Bergquist and Blum, 2007; Laffont et al., 2009; Senn et al., 2010; Perrot et al., 2012; Blum et al., 2013; Das et al., 2013). Most of these studies have reported significantly positive Δ^{199}Hg values in organisms, while δ^{202}Hg values exhibited a wide range of negative and positive values. Since Hg MIF isotopic signatures are preserved during *in vivo* processes, aquatic organisms (mainly fish) have been used to provide valuable information about MeHg bioaccumulation and its degree of degradation before it is incorporated into food webs (Bergquist and Blum, 2009).

2.4.2 Tracking Hg sources and processes in freshwater and marine ecosystems

Hg isotopic signatures have been widely applied for studying biogeochemical processes in different aquatic compartments; such as lakes (Gantner et al., 2009; Perrot et al., 2012; Sherman et al., 2013), rivers (Tsui et al., 2012) or oceans (Senn et al., 2010; Point et al., 2011; Gehrke et al., 2011; Blum et al., 2013). Fish have been usually applied for investigation of Hg sources and exposure pathways to the food web. Variations in Hg isotopic signatures between oceanic and

coastal compartments have been attributed to both different sources and Hg cycles in the two reservoirs (Gantner et al., 2009; Senn et al., 2010; Point et al., 2011; Gehrke et al., 2011; Blum et al., 2013). Although marine organisms characteristically exhibit positive δ^{202}Hg values (Senn et al., 2010; Point et al. 2011), geologic samples such as sediments or rocks typically report negative δ^{202}Hg and close-to-zero Δ^{199}Hg values (Smith et al., 2008; Feng et al., 2010; Gehrke et al., 2011; Donovan et al., 2013; Mil-Homens et al., 2013; Sherman et al, 2013; Yin et al., 2015). Some studies also revealed that coastal organisms are influenced by continental inputs and thus reflect Hg coming from a recent geological source (δ^{202}Hg values~0‰) (Senn et al. 2010; Day et al., 2012; Perrot et al., 2010). A compilation of Hg isotopic composition in pelagic and coastal fish, as well as other organisms (whales, birds) of other aquatic compartments (large lakes, estuaries), is illustrated in Figure 1.19.

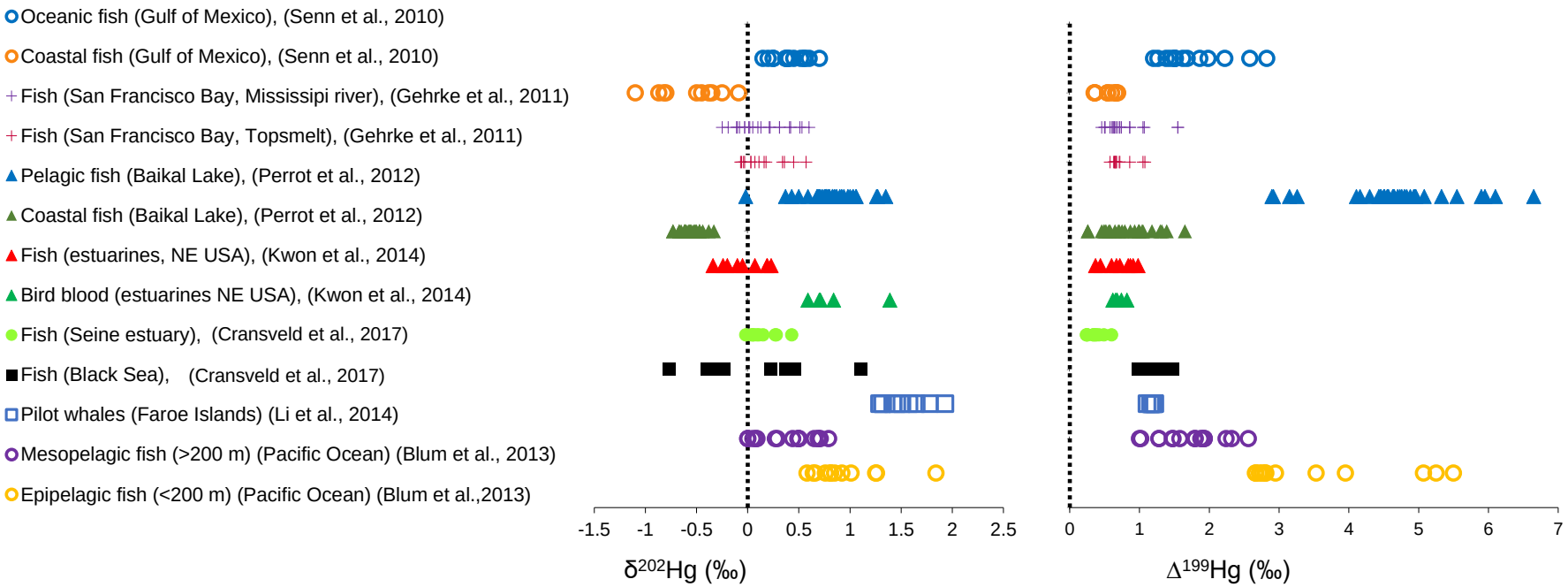

Figure 1.19. Compilation of Hg isotopic composition ($\delta^{202}Hg$, $\Delta^{199}Hg$) in marine and freshwater organisms (fish, whales and bird blood) in literature.

By way of example, one study in fish from the Gulf of Mexico depicted clear Hg isotopic differences between coastal and oceanic species, which was associated to distinct sources of MeHg since coastal species were highly influenced by Hg input from the Mississippi river (Senn et al., 2010). Differences in Hg isotopic signatures between coastal and oceanic fish were in the order of ~0.8‰ for δ^{202}Hg and ~1‰ for Δ^{201}Hg values visibly indicating different sources of MeHg and different photodemethylation extent between the two reservoirs. Another study in Lake Baikal (Russia) revealed much higher Δ^{199}Hg values in the pelagic food web (3.15−6.65‰) in comparison to coastal fish (0.26−1.65‰), allowing then to discriminate between the coastal and pelagic sources and cycling of MeHg (Perrot et al., 2012, Figure 1.20)

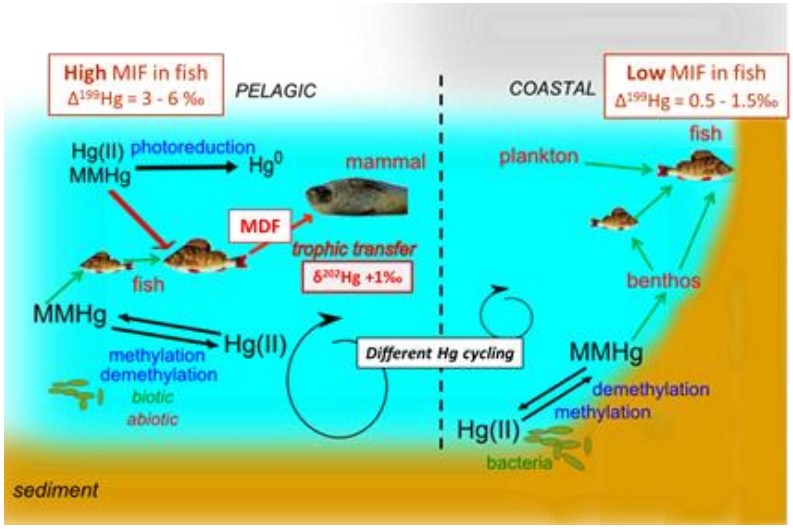

Figure 1.20. Schematic design of Hg isotopic results in the food web (amphipods, phytoplankton, zooplankton, fish and seals) of Lake Baikal (Russia) revealing the existence of different Hg cycling between coastal and pelagic food webs (Perrot et al., 2012).

Likewise, studies on seabirds have also demonstrated the efficiency of Hg isotopic analyses in avian eggs for investigation and identification of different Hg sources between coastal and oceanic environments in the Arctic (Day et al., 2012). It has been assumed that the oceanic MeHg is submitted to a substantial degree of photochemical processes, hence oceanic organisms present more positive MIF (Δ^{199}Hg and Δ^{201}Hg). In the contrary, coastal organisms reflect an Hg coming from contribution of benthic sources and have undergone more limited extent of photochemical reactions, then display lower MIF values.

Other studies have focused in the gradient of δ^{202}Hg, Δ^{199}Hg and Δ^{201}Hg values for depicting MeHg sources and pathways in the open ocean. One study demonstrated the relationship between Hg MIF values (Δ^{199}Hg and Δ^{201}Hg) and foraging depth of fish foraging in the Pacific Ocean (Blum et al., 2013), due to a higher extent of photochemical reactions in the surface layer. These authors evidenced the occurrence of microbial methylation in the pycnocline that produces

additional MeHg without MIF, and thus dilutes the MIF of MeHg exported from the surface mixed layer (Blum et al., 2013).

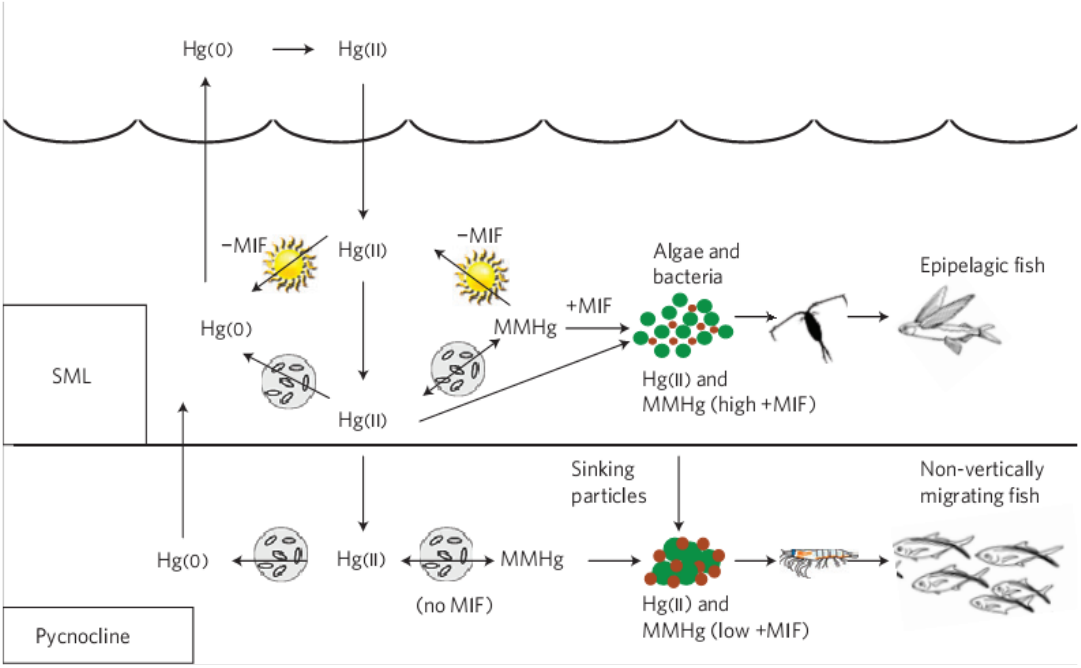

Figure 1.21. Schematic representation of a simplified model for Hg cycling between atmosphere, surface mixed layer, pycnocline and marine food web (figure from Blum et al., 2013).

In polar marine ecosystems, two studies have revealed the influence of ice cover on Hg marine photochemistry by the investigation of Hg isotopic signatures of seabird eggs (Point et al., 2011) and seal livers (Masbou et al., 2015) over a latitudinal gradient in different regions of the Gulf of Alaska. These studies observed a decrease of MIF signatures with the effect of the sea ice cover, which prevents light penetration and thus inhibit photochemical reactions. These authors estimated that the disappearance of ice cover in the Arctic Ocean as a result of global warming would therefore intensify the evasion of MeHg to the atmosphere via photodemethylation.

The biogeochemical cycle of Hg in polar ecosystems is mainly controlled by interactions between the atmospheric and oceanic compartments. AMDEs have been assumed to constitute a substantial pathway of Hg input in the polar marine environment and several studies have explored the mechanisms associated to the oxidation of Hg^0 during these processes (e.g, Ariya et al., 2002; Lindberg et al., 2002). Substantial negative MIF has been observed in Arctic snow after deposition of iHg by AMDEs ($\Delta^{199}Hg < -1.2‰$), meaning that Hg is depleted in odd Hg isotopes during halogen oxidation (Sherman et al., 2010). $\Delta^{199}Hg/\Delta^{201}Hg$ ratios observed for air-snow and snow-frost flowers were, respectively, 1.07± 0.04‰ (Sherman et al., 2010) and 1.26±0.10‰

(Sherman et al., 2012b). Since there is well-supported evidence that AMDEs are related to bromine and chlorine radicals (Barrie et al., 1988; Mao et al., 2010), being Br and BrO the dominant oxidizers (Stephens et al., 2012), Hg isotope fractionation during gas-phase oxidation of Hg^0 by Cl and Br atoms were studied to better recognise the initiation of these processes occurring in polar regions (Sun et al., 2016). Nevertheless, a recent study demonstrated that direct Hg^0 deposition was the dominant source to the Arctic tundra (70%), which is enhanced during summertime, meanwhile AMDEs represent a minor contribution to Hg input (Obrist et al., 2017).

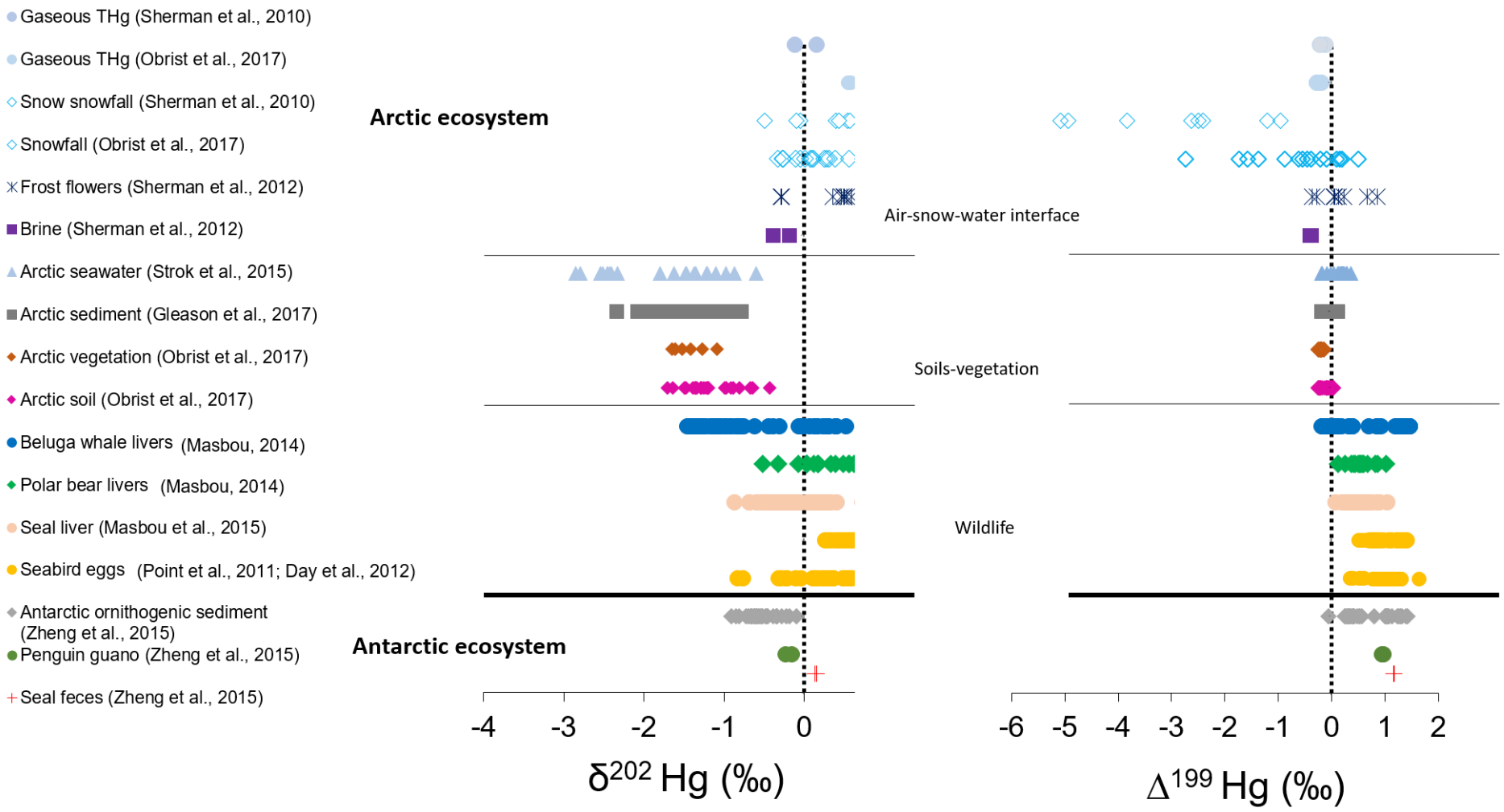

Figure 1.22. Hg isotopic composition in environmental samples from Polar Regions (Arctic and Antarctic) from literature.

As observed in Figure 1.22, Hg isotopic studies in the Antarctic Polar Regions are still scarce comparing to Arctic environments. To date, Hg isotopic signatures have only been measured measured in ornithogenic sediments in the coastal Antarctica (Ross Sea) and in fresh seal and penguin feces (Zheng et al., 2015). This study explored Hg isotopic composition in historical and modern biological deposits in order to trace temporal trends in Hg sources and cycling in the Antarctic Ocean and to discern different bioaccumulation pathways in Antarctic marine biota. Sediment cores were collected from the top to 38 cm depth permitting to assess Hg contamination sources between the present time and around the year 1280 AD. Regarding the trends observed for the more ancient deep layers, seal and penguin excrements were considered the major contributor of Hg inputs into the sediment respectively for the first period (1280-1400 AD) and for the second period (1400-1650 AD), coherent with the increase of penguin population during from that period. During 1650-1990 AD, penguin guano continued to be considered the major source of Hg inputs into the sediment (36-75%), but a lower $\Delta^{199}Hg/\Delta^{201}Hg$ slope observed in this period (1.20±0.04) relative to the precedent period (1.34±0.05) was interpreted as substantial inputs deriving also from bedrock sediment and atmospheric Hg deposition that would explain the dilution in $\Delta^{199}Hg$ signatures. The most top layer, corresponding to 1990 to the present time, recorded higher Hg concentrations and lower $\delta^{202}Hg$ and $\Delta^{199}Hg$ signatures, which was attributed to enhanced atmospheric Hg input due to increasing anthropogenic emissions, also sequestered by terrestrial vegetation or algae in the surface.

2.4.3 $\Delta^{199}Hg/\Delta^{201}Hg$ ratios in aquatic systems

As previously said, it is important to consider that experimental values often represent an approximation of more complex processes in nature. Moreover, the ligands associated with Hg in aqueous solutions (such as organic matter, dissolved cations and halogens in seawater) lead to a slight differences in $\Delta^{199}Hg/\Delta^{201}Hg$ ratios and therefore, the theoretical slopes obtained in laboratory medium are only approximate for interpretation of environmental samples of natural freshwater and marine ecosystems.

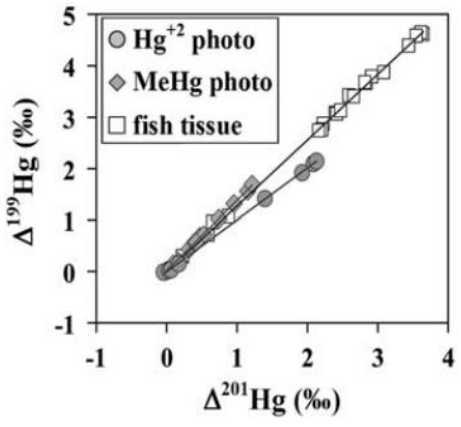

Figure 1.23. $\Delta^{201}Hg$ versus $\Delta^{199}Hg$ for the photochemical reduction experiments and fish tissue samples from the Lake Michigan (Bergquist and Blum 2007).

As observed in Figure 1.23, fish from Lake Michigan presented a $\Delta^{199}Hg/\Delta^{201}Hg$ ratio of 1.28±0.03, corresponding to the accumulation of residual MeHg that has previously undergone photochemical demethylation (Bergquist and Blum, 2007). This is coherent with the predominance of MeHg in fish (~95%) and makes possible to estimate the rate of photodemethylation in the water column of a given ecosystem (Bergquist and Blum, 2007). Latter studies in freshwater fish also reported similar $\Delta^{199}Hg/\Delta^{201}Hg$ ratios close to 1.3 (Laffont et al., 2009; Gantner et al., 2009; Sherman et al., 2013a). However, Hg isotopic studies in marine fish (and seabirds that feed on marine fish) have documented slightly lower $\Delta^{199}Hg/\Delta^{201}Hg$ ratios. For example, fish from the Gulf of Mexico and from the Pacific Ocean exhibited respective $\Delta^{199}Hg/\Delta^{201}Hg$ slopes of 1.20±0.07 (Senn et al., 2010) and 1.20±0.01 (Blum et al. 2013). Hg isotopic studies in seabird eggs from Alaska reported $\Delta^{199}Hg/\Delta^{201}Hg$ slopes of 1.26±0.06 (Point et al., 2011) and 1.09±0.04 (Day et al., 2012).

Although all the MIF slopes compiled in fish derive from MeHg photochemical degradation in both freshwater and marine systems, lower $\Delta^{199}Hg/\Delta^{201}Hg$ can be the consequence of differences in organic matter or the influence of dissolved cations and halogens present in seawater. Moreover, freshwater ecosystems can be impacted by iHg inputs from riverine inputs whereas in opened marine areas Hg atmospheric deposition is considered the main source (Mason et al., 2012)

Table 1.3. Compilation of Hg isotopic composition ($\delta^{202}Hg$, $\Delta^{199}Hg$, $\Delta^{201}Hg$) and $\Delta^{199}Hg/\Delta^{201}Hg$ slopes reported in aquatic/marine biota from the literature.

Study	Sample	Location	n		δ^{202}Hg (‰)	Δ^{201}Hg (‰)	Δ^{199}Hg (‰)	Slope $\Delta^{199}Hg/\Delta^{201}Hg$ (‰)
Freshwater ecosystem								
Bergquist and Blum, 2007	Fish muscle	Michigan Lake (USA)	16	Mean±SD	0.60±0.38	2.79±0.51	3.60±0.65	1.28±0.03
				(min,max)	(-0.29,+1.17)	(+2.16,+3.64)	(+2.73,+4.64)	
Gantner et al, 2009	Fish muscle	Arctic Lakes (Canada)	64	Mean±SD	-0.34±0.78	1.39±0.87	1.83±1.07	1.21±0.13
				(min,max)	(-1.68,+1.28)	(-0.11,+3.89)	(0.0,+4.90)	
Laffont et al., 2009	Fish muscle	Amazon lakes (Bolivia)	20	Mean±SD				1.28±0.12
				(min,max)	(-0.92,-0.40)	(-0.14,+0.38)	(-0.09, +0.55)	
	Hair fish consumers	Amazon lakes (Bolivia)	13	Mean±SD	1.15±0.16	0.12±0.08	0.19±0.06	1.16±0.04
				(min,max)	(+1.04,+1.42)	(+0.25,+0.81)	(+0.15, +0.66)	
Perrot et al, 2010	Fish muscle (perch)	Baikal Lake (Russia)	12	Mean±SD	-0.48±0.14	0.89±0.33	1.14±0.46	1.28±0.05
				(min,max)	(-0.57,-0.33)	(-0.05,+0.08)	(+0.87,+1.39)	
	Fish muscle (roach)	Baikal Lake (Russia)	12	Mean±SD	-0.61±0.14	0.44±0.21	0.58±0.30	1.30±0.05
				(min,max)	(-0.73,-0.47)	(+0.20,+0.59)	(+0.26,+0.79)	
	Fish muscle (perch)	Bratsk Reservoir (Russia)	12	Mean±SD	-0.55±0.45	0.39±0.41	0.52±0.50	1.37±0.10
				(min,max)	(-0.90,-0.16)	(+0.13,+0.79)	(+0.20,+1.04)	
	Fish muscle (roach)	Bratsk Reservoir (Russia)	12	Mean±SD	-0.37±0.30	1.08±0.29	1.28±0.38	1.34±0.04
				(min,max)	(-0.80,-0.22)	(0.30,1.39)	(+0.41,+1.87)	
Sherman et al., 2013	Freshwater fish	Florida Lake (USA)	22	Mean±SD	0.09±0.38		1.35±1.22	1.30±0.01
				(min,max)	(-0.60, 0.68)		(+0.18, +4.43)	
				Mean±SD				1.25±0.03
Li et al., 2016	Freshwater fish	Lake Melville (Canada)	28	(min,max)	(-0.76, +0.15)		(+0.72, 3.14)	
Marine ecosystem								
Senn et al, 2010	Fish muscle	Gulf of Mexico	32	Mean±SD	0.03±0.48	0.93±0.52	1.18±0.62	1.20±0.07
				(min,max)	(-1.10,+0.70)	(+0.24,+2.30)	(+0.35:+2.82)	
Gehrke et al, 2011	Fish muscle	San Francisco Bay	34	Mean±SD	0.15±0.23	0.61±0.20	0.78±0.26	1.26±0.01

				(min,max)	(-0.25,+0.60)	(+0.38,+1.25)	(+0.46,+1.55)	
Blum et al, 2013	Fish muscle	North Pacific Ocean	28	Mean±SD	0.63±0.41	1.95±1.08	2.50±1.19	1.20±0.01
				(min,max)	(+0.00,+1.84)	(+0.16,+4.59)	(+1.00,+5.50)	
Kwon et al, 2014	Fish muscle	Northeastern coast USA	9	Mean±SD	-0.03±0.20	0.58±0.17	0.71±0.20	
				(min,max)	(-0.34,+0.23)	(+0.29,+0.77)	(+0.37,+0.98)	
	Mussel	Northeastern coast USA	7	Mean±SD	0.06±0.36	0.12±0.09	0.38±0.10	
				(min,max)	(-0.31,+0.77)	(+0.02,+0.27)	(+0.21,+0.52)	
	Crab	Northeastern coast USA	6	Mean±SD	-0.11±0.23	0.29±0.27	0.59±0.23	1.22±0.07
				(min,max)	(-0.45,+0.15)	(+0.03,+0.72)	(+0.23,+0.87)	(overall data)
	Bird blood (eider)	Northeastern coast USA	5	Mean±SD	0.85±0.28	0.53±0.07	0.70±0.07	
				(min,max)	(+0.59,+1.39)	(+0.46,+0.63)	(+0.62,+0.82)	
Point et, al 2011	Seabird eggs (murre)	Alaska	43	Mean±SD	0.51±0.55	0.91±0.19	1.05±0.26	1.26±0.06
				(min,max)	(-0.84,+1.45)	(+0.40,+1.12)	(+0.35,+1.63)	
Day et al, 2012	Seabird eggs (murre)	Alaska	45	Mean±SD	0.69±0.25	0.72±0.25	0.88±0.28	1.09±0.04
				(min,max)	(+0.26,+1.18)	(+0.33,+1.21)	(+0.50,+1.41)	
Masbou et al. 2015	Ringed seal liver	Alaska	53	Mean±SD	-0.17±0.33	0.41±0.17	0.51±0.17	0.97±0.03
				(min,max)	(-0.87,+0.72)	(-0.04,+0.91)	(+0.07,+1.04)	

Part 3. Presentation of the doctoral work: scientific context, bioindicators and main objectives

3.1 Scientific context: The Southern Ocean (Indian sector)

3.1.1 Oceanographic characteristics

The Southern Ocean corresponds to all the water masses at the south of the Subtropical Front (40 ° S). The hydrological features of the Southern Ocean play an important role in the worldwide oceanic circulation since it is the nexus of the water masses belonging to the three main oceans of the globe: the Pacific, Indian and Atlantic Oceans. The Southern Ocean helps to drive the global ocean circulation, and stores and recirculates heat, oxygen or carbon. It is characterized by a predominance of strong westerly winds (The Roaring Forties) which are not stopped by any land and then involve a hydrological annular structure around the Antarctic continent (called Antarctic circumpolar current). This results in the presence of different water masses defined by oceanic fronts that separate physically the Southern, Atlantic, Indian and Pacific Ocean basins (Sokolov and Rintoul, 2007).

The climatic and environmental zones strongly influence the environmental conditions of the different ecosystems surrounding the Antarctic continent, distributed here as the **Antarctic zone (**situated between the South Pole and the Polar Front), the **Subantarctic zone** (between the Polar Front and the Subtropical Front) and the **Subtropical zone (**north the Subtropical Front). The Subtropical Zone does not strictly make part of the Southern Ocean since it comprises the area further north of the Subtropical Zone, but in this doctoral work it is included as a Southern Ocean locality for simplification. These regions correspond to the French Southern and Antarctic Territories and cover a long north-south gradient. In this doctoral work, avian samples were collected from 4 territories:

- **Adélie Land**, on the Antarctic continent (66°39′S, **Antarctic Zone**)

- **Kerguelen** (49°21′S, 70°18′E) and **Crozet** Islands (46°25′S, 52°E) (**Subantarctic Zone**)

- **Amsterdam** Island, (37°47'S, **Subtropical Zone**)

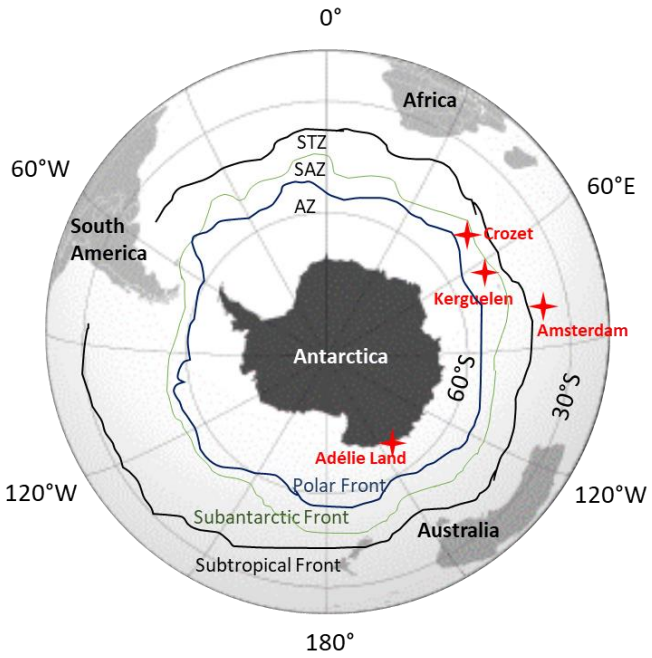

Figure 1.24. Map of the studied zones of the Southern Ocean divided into the three zones AZ (Antarctic Zone), SAZ (subantarctic zone) and STZ (subtropical zone) corresponding to different water masses determined by the oceanic fronts: Polar Front, Subantarctic Front and Subtropical Front.

3.1.2 Biogeochemical characteristics

3.1.2.1 Carbon cycle and stable carbon isotopes

There is evidence of the important role of organic carbon remineralization on the production of Hg methylated compounds in the open Ocean (Sunderland et al., 2009; Cossa et al., 2009). Oceanic carbon cycle can be impacted by physical mechanisms such as upwelling (Marshall and Speer 2012) or the biological pumps (Ducklow et al., 2001). Stable carbon signatures, reported as $\delta^{13}C$, are slightly affected with trophic level and are widely used to determine primary carbon sources in a food web. The Southern Ocean is defined by a well-recognised latitudinal $\delta^{13}C$ gradient which effectively characterise different water masses at the basal food web (Trull and Armand, 2001) and which is preserved in consumers at higher trophic levels (Cherel and Hobson, 2007; Jaeger et al., 2010). In the marine environment, $\delta^{13}C$ values enables the determination of inshore-offshore and pelagic-benthic gradients as well as large latitudinal scales. Indeed, this isotopic method has been successfully applied in areas surrounding Southern Ocean islands to discriminate pelagic from neritic feeders (Cherel and Hobson, 2007) permitting the utilisation of $\delta^{13}C$ signatures to assess the main foraging zones of seabirds (Cherel et al., 2013; Cherel and Hobson, 2007). Furthermore, phytoplankton $\delta^{13}C$ values are positively correlated to higher primary productivity, which is known to be extremely elevated in the vicinity of subantarctic islands during austral summer (Blain et al., 2001; Pollard et al., 2002). Importantly, although $\delta^{13}C$ signatures provide valuable latitudinal trends of the foraging zones, they do not offer indication about longitude variations.

3.1.2.2 Primary production

The Southern Ocean is also characterised by spatial and seasonal heterogeneity in primary production. Generally, these southern marine regions present high nutrient concentrations such as nitrate, phosphate or manganese; whereas phytoplankton production is contrastingly low (Boyd et al., 2000; Blain et al., 2001; Sanial et al., 2014), considered then as "high nutrient-low chlorophyll" waters. Factors such as sunlight incidence, water temperature and complex hydrodynamics have been proposed as influential factors on biological activity rates (Boyd, 2002). Low Fe concentrations in these waters have been shown to limit phytoplankton growth (Boyd et al., 2000). Nevertheless, the Southern Ocean areas experience seasonal supply of Fe and other macro and micro-nutrients that arrive to the surface, resulting in high primary production and phytoplankton bloom during the austral summer (Mongin et al., 2009; Blain et al., 2007), especially in the Antarctic zone by the transit of the circumpolar deep waters (Cossa et al. 2011). In Antarctic coastal zones, this phytoplankton bloom phenomenon is known to be enhanced by sea ice melting during spring and summer seasons (Sokolov, 2008; Riaux-Gobin et al., 2013), demonstrating that sea ice from Adélie Land contains high biomass concentrations and primary production (RiauxGobin et al., 2000), especially fast ice, which is associated to high microalgal biomass and nutrient regeneration. Determined areas of the Subantarctic Zone are highly productive due to seasonally release of nutrients in regions of the Kerguelen Plateau, a phenomenon known as "island fertilisation effect" because nutrients are deposited on the borders of the Crozet, Kerguelen and South Georgia archipelagos (Blain et al., 2001; Korb and Whitehouse, 2004; Sanial et al., 2014). Upwelling waters are also characteristic of these zones and drive the supply of nutrients to surface waters (Plancke, 1977).

3.2 Bioindicators models of the study: seabirds of the Southern Ocean

3.2.1 Seabirds as bioindicators of Hg contamination

A bioindicator of chemical contamination is considered an organism able to reflect the contaminant exposure in a given ecosystem by integration of local and global sources of contamination over different spatial and temporal scales. Wildlife bioindicators present several advantages because they reflect the contamination of the food webs on which they depend and thus allow assessing and understanding the contamination in the ecosystems. The choice of an appropriate bioindicator must be based on its capacity to bioaccumulate the concerned contaminants and, ideally, the environmental concentrations and measurements in the tissues of the bioindicator should be proportionally related. Such direct proportionality is verified for mammals and seabirds for biomagnifiable contaminants such as Hg. The effect of physiologic

factors (metabolism and detoxification processes) and ecological aspects (specific life-history and foraging behaviour) must also be taken into consideration when marine mammals and seabirds are used for a correct interpretation of the measured concentrations or interspecific variations.

Birds have demonstrated to be satisfactory bioindicators of ecosystems health in general and of chemical contamination in particular (Furness and Camphuysen, 1997). Thus they have been widely used for contamination biomonitoring, particularly in marine ecosystems (Burger and Gochfeld, 2004). In some cases they have contributed to unchain regulation or prohibition of pollutant chemicals. This is the case of peregrine falcon whose population became endangered due to the extensive use of some pesticides, mainly DTT, before its ban in 1970 (Ratcliffe, 2012; Walker, 2003).

Since they are top predators within marine food webs, seabirds are exposed to high levels of Hg by dietary uptake, especially under the form of MeHg, leading to Hg-related health effects. Severe consequences of Hg toxicity have been documented on seabirds at the individual level. Since Hg is an endocrine disrupter, it has led to reproductive disturbance and decreased hatching rates (Tartu et al., 2013), resulting in substantial demographic decline (Goutte et al., 2014ab). Therefore, it is hypothesized that an increase in the incorporation of MeHg in the trophic webs, as a consequence of the progressive warming of the ocean (Cossa, 2013), could provoke the decrease in seabird populations due to the reprotoxic effects of Hg (Goutte et al., 2014b).

The use of seabirds to study the sources of Hg and the processes associated to its geochemistry in the ocean is particularly interesting since they forage in diverse positions at sea, in the horizontal and vertical scales, according to the species. Seabirds present some ecological characteristics that make them ideal models for evaluation of Hg fate and bioavailability in marine ecosystems:

i) they present different foraging strategies among species, involving different trophic and different compartments of the food web;
ii) they have a long life span, leading to high Hg concentrations in their tissues;
iii) they are generally colonial and philopatric, allowing to easily sample several individuals simultaneously during the reproduction and follow these individuals repeatedly over time;
iv) they reflect Hg contamination from vast and remote areas, otherwise difficult to sample and monitor with conventional sampling methods.

Figure 1.25. Northern giant petrel at Crozet Islands. Photo: Yves Cherel.

Although some of seabird characteristics could present disadvantages for environmental monitoring studies (such as their high mobility and exploitation of large areas), a careful choice of species whose ecological characteristics are well-known may ensure the procurement of relevant information about of Hg contamination and its correct interpretation (Thompson et al., 1993ab; Blévin et al., 2013; Carravieri et al., 2014ab). During this doctoral dissertation, the principles of selection of the most appropriate seabird models were detailed and justified according to the specific objective of each study (Chapters 3 and 4). Combining information from previous studies on satellite-tracking, carbon isotopic measurements and direct field observations (Jaeger et al., 2010; Cherel and Hobson, 2007; Lescroël and Bost, 2005) enabled to create a primary database of the specific foraging strategies of each seabird species. Furthermore, a previous doctoral work (Carravieri, 2014) already provided key insights for the identification of the most relevant bioindicator species for long-term monitoring of Hg contamination, by measurements of Hg concentrations in more than 30 seabird species with contrasting feeding ecology of the Southern Indian Ocean. Among others indications, Carravieri (2014) highlighted the importance of food intake as the main pathway of exposure of seabirds to contaminants, diet being the first factor explaining Hg concentrations across a single seabird community (Carravieri et al., 2016). Nevertheless, numerous other factors such as phylogeny, moulting patterns, sex, life span and diet composition are likely to influence Hg bioaccumulation in seabird tissues.

3.2.2 Biodiversity of seabirds in the Southern Ocean and ecological characteristics

French Southern and Antarctic territories represent the ideal region for scientific ecological research because they encompass a great biodiversity characterized by massive colonies of birds

and marine mammals. A large number of seabirds of the Southern Indian Ocean (about 380 millions of individuals) return to these localities to breed each year (Van Franeker et al., 1997), of which penguins correspond to the largest biomass (90%) (Woehler, 1995). Another abundant seabird community corresponds to the family Procellariiformes (albatrosses and petrels), including emblematic species such as the wandering albatross, for which the highest feather Hg concentration has been reported (40 µg g^{-1} on average, and up to 95 µg g^{-1} recorded for a single individual, Bustamante et al., 2016). These species are extremely long-lived seabirds, in some cases achieving 80 years old, so are ideal models for monitoring temporal evolution of seabird populations investigating their life history, reproduction, mortality, survival and physical conditions.

Breeding period takes place during the austral summer for the most part of seabird species although there are also some exceptions of winter breeders such as the emperor penguin. While breeding, seabird individuals are constrained to return frequently to their breeding colonies in order to incubate or provision their offspring, thus they are spatially restricted to surrounding areas when foraging at sea. Therefore, seabird diet at this time is mainly composed of local prey. One exception are king penguins that are known to forage in the waters of the Antarctic Polar Front irrespectively of their breeding location (Pütz, 2002). During the breeding season, sampling collection is thus more accessible and feather and blood can be sampled on live adult individuals and chicks.

Outside the breeding period, seabirds are not linked to a central place and have developed specific and contrasting feeding strategies to optimise food resources and elude inter and intraspecific competition. Migratory seabirds can cover long distances during their non-breeding period, in some cases arriving up to North Atlantic and Pacific Ocean zones. The use of migratory seabirds as a bioindicator could thus be perceived as problematic, but their mobility also has some advantages. Indeed, compared to resident species that reflect contamination of a specific exposure zone, migratory seabirds integrate Hg into different areas: breeding and wintering areas. Nevertheless, this characteristic requires the ability to discriminate Hg accumulated in each of these zones, as previously mentioned by combination of Hg measurements and spatial ecology studies, in order to monitor the movement and determine the distribution of organisms during their life cycle (Fort et al., 2014). Penguins, and other diving seabirds, disperse over wide marine areas exploiting different depths of the water column, foraging at epipelagic, mesopelagic or benthic zones depending on species.

Figure 1.26. King penguins breeding at colonies of Crozet Islands. Photo: Paco Bustamante.

Moulting is a necessary process in seabirds for preservation of their thermic isolation and flying capacities. Most flying birds moult annually during the less productive austral winter (Jaeger and Cherel, 2011). Their feather replacements is sequential and prolonged generally over 2-3 months to one year (Bridge, 2006), between two breeding periods. Some seabird species present more complex moulting patterns such as the wandering albatross that moults intermittently over several inter-breeding periods (Weimerskirch, 1991). Unlike flying seabirds, adult penguins renew their whole plumage in the course of austral summer immediately before or after breeding during 2–5 weeks. This process is crucial in the annual cycle of penguins since they experience a progressive thermal reduction that prevents them from going at sea. Therefore, they evolve a previous foraging period of hyperphagia at sea to build up the energy reserves required during moult (e.g, Thiebot et al., 2014). Penguins exhibit a synchronous moult as a consequence of their entire feather renewal, therefore their feathers present a quite homogenous chemical composition (Brasso et al. 2013; Carravieri et al. 2014a). Moreover, since penguins stay on land during extended periods while fasting, they are easily accessible in particular at the beginning of the breeding cycle and during moult.

As previously mentioned, the synthesis of feathers represents a major pathway for excretion of Hg that is remobilized from storage tissues at the time of moulting. Approximately 80% of the Hg contained in the internal tissues is excreted in feathers (Honda et al., 1986; Braune, 1987). Once feathers are synthesized, Hg concentrations do not change and therefore are assumed to

reflect the Hg accumulated over two moulting periods. Consequently, feathers analyses provides information on the integrated Hg contamination over different periods of several months. In migratory seabirds such as Alcids, analysis on feathers thus make possible to discriminate the Hg exposure at their breeding and wintering sites (Fort et al., 2014). In chicks, feathers are synthesized continuously throughout their rearing period, providing access to local Hg contamination over that time since their parents nourish them with prey in the vicinity of the colony. Thus, the use of chick feathers is very relevant for monitoring of Hg contamination of the environment because the integration time and spatial resolution of Hg exposure are clearly defined (Carravieri, 2014; Blévin et al., 2013; Carravieri et al., 2014a). Meanwhile, blood presents a different Hg turnover as it a metabolically active tissue representative of recent Hg exposure that is accumulated dynamically in storage tissues. Therefore, blood reflects a shorter-term Hg intake than feathers, in the order of few weeks/months before sampling (Bearhop et al., 2000b) and, since it is collected during the breeding period, both adult and chick blood samples are assumed to provide information about Hg contamination near the colonies.

Seabirds from the Southern Ocean are considered competent samplers to investigate Hg contamination since they provide access to different marine environmental compartments exploiting interspecific foraging strategies and feeding on large diversity of prey horizontally (from coastal to oceanic) and vertically (epipelagic to mesopelagic zones). Besides, investigating ubiquitous species breeding at colonies of the different locations of the Southern Indian Ocean enables to explore a vast latitudinal gradient from Antarctica (Adélie Land) to the subtropics (Amsterdam Island). In a last instance, exploration of diverse avian tissues (feathers, blood or internal tissues) can give information of different integration times of Hg exposure and/or metabolic response face to Hg contamination.

3.3 Main objectives of this doctoral work

Despite its distance from anthropogenic pressure, the Southern Ocean and Antarctic zones are affected by inputs of contaminants, such as Hg, mainly by oceanic currents and atmospheric deposition (Pacyna et al., 2010). As a globally distributed contaminant, Hg can be easily transported over long distances and is present in substantial levels in these considered pristine ecosystems (Cossa et al., 2011). Several studies have documented meaningful levels of Hg bioaccumulation in tissues of biota and in particular of top predators (e.g., Bocher et al., 2003; Anderson et al., 2009; Carravieri et al., 2014a; Bustamante et al., 2016). Nevertheless, Hg contamination in the Southern Ocean, especially in the Indian sector, remains largely unknown and determining the origin and fate of Hg in such remote areas involves a major challenge. Indeed, previous results of Hg latitudinal variations reported in marine birds and in the water column have

exhibited a reverse gradient. While MeHg concentrations seemed to be higher in Antarctic than in the subantarctic and subtropical waters (Cossa et al. 2011), analyses on seabird tissues have documented increasing MeHg concentrations from Antarctic through subantarctic to subtropical colonies (Blévin et al., 2013; Carravieri et al., 2014b; Goutte et al., 2014; Carravieri et al. 2017). Under these circumstances, a better understanding of the formation sources of MeHg in these ecosystems remains necessary. Therefore, **the main objective of the present doctoral work is the characterisation of the exposure pathways of MeHg accumulated in seabirds to identify the sources and processes involved in the Hg biogeochemical cycle in these remote marine environments**. With this intention, the proposed methodological approach consists on the **determination of Hg isotopic signatures (δ^{202}Hg, Δ^{199}Hg) and Hg species distribution in tissues of an accurate selection of seabirds of the Southern Ocean** (French Southern and Antarctic territories). The combination of Hg speciation and isotopic composition, together with the information of trophic and habitat isotopic tracers (δ^{13}C, δ^{15}N), is expected to provide useful insights for the elucidation the sources of MeHg in these few explored marine areas.

This doctoral work is based in important insights documented in the doctoral work of A. Carravieri (Carravieri, 2014) that enabled a better understanding of the intrinsic and extrinsic factors influencing Hg exposure in seabird as a function of their ecological characteristics, and therefore, provided valuable information concerning the selection of the most preferable bioindicators species. The present work continues the evaluation of the main factors influencing Hg exposure pathways and aims to achieve further innovative information such the determination of the origin (or formation sources) of MeHg accumulating in marine birds according to the latitude, trophic level and ecology of these organisms. This work comprises totally innovative results of Hg isotopic composition of seabird tissues, representing the first data of Hg isotopic composition in the Southern Ocean, including Antarctic Polar Regions, thus providing valuable information about distinct and variable marine ecosystems of these remote zones.

This dissertation has been focused in different aspects and methodological actions that have been previously assessed in order to ensure the procurement of valuable information by Hg isotopic measurements in different avian tissues and to guarantee its correct interpretation and application for elucidating Hg biogeochemical processes. In a first step, an optimisation and **validation of analytical methods and techniques** (Chapter 2) was required for some avian matrixes that were analysed by Hg speciation and Hg isotopic composition studies (principally feathers and blood). Secondly, a **methodological approach** (Chapter 3) was addressed with the triple objective of i) inquire the detoxification mechanisms and metabolic response of seabirds face to Hg by analyses of different avian tissues (feathers, blood and diverse internal tissues and organs), ii) evaluate the level of information provided by tissue-specific isotopic signatures and iii) determine the most effective tissue for biomonitoring depending on the scientific purpose.

Once the methodological features were assessed and the choice of the most pertinent bioindicator tissue was justified, we focused on the exploration of the **ecological and environmental aspects** of this doctoral work (Chapter 4). In this chapter, a first part was focused on the investigation of MeHg exposure pathways as a function of specific ecological characteristics of seabirds (i.e., trophic ecology and foraging strategies) in order to determine distinct environmental MeHg sources at variable marine compartments in a same ecosystem (i.e., the Crozet Islands). The second part was focused at a larger scale (i.e., latitudinal gradient) with the objective of exploring potential MeHg sources and major processes involved in the Hg biogeochemical cycle across the Southern Ocean, from Antarctica to the subtropics, by interpretation of Hg isotopic variations in marine birds. The main **conclusions and perspectives** of the doctoral work, including the descriptive aspects, are presented in Chapter 5.

Chapter 2.

Analytical methods and techniques

Chapter 2. Analytical methods and techniques

Part 2.1: Hg speciation analyses: optimisation of Hg extraction techniques in avian samples

1.1 Assessment of mercury speciation in feathers using species-specific isotope dilution analysis

(Published in Talanta journal in 2017, N°174, pp. 100–110)

Marina Renedo[1,2*], Paco Bustamante[1], Emmanuel Tessier[2], Zoyne Pedrero[2], Yves Cherel[3], David Amouroux[2*]

[1] Littoral Environnement et Sociétés (LIENSs), UMR 7266 CNRS-Université de la Rochelle, 2 rue Olympe de Gouges, 17000 La Rochelle, France

[2] CNRS/ UNIV PAU & PAYS ADOUR, Institut des Sciences Analytiques et de Physico-chimie pour l'Environnement et les Materiaux , UMR5254, 64000, Pau, France

[3] Centre d'Etudes Biologiques de Chizé (CEBC), UMR 7372 CNRS-Université de La Rochelle, 79360 Villiers-en-Bois, France

**Corresponding authors:* marina.renedoelizalde@univ-pau.fr; david.amouroux@univ-pau.fr

Abstract

Seabirds are considered as effective sentinels of environmental marine contamination and their feathers are extensively used as non-lethal samples for contaminant biomonitoring. This tissue represents the main route for mercury (Hg) elimination in seabirds and contains predominantly methylmercury (MeHg). In this work, we developed a robust analytical technique for precise and accurate simultaneous quantification of MeHg, inorganic Hg (iHg) and consequently total Hg (THg), in feathers by gas-chromatography (GC)-ICPMS analyses using species-specific isotope dilution technique. An optimisation of the extraction method was carried out by testing different extraction systems, reagents and spiking procedures using an feather IRM. The procedure was validated for MeHg and THg concentrations with a human hair certified reference material. Microwave nitric acid extraction with spike addition before the extraction provided the best recovery and was chosen as the most appropriate species simultaneous extraction method (SSE). An additional assessment was performed by comparison of our developed extraction method and a MeHg specific extraction technique (MSE) classically used for Hg speciation studies on feathers. The developed method was applied to feather samples from a large number of seabirds from the Southern Ocean (penguins, albatrosses, petrels and skuas) to investigate the variability of Hg speciation across a large range of Hg exposure conditions and concentrations. In all cases, MeHg accounted for > 90% of THg, thus verifying the predominance of organic Hg over iHg in feathers.

Keywords: seabirds, Southern Ocean, GC-ICPMS, methylmercury, inorganic mercury, inter-species transformations, keratin

Introduction

Mercury (Hg) is a globally distributed pollutant of major concern for humans and wildlife, whose toxicity is known to be dependent on its molecular speciation. Methylmercury (MeHg) is considered the most toxic Hg species and, once acquired by dietary uptake, it accumulates in organisms and biomagnifies within the food webs (Bargagli et al., 1998; Bargagli et al., 2005). In aquatic systems, anaerobic microorganisms such as sulphate and iron reducing bacteria (SRB and IRB) transform inorganic Hg (iHg) in MeHg (Benoit et al., 2002; Hammerschmidt and Fitzgerald, 2004; Fleming et al., 2006), resulting in its incorporation into the food chain. Hence top predators, particularly those linked to aquatic ecosystems, are at highest risk for increased dietary Hg exposure, especially MeHg, leading to potential Hg-related health effects (Wiener et al. 2003) and to consequences at the population level (Goutte et al. 2014a).

Birds have been extensively used as effective bioindicators of Hg contamination in the environment, particularly of marine ecosystems (Burger and Gochfeld, 2004). Due to their high position on the aquatic food webs and their long life span, seabirds accumulate significant levels of Hg in their tissues. Feathers are interesting samples to analyse because they represent the main route of Hg elimination in seabirds, so contain most of their Hg body burden (Braune, 1987; Monteiro et al., 1996; Honda et al., 1986; Furness et al., 1986). Moreover, feathers can be easily and non-destructively sampled on live individuals. During moult, most of the Hg stored within internal tissues (70-90%) is remobilised into growing feathers (Honda et al., 1986), where it is sequestered in the sulphydryl groups of the keratin molecules and cannot be reincorporated into internal tissues. Once bound to keratin, Hg is physically and chemically stable (Appelquist et al., 1984) and resistant to a variety of rigorous treatments (Thompson et al., 1998a). Although other metals such as lead or cadmium are supposed to be incorporated in feathers by atmospheric input, the homogenous distribution pattern of Hg previously observed in feathers has led to hypothesize that Hg contamination is more likely due to endogenous causes (food and physiology) and is not affected by atmospheric exposure (Hahn et al., 1993). Nevertheless, gaseous Hg adsorption has been recently demonstrated in human hair under Hg vapour exposure (Queipo Abad et al., 2016; Laffont et al., 2011), suggesting the possibility of direct Hg deposition also in feathers under high gaseous Hg ambient concentrations which could potentially have a repercussion on the use of bird feathers from museum collections for retrospective investigation on Hg temporal trends. However, this process is unlikely to occur in feathers of seabirds inhabiting non-contaminated areas. The first research study of Hg speciation in feathers was carried out by Thompson and Furness (Thompson and Furness 1989a) in various seabird species, in which they found that Hg incorporated into this tissue was mainly composed of MeHg (77-118%). A dominance of MeHg in feathers was also observed in following studies (Kim et al., 1996; Thompson et al., 1998b; Bond et al., 2009). Hg has been therefore assumed to be present almost exclusively under its

organic form in feathers while no accurate determination of iHg has been achieved so far. Total Hg concentrations (THg) are often measured for MeHg quantification in feathers as an economical alternative to speciation analyses. Actually, direct analyses of MeHg in feathers are usually considered on studies focused on temporal variations on Hg concentrations using historical feather collections from museums, e.g (Thompson et al., 1992; Thompson et al., 1993b; Furness et al., 1995; Bond et al., 2015); where a potential contamination of iHg has been found to be produced by the successive application of preservatives containing $HgCl_2$ and methyl-bromide (Vo et al. 2011). Analyses of Hg speciation in feathers are therefore essential to better evaluate Hg exposure and metabolic processes in birds.

Different analytical methods for Hg speciation in feather samples have been reported in previous studies. Thompson and Furness (Thompson and Furness 1989b) proposed the first method to determine concentrations of THg and MeHg in feathers by MeHg selective extraction (adapted from Uthe et al. (Uthe et al., 1972)) for subsequent analyses by cold-vapour atomic fluorescence spectroscopy (CV-AFS). This procedure has been widely used by studies of Hg speciation in feathers (Thompson et al., 1992; Thompson et al., 1993ab; Kim et al., 1996; Monteiro and Furness, 1997; Thompson et al., 1998b; Spalding et al., 2000). More developed analytical techniques were later performed by using gas chromatography in order to separate Hg species: gas chromatography coupled to atomic fluorescence spectroscopy (GC-AFS) (Bond et al. 2009; Mallory et al., 2015); gas chromatography coupled to electron-capture detector (GC-ECD) (Kehrig et al., 2015), and single isotope dilution analysis by gas chromatography coupled to ICPMS (S-IDA-GC-ICPMS) with single isotope spike (only isotopically labelled MeHg was added) (Vo et al., 2011). However, these analytical techniques do not allow correcting possible losses or transformations between Hg species and provide uniquely the quantification of MeHg and THg concentrations, so the determination of iHg concentrations needs to be calculated as the difference between both compounds' concentrations. A synthesis of the results published in previous studies have been compiled in Table 2.1. It can be observed that in some cases MeHg proportion values of feathers exceed 100% of THg, indicating a lack of accuracy or precision in MeHg quantification by classical techniques. This observation enhances the interest of our developed method for accurate and precise Hg species analyses.

The quantification of both Hg species involves an analytical challenge due to potential losses or species transformation reactions (i.e., MeHg demethylation or iHg methylation processes) which could occur during the whole analytical procedure, leading to erroneous results in the quantification of Hg species concentrations (Clémens et al., 2011). GC–ICPMS using a double isotopic dilution method provides the simultaneous measurement of both MeHg and iHg, and subsequently THg as THg = MeHg + iHg, with high precision (Rodríguez-González et al. 2005; Clémens et al. 2012). Obtained data can also be processed by Isotope Pattern Deconvolution

(IPD), a general model for isotope dilution that takes into consideration both spikes (isotopically enriched solutions) and natural species, and enables the determination of potential interconversion reactions and the consequent correction of Hg species concentrations (Clémens et al., 2011). Accordingly, isotope dilution methods guarantee a better precision and accuracy than conventional quantification by external calibration (Clémens et al., 2012). Previous studies published method developments (extraction and derivatisation) for Hg speciation by ID-GC-ICPMS in biological samples, such as seafood (Clémens et al., 2012) or human hair (Laffont et al., 2013). Preliminary work was carried out on human hair thus allowing an initial approach of Hg species analyses on keratin samples by evaluating different extraction methods (Laffont et al., 2013).

Our research work includes the assessment of two keratin-based materials (feathers and hair) and considers further analytical strategies, such as the isotopically enriched spiking technique in all the extraction methods tested or the additional evaluation of classic MeHg selective extraction. This study evaluates in depth analytical performances on keratin samples and provides information about non-desirable reactions occurring during both extraction and derivatisation of each analytical procedure tested. Hg speciation in feathers of a great number of seabirds from the Southern Ocean have been successfully determined by applying the developed method.

Table 2.1. Synthesis of main previous studies on Hg speciation in feathers in order of publication. Result values are represented as mean±SD.

Hg speciation approach	Analytical method	Species	Region	N	THg ($\mu g \cdot g^{-1}$)	iHg ($\mu g \cdot g^{-1}$)	MeHg ($\mu g \cdot g^{-1}$)	MeHg (%)	Ref
Hg species measured: MeHg, THg MeHg specific extraction	CV-AFS	Wandering albatross complex	Gough Island (South Atlantic Ocean) Marion Island (Indian Ocean)	26	30.7±11.7	n/a	29.2±11.6	95	[1]
		Sooty albatross	Gough Island (South Atlantic Ocean)	7	9.4±3.9	n/a	9.1±4.0	97	
		Northern fulmar	Foula (Shetland)	15	1.8±0.8	n/a	2.0±0.7	111	
		European shag	Foula (Shetland)	14	1.7±0.7	n/a	2.0±0.8	118	
		Great skua	Foula (Shetland)	14	6.8±4.4	n/a	7.3±5.5	107	
		Arctic skua	Foula (Shetland)	9	2.2±1.7	n/a	1.7±1.8	77	
		Kittiwake	Foula (Shetland)	14	2.4±0.6	n/a	2.2±0.7	92	
		Razorbill	Foula (Shetland)	16	2.1±0.3	n/a	2.1±0.6	100	
		Common guillemot	Foula (Shetland)	17	1.5±0.4	n/a	1.7±0.5	113	
		Puffin	Foula (Shetland)	10	5.2±2.7	n/a	5.1±2.1	98	
Hg species measured: MeHg, THg MeHg specific extraction	CV-AFS	Oldsquaw	Chaun (Northeast Siberia)	5	0.7±0.2	n/a	0.9±0.2	128	[2]
		Herring gull	Chaun (Northeast Siberia)	5	6.1±4.6	n/a	6.5±4.5	106	
		Arctic tern	Chaun (Northeast Siberia)	5	0.9±0.1	n/a	1.1±0.1	122	
Hg species measured: MeHg, THg MeHg specific extraction	CV-AFS	Great egret	Everglades (Florida)	6	2.0±0.2	n/a	n/a	120	[3]
Hg species measured: MeHg, THg MeHg specific extraction	GC-AFS	Arctic tern	New Brunswick (Canada)	5	0.9±0.5	n/a	0.8±0.3	95±15	[4]
		Common murre	New Brunswick (Canada)	5	1.0±0.4	n/a	1.2±0.3	133±33	
		Common tern	New Brunswick (Canada)	5	1.4±0.6	n/a	1.6±1.8	114±65	
		Razorbill	New Brunswick (Canada)	5	1.8±0.7	n/a	1.1±0.4	82±35	
		Atlantic puffin	New Brunswick (Canada)	5	4.9±2.8	n/a	1.6±0.7	100±50	
		Leach's storm petrel	New Brunswick (Canada)	5	4.9±2.8	n/a	5.3±3.4	99±40	
Hg species measured: MeHg, iHg,THg Chromatographic separation	ID-GC-ICPMS	Black-footed albatross (post-1990)	Pacific Ocean	10	47.9±35.7	0.5±1.2	42.1±30.9	89±14	[5]
Hg species measured: MeHg, THg MeHg specific extraction	CV-AFS	Ivory gulls (post-1975)	Canada	5	3.5±2.1	n/a	2.7±2.2	68±37	[6]

Hg species measured: MeHg, THg Chromatographic separation	GC-ECD	Magellanic penguins	Southern Brazilian coast	22	0.8±0.4	n/a	0.6±0.3	n/a	[7]
Hg species measured: MeHg, iHg, THg Chromatographic separation	GC-AFS	Ivory gulls	Canada	4	11.6±6.5	n/a	9.4±5.3	81±4	[8]
		Glaucous gull	Canada	4	2.3±1.7	n/a	2.1±1.7	91±4	
		Black-legged kittiwake	Canada	2	3.6±0.9	n/a	3.3±0.9	91±n/a	
		Common eider	Canada	10	0.6±0.2	n/a	0.5±0.2	87±2	
		Thick-billed murre	Canada	10	1.9±0.6	n/a	1.7±0.6	90±1	
		Northern fulmar	Canada	10	2.7±0.7	n/a	2.4±0.6	88±1	

References: [1] Thompson and Furness 1989a, [2] Kim et al. 1996, [3] Spalding et al. 2000, [4] Bond et al., 2009, [5] Vo et al. 2011, [6] Bond et al., 2015, [7] Kehrig et al. 2015, [8] Mallory et al. 2015.

Experimental

Feather samples and reference materials

Due to the non-existence of commercialised feather reference material, we prepared a pool sample of feathers collected from different individuals of king penguin (*Aptenodytes patagonicus*) from Crozet Islands which was used as internal reference standard (IRM) for our laboratory feather analyses and named F-KP. For the validation of the results, all the analyses were performed on a human hair certified reference material (NIES-13). Human hair has been chosen as the most appropriate matrix for validation of feather analysis since they have a similar composition, almost completely composed of keratin. NIES-13 presents high Hg concentrations and contains ~90% of MeHg ([THg]= 4420 ± 200 ng·g^{-1} and [MeHg]= 3800 ± 400 ng·g^{-1}, certified values).

The evaluation of MSE and SSE methods was accomplished with feather samples of two marine bird species: the white-chinned petrel (*Procellaria aequinoctialis*) and Antarctic prion (*Pachyptila desolata*). A pool of feathers from a raised pheasant (*Phasianus colchicus*) was used as a control since terrestrial birds are known to accumulate lower amounts of Hg in their tissues than aquatic birds (Burger and Gochfeld, 2004).

The developed SSE method was applied to feathers from several seabird species exhibiting a large range of Hg concentrations. The selection of marine birds comprises seven species of penguins: emperor (*Aptenodytes forsteri*), king (*A. patagonicus*), Adélie (*Pygoscelis adeliae*), gentoo (*P. papua*), macaroni (*Eudyptes chrysolophus*), southern rockhopper (*E. chrysocome filholi*) and northern rockhopper (*E. chrysocome moseleyi*) penguins, and the wandering albatross (*Diomedea exulans*), northern (*Macronectes halli)* and southern (*M. giganteus*) giant petrels, Antarctic prion (*Pachyptila desolata*) and Antarctic (*Catharacta maccormicki*) and subantarctic (*C. lönnbergi*) skuas. Feather sampling was conducted in four sites of the French Southern and Antarctic Territories: Adélie Land (66°40'S, 140°10'E), Crozet Islands (46°26'S, 51°45'E), Kerguelen Islands (49°21′S, 70°18′E) and Amsterdam Island (37°50'S, 77°31'E). Feather sampling dates of each seabird species are indicated in Table 2.4

Sample preparation and extraction procedures

Feathers were cleaned in a 2:1 chloroform:methanol solution for 5 min in an ultrasonic bath, followed by two methanol rinses to remove surface impurities, and then oven dried at 50ºC during 48h (Carravieri et al., 2013). They were afterwards well homogenised in order to acquire accurate analytical results avoiding within-feather variation in Hg sequestration, which could produce fluctuations in observed Hg measurement (Hahn et al., 1993). Feathers were finely cut with

scissors to obtain a homogenous sample. In the particular case of king penguin (F-KP), white-chinned petrel and Antarctic prion (used for the extraction method assessment since more quantity of sample was available), feathers were cut with scissors and additionally grinded in a planetary ball mill (Retsch PM400) at 400 rpm. We noted that during homogenization with planetary ball mill, a potential contamination of iHg could occur and therefore, this homogenisation method was later discarded.

Different reagents were tested for the optimisation of the extraction method: acid digestion using nitric acid (HNO_3·6N, INSTRA quality) and alkaline digestion by tetramethylammonium hydroxide (25% TMAH in H_2O, Sigma Aldrich). Sample amounts between 0.20-0.25 g were digested in 5 mL of reagent. Two different extraction systems were also tested: microwave (MW) and Hotblock (HB) (Figure 2.1). MW assisted extraction was performed using a CEM MW system (Discover SP-D, CEM Corporation) coupled to an autosampler Explorer 4872 96 (USA). The extraction was carried out in CEM Pyrex vessels by 1 min of warming up to 75ºC and 3 min at 75ºC with magnetic agitation to homogenise the samples. HB extractions were performed in closed PFA vessels (Savillex) of 50 mL at 85ºC during 2 hours in a SC100-36 Hotblock (Environmental Express, South Carolina, USA). The addition of isotopic enriched standard solutions was tested before and after the extraction process. In the case of spike addition before extraction, standard solutions were added directly to the solid sample whereas for spike addition after extraction solutions were added to the extract. All samples were extracted in triplicate.

Prior to Hg species analyses, samples were derivatized at pH 4 by ethylation using sodium tetraethylborate ($NaBEt_4$, 5%), in order to produce volatile ethylated forms of Hg that could be separated by gas chromatography, and then extracted in isooctane by mechanical shaking using an orbital shaker during 20 min. Hg species analyses were carried out by GC-ICPMS Trace Ultra GC equipped with a Triplus RSH autosampler coupled to an ICP-MS XSeries II (Thermo Scientific, USA) as detailed in previous works (Clémens et al., 2011).

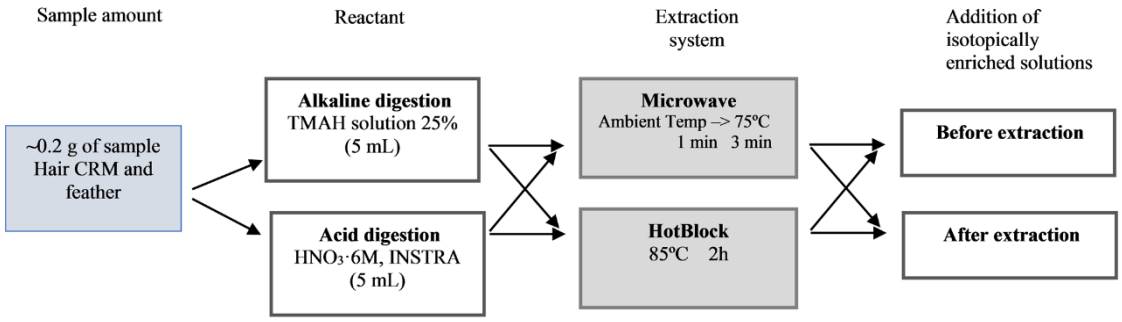

Figure 2.1. Optimisation procedure for Hg speciation analyses in feathers: scheme of the extraction methods tested.

Total Hg analyses

Total Hg concentrations were quantified by using an advanced Hg analyser spectrophotometer (AMA-254, Altec). Homogenised samples (aliquots between 10 and 15 mg) were analysed after thermal destruction and gold amalgamation (drying time 60 s, decomposition time 180 s, waiting time for quantitative trapping of released mercury on the gold amalgamator 45 s). A matrix dependent calibration was performed with human hair reference material (NIES-13) by addition of different masses of sample, following EPA method 7473 (US EPA 2007). This calibration was validated by quantification of a second human hair reference material (IAEA-086), providing an accuracy of 92±5% (n=5) relative to recommended reference value. Feather THg concentrations were calculated by this calibration in order to correct matrix effects associated to keratinised samples. Several blanks were analysed at the beginning of each analytical session. Limit of detection (LOD), calculated for blank average values (15 blanks) plus three times the standard deviation (SD) of these blanks (IUPAC), was 0.15 ng g^{-1}.

Quantification methods for isotopic dilution calibration

Hg species concentrations were determined by different quantification approaches in order to deeply assess analytical performances on keratin samples. Two quantification methods for isotope dilution technique were used: single-IDA and IPD. The concentrations were calculated by both methods and the transformation factors were calculated using IPD, allowing to evaluate interconversion reactions (M% and D%) that occur during both extraction and derivatisation of each analytical procedure tested. For double isotope dilution technique, the sample is spiked with known amounts of two isotope tracers (in this case ^{199}iHg and ^{201}MeHg) to alter the natural isotopic abundance of the studied endogenous species (^{202}iHg and ^{202}MeHg). Quantification is then based on the measurement of the mixed isotope ratios, as explained elsewhere (Clémens et al. 2012; Rodríguez-González et al., 2005). Single-IDA model consists on the specific measurement of Hg species separately. Only two isotopes are considered for the quantification of each Hg species ($R^{202/201}$ for MeHg and $R^{202/199}$ for iHg). IPD takes into account all the different isotopic patterns of both spikes and endogenous species, providing the determination of possible inter-species transformations (M% and D%) and the consequent correction of concentrations (Clémens et al. 2012). The reported results of [THg] were calculated as the sum of [MeHg] and [iHg] determined by ID-GC-ICPMS, and were compared to [THg] determined by AMA-254 in order to evaluate their similarity and verify the recovery of the extraction.

Adaptation of MeHg selective extraction method (MSE)

A specific extraction technique of MeHg was applied in feather samples for the analysis of Hg speciation by ID-GC-ICPMS. The method, adapted from Uthe et al. (Uthe and Grift, 1972),

consists in a first extraction of MeHg in an organic phase (toluene) followed by a reverse extraction in aqueous phase. F-KP and feather samples from different marine bird species (Antarctic prion and white-chinned petrel) and one terrestrial species (pheasant) were used to assess the selectivity of this method, as they exhibit a wide range of Hg concentrations and different Hg species distribution. NIES-13 was also extracted in triplicate and analysed.

Firstly, 0.15-0.20 g of feather samples were extracted by alkaline extraction in a HB system in Savillex vessels with sodium hydroxyde (NaOH [reagent grade], 10M, 4 mL) during 2 h at 60ºC, following Thompson et al. (Thompson and Furness 1989b). Then, 0.5 mL of extract was diluted with 4.5 mL of milliQ water in 50 mL tubes and neutralized afterwards with 0.1 mL of sulfuric acid (H_2SO_4, ACS Grade 95-98%). 5 mL acidic NaBr (30% w/w NaBr [Ultragrade, 99.5%] in H_2SO_4 4 M), 10 mL of aqueous $CuSO_4$ (2.5% w/w [reagent grade, 99%]) and 10 mL of toluene (anhydrous, 99.8%) were added to the extracts. Samples were agitated at 420 rpm for 1 hour in an orbital shaking table. Secondly, an amount of 4 mL of toluene (MeHg passes into the organic phase) was transferred in a Falcon tube with 4 mL of sodium thiosulphate ($Na_2S_2O_3$, 0.005 M [ACS grade, 98%]). Samples were vortexed during 1 min. An aliquot of sodium thiosulphate (MeHg-thiosulphate) was collected in 5 mL tubes and kept at 4ºC until analyses. The addition of isotopically enriched solutions (^{201}MeHg and ^{199}iHg) was tested in two different steps: 1) before NaOH extraction and 2) before specific MeHg extraction (after NaOH extraction) (Figure 2.2). Prior to derivatisation, the addition of a solution of HCl to the MeHg-thiosulphate extract is required to reduce competition with sulphur groups during derivatisation, then different concentrations of HCl solution were tested. The concentrations of the $NaBEt_4$ solution for ethylation were as well optimised. These tests were performed and validated for NIES-13. The best results were achieved when adding 2 mL of HCl solution (5% v/v) and 200 µL of $NaBEt_4$ (5% v/v) to 200 µL of thiosulphate extract. The limit volume of thiosulphate extract for derivatisation is 500 µL, since a higher volume involved matrix effects.

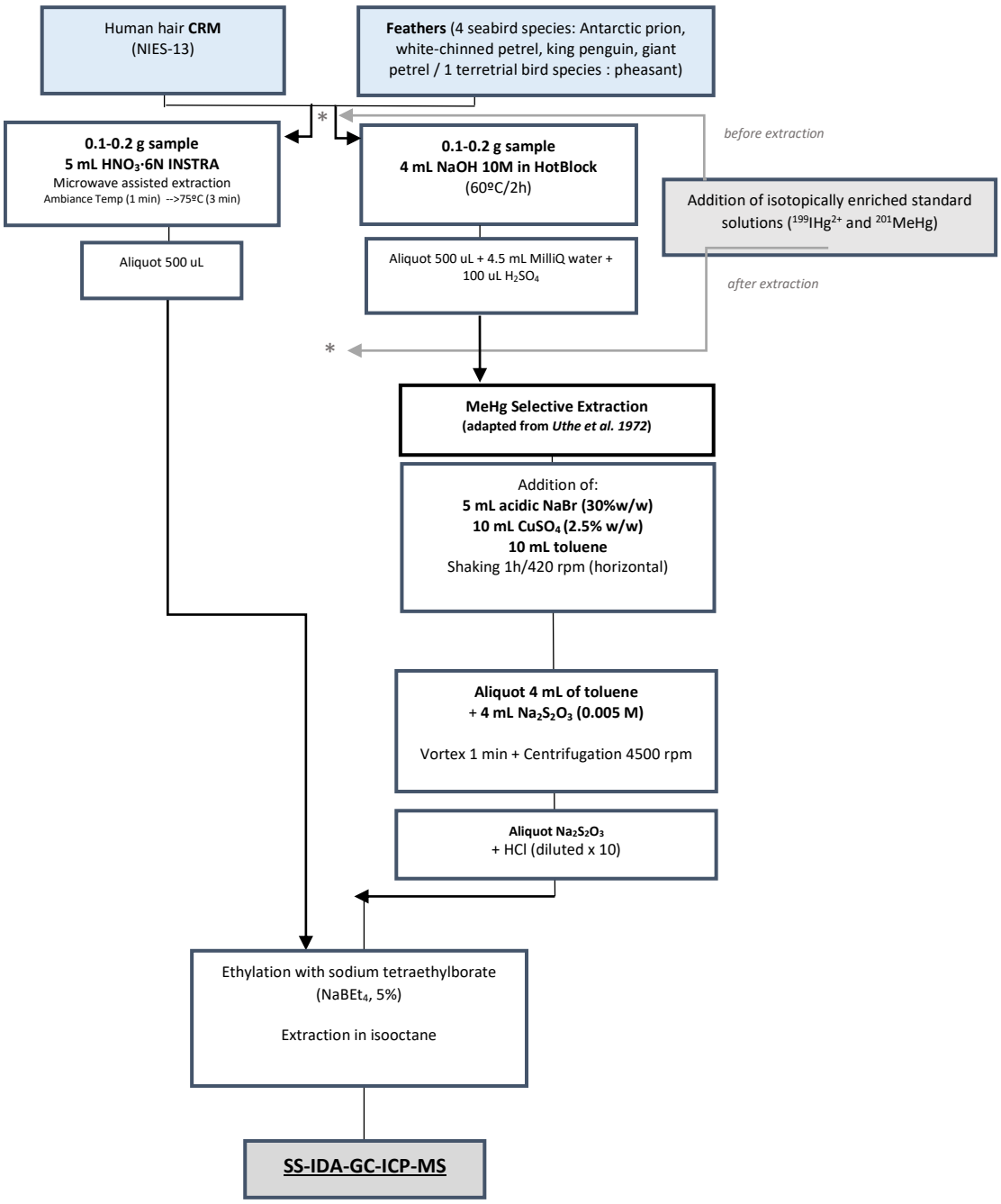

Figure 2.2. Sample preparation flow chart of the two methods compared: speciation extraction and MeHg specific extraction in human hair and feather samples.

Statistical tests for environmental feather samples

Statistical analyses were performed using XLSTAT 2016. Normality and homoscedasticity were firstly checked for the whole dataset by using Shapiro-Wilk and Breusch-Pagan tests, respectively. Since not all the results all the samples presented a normal distribution and homoscedasticity, non-parametric test was used (Kruskal-Wallis coupled to Conover-Iman procedure with Bonferroni correction). The significance level was fixed of α=0.05 for all tests. Values are means ± SD.

Results and discussion

Comparison of speciation extraction procedures: optimisation

Results of [MeHg], [iHg] and [THg] (as [MeHg]+[iHg]) determined by single-IDA and IPD and transformation factors (M% and D%) calculated by IPD for each selected extraction procedure are presented for both reference materials NIES-13 (Table 2.2) and F-KP (Table 2.3).

All the extraction methods tested provided satisfactory results for Hg concentrations for the two reference materials, except acid extractions with spike addition after extraction, which resulted in an insufficient recovery for both Hg species. In the case of NIES-13, recoveries for MW acid extractions with spike addition after extraction were 80.6±1% and 76.5±4.6% for MeHg and THg, respectively, while recoveries of 96.0±1.2% and 95.9±0.2% were achieved for spike addition before extraction. For F-KP, differences between both spiking procedures were not as remarkable as for NIES-13, but better results of THg were obtained when spike addition was added before ([THg]=3899±62 $ng \cdot g^{-1}$) than after MW acid extraction ([THg]=3249±118 $ng \cdot g^{-1}$). This result indicates that spike addition before extraction is highly recommended for hair and feather samples for correcting possible losses and/or species interconversion processes occurring also during the acid extraction step.

TMAH extracts exhibited lower sensitivity for both keratinised matrixes, which consequently induced a higher standard deviation (SD) in determination and a source of error in quantification, even if no substantial alteration of the obtained isotopic ratio was observed. This response demonstrates the occurrence of undesirable competing reactions during derivatisation when using TMAH as extraction reagent. In an acid medium, MeHg from the spike solution is less complexed with the thiol ligands of keratin. Thus, MeHg is more available for ethylation so the derivatization step will be more effective. In the opposite case, in an alkaline medium there is a stabilization of the MeHg by the complexes formed with the thiols, a minor degradation exists but, at the same time, MeHg will be less reactive and there could be interferences by other derivatized molecules (competition) (Tseng et al., 1997). Thus, when extracting keratinised samples in alkaline medium the risk of error by integration of attenuated peaks must be taken into account.

Generally, no significant differences in concentration values were observed between single-IDA and IPD quantification methods for our two reference materials. The only exception was found in the case of NIES-13 MW TMAH with spike addition before extraction. The correction of a substantial D% factor by IPD (26.6±1.0%) involved a significant difference on iHg concentrations calculated by single-IDA (1463±398 $ng \cdot g^{-1}$) and IPD (574±68 $ng \cdot g^{-1}$). This phenomenon also occurred under the same extraction conditions for F-KP, which exhibited a D% of 11.3±10.4%. According to the results obtained for the rest of extraction methods when spiked

solutions were added before extraction, lower but also important D% factors was obtained: MW acid (5.5±1.0% and 4.5±0.2%), HB acid (8.4±0.1% and 3.3±0.8%) and HB alkaline (7.7±0.3% and 6.5±1.5%) for NIES-13 and F-KP samples, respectively. Indeed, for the same extraction conditions but spike addition after extraction, no significant D% were observed on hair and feathers. This result means that significant demethylation reactions mainly occurred during extraction, particularly in the case of MW extraction with TMAH. This could be explained by an influence of different behaviour or transformation rates between endogenous Hg and isotopically enriched Hg from spike solutions (Point et al., 2008). Differences of complexation and lability patterns between Hg from matrix and enriched Hg potentially occur during the extraction procedure, affecting the accuracy of Hg analysis by species-specific isotope dilution. In the previous assessment on human hair samples (Laffont et al., 2013), demethylation during extraction was uniquely observed for HNO_3 oven extraction at 80 °C (4.6±2.5%). Contrary to our results, no demethylation reactions occurred during TMAH extraction.

Concerning the results obtained for procedures with spike addition after extraction, a significant M% was observed for alkaline extractions of F-KP by both systems: MW (8.8±1.9%) and HB (11.9±8.6%). Much lower M% factors were obtained in the case of hair TMAH extracts by MW (3.0±1.5%) and HB (1.3±1.0%). Therefore, important methylation reactions occurred in feather TMAH extracts when spike was added after but not when it was added before. It should also be considered that an additional source of error could exist in quantification of TMAH extraction due to low-sensitivity. No significant D% was obtained for extractions with spike addition after extraction, which means that demethylation artefacts barely occurred during derivatisation step whatever the reagent used. Laffont et al. (Laffont et al., 2013) did not observe methylation but considerable demethylation (4.2±0.8%) during derivatisation of hair TMAH extracts. Notable demethylation reactions occurred during extraction whatever the reagent and extraction system used, and particularly when using TMAH. Due to the existence of important inter-species conversion reactions during extraction and derivatization of keratin-based material samples, the addition of the enriched solutions before acid or alkaline extraction is highly recommended independently of the method used.

Table 2.2. Results of Hg species concentrations and recoveries obtained for the different extraction methods tested in CRM (NIES-13) and calculated by the two different quantification methods (Single-IDA and IPD). Species interconversion factors were calculated by IPD. N is referred to number of extractions.

NIES-13	**Human hair CRM**				**Concentrations ($ng \cdot g^{-1}$)**			**Recoveries (%)**		**Interconversion factors (%)**	
Calculation method	**System**	**Reagent**	**Spike addition**	***n***	**MeHg**	**iHg**	**THg**	**MeHg (%)**	**THg(%)**	**M (%)**	**D (%)**
			Certified values		**3800 ± 400**		**4420 ± 200**				
Single-IDA	Microwave	HNO_3·6N	after extraction	*3*	3064 ± 55	319 ± 148	3383 ± 158	81 ± 1	77 ± 5		
			before extraction	*3*	3647 ± 46	591 ± 53	4238 ± 52	96.0 ± 1.2	95.9 ± 0.2		
	Microwave	TMAH	after extraction	*3*	3467 ± 236	594 ± 8	4202 ± 104	96 ± 3	95 ± 2		
			before extraction	*3*	3651 ± 417	1463 ± 398	5114 ± 589	96 ± 11	116 ± 13		
	HotBlock	HNO3·6N	after extraction	*3*	3022 ± 157	661 ± 16	3683 ± 149	80 ± 4	83 ± 3		
			before extraction	*3*	3403 ± 28	621 ± 64	4025 ± 48	90 ± 1	91 ± 1		
	HotBlock	TMAH	after extraction	*3*	3364 ± 150	845 ± 99	4210 ± 192	89 ± 4	95 ± 4		
			before extraction	*3*	3549 ± 263	964 ± 257	4514 ± 499	93 ± 7	102 ± 11		
IPD	Microwave	HNO_3·6N	after extraction	*3*	3022 ± 18	218 ± 53	3240 ± 62	79.5 ± 0.5	73 ± 1	2.8 ± 1.2	0.3 ± 0.1
			before extraction	*3*	3578 ± 53	565 ± 82	4143 ± 103	94 ± 1	94 ± 2	1.5 ± 1.2	5.5 ± 1.0
	Microwave	TMAH	after extraction	*3*	3574 ± 104	616 ± 56	4191 ± 92	96 ± 1	96 ± 2	3.0 ± 1.5	1.3 ± 0.6
			before extraction	*3*	3803 ± 112	574 ± 68	4377 ± 44	100 ± 3	99 ± 1	1.0 ± 0.3	26.6 ± 1.0
	HotBlock	HNO3·6N	after extraction	*3*	2826 ± 23	704 ± 9	3529 ± 31	74 ± 1	80 ± 1	0.7 ± 0.2	-1.1 ± 0.1
			before extraction	*3*	3421 ± 45	479 ± 22	3900 ± 23	90 ± 1	88 ± 1	1.0 ± 0.3	8.4 ± 0.1
	HotBlock	TMAH	after extraction	*3*	3146 ± 186	654 ± 37	3800 ± 148	83 ± 5	86 ± 3	1.3 ± 1.0	2.9 ± 0.4
			before extraction	*3*	3346 ± 32	494 ± 55	3840 ± 87	88 ± 1	87 ± 2	2.7 ± 1.4	7.7 ± 0.3

Table 2.3. Results of Hg species concentrations and recoveries obtained for the different extraction methods tested in feather IRM sample (F-KP) and calculated by the two different quantification methods (Single-IDA and IPD). Species interconversion factors were calculated by IPD. N is referred to number of extractions.

F-KP	**King penguin feathers (IRM)**				**Concentrations ($ng \cdot g^{-1}$)**			**Interconversion factors (%)**	
Calculation method	**System**	**Reagent**	**Spike addition**	***n***	**MeHg**	**iHg**	**THg**	**M (%)**	**D(%)**
			THg AMA-254 (n=12)				**3816 ± 275**		
Single-IDA	Microwave	HNO_3·6N	after extraction	*3*	2219 ± 50	1029 ± 106	3249 ± 118		
			before extraction	*3*	2539 ± 39	1360 ± 49	3899 ± 62		
	Microwave	TMAH	after extraction	*3*	2461 ± 159	928 ± 83	3389 ± 179		
			before extraction	*3*	2581 ± 256	1592 ± 311	4173 ± 237		
	HotBlock	HNO_3·6N	after extraction	*3*	2238 ± 40	1267 ± 77	3506 ± 87		
			before extraction	*3*	2376 ± 22	1315 ± 13	3691 ± 28		
	HotBlock	TMAH	after extraction	*3*	2733 ± 70	1003 ± 50	3737 ± 86		
			before extraction	*3*	2384 ± 192	1438 ± 137	3822 ± 225		
IPD	Microwave	HNO_3·6N	after extraction	*3*	2175 ± 43	1162 ± 91	3337 ± 101	1.3 ± 1.1	0.5 ± 0.7
			before extraction	*3*	2585 ± 22	1405 ± 46	3990 ± 51	0.3 ± 0.3	4.5 ± 0.2
	Microwave	TMAH	after extraction	*3*	2161 ± 23	964 ± 67	3125 ± 71	8.8 ± 1.9	0.2 ± 0.3
			before extraction	*3*	2505 ± 284	1217 ± 114	3722 ± 323	0.1 ± 0.8	11.3 ± 10.4
	HotBlock	HNO_3·6N	after extraction	*3*	2165 ± 106	1240 ± 77	3404 ± 131	2.8 ± 1.5	0.2 ± 0.2
			before extraction	*3*	2374 ± 24	1194 ± 24.4	3568 ± 40	0.5 ± 0.2	3.3 ± 0.8
	HotBlock	TMAH	after extraction	*3*	2118 ± 138	1110 ± 47	3228 ± 145	11.9 ± 8.6	1.0 ± 0.9
			before extraction	*3*	2452 ± 156	1266 ± 90.9	3718 ± 184	1.4 ± 1.3	6.5 ± 1.5

Comparison of analytical performances

Since no significant differences were observed between MW and HB extraction systems, MW was chosen as the most suitable extraction system since it provides a better-quality control of the extraction, permitting a homogenisation of the sample by electromagnetic stirring and automatic and individually controlled temperature and pressure conditions. Results of MW extraction with spike addition before extraction were evaluated in order to choose the most appropriate reagent. The sensitivity was assessed by the measurement of calibration slopes calculated as the relation of the peak area obtained for ^{202}MeHg (counts per second, cps) divided by the concentration of MeHg injected ($ng \cdot L^{-1}$) for the injection in 2 µL of isooctane. Much higher sensitivity was obtained for HNO_3 than for TMAH extracts obtained for both hair and feathers. Better precision (RSD) was achieved by HNO_3 extraction than by TMAH for the two reference samples. Such important difference is also a consequence of lower sensitivity achieved after alkaline extraction. Accuracy was calculated by recoveries of MeHg and THg relative to NIES-13 certified values. Although the most satisfactory recoveries (for both MeHg and THg of NIES-13) were obtained for TMAH MW extraction with spike addition before the extraction by IPD quantification, this kind of extraction was refused as an pertinent method due to the low sensitivity obtained when using TMAH reagent. Nitric acid MW extraction with spike addition before extraction provided much higher sensitivity and precision, consequently it was chosen for simultaneous species extraction (SSE) on hair and feather samples. For this selected SSE method, mean recoveries for MeHg and THg in NIES-13 quantified by single-IDA (96.0±1.2% and 95.9±0.2) and IPD (94.2±1.4% and 93.7±2.3%) were satisfactory and very similar, suggesting the possibility of using both quantification approaches as valid analytical solutions. Due to practical reasons, single-IDA was chosen in this study to avoid the long data treatment required by IPD. Nevertheless, IPD permits the calculation of conversion reactions among Hg species and the consequent correction of concentrations related to these transformations and therefore, it is considered a more powerful approach. Indeed, IPD generally provides more accurate results than a single-IDA except under particular circumstances in which Hg species concentrations are substantially different within the same sample (Monperrus et al., 2008). In the rest of cases, the level of accuracy of IPD is higher, although it is less precise because the correction of species interconversion is carried out at the expense of the precision of the obtained amount of interconverting analytes (Meija et al., 2009). In conclusion, since satisfactory results were obtained either using single-IDA or IPD in hair and feather samples, IPD remains a reference accurate method for metrology and analytical development while single-IDA can be easily used for routine monitoring analyses.

Intercomparison methods for THg concentrations quantification

Results of THg concentrations were compared for direct quantification by AMA-254 and for the sum of Hg compounds by speciation analyses (SSE) (Table 2.S1). F-KP feather sample was analysed several times in order to obtain a representative THg concentration value ([THg]=3816±275 $ng \cdot g^{-1}$, n=12). Feather THg concentrations obtained by both methods were satisfactory, with recoveries higher than 97% when comparing AMA-254 to SSE values. Precision (RSD) was higher by SSE method (0.3-1.6%) than by AMA-254 (4.3-7.2%) even if for SSE method analyses are performed for triplicate extraction.

Intercomparison between MeHg selective extraction (MSE) and simultaneous species extraction (SSE)

Feather samples were extracted by our previously optimised method for Hg speciation in feathers (SSE) and by MeHg selective extraction (MSE). Results of MeHg concentrations for both methods are given in Table 2.S2. Recoveries of MSE for NIES-13 were calculated relative to MeHg certified values. For the rest of the samples, recoveries were calculated in function to MeHg concentrations obtained by SSE method. Non-significant differences between the mean concentrations obtained for blank extractions and iHg fractions quantified by isotope dilution were found for the MSE extracts, meaning that exclusively MeHg was extracted. We observed notable differences between concentrations values for both types of spiking procedures for MSE. In all cases, spike addition before NaOH extraction provided better results. For NIES-13 recoveries of [MeHg] were satisfactory for SSE (96±3%) and MSE with spike addition before (97±6%), but not sufficient for MSE with spike addition after extraction (80±4%). F-KP presented recoveries of [MeHg] of 76±7% and 82±10% for MSE with spike addition after and before extraction, respectively. Precision (as RSD) was similar for MSE with spike addition after extraction than before extraction. For NIES-13 and F-KP reference samples, extracted in triplicate, precision of MSE with spike after extraction was 4.7% and 9.0%; whereas precision obtained for MSE with spike addition before was 6.3% and 12.3%, respectively. For feather samples, extracted only once, mean RSD was 3.2% (2.6-4.0%) and 2.2% (1.8-4.8%) for spike addition after and before, respectively. Better results were achieved for MSE with spike addition before NaOH extraction as it enables the correction of methylation or demethylation reactions occurring during the whole procedure, which in the case of MSE involves several steps that could induce undesirable interconversion reactions.

A logarithmic representation of obtained [MeHg] values for all the samples tested is shown in Figure 2.3. Since the addition of spike before NaOH extraction resulted in better recoveries, only these results of MSE are plotted to compare to SSE. The precision in MeHg quantification

appeared to be much higher for SSE method for reference materials (1.26% for NIES-13 and 1.53% for F-KP) and feather samples (mean value 1.17% (0.27-2.32%)). This could mean that MSE is less precise, maybe due to its higher complexity and elevated number of analytical steps. As a general trend, results for both extraction methods agree with the expected values for reference materials and matched for the rest of feathers samples (R^2= 0.997).

MSE can be thus considered as an efficient and valid method to quantitatively extract MeHg in hair and feather samples covering a great range of Hg concentrations. However, it is important to highlight that, in this study, MeHg extracted by MSE has been measured by isotope dilution and not by external calibration, allowing to obtain more precise measurements and to correct possible losses or transformations during the whole analytical procedure and providing a more precise quantification of MeHg concentrations. Determination of Hg concentrations by external calibration, as it was performed by previously published studies on Hg speciation using MSE (Thompson and Furness, 1989a; Thompson et al., 1991; Kim et al., 1996; Thompson et al., 1998b), could induce a lack of accuracy and precision and therefore errors in MeHg quantification.

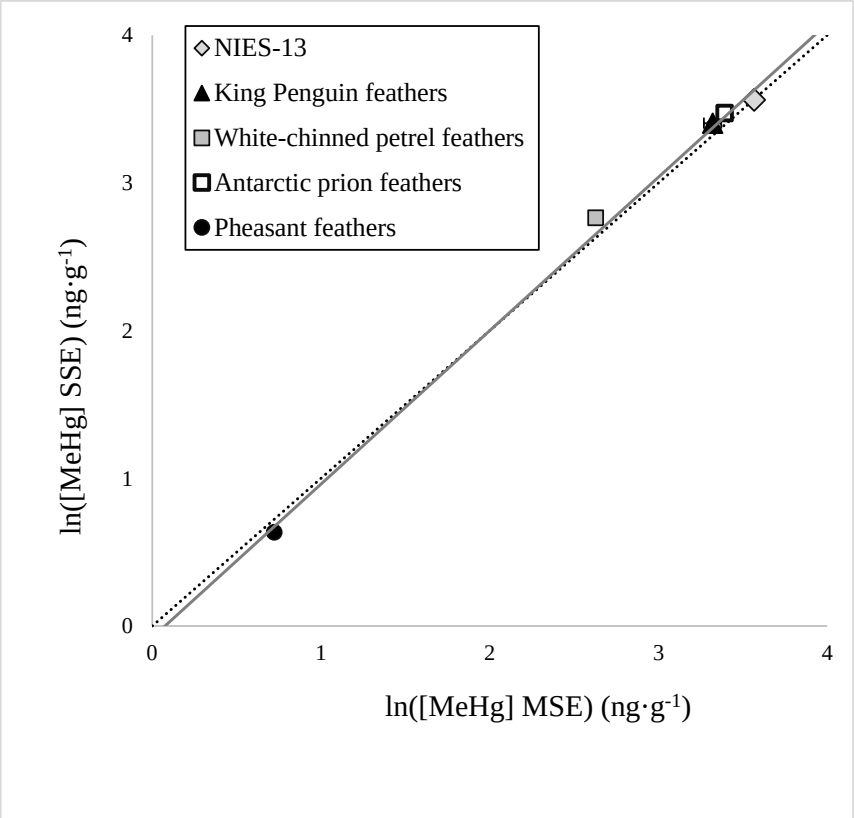

Figure 2.3. Comparison of MeHg concentrations (ng·g-1, logarithmic representation) obtained by simultaneous species extraction (SSE) and MeHg selective extraction (MSE) methods by isotope dilution analyses with spike addition before extraction in certified reference material (NIES-13) and feather samples for the key species studied. Trend line y = 1.0399x - 0.0798 (Pearson's correlation, r=0.998, p<0.001, n=5)

Hg speciation in feathers from Southern Ocean seabirds

The optimised SSE method was applied on feather samples from a large number of marine birds from the Southern Ocean. This selection of seabird species exploiting different ecological characteristics (such as feeding habits, trophic positions and thus different Hg exposure conditions) permits to use our developed speciation method in feathers covering a large range of Hg concentrations (from 375±87 to 39924±29412 ng THg·g^{-1}, corresponding to Adélie penguins and wandering albatrosses, respectively). Values of MeHg, iHg and THg concentrations (as MeHg+iHg) are presented in Table 2.4. THg concentrations values obtained by AMA-254 and those calculated as the sum of MeHg and iHg concentrations by SSE method for all the feather samples were highly correlated (Pearson's correlation, r=0.985, p<0.001, n=175) (Figure 2.S1).

Generally, penguins displayed the lowest feather MeHg concentrations whereas southern and northern giant petrels, subantarctic skuas and wandering albatrosses presented significantly higher MeHg concentrations (Kruskal-Wallis, H= 156.27, p<0.0001, *n=175*). Considering the proportion of MeHg in the feathers, no substantial differences were found among the different analysed species (Kruskal-Wallis, H= 73.06, p<0.0001, *n=175*), with MeHg being the major Hg compound for all the individuals. As it was expected, all the feathers displayed more than 80% of Hg as MeHg. This result is coherent with a dominant presence of MeHg in feathers obtained in previous studies on seabirds from different localities (Kim et al., 1996; Thompson et al., 1998b; Bond et al., 2009). It indicates that Hg speciation in feathers is not influenced by the levels of Hg concentrations, with MeHg being the most abundant compound since it is preferentially excreted via feathers for detoxification purposes (e.g., Thompson et al., 1998b; Bearhop et al., 2000)). Despite the predominance of MeHg in seabird feathers, the amounts of iHg appeared to be non-negligible (reaching almost 20% of total Hg in some individuals). This result highlights the necessity of measuring both Hg compounds in feathers to better investigate Hg exposure and metabolic response of birds.

Table 2.4. Results of MeHg, iHg and THg concentrations obtained for feathers of 13 seabird species of the Southern Ocean. Values are expressed as mean±SD. N means number of individuals analysed. Groups with different letter presented statistically different values (Kruskal-Wallis).

Species	Locality	Sampling dates	Status	Chick diet	n	THg		iHg	MeHg				
						(ng g^{-1})		(ng g^{-1})	(ng g^{-1})	Statistic	%		Statistic
Spheniscidae													
Emperor penguin	Terre Adélie	Nov 2011	Chicks	pelagic fish	10	812±100	(662-1047)	48±19	764±96	A,B	94±2	(88-97%)	B,C.D.E
King penguin	Crozet	Oct 2011	Adults	pelagic fish	11	2291±704	(1658-4141)	178±82	2113±633	D,E,F	92±2	(89-95%)	A,B,C,D
Adélie penguin	Terre Adélie	Feb 2012	Adults	pelagic crustaceans & fish	10	375±87	(289-532)	28±16	347±76	A	93±3	(88-98%)	A,B,C,D,E
Gentoo penguin	Crozet	Oct 2011	Adults	crustaceans & fish	11	4330±1853	(1548-7590)	430±181	3899±1686	E,F	90±2	(87-92%)	A
Macaroni penguin	Crozet	Jan 2012	Adults	pelagic crustaceans & fish	10	2274±244	(1852-2575)	222±49	2053±231	F,G	90±2	(87-94%)	A
Southern rockhopper penguin	Crozet	Feb 2012	Adults	pelagic crustaceans & fish	10	1388±243	(1055-1685)	110±36	1279±214	A,B,C	92±2	(90-95%)	A,B,C
Northern rockhopper penguin	Amsterdam	Nov 2011	Adults	pelagic crustaceans, fish & squid	10	1692±241	(1250-2033)	122±43	1571±243	B,C,D	93±3	(88-95%)	A,B,C,D,E

Diomedeidae													
Wandering albatross	Crozet	Dec 2007-Mar 2008	Adults	cephalopods	10	39924±29412	(6334-91651)	3044±2846	35880±28229	J	90±6	(81-99%)	A,B,C
Procellariidae													
Northern giant petrel	Crozet	Jan 2009	Chicks	seabirds	10	5760±1675	(3935-8867)	447±145	5317±1543	G,H	92±1	(90-94%)	A,B,C
Northern giant petrel	Crozet	Nov 2008	Adults	seabirds	10	12714±6904	(4730-28823)	541±364	12173±6563	I,J	96±1	(90-94%)	E
Southern giant petrel	Crozet	Feb-Mar 2009	Chicks	seabirds	11	5795±821	(4899-7733)	532±146	5263±829	G,H	91±3	(84-93%)	A,B
Southern giant petrel	Crozet	Oct 2009	Adults	seabirds	10	11082±4623	(5066-19966)	587±301	10495±4438	I,J	95±2	(89-96%)	C,D,E
Antarctic prion	Kerguelen	Jan 2012	Adults	crustaceans	10	2568±918	(1219-3985)	152±68	2416±888	D,E,F	92±1	(89-94%)	A,B,C
Stercorariidae													
Antarctic skua	Terre Adélie	Dec 2011-Jan 2012	Chicks	penguins	11	1933±284	(1338-2393)	165±80	1817±266	C,D,E	92±3	(84-95%)	A,B,C
Subantarctic skua	Kerguelen	Dec 2011	Chicks	petrels	10	6978±116	(4134-8210)	500±189	6493±1082	H,I	93±2	(89-96%)	A,B,C,D,E
Subantarctic skua	Crozet	Jan-Feb 2012	Chicks	penguins & rats	11	4911±162	(2293-6328)	273±173	4642±1507	G,H	95±2	(89-97%)	C,D,E
Subantarctic skua	Amsterdam	Dec 2011	Chicks	unknown (seabirds?)	10	12366±2443	(9271-17667)	584±130	11782±2376	I,J	95±1	(94-96%)	D,E

Conclusions

A method for the simultaneous determination of Hg speciation in feathers was optimised and validated. The evaluation of different extraction procedures, spiking strategies and quantification methods was performed, concluding that nitric acid microwave assisted extraction with spike addition before the extraction was found the most adequate for feathers (and hair) samples. Both single-IDA and IPD quantification methods are proposed as valid analytical approaches for either routine analysis or monitoring issues (single-IDA) or metrology and analytical development purposes (IPD). In our case, due to the high number of feather samples, single-IDA was favoured because it is a more practical option. The developed method demonstrates the capability of the GC-ICPMS by using species-specific isotope dilution for the precise and accurate measurement of MeHg, iHg and thus THg as MeHg+iHg concentrations and the correction of potential transformations between MeHg and iHg compounds during the different analytical steps. It was successfully applied in environmental feather samples where MeHg appeared to be the major species for all the feathers analysed independently of THg concentrations. This finding fits well with the evidence that seabirds excrete MeHg in moulting feathers as a Hg detoxification strategy. However, non-negligible amounts of iHg were present in feathers from some individuals. This finding, together with the existence of accidental iHg contamination in feather museum collections, supports the recommended application of methods measuring both Hg compounds' concentrations in feathers.

1.2 Method optimisation for Hg speciation analyses in avian blood and internal tissues

Introduction

The performance of an analytical technique for Hg speciation by GC-ICPMS requires the optimisation of different procedures and parameters such as sample preparation, extraction, derivatisation, chromatographic separation and selective detection. Moreover, when applying the isotope dilution technique, the optimisation of the spike procedure (addition before or after extraction) and the choice of the quantification method are crucial for the assessment and correction of possible Hg species interconversions during the whole analytical procedure. Most of the studies focusing on Hg species extraction, especially in organs and other biological tissues, used MW assisted extraction with a preference for alkaline extraction in TMAH since it enables the total hydrolysis of biological tissues conserving intact C-Hg bounds (Rodriguez Martin-Doimeadios et al., 2002; Point et al., 2007; Monperrus et al., 2008; Clémens et al., 2011; Navarro

et al., 2013). Accurate and precise quantification of Hg speciation requires exigent parameters such as quite low LOQ in the order of ng L^{-1}, important specificity to avoid matrix effects and satisfactory repeatability and reproducibility of the analytical method. The objective of this assessment was to find the most adequate extraction method for Hg species extraction in seabird internal tissues by testing different systems and reagents. The procedures were validated for MeHg and THg concentrations with a CRM (liver and muscle) and IRM (blood).

Experimental

Samples and reference materials

Internal tissues (pectoral muscle and liver) from a dead individual of southern giant petrel (*Macronectes giganteus*) were sampled, weighed and stored individually in plastic bags. This species was used because it is both a large animal when adults and it display high Hg concentrations in its tissues (González-Solís, Sanpera, and Ruiz 2002) so large quantities of tissues were available for the technique development and their assessment. In order to optimise and validate the developed methods for Hg speciation analyses, two CRM were used: DOLT-4 (Dogfish liver, NRCC) and ERM-CE-464 (Tuna fish, IRMM) for liver and muscle extractions, respectively. Both CRM are certified in THg and MeHg concentrations. Since no CRM of bird blood was obtainable, a pool sample of blood collected from different individuals of king penguin was prepared and used as IRM.

Sample preparation and extraction procedures

After dissection, bird tissues were stored at -80°C, and prior to the extraction they were cryogenically pulverized and freeze-dried. Two reagents were tested for extraction of Hg species on the studied avian samples: the classically used alkaline extraction in TMAH and a nitric acid extraction (HNO_3·6N). As for feathers, MW and HB extraction systems were also evaluated and compared, but in this case spike addition procedure was uniquely accomplished after extraction of blood and tissues because the conversion between Hg compounds has not been documented for this kind of samples. Blanks of extraction were performed in triplicate for each reagent and extraction system and then each extract was analysed in triplicate injection. Sample amounts of seabird tissues and CRM (between 0.10-0.15 g) were digested in 5 mL of reagent (Figure 2.4).

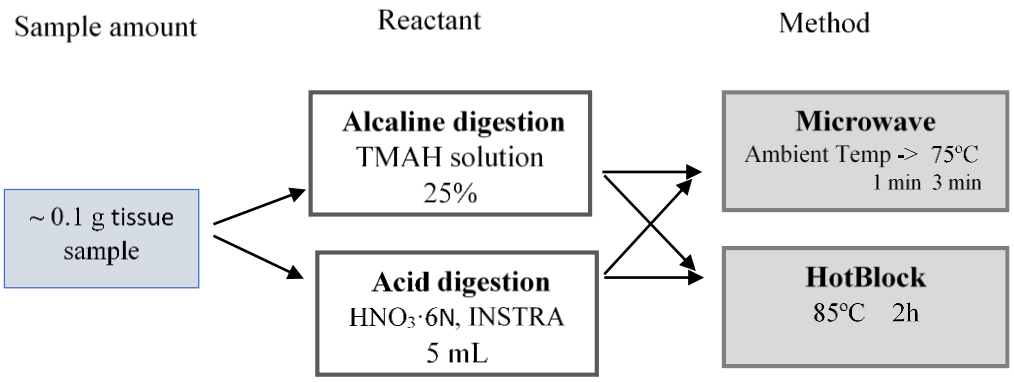

Figure 2.4. Optimisation procedure for Hg speciation analyses in tissues: scheme of the extraction methods tested

Quantification methods for isotopic dilution calibration

As performed for feathers, Hg species concentrations were quantified by both single-IDA and IPD and transformation factors were calculated using IPD, allowing to evaluate interconversion reactions (M% and D%) that occur during derivatisation of each analytical procedure tested. THg concentrations calculated as the sum of MeHg and iHg were compared to the concentrations determined by AMA-254 to calculate the recovery of the extraction.

Total Hg analyses

THg concentrations were quantified by using an advanced Hg analyser spectrophotometer (AMA-254, Altec). Homogenised samples (aliquots between 10 and 15 mg) were analysed in triplicate. Several blanks were analysed at the beginning of each analytical session. Limit of detection (LOD), calculated for blank average values (15 blanks) plus three times the standard deviation (SD) of these blanks (IUPAC), was 0.15 ng g^{-1}.

Results and discussion

Liver samples

All the extraction methods tested in liver samples provided satisfactory results for Hg concentrations except MW acid extraction, which resulted in an insufficient recovery for iHg species relative to CRM values (DOLT-4). The absence of substantial methylation factor observed by IPD results suggests that transformations between Hg compounds during the derivatisation step could not explain the uncomplete extraction for iHg by acid MW method. Two explanations are therefore possible: 1) an important methylation occurred during acid MW extraction (and

could not be corrected since spike solutions were added after extraction); or 2) MW conditions were not adjusted to this kind of extraction. By contrast, acid extraction using HB provided good recoveries for both MeHg (87.8±5.5%) and THg (94.5±2.5%) so it appeared to be a valid reagent for liver sample extraction. Nevertheless, better recoveries were obtained for alkaline extraction in TMAH with both HB (MeHg: 93.4±2.8%, THg: 96.0±2.9%) and MW (MeHg: 95.4±3.4%, THg: 97.5±3.2%) extraction systems, therefore indicating the best recoveries for MW TMAH extraction. Generally, no significant differences in concentration values were observed between single-IDA and IPD calculation methods for DOLT-4 reference material. A slightly higher D% factor was observed for DOLT-4 alkaline extracts by MW (1.4±0.7%) and HB (0.9±0.2%) but did not involve a substantial difference in final Hg species concentrations (Table 2.5).

Table 2.5. Results of Hg species concentrations and recoveries obtained for the different extraction methods tested in CRM (DOLT-4) and calculated by Single-IDA and IPD. Species interconversion factors were calculated by IPD. n is referred to number of extractions.

DOLT-4	**Dogfish liver CRM**										
					Concentrations (ng·g^{-1})			**Recoveries (%)**			
Quant. Method	**System**	**Extr**	**Spike addition**	**n**	**MeHg**	**iHg**	**THg**	**MeHg**	**THg**	**M %**	**D%**
			Certified values		**1330±120**	**~1250**	**2580±220**				
Single-IDA	MW	TMAH	after extraction	3	1202±13	1154±42	2516±81	95.4±3.4	97.5±3.2		
	MW	HNO_3· 6N	after extraction	3	1192±23	735±21	1927±12	89.6±1.7	74.7±0.5		
	HB	TMAH	after extraction	3	1242±37	1235±38	2478±75	93.4±2.8	96.0±2.9		
	HB	HNO_3· 6N	after extraction	3	1134±16	1271±18	2439±64	87.8±5.5	94.5±2.5		
IPD	MW	TMAH	after extraction	3	1236±4	1226±41	2462±44	92.9±0.3	95.4±1.7	0.3±0.2	1.4±0.7
	MW	HNO_3· 6N	after extraction	3	1119±25	737±18	1855±11	84.1±1.9	71.9±0.4	0.4±0.1	0.5±0.2
	HB	TMAH	after extraction	3	1241±32	1174±28	2416±59	93.3±2.4	93.6±2.3	0.5±1.0	0.9±0.2
	HB	HNO_3· 6N	after extraction	3	1168±7	1344±30	2511±37	87.8±0.5	97.3±1.4	0.7±0.3	0.1±0.6

As for the reference liver material, the digestion of giant petrel liver (F-GPA01) also resulted in an insufficient recovery for iHg by MW acid extraction relative to the reference THg concentration value obtained by AMA-254. Calculated recoveries for HB extraction procedures tested in F-PGA01 were satisfactory for acid HB (103.7±6.2%), TMAH HB (94.9±4.0%), and TMAH MW extraction (114.1±9.2%). Although no substantial differences in concentration values were observed between single-IDA and IPD calculation methods for giant petrel liver F-PGA01, important D% factors were obtained for acid HB extract (5.5±3.6%) and for alkaline MW extract (4.9±9.0%), suggesting that this seabird liver sample can potentially undergo demethylation during the derivatisation step independently of the extraction reagent. Despite these relatively high M%, MeHg concentrations calculated by single-IDA and IPD are not significantly different (Table 2.6).

Table 2.6. Results of Hg species concentrations and recoveries obtained for avian liver sample (giant petrel, F-PGA01) and calculated by the two different calculation methods (Single-IDA and IPD). Species interconversion factors were calculated by IPD. n is referred to number of extractions.

F-PGA01					Concentrations (µg·g^{-1})			Recovery (%)		
Quant. method	**System**	**Extr.**	**Spike addition**	**n**	**MeHg**	**iHg**	**THg**	**THg**	**M %**	**D%**
			AMA-254 value				**187.7±22.3**			
Single-IDA	MW	TMAH	after extraction	3	5.1±8.0	209.1±34.2	214.2±34.2	114.1±9.2		
	MW	HNO_3·6 N	after extraction	3	4.1±0.1	118.4±12.4	122.5±12.4	65.3±4.9		
	HB	TMAH	after extraction	3	3.9±0.2	174.2±12.9	178.2±12.9	94.9±4.0		
	HB	HNO_3·6 N	after extraction	3	3.6±0.1	191.1±14.9	194.6±14.9	103.7±6.2		
IPD	MW	TMAH	after extraction	3	4.3±0.3	204.4±24.6	208.7±6.8	111.1±13.3	0.2±0.1	0.4±3.4
	MW	HNO_3·6 N	after extraction	3	3.9±0.1	117.6±9.5	121.5±13.0	64.7±5.1	0.2±0.1	5.5±3.6
	HB	TMAH	after extraction	3	3.4±0.2	166.8±6.8	170.3±24.7	90.7±3.7	0.2±0.1	4.9±9.0
	HB	HNO_3·6 N	after extraction	3	3.1±0.2	185.9±13.0	189.0±9.5	101.0±7.0	0.1±0.1	0.2±2.5

In conclusion, TMAH MW extraction provided the most satisfactory results for Hg species extraction in DOLT-4 CRM relative to reference values (MeHg and THg). For the avian liver, TMAH MW was also chosen since it provided good recoveries relative to AMA-254 obtained concentration. Both single-IDA and IPD quantification methods seemed to be valid analytical approaches for data treatment.

Muscle samples

As observed in livers, acid extractions in MW did not provide sufficient recoveries for MeHg concentrations in tuna fish ERM-CE-464 reference material (45.7±0.5%), indicating an uncomplete extraction. This result could be due to interconversion reactions during extraction or maybe a loss of matter during the extraction step that cannot be corrected by isotope dilution because spike solutions were added later. Although acid HB extraction provided a better recovery for MeHg (86.2±0.9%), the extraction was not complete for iHg species, which was due to the high M% occurring during derivatisation, as indicated by IPD quantification. Regarding the alkaline extraction procedures, good THg recoveries for ERM-CE-464 were exhibited by MW (96.8±1.3%) and HB (96.2±0.3%), indicating the validity of both extraction systems when using TMAH reagent. Nevertheless, it can be observed that for both alkaline systems there was an overestimation of iHg species and underestimation of MeHg concentrations, which could be attributed to interconversion reactions during extraction. Substantial differences in concentration values were observed between single-IDA and IPD quantification methods for HB extractions in

both alkaline and acid medium, meaning the occurrence of interconversion reactions during derivatisation. The calculation of important M% factors (46.5±4.3% for TMAH HB and 41.1±15.2% for acid HB extracts) involves the substantial differences of Hg species concentrations between both quantification methods and indicates the presence of strong methylation reactions occurring during derivatisation of HB extracts. Lower but also important M% factors were found for MW TMAH (7.2±14.7%) and MW acid (16.0±7.9%). Demethylation reactions were however insignificant whatever the extractant used (Table 2.7).

Table 2.7. Table. Results of Hg species concentrations and recoveries obtained for tuna fish CRM (ERM-CE-464) and calculated by the two different quantification methods (Single-IDA and IPD). Species interconversion factors were calculated by IPD. n is referred to number of extractions.

ERM-CE-464	**Tuna fish CRM**				**Concentrations (ng·g^{-1})**			**Recoveries (%)**			
Quant. Method	**System**	**Extr.**	**Spike addition**	**n**	**MeHg**	**iHg**	**THg**	**MeHg**	**THg**	**M %**	**D%**
			Certified values		**5117±158**	**~123**	**5240±100**				
Single-IDA	MW	TMAH	after extraction	3	4809±61	265±11	5074±67	93.9±1.2	96.8±1.3		
	MW	HNO_3· 6N	after extraction	3	2341±26	109±9	2450±29	45.7±0.5	46.7±0.6		
	HB	TMAH	after extraction	3	4858±8	184±18	5042±14	94.9±0.2	96.2±0.3		
	HB	HNO_3· 6N	after extraction	3	4416±66	72±2	4485±49	86.2±0.9	85.6±0.9		
IPD	MW	TMAH	after extraction	3	4829±167	398±12	5227±168	94.4±3.3	99.7±3.0	7.2±14.7	0.8±0.2
	MW	HNO_3· 6N	after extraction	3	2489±28	397±52	2887±60	48.6±0.6	55.1±1.2	16.0±7.9	0.5±0.2
	HB	TMAH	after extraction	3	4354±19	314±14	4668±24	85.1±0.4	89.1±0.6	46.5±4.3	0.2±0.1
	HB	HNO_3· 6N	after extraction	3	4049±45	135±3	4183±45	77.3±0.9	79.8±0.9	41.1±15.2	0.2±0.1

Regarding the results of giant petrel muscle (M-GPA01), MW acid extraction did not provide a complete extraction of MeHg and iHg compounds. The other extraction procedures achieved much better recoveries, especially MW TMAH extraction (THg: 98.9±3.3%) relative to the reference THg concentration value obtained by AMA-254. Despite the great M% factors obtained for HB extracts in the tuna fish CRM, much lower methylation reactions were found to occur in HB extracts of M-PGA01 (2.4±1.5% for TMAH and 2.9±1.0% for acid). In the contrary, a notable D% factor was calculated for MW TMAH extracts (7.2±0.9%). No substantial demethylation reactions seemed to occur during the derivatisation when using other extracts (Table 2.8).

Table 2.8. Results of Hg species concentrations and recoveries obtained for avian muscle (giant petrel, M-PGA01) and calculated by the two different quantification methods (Single-IDA and IPD). Species interconversion factors were calculated by IPD. n is referred to number of extractions.

M-PGA01					**Concentrations (ng·g^{-1})**			**Recovery (%)**		
Quant. Method	**System**	**Extractant**	**Spike addition**	**n**	**MeHg**	**iHg**	**THg**	**THg**	**M %**	**D%**
			AMA-254 value				**4158±256**			
Single-IDA	MW	TMAH	after extraction	3	2086±13	2026±144	4113±144	98.9±3.3		
	MW	HNO_3·6 N	after extraction	3	1907±96	1209±503	3117±512	75.0±11.7		
	HB	TMAH	after extraction	3	2087±228	1839±275	3926±228	90.5±1.5		
	HB	HNO_3·6 N	after extraction	3	1853±311	1842±18	3695±312	88.9±6.5		
IPD	MW	TMAH	after extraction	3	2000±32	1869±146	3869±150	93.1±3.4	0.3±0.6	7.2±0.9
	MW	HNO_3·6 N	after extraction	3	1887±172	1328±404	3215±439	77.3±11.1	0.3±0.5	0.5±0.3
	HB	TMAH	after extraction	3	1710±496	1769±166	3479±253	83.7±15.8	2.4±1.5	0.3±0.4
	HB	HNO_3·6 N	after extraction	3	1940±48	1837±73	3777±88	90.4±3.5	2.9±1.0	0.1±0.3

As for livers, alkaline extraction appeared the most adequate method for muscle digestion. Both HB and MW extraction techniques were suitable and valid for the complete extraction of MeHg and iHg species, however MW is a more robust and easily controlled technique so it was selected for digestion of muscles. Both single-IDA and IPD quantification methods seemed to be valid analytical approaches for data treatment and, as observed for feathers, were proposed and preferred for routine analysis (single-IDA is suggested) or analytical development (IPD). For this work, once the assessment and development of the analytical approaches was accomplished, single-IDA was applied due to practical aspects and the numerous samples to be analysed.

Blood samples

For the blood sample (RBC-KP), satisfactory recoveries were obtained for all the extraction methods and reagents relative to reference concentration value (AMA-254), indicating their suitability for blood samples digestion and also suggesting that the organic matrix of the blood cells is much more easier to digest compare to the other tissues. Slight methylation (M% ~1%) and demethylation reactions (D%~2%) were observed during derivatization of blood samples irrespectively of the method used but no differences were found among the two quantification methods (single-IDA and IPD). Alkaline extraction was preferred because it enables that the matrix is completely dissolved so that extract recuperation is much easier than for acid extracts. Moreover, TMAH MW extraction exhibited the most accurate results (100.4±2.3%) and was thus

preferred among the rest of methods. Single-IDA was chosen since it is the most practical quantification option (Table 2.9).

Table 2.9. Results of Hg species concentrations and recoveries obtained for avian blood samples (red blood cells, RBC-KP) and calculated by the two different quantification methods (Single-IDA and IPD). Species interconversion factors were calculated by IPD. n is referred to number of extractions.

RBC-KP					**Concentrations (ng·g^{-1})**			**Recovery (%)**		
Quant. Method	**System**	**Extr.**	**Spike addition**	**n**	**MeHg**	**iHg**	**THg**	**THg**	**M %**	**D%**
			AMA-254 value				**1980±76**			
Single-IDA	MW	TMAH	after extraction	3	1956±38	62±13	1988±39	100.4±2.3		
	MW	HNO_3·6 N	after extraction	3	1896±32	54±21	1951±42	98.5±2.1		
	HB	TMAH	after extraction	3	1917±43	85±7	2003±45	101.1±2.3		
	HB	HNO_3·6 N	after extraction	3	1979±78	70±16	2079±93	105.0±4.7		
IPD	MW	TMAH	after extraction	3	1989±42	72±9	2061±41	104.1±1.3	0.9±0.5	1.3±0.3
	MW	HNO_3·6 N	after extraction	3	2028±54	64±7	2092±59	105.6±3.0	1.1±0.5	1.9±0.3
	HB	TMAH	after extraction	3	1954±36	77±9	2031±32	102.6±1.6	1.0±0.4	1.7±0.1
	HB	HNO_3·6 N	after extraction	3	1980±78	68±4	2048±76	103.4±3.9	1.1±0.4	1.9±0.2

1.3 Analytical performances and long-term internal reproducibility of the Hg speciation method (SSE)

After the evaluation of different extraction techniques and reagents, we concluded that:

- **MW assisted extraction** was the most robust and easily controlled technique so it was selected for Hg species extraction in all the studied matrixes.
- **Acid extraction** appeared the most suitable technique **for keratinised samples** (human hair and feathers) whereas **alkaline extraction** provided the most satisfactory results **for internal tissues** (livers and muscles) **and blood** samples.
- Both single-IDA and IPD quantification methods were considered valid analytical approaches for data treatment. **Single-IDA is suggested for routine analysis** or when the number of samples is substantial (due to its practical advantages), whereas **IPD is recommended for analytical development**.

Sensitivity, precision and accuracy of the optimised extraction methods were evaluated for the different matrixes (Table 2.10). The sensitivity was assessed by the measurement of calibration slopes calculated as the relation of the peak area obtained for ^{202}MeHg (counts per

second, cps) divided by the concentration of MeHg injected ($ng \cdot L^{-1}$) for the injection in 2 µL of isooctane. Sensitivity is reported as the mean value for the 9 injections. The precision was calculated as the mean RSD of 3 injections of each extract. Accuracy was calculated by recoveries of MeHg and THg relative to certified values for CRM (NIES-13, DOLT-4 and ERM-CE-464).

Table 2.10. Analytical performances of the optimised MW assisted extraction (3 extractions) for the studied matrixes in acid (keratinised samples) and in TMAH (internal tissues and blood samples)

Matrix	**Sample**		**Sensitivity (cps/ng L^{-1})**	**Precision (%)**		**Accuracy (%)**	
				MeHg	**iHg**	**MeHg**	**THg**
Hair	CRM human hair	NIES-13	8.14E+05	0.38±0.05	1.59±0.31	95.9±1.2	95.9±0.2
Feathers	IRM King penguin	F-KP	1.05E+06	1.30±0.34	1.58±0.23	-	102±1.5
Liver	CRM Dogfish liver	DOLT-4	7.07E+07	1.04±1.01	3.64±1.28	95.4±3.4	97.5±3.2
	Giant petrel liver	F-PGA01	8.12E+04	2.87±2.42	1.22±1.19	-	114.1±9.2
Muscle	CRM Tuna fish	ERM-CE-464	6.19E+07	1.30±0.85	4.16±1.20	93.9±1.2	96.8±1.3
	Giant petrel muscle	M-PGA01	4.83E+05	1.61±1.08	2.15±1.34	-	98.9±3.3
Blood	IRM King penguin	RBC-KP	1.32E+06	1.36±1.08	5.48±3.28	-	100.4±2.3

An evaluation of long-term internal reproducibility and repeatability of the optimised method was performed on CRM (NIES-13, DOLT-4 and ERM-CE-464) and on our IRM for feather samples (F-KP) and avian blood samples (RBC-KP). Internal reproducibility was assessed for triplicate injection of the three extracts of each reference material (n=9), prepared following identical protocols and by the same operator and equipment in each analytical session, with 1-6 months of interval. Since the term reproducibility implies the involvement of measurement by different operators and laboratories, we use the term internal reproducibility. Repeatability was estimated by analysing in triplicate the same extract the same day, under identical conditions (n=3). For keratinised matrixes by acid extraction, limits of detection (LOD) and quantification (LOQ) were calculated as the sum of spiked HNO_3·6N blank average values analysed in triplicate (15 blanks of extraction) plus three times the standard deviation (SD) of these blanks for LOD or ten times for LOQ (IUPAC). For extraction of 0.25 g of hair or feathers in 5 mL of HNO_3·6N, LOD obtained is 3.24 ng g^{-1} and 11.62 ng g^{-1} and LOQ is 9.04 ng g^{-1} and 30.37 ng g^{-1}, for MeHg and iHg, respectively.

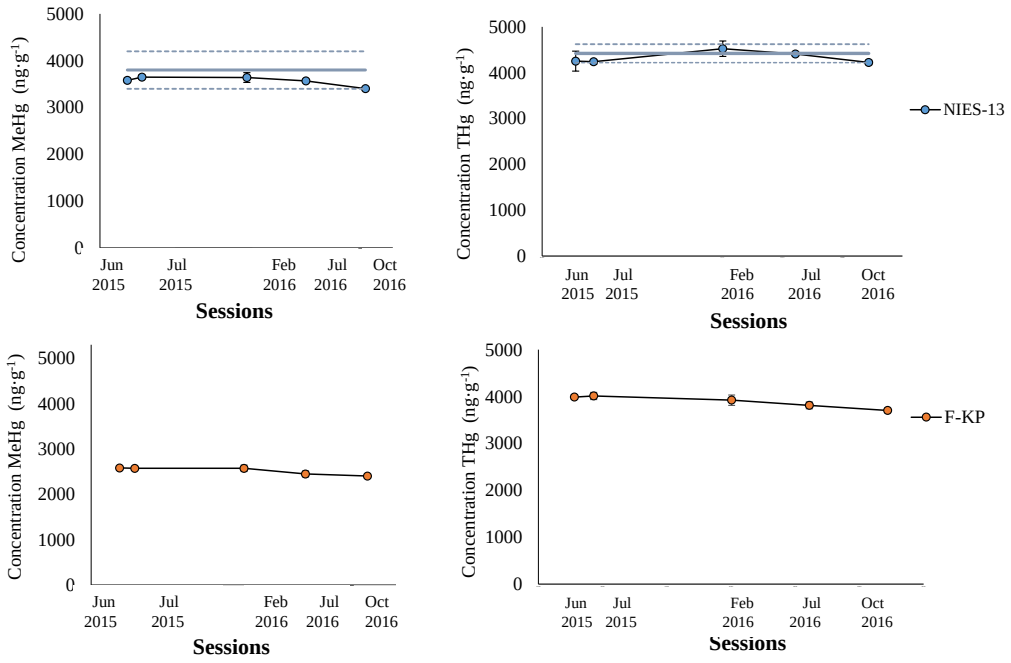

Figure 2.5. Control charts of measured MeHg and THg concentrations for keratinised reference materials NIES-13 and F-KP for each analytical session.

In the case of alkaline extraction for internal tissues and blood (extraction of 0.10 g of blood or internal tissue sample in 5 mL of TMAH), LOD obtained is 4.05 ng g^{-1} and 12.45 ng g^{-1} and LOQ is 11.04 ng g^{-1} and 28.49 ng g^{-1}, for MeHg and iHg, respectively (20 blanks of extraction).

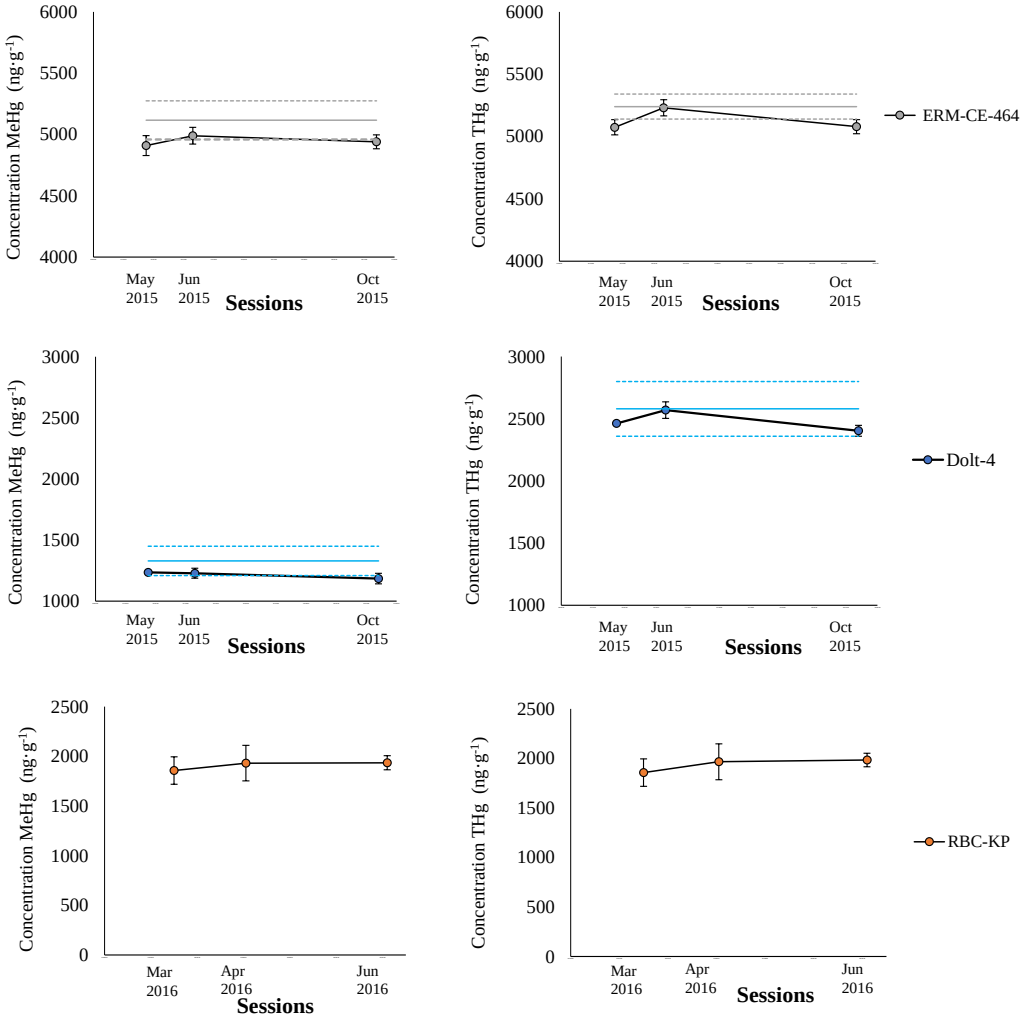

Figure 2.6. Control charts of measured MeHg and THg concentrations for reference materials ERM-CE-464 and DOLT-4 and for IRM RBC-KP for each analytical session.

Part 2.2: Hg isotopic analyses: optimisation of Hg extraction techniques in avian samples (feathers, blood and internal tissues)

Introduction

Total Hg isotopic analyses in biological tissues require a rigorous sample preparation with previous homogenisation and a full extraction of Hg from the matrix. Acid digestion is the most common strategy for Hg extraction in biological samples and is followed by a dilution of the extract in acidic matrix. A complete THg extraction is essential in order to avoid potential Hg isotopic fractionation during sample preparation and to reduce possible matrix effects associated to the presence of lipids or other organic ligands in such complex biological tissues. Numerous tests of sample digestion were performed to assure a complete extraction of Hg in the samples with addition of H_2O_2 in some cases to guarantee a full oxidation of Hg. The final solution of the sample extract in an acidic matrix is 10% HNO_3 and 2% HCl for analyses. Final concentration in these diluted extracts was generally 1 ng g^{-1} and could decrease to a minimum of 0.5 ng.g^{-1} for analyses of low concentrated samples when optimal conditions of sensitivity were achieved.

Experimental

Optimisation of the extraction method

Sample preparation of feathers, internal tissues and blood was carried out as detailed in Part 2.1. Amounts of approximately 0.2 g of feathers and 0.1 g of muscle, liver and blood samples were extracted in 5 mL of HNO_3 (65%, INSTRA quality) after a predigestion step overnight at room temperature. Two different mineralization systems were tested: High Pressure Asher (HPA, Anton Paar, Austria) and HB. HPA mineralization was performed at high conditions of pressure (130 bar) and temperature (temperature ramp: 80ºC–120 ºC (2ºC/min) –300 ºC (2.5 h) – 80 ºC (1 h), total time with cooling = 4.5 h). HB mineralization was effectuated in Savillex Teflon vessels at 75ºC during 8 h (6 h in HNO_3 and 2 h more after the addition of 1/3 of the volume (1.66 mL) of H_2O_2 (30%, ULTREX quality).

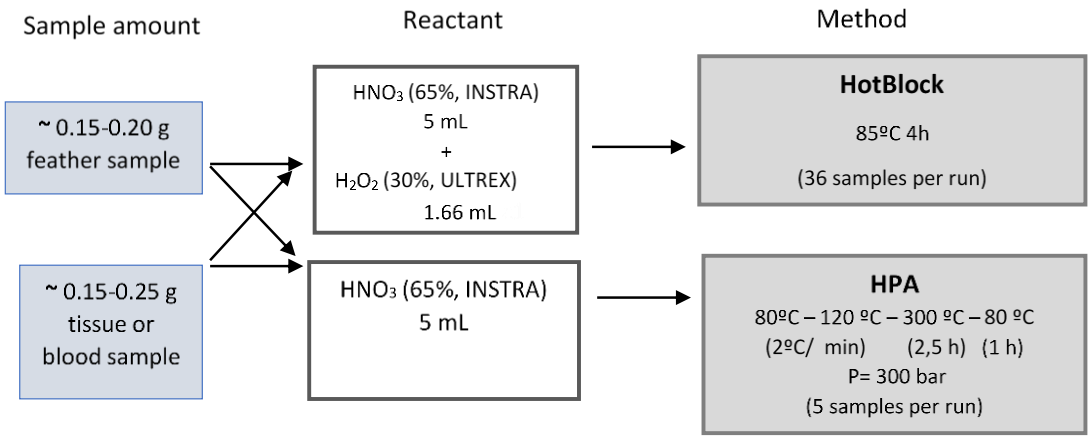

Figure 2.7. Optimisation procedure for Hg isotopic analyses in feathers, blood and internal tissues: scheme of the extraction methods tested

Reference materials of each matrix were used for the optimization: IAEA-086 (human hair), DOLT-4 (dog fish liver) and ERM-CE-464 (tuna fish muscle). IRM of feathers (F-KP), avian blood (RBC-KP) and avian tissues (muscle and liver) from the same individual of southern giant petrel (*Macronectes giganteus*) ad for speciation, were analyzed in triplicate by the two extraction protocols. Blanks of extraction were also prepared in triplicate.

Analytical parameters and instrumentation

Hg isotopic analyses were performed in a Nu Plasma HR MC-ICPMS (Nu Instruments, UK using a continuous flow Cold Vapor Generation (CVG) as sample introduction system (Blum and Bergquist 2007). The dissolved Hg^{2+} is reduced into Hg^0 by tin chloride ($SnCl_2$), separated from the rest of the matrix in a Gas Liquid Separator (GLS) and then is transported by a continuous flow of Ar to the plasma torch of the MC-ICP-MS. A DSN (Desolvating Nebuliser System, Nu Instrument, UK) and a double entry torch were used for the simultaneous introduction of a Tl isotopic standard to correct for instrumental mass bias. The overall instrumental setup is shown in Figure 2.8.

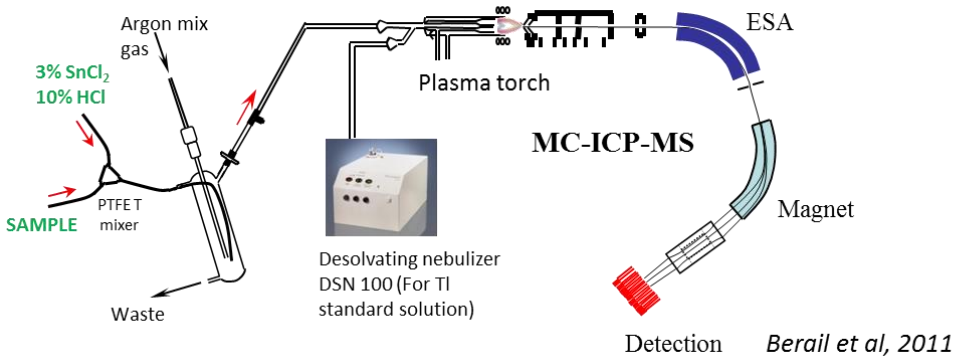

Figure 2.8. Schematic design of sample introduction into MC-ICPMS instrument. Range of [Hg] (0.5-1 ppb) and 10% HNO3 / 2% HCl for the sample. Double entry plasma torch.

Two mass bias corrections are used simultaneously to improve the precision and accuracy of the results: internal and external correction. In the case of internal mass-bias correction, NIST-SRM-997 Tl solution was used as internal standard for the correction of instrumental mass bias. Tl is used because its fractionation in the instrument is quite similar to Hg and it is located in the same mass range of the analyte. The solution is introduced continuously and the $^{205}Tl/^{203}Tl$ ratio is monitored. Then the instrumental mass-bias is calculated using an exponential law as described below:

$$\left(\frac{^{xxx}Hg}{^{198}Hg}\right)_{true} = \left(\frac{^{xxx}Hg}{^{198}Hg}\right)_{meas.} \times \frac{1}{\left(\frac{M_{xxx}}{M_{198}}\right)^{\beta}} \qquad \beta = \ln\left(\frac{\left(\frac{^{205}Tl}{^{203}Tl}\right)_{meas.}}{\left(\frac{^{205}Tl}{^{203}Tl}\right)_{true}}\right) \times \frac{1}{\ln\left(\frac{M_{205}}{M_{203}}\right)}$$

The external mass bias correction used is simply a direct consequence of the use of the delta notation against the NIST 3113 using a standard-sample bracketing sequence. This correction supposes the instrumental mass bias is the same for the sample and the NIST 3133 standard. Another secondary standard UM-Almadén (now distributed as NIST 8610) is introduced during the analysis to validate the measurements and is prepared from cinnabar ore from Almadén (Spain).

Results and discussion

Secondary standard UM-Almadén was analyzed several times during the session focused on method optimization and displayed a mean δ^{202}Hg value of −0.54±0.17‰ (Mean±2SD, n = 45), coherent with certified δ^{202}Hg value, permitting to validate the analytical session for extraction method optimization. Regarding the results obtained for Hg extraction in the three reference materials evaluated, both HPA and HB provided accurate results for human hair IAEA-086 and dogfish liver DOLT-4, according to previous isotopic values from the literature (Table 2.11). Therefore, both HPA and HB extractions appeared appropriate extraction methods for human hair and fish liver samples. However, in the case of fish muscle tissue (i.e., tuna fish muscle ERM-CE-464), HB extracts exhibited satisfactory Δ^{199}Hg values whereas δ^{202}Hg values were lower than reference values, indicating that HB digestion did not provide a full Hg extraction, even after addition of H_2O_2 and supplementary heating (2h). Therefore, HPA appeared the most suitable extraction method for muscle. It is also important to highlight that the HPA extract of ERM-CE-464 required an additional heating cycle in HB (2h) with H_2O_2 (1.66 mL) to ensure a complete extraction.

A clear limitation of this method for Hg isotopic analyses is that HPA extractions in reference materials were not carried out in triplicate as it was performed for avian samples. Therefore, the precision of HPA method could not be assessed. Precision of Hg isotopic values for HB triplicate extractions (evaluated as 2SD‰ for δ^{202}Hg and Δ^{199}Hg, respectively) were satisfactory for IAEA-086 (0.10 and 0.02 ‰) and DOLT-4 (0.18 and 0.08 ‰) but less precise results were obtained for ERM-CE-464 (0.13 and 0.15 ‰).

Table 2.11. Results Hg isotopic composition obtained for reference materials extracted by the two different mineralisation methods: HPA and Hotblock. Results are compared to values in literature. n means number of extractions.

Certified reference material	**[Hg] (µg g^{-1})**	**Digested mass (mg)**	**δ^{204} Hg**	**δ^{202} Hg**	**δ^{201} Hg**	**δ^{200} Hg**	**δ^{199} Hg**	**Δ^{204} Hg**	**Δ^{201} Hg**	**Δ^{200} Hg**	**Δ^{199} Hg**	*n*
Human hair (IAEA-086)	0.57											
HPA extraction		0.21										
Average (‰)			0.74	0.63	0.68	0.29	0.35	-0.20	0.21	-0.03	0.19	*1*
2SD (‰)			-	-	-	-	-	-	-	-	-	
HB extraction		0.15-0.17										
Average (‰)			0.95	0.69	0.75	0.33	0.37	-0.07	0.23	-0.02	0.20	*3*
2SD (‰)			0.38	0.10	0.12	0.07	0.06	0.25	0.04	0.04	0.05	
Yamawaka et al., 2016												
Average (‰)			0.87	0.58	0.64	0.31	0.41	0.00	0.20	0.02	0.26	*3*
2SD (‰)			0.12	0.09	0.09	0.04	0.02	0.04	0.03	0.04	0.02	
Dogfish liver (DOLT-4)	2.58±0.22											
HPA extraction		0.20										
Average (‰)			-0.49	-0.35	0.73	-0.09	1.08	0.03	0.99	0.08	1.17	*1*
2SD (‰)			-	-	-	-	-	-	-	-	-	
HB extraction		0.18-0.19										
Average (‰)			-0.50	-0.35	0.65	-0.16	1.00	0.02	0..92	0.01	1.09	*3*
2SD (‰)			0.08	0.18	0.09	0.05	0.09	0.02	0.18	0.04	0.08	
Masbou et al., 2014												
Average (‰)			-	-0.35	0.71	-0.14	1.03	-	0.98	0.00	1.12	*4*
2SD (‰)			-	0.2	0.06	0.06	0.07	-	0.19	0.03	0.11	
Tuna fish (ERM-CE-464)	5.24±0.10											
HPA extraction		0.17	0.87	0.65	2.36	0.40	2.50	-0.10	1.87	0.07	2.33	*1*
Average (‰)			-	-	-	-	-	-	-	-	-	
2SD (‰)												
HB extraction		0.16-0.18	0.69	0.55	2.31	0.33	2.51	-0.06	1.90	0.05	2.36	*3*
Average (‰)			0.11	0.13	0.08	0.03	0.10	0.00	0.01	0.03	0.15	
Li et al., 2014												
Average (‰)			0.94	0.70	2.49	0.43	2.55	-0.10	1.96	0	2.38	*3*
2SD (‰)			0.06	0.04	0.06	0.05	0.08	0.05	0.06	0.04	0.07	

Concerning avian samples, Hg isotopic results were similar for the two extraction methods in all the matrixes (Table 2.12). King penguin feathers (F-KP) presented identical isotopic values for the two types of extraction methods, as observed for IAEA-086, indicating that both HPA and HB are appropriate for Hg extraction in keratinized matrixes whether hairs or feathers, for a range of THg concentrations in dry material of 0.57-3.25 μg g^{-1} and for a mass a sample digested ranging from 0.22 mg to 0.25 mg. Regarding giant petrel muscle, results for HB extraction presented much lower δ^{202}Hg values in comparison with HPA extracts possibly indicating an incomplete mineralization of the matrix (due to presence of fat, organic matter, etc.) that can create matrix effects in the CVG. Nevertheless, MIF values (Δ^{199}Hg and Δ^{201}Hg) were satisfactory for HB extraction, as it was previously observed for the CRM of tuna fish muscle. Meanwhile, HPA provided satisfactory results for the three extractions and seemed to be the best choice for muscle digestion at this range of THg concentration (4.11-5.24 μg g^{-1}) and for a mass sample digested (0.20-0.25 mg), although it also required an additional heating step with H_2O_2 (during 2h). In the case of southern giant petrel liver, HPA and HB extractions presented similar isotopic values, as obtained for dogfish liver CRM and both were considered suitable extraction methods for a wide range of THg concentrations (2 to 208 μg g^{-1}) and 0.18-0.20 mg of digested sample. The availability of both extraction methods was also observed for king penguin blood sample (RBC-KP) for which HB and HPA provided similar mean delta values for THg concentration of 1.9 μg g^{-1} and 0.15-0.17 mg of digested sample.

In terms of precision (evaluated as 2SD‰), Hg extraction of king penguin feathers showed slightly more precise δ^{202}Hg values for HPA (0.06 ‰) than HB (0.12 ‰), although Δ^{199}Hg values were less precise in HPA (0.12 ‰) than HB (0.05 ‰). In the case of giant petrel liver, HPA also provided more precise δ^{202}Hg values (0.05 ‰) than HB (0.10 ‰), whereas Δ^{199}Hg values were less precise for HPA extraction (0.05 ‰) than HB (0.02 ‰). Precision of extraction in muscles was satisfactory for both delta values (respectively for δ^{202}Hg and Δ^{199}Hg) for HPA (0.09 and 0.01 ‰) whereas quite high 2SD were obtained for HB extraction (0.23 and 0.13 ‰).Slightly more precise delta values were however observed for blood HB extraction (0.10 and 0.02%) than for HPA (0.14 and 0.11 ‰).

Table 2.12. Results Hg isotopic composition obtained for the studied avian samples (feathers, muscle, liver and blood) extracted by the two different mineralisation methods: HPA and Hotblock. n means number of extractions.

	[Hg] (μg g^{-1})	Digested mass (mg)	δ^{204}Hg	δ^{202}Hg	δ^{201}Hg	δ^{200}Hg	δ^{199}Hg	Δ^{204}Hg	Δ^{201}Hg	Δ^{200}Hg	Δ^{199}Hg	*n*
King penguin feathers (F-KP)	3.25±1.18											
HPA extraction		0.23-0.24										
Average (‰)			2.36	1.58	2.70	0.80	2.10	0.00	1.52	0.01	1.70	*3*
2SD (‰)			0.17	0.06	0.07	0.06	0.12	0.14	0.03	0.07	0.12	
HB extraction		0.23-0.25										
Average (‰)			2.35	1.52	2.65	0.76	2.12	0.09	1.51	0.00	1.74	*3*
2SD (‰)			0.15	0.12	0.06	0.07	0.04	0.16	0.07	0.07	0.05	
Giant petrel muscle (M-PGA01)	4.11±0.15											
HPA extraction		0.23-0.24										
Average (‰)			0.49	0.38	1.54	0.17	1.50	-0.08	1.26	-0.02	1.41	*3*
2SD (‰)			0.08	0.09	0.04	0.08	0.04	0.17	0.04	0.04	0.01	
HB extraction		0.23-0.25										
Average (‰)			0.04	0.06	1.23	0.02	1.41	-0.05	1.18	-0.01	1.40	*3*
2SD (‰)			0.35	0.23	0.17	0.12	0.17	0.01	0.03	0.01	0.13	
Giant petrel liver (F-PGA01)	208.7±6.8											
HPA extraction		0.19-0.21										
Average (‰)			-0.44	-0.28	0.98	-0.14	1.27	-0.02	1.19	0.00	1.34	*3*
2SD (‰)			0.30	0.05	0.11	0.08	0.05	0.34	0.12	0.06	0.05	
HB extraction		0.18-0.19										
Average (‰)			-0.29	-0.22	1.04	-0.05	1.33	0.03	1.21	0.05	1.38	*3*
2SD (‰)			0.19	0.10	0.09	0.11	0.02	0.16	0.03	0.07	0.02	
King penguin blood (RBC-KP)	1.98±0.76											
HPA extraction		0.15-0.17										
Average (‰)			1.86	1.27	2.22	0.63	1.79	-0.04	1.27	-0.01	1.47	*3*
2SD (‰)			0.26	0.14	0.09	0.09	0.15	0.04	0.02	0.01	0.11	
HB extraction		0.15-0.17										
Average (‰)			1.95	1.32	2.28	0.65	1.80	-0.01	1.28	-0.01	1.47	*3*
2SD (‰)			0.10	0.10	0.04	0.03	0.04	0.15	0.11	0.03	0.02	

In conclusion on the preparation before stable isotope Hg analyses:

- Both **HPA and HB extractions can be used** as efficient extraction methods **for human hair and feathers, avian blood samples and** also for the **both types of liver** (dogfish CRM and avian liver).
- **Both methods** also showed **similar precision for the triplicate of extraction for feathers and blood**. Thus **HB was chosen due to practical reasons** because it permits a higher number of samples per cycle (36 samples for HB, 5 samples for HPA) and easier sample preparation.
- **In the case of avian liver**, although both extraction methods are suitable, **HPA provided more precise δ^{202}Hg values** (0.05 ‰) than HB (0.10 ‰), as 2SD‰. Therefore, although HPA implies a tedious preparation comparing to HB, it may deliver more satisfactory delta values for this type of matrix.
- In the case of **fish and avian muscles**, HB did not provide a complete mineralisation therefore **HPA is the unique recommended** method.
- Therefore, in this doctoral work, **HB extraction was applied for hair, feathers and blood** samples whereas **HPA was preferred for livers and muscles**.

Medium-term and long-term internal reproducibility

Internal reproducibility of the analytical method was performed on the medium and long-term measurements of CRM and IRM for avian samples (F-KP and RBC-KP) prepared following identical protocols and by the same operator and equipment during each analytical session. This permits the evaluation of both precision of the global method (extraction and MC-ICP-MS measurement) and instrumental precision (MC-ICP-MS) for the same solution analysed. Extractions were performed following the specific developed method for each matrix and one extract of each reference material was also analysed several times during the whole analytical session. Long-term internal reproducibility was also determined with 1-6 months for the different analytical sessions during this doctoral work (Table 2.13).

Since there are no certified reference isotopic values for the used reference materials except for UM-Almadén (NIST-8160), the accuracy of the method was approximate and based on published data in previous studies as reference. Precision (2SD‰) at medium-term reproducibility was evaluated for diary measurements of UM-Almadén during a whole week of analyses showing a mean precision (δ^{202}Hg and Δ^{199}Hg values) of 0.15 ‰ and 0.08 ‰ for the six

performed analytical sessions (n=30-45 analyses/session). Unlike other CRM, avian reference samples were analysed a representative number (see below) of times during each analytical session permitting an evaluation of medium-term reproducibility in this kind of samples. F-KP presented a mean precision at medium term of 0.18 ‰ and 0.10 ‰ (n=5-10 analyses/session) and RBC-KP a mean precision of 0.07 ‰ and 0.07 ‰, (n=3-5 analyses/session), both corresponding to mean precision values for three analytical sessions.

Mean isotopic values for the overall analytical sessions were correct for reference material UM-Almadén according to previously reported values in other studies with a δ^{202}Hg value of -0.55±0.08 ‰ (Mean±2SD, n=173). The precision (2SD) at long-term for Hg isotopic values was satisfactory for the most analysed reference samples: UM-Almadén (0.15 ‰ and 0.05 ‰, n=173), IAEA-086 (0.07 ‰ and 0.07 ‰, n=6), NIES-13 (0.09 ‰ and 0.07 ‰, n=8) and for the avian internal standards F-KP (0.12 ‰ and 0.07 ‰, n=22) and RBC-KP (0.05 ‰ and 0.06 ‰, n=17) for δ^{202}Hg and Δ^{199}Hg values, respectively.

Table 2.13. Results Hg isotopic composition obtained for reference materials (CRM UM-Almadén, human hair, liver, muscle and avian feathers and blood) for the overall analytical sessions performed during this doctoral work. N means number of analyses.

Reference material	Date		$\delta^{204}Hg$	$\delta^{202}Hg$	$\delta^{201}Hg$	$\delta^{200}Hg$	$\delta^{199}Hg$	$\Delta^{204}Hg$	$\Delta^{201}Hg$	$\Delta^{200}Hg$	$\Delta^{199}Hg$	*n*
UM-Almadén (CRM cinnabar)	May 2015	Average (‰)	-0.81	-0.54	-0.44	-0.26	-0.17	0.03	-0.04	0.01	-0.03	*45*
		2SD (‰)	*0.25*	*0.17*	*0.14*	*0.13*	*0.10*	*0.17*	*0.07*	*0.08*	*0.09*	
	June 2015	Average (‰)	-0.81	-0.54	-0.44	-0.26	-0.17	-0.01	-0.04	0.01	-0.03	*45*
		2SD (‰)	*0.25*	*0.17*	*0.14*	*0.13*	*0.10*	*0.15*	*0.07*	*0.08*	*0.09*	
	December 2015	Average (‰)	-1.01	-0.66	-0.50	-0.30	-0.18	-0.03	-0.01	0.03	-0.01	*4*
		2SD (‰)	*0.11*	*0.10*	*0.01*	*0.01*	*0.05*	*0.19*	*0.08*	*0.04*	*0.04*	
	March 2016	Average (‰)	-0.85	-0.57	-0.46	-0.28	-0.16	0.01	-0.03	0.01	-0.01	*29*
		2SD (‰)	*0.23*	*0.18*	*0.13*	*0.13*	*0.10*	*0.18*	*0.12*	*0.09*	*0.11*	
	July 2016	Average (‰)	-0.85	-0.56	-0.46	-0.28	-0.18	-0.02	-0.04	0.00	-0.04	*30*
		2SD (‰)	*0.19*	*0.09*	*0.10*	*0.14*	*0.11*	*0.14*	*0.07*	*0.13*	*0.10*	
	May 2017	Average (‰)	-0.74	-0.49	-0.41	-0.24	-0.16	-0.01	-0.04	0.00	-0.04	*7*
		2SD (‰)	*0.13*	*0.07*	*0.08*	*0.10*	*0.17*	*0.09*	*0.07*	*0.09*	*0.16*	
	Reference values (NIST 8610)	Average (‰)	-0.82	-0.56	-0.46	-0.27	-0.17	-	-0.04	0.00	-0.03	
		2SD (‰)	*0.07*	*0.03*	*0.02*	*0.01*	*0.01*	-	*0.01*	*0.01*	*0.02*	
IAEA-086	June 2015	Value (‰)	1.23	0.81	0.76	0.45	0.50	0.02	0.15	0.04	0.29	*1*
(RM humain hair)	March 2016	Average (‰)	0.94	0.73	0.77	0.37	0.44	-0.14	0.22	0.00	0.26	*5*
		2SD (‰)	*0.25*	*0.13*	*0.09*	*0.11*	*0.16*	*0.26*	*0.08*	*0.09*	*0.15*	
	Yamakawa et al. 2016	Average (‰)	0.87	0.58	0.64	0.31	0.41	0.00	0.20	0.02	0.26	*3*
		2SD (‰)	*0.12*	*0.09*	*0.09*	*0.04*	*0.02*	*0.04*	*0.03*	*0.04*	*0.02*	
NIES-13	June 2015	Value (‰)	2.98	2.07	3.07	1.10	2.29	-0.11	1.51	0.06	1.76	*1*
(CRM humain hair)	March 2016	Average (‰)	2.99	2.11	3.11	1.08	2.34	-0.14	1.52	0.05	1.80	*5*
		2SD (‰)	*0.28*	*0.13*	*0.16*	*0.01*	*0.14*	*0.24*	*0.05*	*0.07*	*0.08*	
	July 2016	Value (‰)	3.08	2.21	3.18	1.18	2.42	-0.22	1.52	0.07	1.87	*1*
	May 2017	Value (‰)	2.96	2.10	3.05	1.05	2.35	-0.01	1.52	0.06	1.85	*1*

	Yamakawa et al. 2016	Average (‰)	2.76	1.89	2.77	0.98	2.13	-0.04	1.36	0.04	1.65	*11*
		2SD (‰)	*0.16*	*0.10*	*0.10*	*0.08*	*0.07*	*0.11*	*0.07*	*0.04*	*0.06*	
DOLT-4	May 2015	Value (‰)	-0.53	-0.35	0.65	-0.16	1.00	0.00	0.92	0.01	1.09	*1*
	June 2015	Value (‰)	-0.47	-0.31	0.67	-0.10	1.02	-0.02	0.90	0.06	1.10	*1*
	Masbou, 2014	Average (‰)	-	-0.35	0.71	-0.14	1.03		0.98	0.02	1.12	*4*
(CRM dogfish liver)		2SD (‰)	-	*0.20*	*0.06*	*0.06*	*0.07*		*0.19*	*0.03*	*0.11*	
	Perrot et al, 2012	Average (‰)	-0.58	-0.34	0.69	-0.14	1.04		-	-	-	*3*
		2SD (‰)	*0.18*	*0.13*	*0.02*	*0.01*	*0.11*		-	-	-	
ERM-CE-464	May 2015	Value (‰)	0.87	0.65	2.36	0.40	2.50	-0.11	1.87	0.07	2.33	*1*
	June 2015	Value (‰)	0.96	0.63	2.38	0.40	2.49	0.03	1.91	0.08	2.33	*1*
	December 2015	Value (‰)	0.62	0.46	2.25	0.30	2.58	-0.06	1.91	0.07	2.47	*1*
(CRM tuna fish)	Sherman et al.,2012a	Average (‰)	-	0.68	2.48	0.43	2.57		1.97	0.09	2.40	*9*
		2SD (‰)	-	*0.06*	*0.03*	*0.05*	*0.08*		*0.03*	*0.04*	*0.07*	
	Li et al., 2014	Average (‰)	0.94	0.70	2.49	0.43	2.55		1.96	0.07	2.38	*9*
		2SD (‰)	*0.06*	*0.04*	*0.06*	*0.05*	*0.08*		*0.06*	*0.04*	*0.07*	
F-KP	May 2015	Average (‰)	2.30	1.52	2.64	0.77	2.11	0.09	1.50	0.00	1.73	*8*
		2SD (‰)	*0.32*	*0.22*	*0.20*	*0.11*	*0.08*	*0.16*	*0.06*	*0.06*	*0.08*	
	March 2016	Average (‰)	2.40	1.58	2.68	0.80	2.11	0.04	1.49	0.00	1.71	*10*
(IRM penguin feathers)		2SD (‰)	*0.24*	*0.26*	*0.17*	*0.15*	*0.18*	*0.31*	*0.12*	*0.06*	*0.15*	
	July 2016	Average (‰)	2.44	1.60	2.70	0.85	2.15	0.05	1.50	0.04	1.74	*5*
		2SD (‰)	0.26	0.15	0.16	0.18	0.15	0.11	0.07	0.12	0.12	
	March 2016	Average (‰)	1.95	1.32	2.28	0.65	1.80	-0.01	1.28	-0.01	1.47	*3*
RBC-KP		2SD (‰)	*0.10*	*0.10*	*0.04*	*0.03*	*0.04*	*0.15*	*0.11*	*0.03*	*0.02*	
	April 2016	Average (‰)	1.60	0.99	2.08	0.52	1.84	0.12	1.34	0.02	1.59	*3*
(IRM penguin blood)		2SD (‰)	*0.37*	*0.20*	*0.29*	*0.36*	*0.08*	*0.15*	*0.14*	*0.25*	*0.05*	
	July 2016	Average (‰)	1.99	1.30	2.26	0.62	1.77	0.05	1.28	-0.03	1.44	*5*
		2SD (‰)	*0.15*	*0.10*	*0.12*	*0.11*	*0.16*	*0.10*	*0.10*	*0.07*	*0.15*	

Chapter 3.

Methodological approach: Biological aspects

Chapter 3. Methodological approach: biological aspects

Part 3.1: Blood and feathers from seabirds as efficient biomonitoring tissues for Hg isotopic studies: implications of using chicks and adults

Abstract

Seabirds bioaccumulate important Hg concentrations in their tissues as a direct consequence of their medium to high trophic position within marine food webs. Blood and feathers are the most targeted avian tissues for environmental biomonitoring studies, as they respectively reflect Hg short and long-term exposure and can be easily and non-destructively sampled on live individuals. Studying Hg isotopic ratios in seabird tissues can provide valuable information for avian ecology studies but it also represents a promising approach for tracking sources and pathways of Hg in marine ecosystems. Nevertheless, a good knowledge of the Hg isotopic differences between blood and feathers is required for the interpretation of the information provided by each tissue. This study presents the first comparison of Hg isotopic composition of blood and feathers, which were sampled on seabird chicks and adults from diverse breeding colonies of the Southern Ocean. Chicks of Antarctic and subantarctic skuas (n=40) and adults from six species of penguins (n=62) were chosen for this purpose. Our results indicated a strong correlation between blood and feathers Hg isotopic ratios in the case of skua chicks, with almost identical values for both tissues in all the individuals (mean difference of -0.01±0.25 ‰ ($p=0.741$) and -0.05±0.12 ‰ ($p=0.008$) for δ^{202}Hg and Δ^{199}Hg, respectively). Conversely, penguin adults displayed a clear divergence between tissue-specific Hg isotopic values (mean differences 0.28±0.19 ‰ ($p<0.0001$) and 0.25±0.13 ‰ ($p<0.0001$) for δ^{202}Hg and Δ^{199}Hg, respectively). Different Hg integration times between tissues and dietary or foraging habitat variations were hypothesized as the main explanatory factors of such Hg isotopic mismatch between blood and feathers in adults. We concluded that both blood and feathers were valid bioindicator tissues for Hg isotopic studies and, in the case of adults, they should be chosen depending on the scientific question: feathers are useful for the investigation of long-term (i.e. annual) monitoring, whereas blood samples are more suitable for short-term (i.e. seasonal) and physiological monitoring.

Keywords: skua, penguins, bioaccumulation, marine ecosystems, isotopes

Introduction

Mercury (Hg) and more specifically methylmercury (MeHg) have been reported as highly toxic environmental pollutants with severe risks for animal and human health. The amount of Hg released into the environment has worthily increased since the pre-industrial times as a consequence of its large utilisation in human activities. Due to its persistence and biomagnification in marine food webs, high levels of Hg have been reported in high trophic level predators. Seabirds, as top predators, present elevated Hg amounts in their tissues and have been reported as efficient bioindicators of the environmental pollution (e.g. Burger and Gochfeld, 2004). Since they display contrasted foraging strategies and feed at different trophic levels, they are considered appropriate models to assess Hg contamination of the marine environment.

Hg exposure in birds is essentially attributed to dietary uptake (especially MeHg) which appears to be easily uptaken and distributed by the blood stream to internal organs and tissues (Thompson and Furness, 1989b; Braune, 1987; Honda et al., 1986). Seabirds present a considerable opportunity of detoxification by their capacity to efficiently excrete environmental contaminants through moulting feathers (annually in the case of most species). Thus, moulting represents the main detoxification route for Hg in most seabird species (Furness et al., 1986). Indeed, Hg is assumed to be sequestered in feathers binding to the keratin molecules (Appelquist et al., 1984), which impedes its reincorporation into internal tissues. Between 70 and 90% of the whole Hg body burden is assumed to be remobilised from internal tissues and excreted into the growing feathers (Honda, Nasu, and Tatsukawa 1986), where the main part of Hg is known to be present under its organic form (more than 90% of THg as MeHg) (Thompson and Furness 1989b; Thompson et al., 1990; Renedo et al., 2017).

In seabirds, blood and feathers are the most frequently used tissues for biomonitoring studies because they do not involve lethal-sampling. However, each tissue presents a specific Hg turnover and they potentially provide access to different temporal scales of Hg exposure. Feathers are representative of Hg incorporation during the inter-moult periods and are metabolically inert after their synthesis. In contrast, blood is a metabolically active tissue representative of a shorter-term Hg intake than feathers, meaning a few weeks/months before sampling (Bearhop et al., 2000b). Therefore, tissue-specific integration times must be considered for the selection of the most appropriate avian tissue depending on the scientific purposes (Carravieri al., 2014a). Since chick moult occurs at the end of the chick-rearing period, both blood and simultaneously-growing feathers reflect recent Hg intake over a similar period (Carravieri al., 2014a). Consequently, sampling chick tissues could allow reducing the temporal mismatch of Hg integration between feathers and blood.

In the last decades, the measurement of Hg isotopic mass-dependent (MDF) and mass-independent fractionation (MIF) has become a documented tool for identifying sources of Hg and biogeochemical processes within the different compartments of the environment (Blum et al., 2014). MDF can occur during all Hg specific transformation processes such as volatilization (Zheng et al., 2007), reduction (Kritee et al. 2007), bacterial methylation or demethylation reactions (Rodriguez Gonzalez et al., 2009; Kritee et al., 2009; Perrot et al., 2013; Perrot et al., 2015) and metabolic processes (Feng et al., 2015; Perrot et al., 2016). Significant Hg MIF is known to be induced exclusively during photochemical reactions and mainly concerns the two odd isotopes (199 and 201) (Bergquist and Blum, 2007; Zheng and Hintelmann 2010a). Unlike MDF, MIF is thus not affected by biological processes (Kritee et al., 2007; Kritee et al., 2009; Perrot et al., 2015) and its signature is thus assumed to be conserved throughout the food web (Kwon et al. 2012b; Feng et al. 2015). Therefore, both MDF and MIF provide complementary information and are used as a double tracers for both Hg potential sources and transformation pathways.

Numerous studies have exploited and demonstrated the usefulness of Hg isotopes for tracing Hg exposure and sources in aquatic organisms (Li et al., 2016; Perrot et al., 2012; Jackson et al., 2008; Gehrke et al., 2011; Senn et al., 2010). Hg isotopic signatures have also been successfully used in ecotoxicology studies for a better understanding of detoxification and excretion processes and Hg metabolic responses, such as hepatic demethylation in marine mammals (Masbou et al., 2015; Perrot et al., 2016) or human exposure by excretion biomarkers such as urine (Sherman et al., 2013) and hairs (Laffont et al., 2009). Concerning avian samples, two studies have revealed the efficiency of Hg isotopic analyses in seabird eggs for investigating factors controlling Hg cycling in aquatic ecosystems (Point et al., 2011; Day et al., 2012).

In this work, we present the first data on Hg isotopic composition of blood and feathers of the same individual seabirds with the double objective of investigating Hg isotopic association between both tissues and of evaluating their suitability as tracers of Hg fate in marine ecosystems. This study was performed on different seabird species exhibiting contrasted ecological characteristics and breeding in distant sites in order to cover a wide range of Hg concentrations. Assuming that Hg integrated in chick blood and feathers correspond to a similar time frame, we first focused on chicks for exploring inter-tissue isotopic relationships and the allocation of Hg following transport and fractioning from blood to feathers. Potential biologic processes or transport among the two tissues were hypothesized to induce Hg MDF, leading to differences in Hg MDF values between blood and feathers. Because the temporal mismatch between chick tissues is supposed to be reduced and Hg MIF is not induced by *in vivo* processes, Hg MIF values in blood and feathers of chicks were predicted to be similar. Chicks of two very close species of skua were chosen to test these hypotheses. Complementary to this, we investigated feathers and

blood samples of adult seabirds to verify the potential influence of different tissue-specific temporal windows of Hg exposure on Hg isotopic signatures. We expected that shifts on foraging habits and zones during adult annual cycle could produce significant Hg isotopic variations among tissues. Penguins from six different species, all belonging to different populations, were selected to confirm this hypothesis.

Material and methods

Sites, field collection and ecological characteristics of sampled seabirds

Sample collection was conducted during the austral summer 2011-2012 (from October to February) in the four sites of the Terres Australes et Antarctiques Françaises, depending on the seabird species: Pointe Géologie, Adélie Land (Antarctic Zone, 66°40'S, 140°10'E), Crozet Islands (Subantarctic Zone, 46°26'S, 51°45'E), Kerguelen Islands (Subantarctic Zone, 49°21′S, 70°18′E) and Amsterdam Island (Subtropical Zone, 37°50'S, 77°31'E). Exact dates of sample collection of each seabird species are specified in SI (Table 3.S1).

Reference materials, sample preparation and total Hg analysis

Due to the absence of feather and bird blood certified reference materials (CRM), two internal reference samples were prepared with pooled samples collected from different individuals of king penguin (KP) from Crozet Islands: F-KP (feathers) and RBC-KP (red blood cells). The two reference samples were analysed at each session. For the validation of the results, human hair CRM (IAEA-086) was additionally analysed due to its similar chemical composition to feathers (keratin). Feathers samples were cleaned, oven dried and homogenised as detailed in (Carravieri et al. 2013). Blood samples were collected from a wing vein, centrifuged, and red blood cells were kept frozen at -20°C until analysis. Total Hg concentration was also quantified by using an advanced Hg analyser spectrophotometer (AMA-254, Altec) thus allowing intercomparing with Hg total concentrations obtained by Hg speciation analyses, meaning the sum of inorganic and organic Hg. For feather analyses, a matrix dependent calibration was performed with human hair reference material (NIES-13) as described in (Renedo et al., 2017). Blood samples analyses were performed as described in (Carravieri et al., 2017).

Hg species concentrations analysis

Feathers were prepared following a previously developed method (Renedo et al., 2017). Hg from blood samples (0.10-0.15 g) was extracted by alkaline microwave digestion with 5 mL of tetramethylammonium hydroxide (25% TMAH in H_2O, Sigma Aldrich) (Rodrigues et al., 2011). Details of the extraction method, analysis and quantification of Hg species are included in (Renedo et al. 2017).

Total Hg isotopic composition analysis

Samples (0.05-0.10 g) were digested with 3 or 5 mL of HNO_3 acid (65%, INSTRA quality) after a predigestion step overnight at room temperature. Two different mineralisation systems were successfully tested and used: High Pressure Asher (HPA) and Hotblock. HPA mineralisation was performed at high conditions of pressure (130 bar) and temperature (temperature ramp: 80ºC–120 ºC (2ºC/min) –300 ºC (2.5 h) – 80 ºC (1 h)). Hotblock mineralisation was effectuated in Savillex vessels at 75ºC during 8 h (6 h in HNO_3 and 2 h more after the addition of 1/3 of the total volume of H_2O_2 (30%, ULTREX quality)). Hg isotopic composition was determined using cold-vapour generator (CVG)-MC-ICPMS (Nu Instruments), as detailed in (Perrot et al. 2012). Hg isotopic values were reported as delta notation, calculated relative to the bracketing standard NIST SRM-3133 reference material to allow inter-laboratory comparisons, as described in SI. NIST SRM-997 thallium standard solution was used for the instrumental mass-bias correction using the exponential law.

Recoveries of extraction were verified for all samples by checking the signal intensity obtained on the MC-ICPMS for diluted extracts relative to NIST 3133 standard (with an approximate uncertainty of +/-15%). Total Hg concentrations in the extract solution were compared to the concentrations found by AMA-254 analyses. Average recoveries obtained were 98 ±14% for feathers (n=104) and 111 ±11% for blood samples (n=102). Accuracy was evaluated by analyses of human hair IAEA-086 and NIES-13 reference materials for keratin matrixes and tuna fish ERM-CE-464 for soft-tissues. Internal reference samples of feathers (F-KP) and avian blood (RBC-KP) were also measured. Repeatability was estimated by analysing the same extract of each reference material on the long term (during 2 weeks of analysis). Uncertainty for delta values was calculated using 2SD typical errors for each internal reference material (Table 3.S2). Internal reproducibility was also assessed for numerous measurements of the two internal reference samples of feathers (F-KP) and avian blood (RBC-KP) within 2-10 months of interval (Table 3.S3).

Results

Skua chicks

Mean skua chicks' δ^{202}Hg values of feathers (blood) ranged widely between populations, varying from 0.00±0.36 ‰ (0.23±0.13 ‰) in Adélie Land to 1.56±0.08 ‰ (1.51±0.20 ‰) in Amsterdam Island. Lower variability was found in Δ^{199}Hg between the four sites, with mean values of feathers (blood) ranging from 1.46±0.07 ‰ (1.51±0.08 ‰) in Adélie Land to 1.76±0.05 ‰ (1.70±0.05 ‰) in Amsterdam Island (Table 3.1).

Individual paired differences of δ^{202}Hg and Δ^{199}Hg (feathers minus blood) were respectively -0.01±0.25‰ and -0.05±0.12‰, when pooling all the individuals. In general, insignificant differences in tissue-specific Hg isotopic ratios were found, with the highest δ^{202}Hg difference obtained for Adélie Land (-0.16±0.33‰) and Kerguelen (0.19±0.18‰) and the highest Δ^{199}Hg difference for the Crozet population (-0.06±0.17‰). No statistically differences between feathers and blood δ^{202}Hg values were observed for the 40 individuals of skua. However, when evaluating each skua population separately, only Kerguelen individuals presented significant differences between feather and blood δ^{202}Hg values, probably associated to high SD of tissues-paired differences (δ^{202}Hg difference = 0.19±0.18‰). Δ^{199}Hg mean paired differences observed in skua chicks were statistically significant for the overall data set. Paired differences in Amsterdam individuals were marginally significant (Table 3.1).

Linear regressions between blood and feather Hg isotopic values were determined for all the individuals (Figure 3.1) showing high and linear correlation for δ^{202}Hg values (Pearson correlation, $r=0.91$, $p<0.0001$, $n=40$). Δ^{199}Hg values were also significantly correlated but to a lesser extent (Pearson correlation, $r=0.53$, $p<0.0001$, $n=40$). Regressions slopes were not statistically different from slope 1:1 neither for δ^{202}Hg ($t=-12.68$, $p<0.0001$) nor for Δ^{199}Hg values ($t=-6.54$, $p<0.0001$).

Table 3.1. Blood (red blood cells) and feather $\delta^{202}Hg$ and $\Delta^{199}Hg$ values, associated statistics, and isotopic differences between feathers and blood of skua chicks. Both tissues were sampled simultaneously in large chicks. Statistically significant results are marked in bold. Values are means ± SD

Species	Location	n	Blood $\delta^{202}Hg$ (‰)	Feathers $\delta^{202}Hg$ (‰)	Paired t- test ($\delta^{202}Hg$ values)		Paired $\delta^{202}Hg$ differences ($\delta^{202}Hg$ (‰)
			Mean ± SD	Mean ± SD	t	p	Mean ± SD
Antarctic skua	Adélie Land	9	0.23±0.13	0.00±0.36	1.455	0.184	-0.16±0.33
Subantarctic skua	Kerguelen	10	1.04±0.08	1.22±0.19	**-0.680**	**0.009**	0.19±0.18
	Crozet	11	1.39±0.18	1.35±0.14	-3.209	0.512	-0.04±0.18
	Amsterdam	10	1.56±0.08	1.51±0.20	0.884	0.400	-0.07±0.20
	All populations	40			-0.333	0.741	-0.01±0.25

Species	Location	n	Blood $\Delta^{199}Hg$ (‰)	Feathers $\Delta^{199}Hg$ (‰)	Paired t- test ($\Delta^{199}Hg$ values)		Paired $\Delta^{199}Hg$ differences (‰)
			Mean ± SD	Mean ± SD	t	p	Mean ± SD
Antarctic skua	Adélie Land	9	1.51±0.08	1.46±0.07	-1.096	0.305	-0.04±0.11
Subantarctic skua	Kerguelen	10	1.61±0.06	1.55±0.12	-1.166	0.271	-0.05±0.12
	Crozet	11	1.69±0.11	1.64±0.12	-1.454	0.180	-0.06±0.17
	Amsterdam	10	1.76±0.05	1.70±0.05	**-2.440**	**0.037**	-0.05±0.08
	All populations	40			**-2.745**	**0.008**	-0.05±0.12

Penguins

Penguins' feathers (blood) mean δ^{202}Hg values increased from Adélie penguins (0.56±0.20 ‰ (0.67±0.13 ‰)) to northern rockhopper penguins (2.16±0.14 ‰ (2.42±0.13 ‰)). In the case of Δ^{199}Hg values, gentoo penguins displayed the lowest values (1.41±0.06 ‰ (1.51±0.12 ‰)) and northern rockhopper penguins the highest ones (1.89±0.12 ‰ (2.22±0.10 ‰)) (Table 3.2).

Significantly different Hg isotopic signatures (feathers minus blood) were observed among penguin tissues. Feathers displayed heavier δ^{202}Hg and Δ^{199}Hg values than blood in almost all the individuals (except some individuals of gentoo penguins). Respective mean paired differences for δ^{202}Hg and Δ^{199}Hg were 0.28±0.19 ‰ and 0.25±0.13 ‰, when considering the 62 individuals. Gentoo penguins showed much lower mean paired differences -0.02±0.12 ‰ (for δ^{202}Hg) and 0.10±0.12 ‰ (for Δ^{199}Hg) comparing to other penguin species. King penguins displayed the highest δ^{202}Hg difference (0.45±0.19‰) and northern rockhopper penguins the highest Δ^{199}Hg difference (0.33±0.08‰). Paired differences were statistically significant for both δ^{202}Hg values and Δ^{199}Hg values considering the six populations. Regarding each population separately, feather and blood δ^{202}Hg values were statistically similar only for Adélie and gentoo penguins. However, differences of Δ^{199}Hg values between the two tissues were substantial for every penguin population.

A high linear correlation among tissues was obtained for both δ^{202}Hg (Pearson correlation, R^2=0.93 p<0.0001, n=62) and Δ^{199}Hg values (Pearson correlation, R^2=0.87, p<0.0001, n=62) in all the penguin individuals (Figure 3.2). Regressions slopes were not statistically different from slope 1:1 neither for δ^{202}Hg (t=-22.01, p<0.0001) nor for Δ^{199}Hg values (t=-14.41, p<0.0001).

Table 3.2. Blood (red blood cells) and feather $\delta^{202}Hg$ and $\Delta^{199}Hg$ values, associated statistics, and isotopic differences between feathers and blood. Both tissues were sampled simultaneously in adults. Statistically significant results are marked in bold. Values are means ± SD

			Blood $\delta^{202}Hg$ (‰)	Feathers $\delta^{202}Hg$ (‰)	Paired t- test ($\delta^{202}Hg$ values)		Paired $\delta^{202}Hg$ differences (‰)
Species	Location	n	Mean ± SD	Mean ± SD	t	P	Mean ± SD
Adélie penguin	Adélie Land	10	0.56±0.20	0.67±0.13	2.147	0.060	0.11±0.16
Gentoo penguin	Crozet	10	1.45±0.12	1.44±0.10	-0.422	0.682	-0.02±0.12
King penguin	Crozet	11	1.49±0.11	1.95±0.15	**7.909**	**<0.0001**	0.45±0.19
Macaroni penguin	Crozet	10	1.66±0.11	2.01±0.15	**5.453**	**<0.0001**	0.35±0.20
Eastern rockhopper penguin	Crozet	10	1.93±0.18	2.31±0.12	**8.379**	**<0.0001**	0.38±0.14
Northern rockhopper penguin	Amsterdam	10	2.16±0.14	2.42±0.13	**5.601**	**<0.0001**	0.27±0.15
	All populations	72			**-8.795**	**<0.0001**	0.26±0.23

			Blood $\Delta^{199}Hg$ (‰)	Feathers $\Delta^{199}Hg$ (‰)	Paired t- test ($\Delta^{199}Hg$ values)		Paired $\Delta^{199}Hg$ differences (‰)
Species	Location	n	Mean ± SD	Mean ± SD	t	P	Mean ± SD
Adélie penguin	Adélie Land	10	1.54±0.11	1.80±0.14	**8.330**	**<0.0001**	0.26±0.10
Gentoo penguin	Crozet	10	1.41±0.06	1.51±0.12	**2.902**	**0.016**	0.10±0.12
King penguin	Crozet	11	1.60±0.04	1.82±0.09	**7.215**	**<0.0001**	0.22±0.10
Macaroni penguin	Crozet	10	1.54±0.06	1.86±0.08	**11.410**	**<0.0001**	0.31±0.09
Eastern rockhopper penguin	Crozet	10	1.77±0.13	2.09±0.09	**-7.290**	**<0.0001**	0.32±0.14
Northern rockhopper penguin	Amsterdam	10	1.89±0.12	2.22±0.10	**59.061**	**<0.0001**	0.33±0.08
	All populations	72			**-15.390**	**<0.0001**	0.23±0.13

Discussion

The information about Hg speciation in each tissue is essential for the interpretation of total Hg isotopic signatures. Feather and blood samples analysed in this study presented a vast majority of MeHg content (data already published Renedo et al. 2017). This observation is consistent with previous reported results indicating that MeHg accumulates in seabirds' feathers as a detoxification mechanism, where it typically comprises the most abundant proportion of total Hg (Thompson and Furness 1989a; Renedo et al. 2017) and reporting blood as a Hg transport tissue within the organism (Bearhop, Ruxton, and Furness 2000b).

Chicks: identical Hg isotopic composition in feathers and blood

Skua chicks exhibited identical Hg MIF (Δ^{199}Hg) and MDF (δ^{202}Hg) values in blood and feathers, suggesting that both tissues reflect equally Hg acquisition during a similar temporal window. This finding represents substantial practical advantages for avian ecology studies, firstly because during fieldwork the sampling can be done indifferently on feathers or blood of chicks; and secondly, and more importantly, because blood and feathers of all the individuals can be compared in interpretative terms directly without applying corrections, as it must be done for carbon and nitrogen stable isotopes (Cherel et al. 2014).

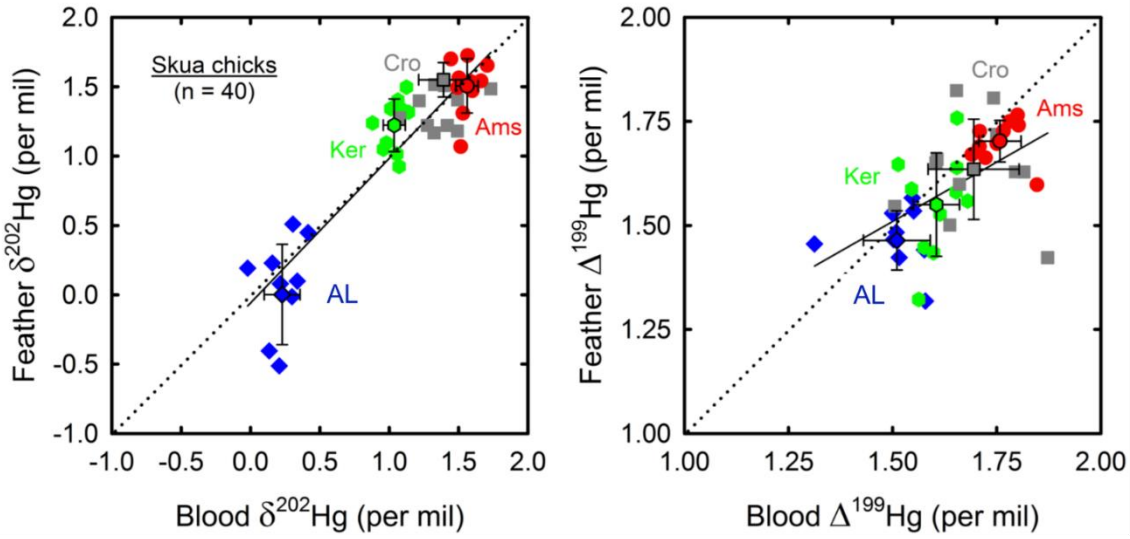

Figure 3.1. Feather versus blood (red blood cells) δ^{202}Hg and Δ^{199}Hg values in skua chicks (individual values and mean population values). Regression equations for δ^{202}Hg blood-feather and Δ^{199}Hg blood-feather values are y=1.12x-0.17 (R^2=0.81, p<0.0001), and y=0.63x-0.56 (R^2=0.33, p<0.0001), respectively. Abbreviations for the different populations are AL (Adélie Land), Ker (Kerguelen), Cro (Crozet) and Ams (Amsterdam).

Differences in Hg isotopic differences between feathers and blood of adult penguins

Compared to skua chicks, penguin adults generally displayed a higher degree of variations between tissue-specific Hg isotopic values, with feathers showing slightly heavier δ^{202}Hg and Δ^{199}Hg values. Potential explanatory factors of those inter-tissues isotopic differences are discussed in the following sections.

Differences between feathers and blood: metabolic origin

Metabolic processes are complex and constituted by several steps that potentially induce MDF between internal tissues. Intrinsic processes such as inter-tissue transport or Hg complexation to proteins could therefore induce significant MDF between blood and feathers. The similar Hg isotopic signatures observed between blood and feathers of skua chicks could be interpreted as an absence of Hg isotopic fractionation during internal mechanisms in chick tissues. However, we cannot ensure an absence of Hg isotopic fractionation between blood and feathers in chicks because this effect could be linked to specific conditions of their young age such as a low Hg bioaccumulation in which no limiting-step is responsible of significant MDF during the different metabolic steps. However, penguins exhibited heterogeneous blood and feather paired differences between the six penguin populations, with some species exhibiting similar values for both samples (primarily gentoo penguins) while other species displayed high discordance between tissue-specific isotopic signatures. Since blood and feather paired isotopic differences do not follow a similar pattern within all the penguins' populations, intrinsic metabolic processes do not seem the major cause of MDF. Therefore, the influence of extrinsic factors related to the specific ecological characteristics for each penguin species (such as geographical and temporal mismatch among tissues) seems to be a more plausible explanatory factor of Hg isotopic variations within adults' blood and feathers. Furthermore, this is consistent with MIF differences between blood and feathers, which are not likely linked to metabolic processes.

Geographical and ecological influence

The accumulation of a greater extent of heavier (δ^{202}Hg) and odd (Δ^{199}Hg) Hg isotopes in adult' feathers relative to blood could be likely the consequence of significant shifts in feeding ecology (foraging habitat and prey) that take place during the different stages of their annual cycle. Since feathers of adult penguins are assumed to reflect Hg acquisition during approximatively one complete year, we expected that significant changes in foraging habitats during this time would alter feather Hg isotopic signatures as a result of integration of Hg from diverse sources. This integrative effect could explain the dissimilarities obtained here between gentoo penguins, considered to be resident all year long (Lescroël et al., 2004), and the other five

penguin populations, known to spread out during winter. Gentoo penguins displayed limited isotopic differences among tissues (-0.02±0.12 ‰ for δ^{202}Hg and 0.10±0.12 ‰ for Δ^{199}Hg), whereas the other penguins provided statistically different tissue-specific isotopic values. Based on our hypothesis, feathers of gentoo penguins would hypothetically reflect Hg exposure from more restricted areas diminishing the Hg isotopic differences between blood and feathers.

Owing to their flightlessness, adult penguins are known to be restricted to the Southern Ocean during their wintery dispersion. In contrast, flying seabirds reproducing in this area are able to cover long distances during their non-breeding period at the time of feather growth, and therefore, Hg accumulated into their feathers represents the acquisition of remote and extended areas (Fort et al. 2014). Therefore, the higher shifts in latitudinal zones or depths that are produced during the different stages of the annual cycle (inter-moult and breeding periods) could potentially enhance Hg isotopic differences between blood and feathers tissues (Chapter 3.2). Alternatively, measurements of Hg isotopic composition in feathers of flying migratory seabirds open a new perspective for exploring Hg cycle and fate since they denote a powerful tool to trace Hg exposure pathways in large zones of the marine environment.

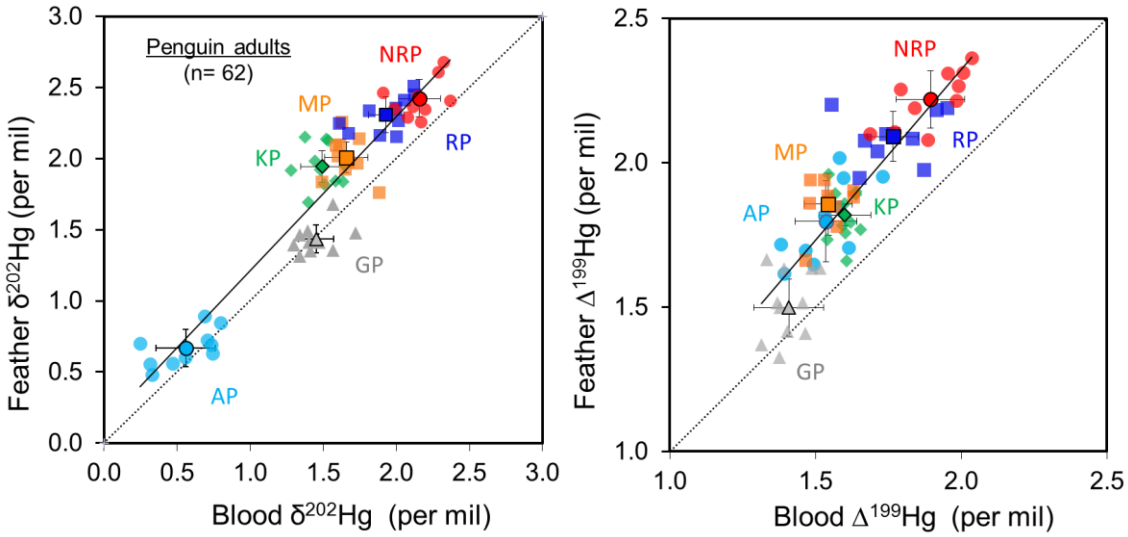

Figure 3.2. Feather versus blood (red blood cells) δ^{202}Hg and Δ^{199}Hg values in adult penguins (individual values and mean population values). Regression equations for δ^{202}Hg blood-feather and Δ^{199}Hg blood-feather values are y=1.08x+0.13 (R^2=0.86, p<0.0001) and y=1.18x-0.04 (R^2=0.75, p<0.0001), respectively. Abbreviations for the different populations are AP (Adélie penguin), GP (gentoo penguin), KP (king penguin), MP (macaroni penguin), RP (eastern rockhopper penguin) and NRP (northern rockhopper penguin).

Influence of different integration times

The mismatch of Hg isotopic signatures between blood and feathers of adults could also be the result of the different Hg integration times among both tissues. Adults' feathers sequestrate the Hg acquired between two moults (approximatively 12 months in our seabird species), presenting a much longer Hg accumulation interval compared to blood. In contrast, chicks start synthetizing their first feathers at the second part of their rearing-period (which is about 2 months of total duration in the case of skuas) and therefore the two tissues should represent similar periods of Hg dietary intake reducing this mismatch.

Contrary to other adult flying seabirds, penguins present a synchronous moult so they renew their whole plumage entirely in a single venue, resulting in high homogeneity in feathers in terms of chemical composition, including THg (Brasso et al., 2013; Carravieri, et al., 2014a). The discordance in Hg isotopic composition between feathers and blood observed in adult penguins at the individual level supports the expected influence of longer Hg integration times in feathers. Our results suggest that Hg isotopic studies on recent contamination or physiological monitoring should be preferentially applied on adult blood samples instead of feathers. Working on adult seabirds' feathers is however suitable for tracking whole annual Hg contamination.

Choice of the most adequate monitoring sample

For the selection of the most pertinent avian sample for Hg isotopic studies, it is important to consider the advantages and limitations of each tissue. According to practical issues, feathers permit an easy collection, storage and long-term conservation which is clearly advantageous for retrospective studies on environmental pollution and make them a relevant tissue for comparison between bird biomonitoring studies. Otherwise, blood requires a more invasive sample collection compared to feathers and it is more problematic to collect, preserve and store in the field. Apart practical considerations, the use of adult feathers present several constraints such as the potentially higher degree of heterogeneity within individuals (except penguins, see above), the asynchronous growth occurring in some species (Carravieri et al., 2014a) and the reflect of year round exposure for adults (especially in flying adults that migrate over large distances and change their diet). Hence, chick feathers should be preferred for local and recent contamination whereas adult feathers could be interesting for investigating Hg contamination over their whole annual cycle. However blood is more appropriate if we want information about recent assimilation or local contamination in adult individuals sampled at the colonies during their breeding period.

Conclusion

This work presents the first measurements of Hg isotopic composition on seabirds' blood and feathers of the same individuals and validates the efficient utilisation of both as effective key target tissues for tracing local Hg isotopic signatures. Briefly, feathers are interesting tissues for the investigation of historical contamination trends and annual monitoring whereas blood samples represent ecosystem-specific tissues more suitable for seasonal and physiological monitoring. Our study also highlights the great potential of combining Hg isotopes studies and seabirds for depicting Hg routes in marine ecosystems and a better understanding of the Hg cycle.

Main **findings** of this work

- Blood and feather Hg stable isotopes were measured in skua and penguin populations from distant sites in the Southern Ocean, from the fringing subtropics to Antarctica.
- In **adult birds**, Hg isotopic composition differed between **blood and feathers**, most likely as a consequence of **different tissue-specific temporal windows of Hg exposure**.
- In **chicks**, **blood and feathers** had identical Hg isotopic values meaning that the two tissues carry the **same amount of information** and can be easily compared with each other without any correction factor.
- **Hg isotopic studies in blood and feathers** open a **new perspective for exploring Hg cycle** and exposure pathways within marine ecosystems.

Acknowledgements

The present work was supported financially and logistically by the Région Poitou-Charentes through a PhD grant to MR, and by the Institut Polaire Français Paul Emile Victor (IPEV, program no. 109, H. Weimerskirch) and the Terres Australes et Antarctiques Françaises (TAAF) and by the Agence Nationale de la Recherche (program POLARTOP, O. Chastel). The IUF (Institut Universitaire de France) is acknowledged for its support to PB as a Senior Member. The authors thank all the fieldworkers that contributed to the collection of samples. Field procedures were authorised by the Ethics Committee of IPEV and by the Comité de l'Environnement Polaire.

Part 3.2: Hg isotopic composition of key tissues documents Hg metabolic processes in seabirds

Abstract

Seabirds bioaccumulate significant Hg amounts in their tissues as a consequence of their medium to high position in marine food webs and of their long-life span. Since they display contrasted foraging strategies, feeding on different trophic levels, seabirds are appropriate models to assess Hg bioaccumulation processes as well redistribution and detoxification mechanisms in their organism. The aim of this work is thus the evaluation of Hg metabolic responses by analyses of different tissues of seabirds from the Southern Ocean. Internal tissues (pectoral muscle, liver, brain, kidneys and blood) and feather samples were studied by the combination of Hg speciation and Hg isotopic composition analyses. Three seabird species with contrasting feeding ecology were chosen for this assessment: Antarctic prion (zooplankton eaters), white-chinned petrel (mesopelagic fish consumers) and southern giant petrel (other-seabird meat and carrion eaters). High variability in Hg speciation between tissues evidenced their different roles in metabolic processes such as demethylation in liver, recognized as a Hg detoxification organ. Hg isotopic signatures exhibited the same trend in the three seabird species, with increasing mass-dependent fractionation (MDF, δ^{202}Hg) values from livers through muscles to feathers, attributed to preferential demethylation of isotopically lighter Hg in liver and preferential sequestration of isotopically heavier Hg in feathers (preferential complexation of heavier isotopes and/or integration of distinct Hg sources). Mass-independent fractionation (MIF, Δ^{199}Hg) values differed widely between internal tissues and feathers, suggesting the existence of different Hg sources due to distinct Hg turnover between tissues, consistent with organs as long-term accumulative tissues and feathers as representative of annual Hg contamination between inter-moult periods.

Keywords: isotopes, methylmercury, demethylation, excretion, seabirds, metabolism

Introduction

Hg presents several adverse effects which involves serious consequences for the health of avian species, affecting particularly their behaviour, physiology and development (Evers et al., 2008; Tan et al., 2009) with consequences at the population level (Goutte, et al., 2014ab). Hg intake in seabirds occurs mainly by ingestion of prey containing MeHg, which is readily absorbed into the blood and transported to internal tissues, especially liver, kidney, brain and muscles by the blood stream (Wolfe et al., 1998). Dietary MeHg is also efficiently transferred to avian eggs and therefore, reproduction is consequently one of the most affected aspects of Hg toxicity in seabirds (Wolfe et al., 1998). The main route for Hg elimination in seabirds is excretion by moulting feathers (Thompson and Furness 1989b; Thompson et al., 1990), where Hg (predominantly under its MeHg form, Renedo et al., 2017) is sequestered in relatively high concentrations. These feather Hg concentrations are correlated with blood Hg levels at the time of feather growth (Bearhop et al., 2000). Feathers are thus considered as archives of Hg exposure since the previous feather synthesis and they reflect both site-specific dietary uptake of MeHg and the stored then remobilised body burden Hg (Monteiro et al., 1996). During seasonal moult, Hg accumulated in muscles is remobilised into growing feathers, and the Hg accumulated in the organism is gradually reduced (Braune, 1987; Furness et al., 1986). Hg dynamic in seabirds are consequently complex and highly variable between species, since detoxification rates and strategies are potentially influenced by their degree of exposure to Hg, their moult frequency and the efficiency of Hg excretion by moulting (Bearhop et al. 2000).

Metallothioneins are cysteine-rich proteins with high affinity to Hg (and other trace elements, such as Cd or Zn) that have been suggested to play an important role in Hg detoxification. These proteins have been detected in the tissues of seabirds (Elliott and Scheuhammer, 1997; Elliott et al., 1992; Andrews et al., 1996) and their amount is proportional to iHg concentrations in the liver (Kehrig et al., 2015). To date, the binding Hg-metallothioneins has only been identified in dolphin livers (Pedrero et al., 2012b). Additionally, Hg has also been found to accumulate significantly as an inert Hg-Se complex called tiemannite in the liver of marine mammals (Palmisano et al., 1995; Nakazawa et al., 2011) and seabirds (Arai et al., 2004; Ikemoto et al., 2004), thus reducing its bioavailability and impeding its remobilisation (Cuvin-Aralar and Furness, 1991). Demethylation of MeHg into less toxic iHg in the liver appears to be a significant detoxification mechanism in seabirds (Thompson and Furness 1989b; Thompson et al., 1993b) and is supposed to be a complementary process to Hg excretion by feathers (Muirhead and Furness, 1988; Nigro and Leonzio, 1996). Consequently, seabird species that present both a Hg-rich diet and a complex moulting pattern associate excretion of MeHg into feathers with a high capacity of hepatic demethylation (Kim et al., 1996). This overall process appears to be especially significant in

Procellariiforms, such as albatrosses and petrels (Wolfe et al., 1998). Understanding Hg bioaccumulation, inter-tissue distribution and detoxification or excretion processes in seabirds represents a great challenge. Numerous studies have investigated Hg levels and speciation in internal tissues in the last decades focusing on the toxicokinetics (Monteiro and Furness, 2001; Spalding et al., 2000) or on their use as bioindicators of Hg contamination (Norheim and Frøslle, 1978; Dietz et al., 1990; Kim et al., 1996; Kehrig et al., 2015). Here, we measured for the first time Hg isotopic composition in several avian tissues from the same individuals to investigate Hg biotransformation processes within the whole body. Since each tissue presents a different metabolic turnover, they are supposed to provide variable Hg speciation and Hg isotopic signatures, which both combined, can provide some information about the occurring biological processes and Hg fate in seabird tissues.

Hg isotopes can undergo mass-dependent and mass-independent isotope fractionation (MDF and MIF, respectively). MDF is known to affect all Hg isotopes and is induced during transformations such as methylation and demethylation (Rodriguez Gonzalez et al., 2009; Kritee et al., 2009; Perrot et al., 2013; Perrot et al., 2015), reduction (Kritee et al. 2007) and volatilization (Zheng et al., 2007). Numerous studies have evidenced Hg MDF during trophic transfer leading to accumulation of isotopically heavier MeHg in predators relative to their prey (Perrot et al., 2010; Senn et al. 2010; Li et al., 2014). Therefore, *in vivo* processes such as Hg species-specific accumulation in target organs, inter-tissue transport or Hg detoxification mechanisms (such as demethylation in the liver) involve Hg MDF, which has been widely used as a proxy of these processes in aquatic organisms such as fish (Feng et al., 2015; Kwon et al., 2012a; Zhu et al., 2013) and marine mammals (Masbou et al. 2015; Perrot et al. 2016). In contrast, Hg MIF seems not to be induced by biological processes (Kritee et al. 2007; Kritee et al., 2009; Feng et al. 2015); hence, Hg MIF is assumed to not vary within food webs. Significant Hg MIF variations are driven by photochemical reactions, the only mechanism known to date (Bergquist and Blum, 2007; Zheng and Hintelmann 2010a). The interest of this study is the combination of Hg speciation and Hg isotopic composition analyses of avian internal tissues (pectoral muscle, liver, brain, kidney and blood) and feather samples to i) contribute to the elucidation of Hg transformations and metabolic fate of Hg among seabird tissues and ii) evaluate the level of information on Hg contamination provided by the most targeted non-lethal samples: feathers and blood. We hypothesize that hepatic demethylation of ingested MeHg may induce a Hg MDF between tissues, resulting in the accumulation of lighter isotopes in the produced iHg in liver and heavier isotopic composition in the remaining MeHg with its potential remobilisation into feathers during moult. Due to the assumed absence of Hg MIF during *in vivo* processes, no anomalous Hg fractionation was expected between internal tissues. However, the different integration times and turnover of Hg between feathers and internal tissues was presumed to potentially influence Hg MIF variations

between internal tissues (muscle and liver) and feathers, as previously observed between feathers and blood in adult individuals (Chapter 3.1).

Material and methods

Description of ecological characteristics of the studied seabirds

The Antarctic prion (*Pachyptila desolata)* is a small petrel that moves far from the colonies between breeding periods (mainly to subtropical waters) and returns to breed in the Southern Ocean (Cherel et al., 2016). Antarctic prions obtain most of their food near the surface. They are opportunistic epipelagic foragers, feeding on the most available swarming crustaceans, mainly the hyperiid amphipod *Themisto gaudichaudii* and the subantarctic krill *Euphausia vallentini* (Cherel et al., 2002). In Kerguelen Islands, they forage from subantarctic to Antarctic waters during the chick-rearing period (Cherel et al. 2002).

White-chinned petrel (*Procellaria aequinoctialis*) is a large petrel and one of the most abundant seabirds in the Southern Ocean. This species is known to be effective competitors and excellent divers (Péron et al., 2010). In Kerguelen, their diet is mostly composed of fish, but it also includes crustaceans, cephalopods, and offal and discards from fishing vessels (Delord et al., 2010). During the chick rearing period, seabirds from the Kerguelen Islands forage from subantarctic to Antarctic waters (Delord et al., 2010), and they winter in the Benguela Current where they feed primarily on fish (Péron et al., 2010; Jackson, 1988).

Together with the closely-related northern giant petrel (*Macronectes halli*), the southern giant petrel (*M. giganteus*) is the largest petrel and the dominant scavenger in the Southern Ocean (González-Solís et al., 2002). During the breeding period, the species presents sex-related foraging strategies, with males mainly scavenging on land and females primarily feeding at sea (Thiers et al., 2014). During the inter-breeding periods, both males and females are pelagic within the southern Indian Ocean (Thiers et al., 2014). As white-chinned petrels, giant petrels are ship-followers, being thus at risk to be killed by fishing gears.

Sample collection, preparation and reference material used

Dead individuals of Antarctic prions (n=10) and white-chinned petrels (n=10) were collected at the Kerguelen archipelago (49°21′S, 70°18′E) in January 2012 and October 2003, respectively. Loss of labels precludes precise knowledge of both origins and sampling dates of southern giant petrels (n=3); however seabirds were collected dead either at Crozet Islands (subantarctic waters) and/or in Adélie Land (high-Antarctica). Internal tissues analysed in this study (pectoral muscle, liver, kidney and brain) were sampled, weighed and stored individually in plastic bags. Blood samples were obtained by collecting clotted blood from heart atria and stored in Eppendorf

microtubes. After dissection, all the samples were stored at -20°C. Body feathers were removed from breast and stored dry. Flying feathers from white-chinned petrels were also collected. Prior to the analyses, tissue samples were cryogenically pulverised and freeze-dried. Feathers were cleaned, oven-dried and homogenised as detailed in previous work (Carravieri et al. 2013). Feathers, muscles and livers from the 10 individuals of both Antarctic prions and white-chinned petrels were analysed, as were kidneys, brains and blood samples of the three southern giant petrels.

Three certified reference materials (CRM), with certified concentration values of both THg and MeHg, were used in this study for validation of our speciation and isotopic results: NIES-13 (human hair), DOLT-4 (dogfish liver) and ERM-CE-464 (tuna fish). Human hair CRM IAEA-086 was also used for validation of Hg isotopic analyses. King penguin feather and red blood cells samples (F-KP and RBC-KP, respectively) were used as internal reference materials.

Hg species concentration analysis

Samples were digested by microwave-assisted extraction using a CEM microwave system (Discover SP-D, CEM Corporation) coupled to an autosampler Explorer 4872 96 (USA). The extraction was carried out in CEM Pyrex vessels by 1 min of warming up to 75ºC and 3 min at 75ºC with magnetic agitation to homogenise the samples. Feathers (~ 0.10 g) were extracted using nitric acid (HNO_3·6N, INSTRA quality) with addition of isotopic enriched standard solutions before the extraction process as detailed in previous work (Renedo et al., 2017). Blood and internal tissues (0.10-0.15 g) were extracted by alkaline digestion with 5 mL of tetramethylammonium hydroxide (25% TMAH in H_2O, Sigma Aldrich). Quantification of Hg species was carried out by isotope dilution analysis, using a GC-ICP-MS Trace Ultra GC equipped with a Triplus RSH autosampler coupled to an ICP-MS XSeries II (Thermo Scientific, USA) as detailed elsewhere (Clémens et al., 2011). THg concentrations were also quantified by using an advanced Hg analyser spectrophotometer (AMA-254, Altec) for method intercomparison and corroboration of Hg total concentrations obtained by Hg speciation analyses. Hg speciation results were validated for each CRM (Table 3.S4).

Hg isotopic composition analysis

Amounts of 0.10-0.15 g of sample were digested with 5 mL of HNO_3 acid (65%, INSTRA quality) after a predigestion step overnight at room temperature. Feathers and blood samples were extracted by Hotblock effectuated in Savillex vessels at 75ºC during 8 h (6 h in HNO_3 and 2 h more after the addition of 1.66 mL of H_2O_2, 30% ULTREX quality). Internal tissues (muscle, liver, kidney and brain) were extracted by High Pressure Asher (HPA) mineralisation performed at high conditions of pressure (130 bar) and temperature (temperature ramp: 80ºC–120ºC

(2ºC/min) –300ºC (2.5 h) – 80ºC (1 h)). Hg isotopic composition was determined for the six most abundant stable Hg isotopes (^{198}Hg, ^{199}Hg, ^{200}Hg, ^{201}Hg, ^{202}Hg and ^{204}Hg) using cold-vapour generator (CVG)-MC-ICPMS (Nu Instruments), as detailed in (Perrot et al., 2012). Hg isotopic values were reported as delta notation, calculated relative to the bracketing standard NIST SRM-3133 CRM to allow inter-laboratory comparisons. NIST SRM-997 thallium standard solution was used for the instrumental mass-bias correction using the exponential law. Uncertainty for delta values was calculated using 2 SD typical errors for each reference material (Table 3.S5).

Statistical analyses

Statistical tests were performed using RStudio. Before analyses, data were checked for normality of distribution and homogeneity of variances using Shapiro–Wilk and Breusch-Pagan tests, respectively. According to this, parametrical (One-way ANOVA) or non-parametrical tests (Kruskal–Wallis with Conover-Iman test) were performed. Statistically significant results were set at $\alpha = 0.05$.

Results

Antarctic prions

THg concentrations, Hg species distribution and Hg isotopic composition in Antarctic prions samples varied significantly depending on the type of tissue analysed (Table 3.3, Figure 3.3). All the 10 individuals exhibited highest mean THg levels in feathers and livers, with lower concentrations in muscle (2.6±0.9, 2.1±0.5, 0.3±0.1 $\mu g \cdot g^{-1}$, respectively; Kruskal-Wallis, H= 19.86, p<0.0001). Feather and liver Hg concentrations were highly variable between individuals, although muscle exhibited quite homogenous THg concentrations. Kidney and blood from five Antarctic prions were also analysed, providing intermediate mean THg concentrations (0.9±0.2 and 0.7±0.1 $\mu g \cdot g^{-1}$; respectively).

Hg species distribution was also variable among the different tissues (Kruskal-Wallis, H= 24.28, p<0.001). As expected, MeHg was the most abundant Hg species in both feathers and muscle of Antarctic prions (94±3 and 84±5%, respectively). MeHg also predominates in the liver (mean 66±6%, up to 74%) (Table 3.3).

Hg isotopic composition showed large MDF variations among internal tissues and feathers (Kruskal-Wallis, H= 18.10, p<0.0001), with individual δ^{202}Hg values ranging from -0.28 to 1.55 ‰. Liver and muscle exhibited the lowest mean δ^{202}Hg signatures (0.01±0.25 and 0.37±0.41 ‰, respectively) whereas feathers presented significantly heavier values (1.32±0.13 ‰). MIF signatures were also significantly different between internal tissues and feathers (Kruskal-Wallis,

H= 17.36, p<0.0001), ranging from 1.77 to 2.52 ‰. Δ^{199}Hg values were similar in liver and muscle, whereas they were 0.95 ‰ higher in feathers relative to muscles.

Table 3.3. THg, Hg speciation (iHg, MeHg), and Hg isotopic composition (δ^{202}Hg, Δ^{199}Hg) in Antarctic prions from Kerguelen Islands. Values not sharing the same superscript letter are significantly different. Values are means ± SD

Tissue	**n**	**THg**	**iHg**	**MeHg**		**δ^{202}Hg**	**Δ^{199}Hg**	**Δ^{199}Hg/Δ^{201}Hg**
		µg g^{-1}	µg g^{-1}	µg g^{-1}	%	‰	‰	‰
Liver	5	2.1±0.5 ^{A}	0.71±0.20	1.4±0.4	66±6^{A}	0.01±0.25 ^{A}	1.90±0.05 ^{A}	1.15±0.05 ^{A}
Muscle	10	0.3±0.1 ^{B}	0.05±0.02	0.3±0.1	84±5^{B}	0.37±0.41 ^{A}	1.93±0.14 ^{A}	1.16±0.03 ^{A}
Feathers	10	2.6±0.9 ^{A}	0.15±0.07	2.4±0.9	94±3^{C}	1.32±0.13 ^{B}	2.37±0.10 ^{B}	1.15±0.01 ^{A}

According to theoretical Δ^{199}Hg/Δ^{201}Hg slopes obtained experimentally for MeHg photodemethylation (1.3) and iHg photoreduction (1.0) in aquatic compartments (Bergquist and Blum, 2007), Hg accumulated in Antarctic prions' tissues should have undergone both processes as it represents a Δ^{199}Hg/Δ^{201}Hg slope between both theoretical lines (1.16, for the overall samples). Δ^{199}Hg/Δ^{201}Hg ratios were calculated for each tissue separately, indicating no statistically differences between samples (ANOVA, F=0.005, p=0.995, n=25). Δ^{199}Hg and Δ^{201}Hg values obtained for Antarctic prions' feathers were highly correlated (Pearson correlation, R^2=0.89, p<0.0001) and displayed a MIF slope of 1.11±0.08.

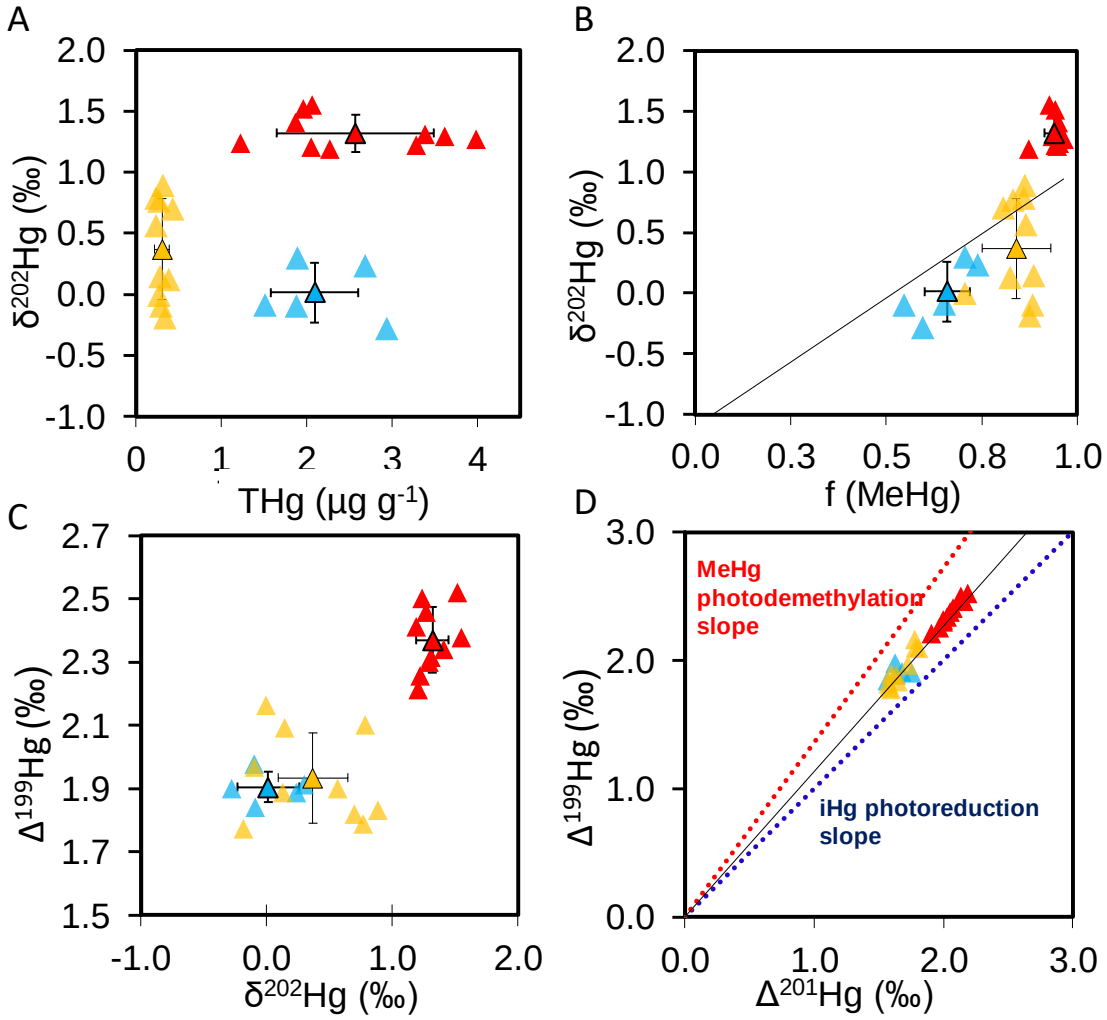

Figure 3.3. A) THg concentrations and Hg MDF (as δ^{202}Hg) in liver (blue), muscle (yellow) and feathers (red) from Antarctic prions. B) Hg MDF relative to the fraction of MeHg (regression line: y=2.11x-1.10, Pearson correlation coefficients R^2=0.76, p<0.0001). C) Hg MDF versus Hg MIF (expressed as δ^{202}Hg and Δ^{199}Hg, respectively) D) Hg MIF signatures (Δ^{199}Hg versus Δ^{201}Hg). The red and blue dashed lines represent the theoretical Δ^{199}Hg/Δ^{201}Hg slope for MeHg photodemethylation and for iHg photoreduction in the water column (Bergquist and Blum, 2007). Δ^{199}Hg/Δ^{201}Hg slope for Antarctic prions was 1.11±0.08 (R^2=0.86, p<0.0001).

White-chinned petrels

All the 10 individuals of white-chinned petrels presented significantly different THg concentrations in their tissues (Table 3.4, Figure 3.4) with higher mean THg concentrations observed in livers in comparison with muscles and feathers (54.3±18.7, 4.7±1.8 and 5.4±2.2, respectively) ($H= 19.355$, $p<0.0001$).

Hg compounds distribution was statistically different among the three studied tissues of white-chinned petrels ($H= 25.81$, $p<0.0001$). Feathers exhibited the highest fraction of MeHg (96±2%) whereas MeHg amount in muscles was less abundant and more variable between individuals (70-88%). Livers presented almost exclusively iHg (84-98%).

Concerning Hg isotopic composition, δ^{202}Hg values also differed among tissues ($H= 25.30$, $p<0.0001$) with livers exhibiting highly negative mean δ^{202}Hg values (-0.64 ‰), contrary to samples with the highest fraction of MeHg (i.e. muscles and feathers) that were characterized by positive δ^{202}Hg signatures (0.30 ‰ and 1.10 ‰, respectively). The enrichment in heavier MDF values is noticeable from livers to muscles (~ +0.94 ‰) and from muscles to feathers (~ +0.80 ‰) of white-chinned petrels. MIF signatures between white-chinned petrels' samples were also significantly different ($H= 20.97$, $p<0.0001$), ranging from 1.05 to 1.71 ‰. Mean Δ^{199}Hg values were 0.20 ‰ higher in feathers than in muscles and 0.08 ‰ higher in muscles than in livers.

Table 3.4. THg, Hg speciation (iHg, MeHg) and Hg isotopic composition (δ^{202}Hg, Δ^{199}Hg) in white-chinned petrels from Kerguelen Islands. Values not sharing the same superscript letter are significantly different. Values are means ± SD

Tissue	**n**	**THg**	**iHg**	**MeHg**		**δ^{202}Hg**	**Δ^{199}Hg**	**Δ^{199}Hg/Δ^{201}Hg**
		µg g^{-1}	µg g^{-1}	µg g^{-1}	%	‰	‰	
Liver	10	54.3±18.7 ^{A}	49.4±18.8	4.9±2.1	10±5^{A}	-0.64±0.27 ^{A}	1.17±0.05 ^{A}	1.14±0.04 ^{A}
Muscle	10	4.7±1.8 ^{B}	1.0±0.3	3.7±1.8	77±9 ^{B}	0.30±0.28 ^{B}	1.29±0.07 ^{B}	1.15±0.04 ^{A}
Feathers	10	5.4±2.2 ^{B}	0.2±0.1	5.2±2.1	96±2 ^{C}	1.10±0.14 ^{C}	1.49±0.21 ^{C}	1.26±0.08 ^{B}

Δ^{199}Hg/Δ^{201}Hg line exhibited by the overall samples of white-chinned petrel presented a slope of 1.46. However, Δ^{199}Hg/Δ^{201}Hg ratios calculated individually for each tissue were significantly different between livers and muscles (1.14±0.04 and 1.16±0.05) and feathers (1.26±0.08) ($H= 13.80$, $p=0.001$).

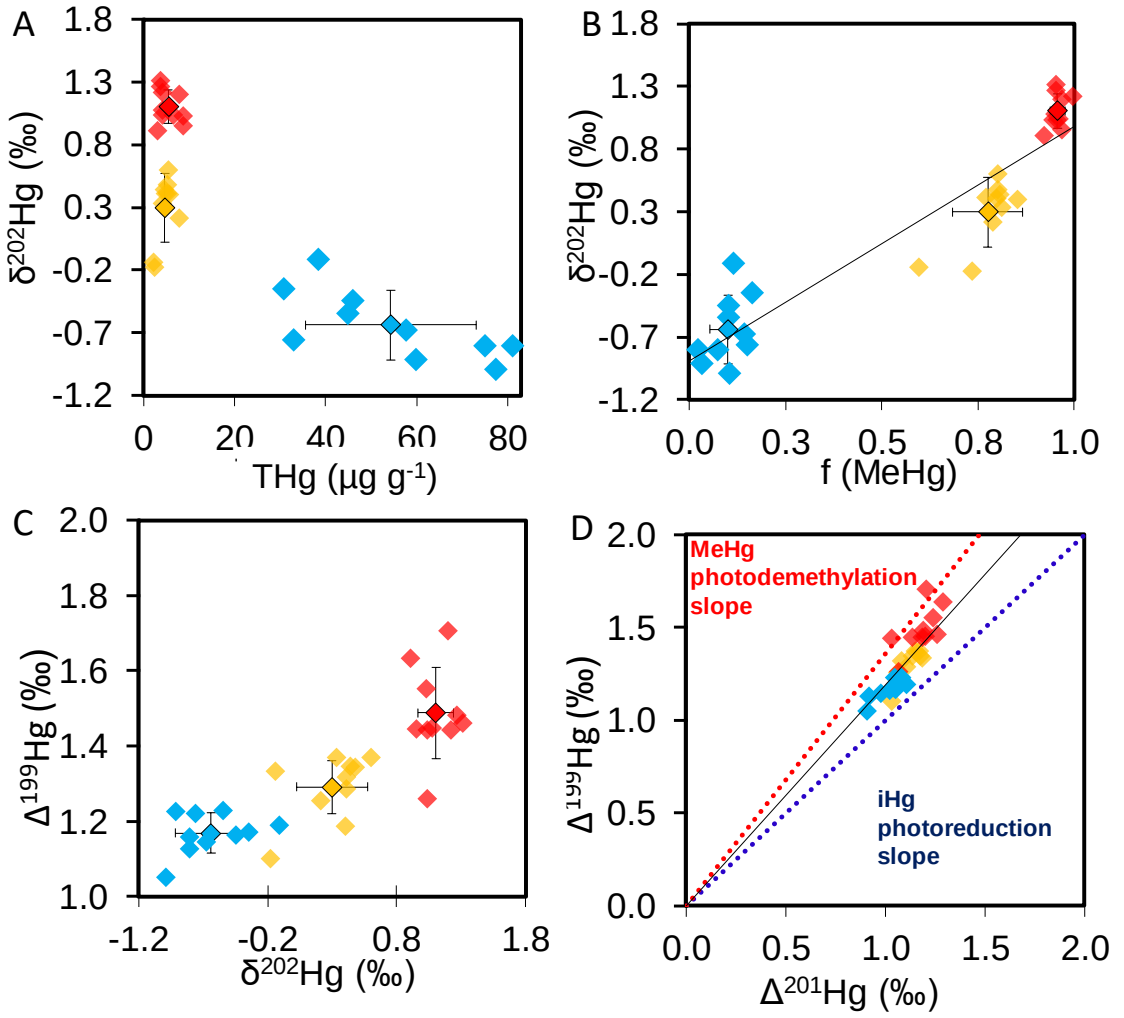

Figure 3.4. A) THg concentrations and Hg MDF (as δ^{202}Hg) in liver (blue), muscle (yellow) and feathers (red) from white-chinned petrels. B) Hg MDF relative to the fraction of MeHg. (regression line: y=1.87x-0.89, Pearson correlation coefficients were R^2=0.93, p<0.0001. C) Hg MDF versus Hg MIF (expressed as δ^{202}Hg and Δ^{199}Hg, respectively) D) Hg MIF signatures (Δ^{199}Hg versus Δ^{201}Hg). The red and blue dashed line represents the theoretical Δ^{199}Hg/Δ^{201}Hg slope for MeHg photodemethylation and for photoreduction of iHg in the water column (Bergquist and Blum 2007). White-chinned petrel samples Δ^{199}Hg/Δ^{201}Hg line regression is 1.19±0.12 (R^2 =0.85, p<0.0001).

Southern giant petrels

As previously observed in the other seabird species, Hg concentrations, speciation and isotopic signatures were highly dependent on the type of tissue analysed. However, in this case, high inter-individual variability was also observed between the three southern giant petrels (Table 3.5). In general, similar trends of Hg concentrations were observed for the three southern giant petrels, with the significantly highest mean THg concentrations in livers and the lowest in brains (309.7±135.1 and 5.9±6.4 $\mu g \cdot g^{-1}$, respectively). Kidneys were also highly concentrated (39.4±11.7 $\mu g \cdot g^{-1}$). Feathers and muscles also showed similar THg concentrations (13.3±6.9 and 11.6±15.2 $\mu g \cdot g^{-1}$, respectively) comparing to other MeHg accumulative tissues, such as blood (9.9±12.1 $\mu g \cdot g^{-1}$) (H= 10.70, p=0.058).

Despite inter-individual variability, Hg species distributions in liver and kidney tissues were characterized by a great predominance of iHg comparing to other tissues (H= 14.36, p=0.012), with livers presenting a slightly higher mean iHg percentage (96±2%) than kidneys (84±16%). The proportion of MeHg was homogenous for the three individuals in both feathers (mean 97.4±0.1%) and blood samples (mean 90±5%). However, Hg speciation in the storage organs differed widely between individuals, with muscles displaying a mean proportion of MeHg of 49% (37-58%), similar to brain 49% (34-74%) (Table 3.S8).

Concerning Hg isotopic composition, southern giant petrels displayed a large range of δ^{202}Hg values (from -0.93 to 2.35 ‰), which were statistically different among tissues (H= 12.47, p=0.029). No significant variations in Δ^{199}Hg values were neither obtained among different tissues (H= 5.54, p=0.353) that ranged between 1.23 and 1.57 ‰.

Table 3.5. THg, Hg speciation (iHg, MeHg), and Hg isotopic composition (δ^{202}Hg, Δ^{199}Hg) in southern giant petrels. Values not sharing the same superscript letter are significantly different. Values are means ± SD.

Tissue	n	THg	iHg	MeHg		δ^{202}Hg	Δ^{199}Hg	Δ^{199}Hg/Δ^{201}Hg
		µg g^{-1}	µg g^{-1}	µg g^{-1}	%	‰	‰	
Liver	2	309.7±135.1 ^{A}	295.4±122.0	14.3±13.0	4±2 ^{A}	0.20±0.68 ^{AB}	1.29±0.08 ^{A}	1.11±0.03 ^{A}
Kidney	3	39.4±11.7 ^{AB}	32.2±6.8	7.2±8.7	16±16 ^{AB}	-0.22±0.77 ^{AB}	1.37±0.08 ^{A}	1.21±0.05 ^{A}
Blood	3	9.9±12.1 ^{AB}	0.6±0.4	9.4±11.7	90±5 ^{CD}	2.01±0.36 ^{BC}	1.48±0.12 ^{A}	1.20±0.01 ^{A}
Muscle	3	11.7±15.2^{AB}	7.1±9.9	4.6±5.3	49±11 ^{BC}	0.45±0.09 ^{AB}	1.37±0.07 ^{A}	1.15±0.03 ^{A}
Feathers	3	13.3±6.9 ^{AB}	0.4±0.2	13.0±6.7	97.4±0.1^{D}	2.33±0.02 ^{C}	1.30±0.05 ^{A}	1.16±0.01 ^{A}
Brain	3	5.88±6.39 ^{B}	3.64±4.51	2.25±1.90	49±21^{ABC}	0.94±0.84 ^{ABC}	1.39±0.04 ^{A}	1.17±0.06 ^{A}

MIF slopes obtained for the overall samples of southern giant petrels displayed a $\Delta^{199}Hg/\Delta^{201}Hg$ slope of 1.17±0.09. $\Delta^{199}Hg/\Delta^{201}Hg$ ratios calculated individually for each tissue were statistically similar between tissues (H= 8.03, p=0.154).

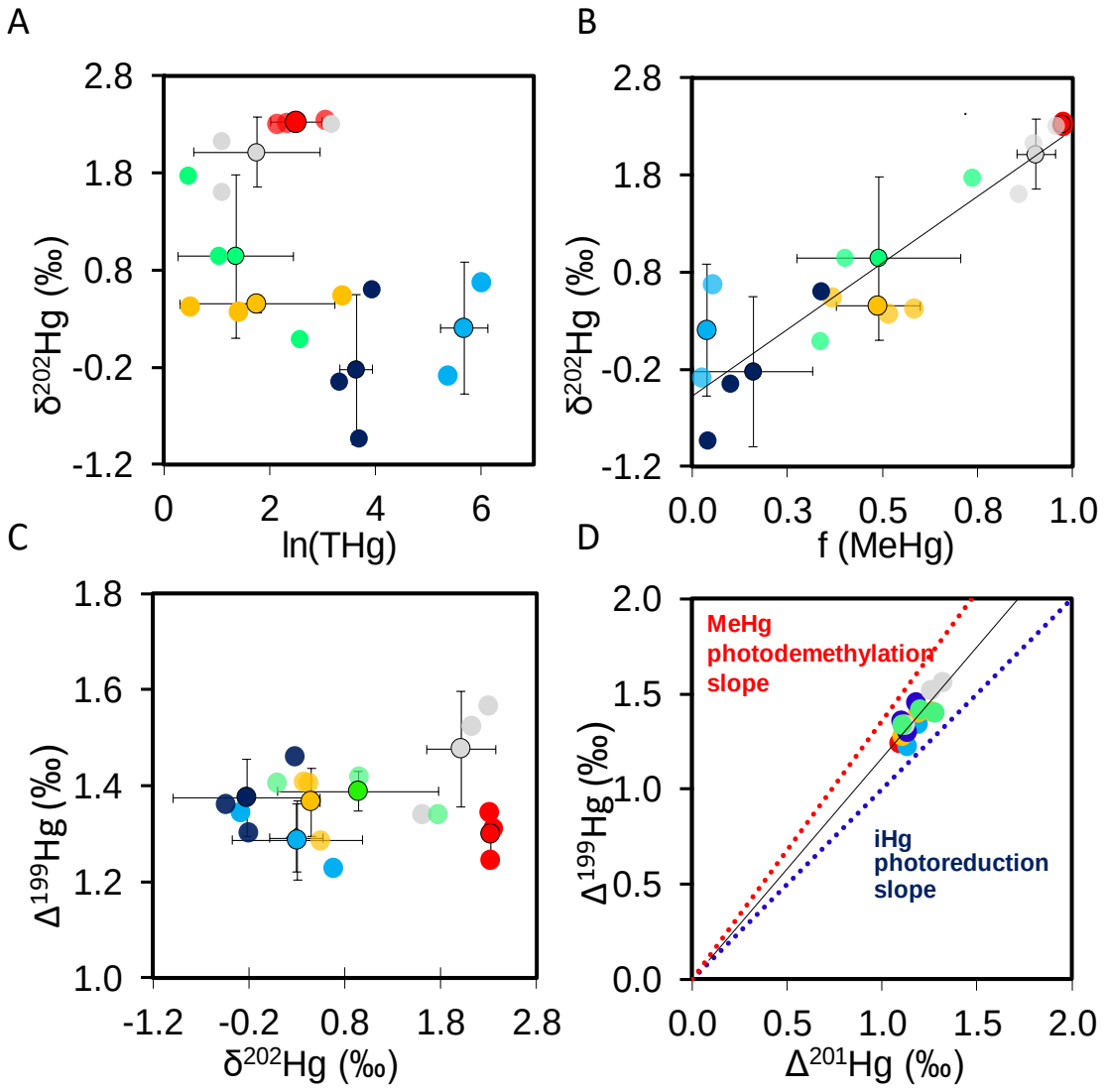

Figure 3.5 A) THg concentrations and Hg MDF (as $\delta^{202}Hg$) in liver (blue), kidneys (dark blue), muscles (yellow), feathers (red), brains (green) and blood (grey) from southern giant petrels. B) Hg MDF relative to the fraction of MeHg (regression line: y=2.75x-0.48, Pearson correlation coefficients were R^2 =0.92, p<0.0001). C) Hg MDF versus Hg MIF (expressed as $\delta^{202}Hg$ and $\Delta^{199}Hg$, respectively) D) Hg MIF signatures ($\Delta^{199}Hg$ versus $\Delta^{201}Hg$). The red and blue dashed line represents the theoretical $\Delta^{199}Hg/\Delta^{201}Hg$ slope for MeHg photodemethylation and for photoreduction of iHg in the water column (Bergquist and Blum 2007). For the southern giant petrel samples $\Delta^{199}Hg/\Delta^{201}Hg$ line regression is 1.17±0.09 (R^2=0.85, p<0.0001).

Discussion

Hg concentrations and isotopic variations within the trophic levels and feeding strategies

Wide ranges of Hg concentrations and isotopic values were obtained among tissues from the three pelagic seabird species investigated in this study. Increasing MDF signatures with trophic level have already been found in aquatic food webs by Hg isotopic analyses in fish or marine mammal muscle. For example, Perrot et al., (2012) measured δ^{202}Hg values in pelagic food web from Lake Baikal ranging from 0.64 ± 0.26‰ in fish (sculpins) to 1.83 ± 0.29‰ in seal muscles. High differences in MDF values were observed in feathers (a tissue that accumulates non-demethylated Hg) among organisms corresponding to different trophic levels, with giant petrels exhibiting higher feather mean δ^{202}Hg values (2.33±0.02 ‰) than Antarctic prions (1.32±0.13‰) and white-chinned petrels (1.10±0.14‰). However, this trend is not coherent with the assumption of heavier δ^{202}Hg values with increasing trophic levels. Since Antarctic prions mainly feed on zooplankton, they are exposed to lower Hg levels by diet than the other two species (Bocher et al., 2003; Fromant et al., 2016). Similarly, white-chinned petrels, which mostly feed on pelagic fish, presented significantly lower Hg concentrations and MDF values than southern giant petrels that scavenge on seal and other seabird carcasses (Cipro et al., 2014). Therefore, an influence of the diet could be proposed as the most plausible explanation of such variations in Hg concentrations and isotopic values among the three species.

Differences on MIF extent were also noticed between the three seabird populations. The highest Δ^{199}Hg values were measured in Antarctic prions' tissues (ranging from 1.77 to 2.52‰) that were significantly greater than those registered in white-chinned petrels (from 1.05 to 1.71‰) and southern giant petrels (from 1.23 to 1.57‰) (Kruskal-Wallis, $H=49.117$, $p<0.0001$, $n=72$). Previous biomonitoring studies have revealed variably positive Hg MIF (Δ^{199}Hg or Δ^{201}Hg) in aquatic organisms that have acquired MeHg that was photochemically degraded in different extents (Bergquist and Blum, 2007; Tsui et al., 2012; Perrot et al., 2010; Point et al., 2011; Senn et al., 2010; Sherman et al., 2013; Sherman et al., 2015). Large variations in Δ^{199}Hg among the two petrel species and Antarctic prions could be due to specific feeding behaviour or distinct foraging zones. Antarctic prions are known to migrate to northern latitudes during inter-breeding periods (Cherel et al., 2016), where photochemical reactions are potentially more substantial. Therefore, the higher MIF in their tissues could be attributed to the exposure to MeHg having undergone greater photodemethylation extent before incorporation to the food web.

Hg species distribution and MDF variations: proxies of metabolic processes

Hg species distribution among tissues followed a general pattern for the three seabird models, with liver and kidneys being predominantly enriched in iHg, relative to muscles and feathers that tend to accumulate mainly MeHg, which is in good agreement with previous studies on seabirds (Thompson and Furness 1989b; Kim, Murakami, et al. 1996; M Vahter et al. 2000; Kehrig et al. 2015). Tissue-specific δ^{202}Hg values were also observed on the three seabird species, since tissues that contained high amounts of iHg exhibited much lighter (in some cases negative) δ^{202}Hg values. In contrast, tissues presenting similar proportions of both Hg compounds (i.e. iHg and MeHg) showed intermediate δ^{202}Hg signatures (muscles and brains). Finally, feathers and blood, which had a majority of MeHg, were characterized by much positive δ^{202}Hg values and higher inter-individual homogeneity. The correlation between MeHg fractions and MDF values can be attributed to intrinsic metabolic processes (such as demethylation and/or inter-organ transport) that would induce changes in Hg isotopic composition before the posterior accumulation of Hg species among different tissues.

As previously mentioned, liver is assumed to play a detoxification role in Hg metabolism by demethylation of MeHg into a less toxic species iHg, as it has been reported extensively in studies on seabirds (Thompson et al., 1990; Kim et al., 1996; Thompson et al., 1998ab; Cipro et al., 2014). Evidences of Hg MDF during MeHg demethylation processes have been reported in experimental studies (Perrot et al., 2013; Rodriguez Gonzalez et al., 2009) and during *in vivo* processes in organisms (Feng et al., 2015; Kwon et al., 2013; Perrot et al., 2016). This is explained by the preferential demethylation of isotopically lighter MeHg (lower δ^{202}Hg values) which produced light iHg and lead to the deposition of residual MeHg fraction enriched in heavier Hg isotopes (greater δ^{202}Hg values). Hg demethylation process seemed to occur in significant degree in livers of white-chinned petrels and southern giant petrels, since both presented almost exclusively iHg and an important enrichment in lighter isotopes from muscles to livers, especially for white-chinned petrels (~ 0.94 ‰). On the contrary, livers from Antarctic prions displayed a minor presence of iHg (from 26 to 45%) and a lower difference in MDF was observed between muscles and livers (~ 0.36 ‰) comparing to the two other seabird species, possibly indicating less efficient MeHg hepatic demethylation.. It is widely recognized that *in vivo* MeHg demethylation is quite dependent on individual maturity and exposition to Hg levels (Wagemann et al., 1998; Wang et al., 2013). Therefore, another non-exclusive explanation is that the apparent slight demethylation extent in livers from Antarctic prions could be attributed to their exposure to low levels of Hg by dietary intake, since they feed at lower pelagic trophic levels comparing to petrels, and therefore, their necessity of Hg detoxification processes such as hepatic demethylation may be less

significant. Furthermore, Antarctic prions presented much higher Hg levels excreted in feathers relative to their concentrations registered in liver (comparing to the two petrel species), suggesting that they possibly present higher capacities of Hg elimination by moulting feathers. Contrastingly, the predominance of iHg in liver and kidney tissues from the two petrel species, together with their very elevated concentrations accumulated in such internal tissues, may be indicative of significant MeHg hepatic (and possibly renal) demethylation (Kim et al., 1996; Cipro et al., 2014).

After *in vivo* demethylation, the remaining non-metabolised and heavier MeHg fraction would be potentially redistributed and accumulated in other organs (muscle, brain) and, in the case of seabirds, excreted by feathers. This effect could explain the MDF variations obtained between storage and target organs in seabirds, which matches with previous observations in fish (Feng et al. 2015). Several toxicokinetic studies on MeHg metabolism and elimination in other organisms, such as fish and humans, have evidenced that faeces and urine excretion are the predominant elimination pathway of iHg resulting from MeHg *in vivo* demethylation and/or from direct ingestion (Van Walleghen et al., 2007; Li et al., 2014; Sherman et al., 2013; Feng et al., 2015). The isotopic characterization of urine/faeces (Li et al., 2014; Feng et al., 2015; Sherman et al., 2013) evidenced that the excreted iHg is isotopically lighter than the remaining Hg in the body, where it is principally present as MeHg.

Variations in MIF and MDF values between feathers and internal tissues

A common trend observed in the three seabird species was the enrichment in higher δ^{202}Hg values from muscles to feathers, which was particularly noteworthy in giant petrels (~ 1.88 ‰), followed by Antarctic prions (~0.95 ‰) and white-chinned petrels (~0.81 ‰). Significant anomalous Hg fractionation (MIF) was also observed between muscles and feathers in white-chinned petrels (enrichment of Δ^{199}Hg values +0.20‰) and particularly in Antarctic prions (+0.44 ‰). However, no substantial Hg MIF was obtained from muscles to feathers in the case of giant petrels.

Taking into account *in vivo* processes, it is well established that MeHg presents a high affinity for thiol-containing compounds such as cysteine, the principal constituent of keratin which forms the growing feather. MeHg-cysteine complexes are known to be transferred across the blood-brain barrier (Clarkson and Magos, 2006) and across membranes to liver and kidneys (Bridges and Zalups, 2010). Therefore, as a first explanation, we could associate increasing δ^{202}Hg values from muscles to feathers to an isotopic fractionation induced by intrinsic process, such as formation and transport of MeHg-cysteine complexes; or even a combination of other reactions occurring during inter-tissue transport or inside the feather itself. A priori, differences in Δ^{199}Hg signatures could be also explained by internal processes related to photochemistry, so inducing

significant MIF, such as a potential photochemical demethylation in the feather. However, this hypothesis appears unlikely because Hg is known to be sequestered in the sulphydryl groups of the keratin molecules where it is supposed to be physically and chemically stable (Appelquist et al., 1984). Therefore, Δ^{199}Hg variations could be mostly explained by the influence of extrinsic factors, such as the combination of different temporal and geographic integration windows between feathers and internal tissues samples. Feathers are known to reflect Hg exposure between two moults, integrating Hg acquired both at the breeding site and during their wintery migration far from their colonies. However, significant shifts in feeding ecology (foraging habitat and prey) that are produced during the different stages of their annual cycle (inter-moult and breeding periods) could potentially enhance Hg isotopic differences (both MDF and MIF) between feathers and internal organs. Changing latitudinal zones or depths during their migration period would also influence the uptake of isotopically different MeHg due to distinct aquatic photochemistry. Indeed, MIF variations between tissues in adult seabirds demonstrated to be an effective proxy of changes in foraging behaviour (horizontal, vertical and latitudinal dimensions) along their annual cycle (Chapter 3.1). Thus, migrating to southern latitudes with higher photochemistry extent would involve integration of MeHg with greater Δ^{199}Hg values into growing feathers. For instance, Antarctic prions exhibited here the highest differences in MIF among organs and feathers, which is consistent with their pre-breeding moult in warmer subtropical waters (Cherel et al. 2016) and supported by the results obtained for δ^{13}C isotopic analyses, for which feathers exhibited a subtropical signature whereas internal tissues showed Antarctic signatures (Figure 3.S6). However, although this hypothesis could explain the variations in MIF between internal organs and feathers observed in Antarctic prions and white-chinned petrels, it is not coherent with the absence of MIF for this tissues on giant petrels. A first suggestion that could explain this effect is the extended moulting time interval of southern giant petrels. Their moult initiates at the end of their breeding period so, possibly, a fraction of Hg integrated in feathers could correspond to their diet at the beginning of moult in the colonies and, consequently, reduce the fluctuations observed in MIF values among internal tissues and feathers. Another possible cause agent of this absence of MIF between feathers and internal organs could be due to the elevated Hg concentrations in the tissues of these apex predators that would induce a "reservoir effect", leading to the attenuation of Hg isotopic composition of recently acquired Hg during inter-organ equilibration producing more homogeneity in MIF values among the different tissues.

White-chinned petrels exhibited also significantly different MIF values among all the three analysed tissues. According to the other seabird species, the difference between internal organs and feathers seems to be clearly due to different Hg sources (as a result of different integration periods). Furthermore, this idea is supported by the observed different Δ^{199}Hg/Δ^{201}Hg ratios between internal tissues and feathers of white-chinned petrels, thus suggesting different

magnitudes of MeHg photodemethylation. As a first hypothesis, MIF differences between muscle and liver of this species could be associated to a difference in the ingested MeHg and iHg. Based on previous studies, dietary iHg is principally accumulated in liver and later redistributed to other organs (Feng et al. 2015). However, the diet of white-chinned petrels is mainly composed on mesopelagic fish and cephalopods, which are known to be almost exclusively constituted by MeHg (more than 90%), thus the potential ingestion of some others organisms contributing to a significant higher iHg fraction is improbable (Monteiro et al. 1996; Bustamante et al. 2006).The similar $\Delta^{199}Hg/\Delta^{201}Hg$ ratios displayed by muscles and livers also supports the idea of a similar source of MeHg between tissues. An alternative explanation could be an influence of different Hg residence time between tissues. Muscles are assumed to reflect Hg acquisition since the last moult, after remobilisation into growing feathers, therefore representing Hg accumulated during one year (considering species with annual moulting). However, Hg in liver (mainly as metabolite iHg) is considered to represent long-term accumulation, although it is known that a part of the produced iHg from hepatic demethylation is excreted by urine or faeces. This different Hg turnover and residence time between muscles and liver could involve distinct sources of Hg accumulated specifically in each tissue.

Conclusion

In conclusion, the exploration of Hg isotopes in tissues from three seabird species with contrasting ecological behaviour (foraging habits, trophic level, type of prey, etc.) and different biological characteristics (metabolic response, detoxification strategies and capacities) enables to evaluate the influence of these factors in Hg exposure pathways and bioaccumulation. The observed MDF variations among internal organs and feathers provided information about detoxification processes occurring in seabirds (Hg hepatic demethylation, inter-organ redistribution or Hg excretion by moulting), indicating different metabolic mechanisms depending on species, physiology or the extent of Hg dietary exposure. The existence of different Hg integration times between feathers and internal organs permits the access to different temporal and geographical windows. Although internal organs can provide valuable information about long-term Hg accumulation and physiological aspects, their longer Hg turnover relative to other "metabolically recent" tissues that give access to more precise Hg temporal integration windows, such as blood (weeks to few months) or feathers (~1 year), makes them less sensitive to trace Hg spatio-temporal exposure.

Main **findings** of this work:

- Hg species distribution among tissues followed a general pattern for the three seabird models, with livers being predominantly enriched in iHg, certainly as a consequence of *in vivo* demethylation, whereas muscles and feathers tend to accumulate mainly MeHg.
- Differences in δ^{202}Hg values between livers and muscles indicates Hg fractionation during MeHg demethylation in livers.
- Different temporal windows of Hg exposure and different Hg turnover between internal tissues (life span accumulation) and feathers (annual incorporation) are reflected in distinct Hg MIF values, with feathers showing significantly greater Δ^{199}Hg values potentially as a consequence of the exposure to distinct Hg sources during wintery migration.
- Heavier δ^{202}Hg values in feathers relative to muscles could be due to a combination of Hg fractionation during metabolic pathways (preferential excretion of isotopically heavier MeHg from muscles to growing feathers during moult) and extrinsic factors linked to different temporal windows of Hg exposure in feathers (wintery acquisition).

Acknowledgements

The present work was supported financially and logistically by the Région Poitou-Charentes through a PhD grant to MR, and by the Institut Polaire Français Paul Emile Victor (IPEV, program no. 109, H. Weimerskirch) and the Terres Australes et Antarctiques Françaises (TAAF) and by the Agence Nationale de la Recherche (program POLARTOP, O. Chastel). The IUF (Institut Universitaire de France) is acknowledged for its support to PB as a Senior Member. The authors thank all the fieldworkers that contributed to the collection of samples. Field procedures were authorised by the Ethics Committee of IPEV and by the Comité de l'Environnement Polaire.

Chapter 4.

Ecological and biogeochemical aspects

Chapter 4. Ecological and biogeochemical aspects

Part 4.1: Identification of sources and bioaccumulation pathways of MeHg in subantarctic penguins: a stable isotopic investigation

Abstract

Methylmercury (MeHg) is a bioaccumulative neurotoxin with severe health risk for humans and wildlife. Seabirds have been widely used as bioindicators of Hg marine contamination and the investigation of their foraging strategies is of key importance for the better understanding of their MeHg exposure pathways and for depicting MeHg environmental sources within the different ecosystems. Here we report stable isotopic values of Hg (δ^{202}Hg, Δ^{199}Hg), carbon (δ^{13}C, proxy of foraging habitat) and nitrogen (δ^{15}N, dietary proxy) in blood of four sympatric subantarctic penguins that breed at the Crozet Islands (southern Indian Ocean). Penguins have species-specific foraging strategies in their horizontal (from coastal to oceanic waters), vertical (from benthic to pelagic dives) and dietary (from crustaceans to mesopelagic fish) components. A progressive increase in blood Hg isotopic composition (δ^{202}Hg and Δ^{199}Hg, respectively) was observed from benthic (1.45±0.12 and 1.41±0.06 ‰), mesopelagic (1.66±0.11 and 1.54±0.06 ‰) to epipelagic (1.93±0.18 and 1.77±0.13 ‰) penguins, indicating a benthic-pelagic gradient of MeHg sources. Nevertheless, the relatively slight variations in both δ^{202}Hg and Δ^{199}Hg suggest the mixing of various MeHg sources from benthic and oceanic origins in waters surrounding the Crozet Islands. Penguins reflect the environmental conditions prevailing in their species-specific foraging habitats, thus allowing depicting distinct MeHg sources at larger scales of the Southern Ocean. The present study provides new and valuable information to help identifying processes involved in the Hg biogeochemical cycle in subantarctic ecosystems of the Southern Indian Ocean.

*Keywords***:** mercury, seabirds, stable isotopes, origin, Southern Ocean

Introduction

As a result of its severe toxicity, mercury (Hg) is considered as a worldwide pollutant of major concern for humans and wildlife (e.g. Tan et al., 2009). It is present in all compartments, transported over long distances and accumulated in the environment, where once methylated, it biomagnifies (e.g. Atwell et al., 1998). In aquatic systems, Hg inorganic forms (iHg) can be methylated by microbiological (Compeau and Bartha, 1985; Jensen and Jernelöv, 1969) or abiotic processes (Celo et al., 2006), leading to the incorporation and posterior biomagnification of methylmercury (MeHg) in marine food webs. Vertical profiles of MeHg concentrations have been globally found in oceans (Cossa et al., 2009; Mason and Fitzgerald, 1990; Hammerschmidt and Bowman, 2012), including the Southern Ocean (Cossa et al., 2011), presenting lower concentrations in surface waters due to the degradation of MeHg into iHg by photodemethylation processes (Bergquist and Blum, 2007) and increasing concentrations with depth peaking at low-oxygen intermediate waters, where microbial methylation is assumed to occur (Mason and Fitzgerald 1990; Heimbürger et al. 2010; Blum et al. 2013). Consequently, an increasing gradient of Hg concentrations was found in fish caught from the surface (epipelagic zone) to deeper waters (mesopelagic zone) (Monteiro et al., 1996; Chouvelon et al., 2012; Blum et al., 2013).

Seabirds are positioned at medium to high trophic levels, being thus exposed to elevated concentrations of MeHg via dietary uptake. They are recognized as efficient bio-indicators of marine Hg contamination at different spatial scales according to their life cycle (Burger and Gochfeld, 2004; Fort et al., 2014). In contrast to flying birds, penguins exploit relatively spatially restricted foraging zones and are thus representative of Hg contamination in more limited areas, which make them interesting models for local biomonitoring studies (Carravieri et al. 2013; Carravieri et al. 2016). Investigating diverse penguin species provide access to different marine environmental compartments since they have species-specific foraging ecologies. They feed on a large diversity of prey in different oceanographic ecosystems, both horizontally (from the neritic to the oceanic domains) and vertically, as they forage at different depths of the water column (from the epipelagic to the mesopelagic zone). Taking advantage of these specificities, we have measured here the stable isotope ratios of Hg in blood samples of four sympatric penguin species that breed at the subantarctic Crozet Islands (southern Indian Ocean) in order to characterize a priori different MeHg exposure pathways.

Mercury has seven stable isotopes that undergo mass dependent fractionation (MDF) as a consequence of many physical, chemical or biological processes (Rodriguez Gonzalez et al. 2009; Kritee et al. 2007; Kritee et al., 2009; Estrade et al. 2009; Zheng and Hintelmann 2010a). Moreover, photochemical reactions induce significant Hg mass independent fractionation (MIF), wherein the odd isotopes are enriched or depleted in reaction products relative to the even isotopes

(Zheng and Hintelmann 2009a; Bergquist and Blum 2007; Sherman et al. 2010; Perrot et al., 2012). However, no substantial MIF has been observed during trophic processes (Kwon et al. 2012b; Perrot et al., 2012), meaning that MIF values can be used as conservative tracer of MeHg sources in predators.

Increasing number of studies have successfully applied Hg isotope analysis for elucidating sources and pathways of MeHg in the environment (e.g. Senn et al., 2010; Gehrke et al., 2011; Day et al., 2012; Chen et al., 2016). In aquatic ecosystems, MIF is highly sensitive to photochemical reactions and varies as a function of light penetration extent at different locations or depths. In a previous study, Blum et al., (2013) evidenced a relationship between fish foraging depth and Hg isotopic values as a consequence of different extent of photochemical degradation of MeHg in the water column. These authors showed that MeHg produced at the subsurface of the open ocean is effectively uptake by fish with higher MIF values in epipelagic fish than in deep ones. Higher magnitudes of MIF have also been observed in pelagic organisms relative to coastal organisms (Senn et al., 2010; Day et al., 2012; Perrot et al., 2012). This gradient was mainly attributed to enhanced light penetration in oceanic waters due to minor water turbidity and lower dissolved organic carbon (DOC), thus leading to higher rate and extent of MeHg demethylation in the pelagic water column.

Stable isotopes of carbon ($\delta^{13}C$) and nitrogen ($\delta^{15}N$) serve as powerful indicators of foraging habitat and trophic position, respectively. Isotopic measurements have already been validated in the Southern Ocean, with seabird $\delta^{13}C$ values indicating their latitudinal foraging grounds and depicting offshore versus inshore consumers and benthic vs pelagic ones, while $\delta^{15}N$ values increased with trophic level (e.g., Cherel et al., 2007; Jaeger et al., 2010). Thus, we used δ13C and δ15N values to explain the potential variations in Hg stable isotopes in seabirds and to trace the origin, trophic transfer and bioaccumulation processes of Hg in marine food webs, as it was previously demonstrated in fish (Senn et al., 2010; Blum et al., 2013; Li et al., 2016; Cransveld et al., 2017).

The main objective of this work was to investigate the effectiveness of Hg stable isotope ratios in seabird tissues to discern and quantify MeHg sources and exposure pathways in the different marine compartments in which they forage. Because blood samples are known to reflect recent Hg exposure (month scale) and penguins are generally restricted to areas near their colonies at the time of sample collection (end of the breeding period), Hg isotopic composition of penguin blood samples were considered as indicative of local Hg values. Thus, we hypothesized that contrasting ecological strategies among penguins (four species) would determine the uptake of distinct environmental MeHg sources and would lead to interspecies differences in blood Hg isotopic composition. According to MIF dynamics in aquatic systems, we did the following

hypothesis that more positive Δ^{199}Hg values are expected for penguins foraging in shallower waters (rockhopper and macaroni penguins) than mesopelagic (king penguins) feeders; while lower Δ^{199}Hg values are predictable for benthic predators (gentoo penguins) relative to the other three pelagic species. The main question addressed in this study is: what is the effectiveness of Hg isotopes to elucidate the environmental origin and exposure pathways of MeHg accumulated in seabirds depending on their ecological characteristics?

Material and methods

Study site and sampling procedure

Sample collection was conducted during the austral summer 2011-2012 (from October to February; Table 4.S1) at Ile de la Possession, Crozet Islands (Subantarctic Zone, 46°26'S, 51°45'E). Ten to 11 randomly-chosen breeding adults were blood sampled at the end of the chick-rearing period by venepuncture of a flipper vein using heparinized syringes. Whole blood was centrifuged to separate plasma from blood cells (hereafter blood). Blood samples were kept frozen at -20°C until Hg and isotopic analyses in France.

Diet and foraging habits of penguin populations

All the four sympatric species of penguins that breed at the Crozet Islands were investigated, including the king *Aptenodytes patagonicus*, gentoo *Pygoscelis papua*, macaroni *Eudyptes chrysolophus* and eastern rockhopper *E. chrysocome filholi* penguins. The king penguins (KP) is a large oceanic species that feed on mesopelagic fish (myctophids) at deep depths (100-300 m) in distant southern foraging grounds located in the vicinity of the Polar Front (Kooyman et al., 1992; Cherel et al., 2007; Bost et al., 2015). In contrast, the medium-sized gentoo penguin (GP) is a coastal neritic species that dive both pelagically and benthically to feed opportunistically on a large diversity of prey, including swarming crustaceans and benthic fish (Bost et al., 1994; Ridoux, 1994). The smaller and closely-related macaroni (MP) and rockhopper (RP) penguins forage in offshore waters where they primarily target swarming crustaceans (euphausiids and hyperiids) in the top 70 m of the water column (Ridoux 1994; Y. Tremblay and Cherel 2003; Cherel et al. 2007; Bon et al. 2015).

Sample preparation and analytical methods

Hg speciation and Hg isotopic analyses

For Hg speciation analyses, Hg was extracted from blood samples (0.10-0.15 g) by alkaline microwave digestion with 5 mL of tetramethylammonium hydroxide (25% TMAH in H_2O, Sigma Aldrich) (Rodrigues et al. 2011). Details of the extraction method, analysis and quantification of Hg species are included in (Chapter 3.1).

Prior to Hg isotopic analyses, blood samples (0.05-0.10 g) were digested with 3 or 5 mL of HNO_3 acid (65%, INSTRA quality) after a predigestion step overnight at room temperature and later extraction in Hotblock at 75ºC during 8 h (6 h in HNO_3 and 2 h more after the addition of 1/3 of the total volume of H_2O_2 (30%, ULTREX quality)). Details of Hg isotopic composition analyses are included in (Chapter 3.1).

For the validation of the analytical results, two certified reference material were analysed: human hair IAEA-086 and tuna fish ERM-CE-464. An internal reference sample was prepared with pool samples collected from different individuals of king penguin from Crozet Islands: RBC-KP (red blood cells) and was analysed at each analytical session. Uncertainty for delta values was calculated using 2SD typical errors for reference material (Table 4.S2).

Carbon and nitrogen stable isotopes analyses

Carbon ($\delta^{13}C$) and nitrogen ($\delta^{15}N$) stable isotope ratios were determined in red blood cells with a continuous flow mass spectrometer (Thermo Scientific Delta V Advantage) coupled to an elemental analyser (Thermo Scientific Flash EA 1112) (aliquots mass: ~0.3 mg). Results are in delta notation relative to Vienna PeeDee Belemnite and atmospheric N_2 for $\delta^{13}C$ and $\delta^{15}N$, respectively. Replicate measurements of internal laboratory standards (acetanilide) indicated measurement errors < 0.15‰ for both $\delta^{13}C$ and $\delta^{15}N$ values.

Statistical analyses

Statistical tests were performed using RStudio. Before analyses, data were checked for normality of distribution and homogeneity of variances using Shapiro–Wilk and Breusch-Pagan tests, respectively. According to this, parametrical (One-way ANOVA) or non-parametrical tests (Kruskal–Wallis with Conover-Iman test) were performed. Statistically significant results were set at $\alpha = 0.05$.

Results

Blood Hg concentrations and Hg isotopic composition

Blood THg concentrations differed amongst penguin species (Kruskal Wallis, H=30.09, p<0.0001), with KP and GP being more contaminated than MP and RP (Table 4.1). Accordingly, blood MeHg was overall different (H=28.87, p<0.0001), with KP and GP showing higher concentrations than MP and RP. All individual penguins presented a large predominance of MeHg in their blood (94±2%, range: 91-98%, n = 42).

Blood samples showed large ranges of individual δ^{202}Hg (MDF) and Δ^{199}Hg (MIF) values (1.28-2.12 ‰ and 1.31-1.95 ‰, respectively, n = 42). Both blood δ^{202}Hg and Δ^{199}Hg values differed amongst penguins (H=26.94 and 32.27, respectively, both p<0.0001), except KP and GP that showed identical δ^{202}Hg values. Blood δ^{202}Hg and Δ^{199}Hg values increased in the order GP = KP < MP < RP and GP < MP < KP < RP, respectively. RP notably showed high inter-individual variability in their blood Δ^{199}Hg values (from 1.55 to 1.93 ‰).

Measured blood δ^{202}Hg values followed the predicted theoretical MDF line. In contrast, measured blood δ^{199}Hg values diverged from the δ^{199}Hg theoretical MDF line (Figure 4.S1), indicating that all blood samples showed MIF of the ^{199}Hg and ^{201}Hg odd isotopes. Overall penguin blood samples displayed a Δ^{199}Hg/Δ^{201}Hg slope of 1.16±0.05 (R^2=0.98, p<0.0001) (Figure 4.1). Individual Δ^{199}Hg/Δ^{201}Hg ratios for each penguin species are included in Table 4.1.

Blood δ^{13}C and δ^{15}N values

Penguins were segregated by their δ^{13}C and δ^{15}N values (Figure 4.S2), with both variables being significantly and negatively correlated (Pearson correlation R^2= -0.74, p<0.0001). The four species presented distinct δ^{13}C values (Kruskal Wallis, H=35.30, p<0.0001), with a progressive ^{13}C enrichment from KP to GP. Blood δ^{15}N values were also different (H=25.24, p<0.0001). They allow splitting species into two groups, with MP, RP and GP differing from KP by their 1.5-1.8 ‰ lower δ^{15}N values (Table 4.1).

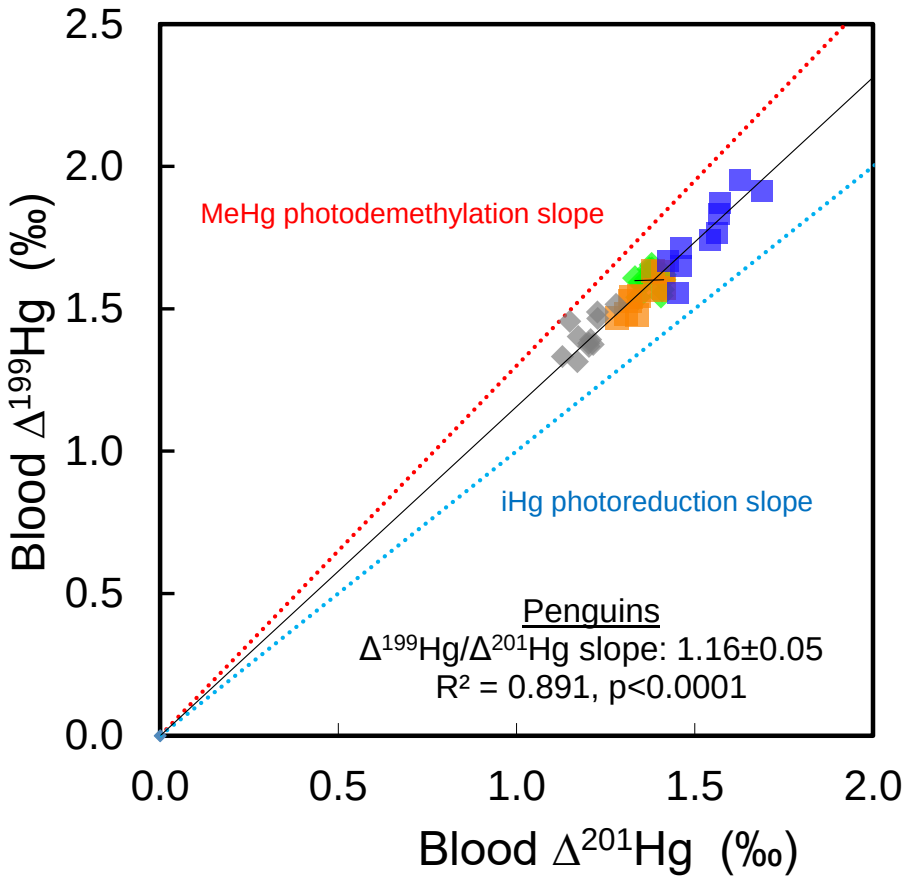

Figure 4.1 Blood Hg MIF values (Δ^{199}Hg versus Δ^{201}Hg) of subantarctic penguins from Possession Island, Crozet archipelago. The solid line represents the $\Delta^{199}Hg/\Delta^{201}Hg$ slope of the samples. The red dashed line represents the theoretical $\Delta^{199}Hg/\Delta^{201}Hg$ slope for MeHg photodemethylation in the water column, and the blue dashed line represents the theoretical $\Delta^{199}Hg/\Delta^{201}Hg$ slope expected for photoreduction of iHg in the water column (Bergquist and Blum, 2007).

Relationship between blood Hg isotopic composition and δ^{13}C and δ^{15}N values

Without considering KP population, highly negative correlations were found for δ^{13}C values with δ^{202}Hg values (R^2=-0.73, p<0.0001) and with Δ^{199}Hg values (R^2=-0.71, p<0.0001) (). An absence of correlation was observed between blood Δ^{199}Hg and δ^{15}N values (R^2=0.03, p=0.30) and between blood δ^{202}Hg and δ^{15}N values for the overall individuals (R^2=-0.10, p=0.52) (Figure 4.S3).

Table 4.1. Food and feeding ecology, including blood $\delta^{13}C$ (foraging habitat) and $\delta^{15}N$ (diet) values, together with blood Hg characteristics of subantarctic penguins from Possession Island, Crozet archipelago (n, number of individuals). Values not sharing the same superscript letter are statistically different. Values are means ± SD.

Species	**Diet**	**Diving behaviour**	**N**	**$\delta^{13}C$** (‰)	**$\delta^{15}N$** (‰)	**THg** (µg g^{-1})	**MeHg** (µg g^{-1})	**MeHg** (%)	**$\delta^{202}Hg$** (‰)	**$\Delta^{199}Hg$** (‰)	**$\Delta^{199}Hg/\Delta^{201}Hg$ ratio**
King penguin	fish	mesopelagic	11	-21.8±0.4 ^{A}	10.1±0.2 ^{A}	2.01±0.29 ^{A}	1.88±0.28^{A}	93±1	1.49±0.11 ^{A}	1.60±0.04 ^{A}	1.16±0.04 ^{A}
Gentoo penguin	crustaceans, fish	epipelagic, benthic	11	-18.6±0.3 ^{B}	8.2±0.6 ^{B}	2.04±1.00 ^{A}	1.89±0.93^{A}	93±1	1.45±0.12 ^{A}	1.41±0.06 ^{B}	1.18±0.04 ^{A}
Macaroni penguin	crustaceans (fish)	epipelagic	10	-20.0±0.7 ^{C}	8.6±0.4 ^{B}	1.06±0.16 ^{B}	1.01±0.15 ^{B}	96±2	1.66±0.11 ^{B}	1.54±0.06 ^{C}	1.14±0.02 ^{A}
Eastern rockhopper penguin	crustaceans (fish)	epipelagic	10	-20.8±0.3 ^{D}	8.6±0.4 ^{B}	0.97±0.20 ^{B}	0.93±0.19 ^{B}	95±1	1.93±0.18 ^{C}	1.77±0.13 ^{D}	1.15±0.04 ^{A}

Discussion

Because MeHg is the predominant Hg species in all the blood samples, irrespective of THg concentration or penguin species, the measured Hg isotopic composition of this tissue corresponds essentially to MeHg values. This predominance of MeHg in blood allows directly comparing the four penguin species, and the exploration of MDF and MIF values to trace MeHg pathways in each marine compartment used by penguins in Crozet waters. In the following sections, variations of Hg isotopic composition among penguins are discussed and interpreted in function of their specific ecological characteristics in order to estimate sources and processes involving MeHg.

Variations in foraging habitats ($\delta^{13}C$) between penguin populations

In areas surrounding subantarctic islands, $\delta^{13}C$ values decrease from neritic to oceanic waters (inshore-offshore $\delta^{13}C$ gradient), and from warm to cold waters (latitudinal $\delta^{13}C$ gradient), thus allowing using $\delta^{13}C$ values to assess the main foraging grounds of seabirds (Cherel et al. 2013; Cherel and Hobson, 2007). A large range of $\delta^{13}C$ values was observed across penguin populations with decreasing values from GP to KP (a 3.6 ‰ difference). KP exhibited much lower $\delta^{13}C$ values than the other two oceanic penguins (MP and RP), which is in agreement with their well-known southern foraging grounds down to the Polar Front (Cherel et al., 2007; Bost et al., 2015). RP showed significantly lower $\delta^{13}C$ values than MP, indicating that they forage at more southern latitudes than MP during the breeding period (Cherel and Hobson, 2007). Finally, the more positive $\delta^{13}C$ values of GP compared to the other species are in agreement with the inshore feeding habits of the species (Cherel and Hobson, 2007). Species-specific $\delta^{13}C$ values clearly demonstrate that the four penguins breeding at the Crozet Islands document each a different marine environment, thus allowing studying processes affecting Hg behaviour and its fate in the Southern Ocean.

Relation between Hg isotopes and trophic ecology ($\delta^{15}N$)

Independently of the species, the lack of correlation between blood $\Delta^{199}Hg$ and $\delta^{15}N$ values is consistent with the absence of MIF during trophic transfer (Laffont et al., 2009; Perrot et al., 2010; Sherman et al., 2013; Li et al., 2014). While MDF could be produced during trophic transfer (Laffont et al., 2009; Perrot et al., 2010), no correlation was observed between $\delta^{202}Hg$ and $\delta^{15}N$ values. Differences in dietary composition amongst pelagic penguins is well illustrated by $\delta^{15}N$ values being higher in the fish-consumer species (KP) than in crustacean feeders (MP and RP). KP preferentially rely on mesopelagic fish so they have a higher trophic position than MP and RP that rely mainly on swarming euphausiids and hyperiids (Cherel et al. 2007). Moreover,

mesopelagic fish are known to accumulate elevated MeHg concentrations as a result of enhanced Hg methylation in deep waters (Monteiro et al., 1996; Chouvelon et al., 2012). Both the higher trophic position and the mesopelagic foraging habitat of KP explain why their THg and MeHg concentrations were twice higher compared to the epipelagic crustacean-eaters MP and RP. Based on the existing knowledge of Hg isotopic fractionation dynamics, we hypothesized that the observed MIF variations between penguin species are linked to distinct MeHg sources having undergone different degrees of photochemical reactions. Since no effect of trophic level was found for δ^{202}Hg and Δ^{199}Hg values, the most plausible explanation of Hg isotopic variations is the consequence of species-specific foraging habitats within the marine environmental compartments.

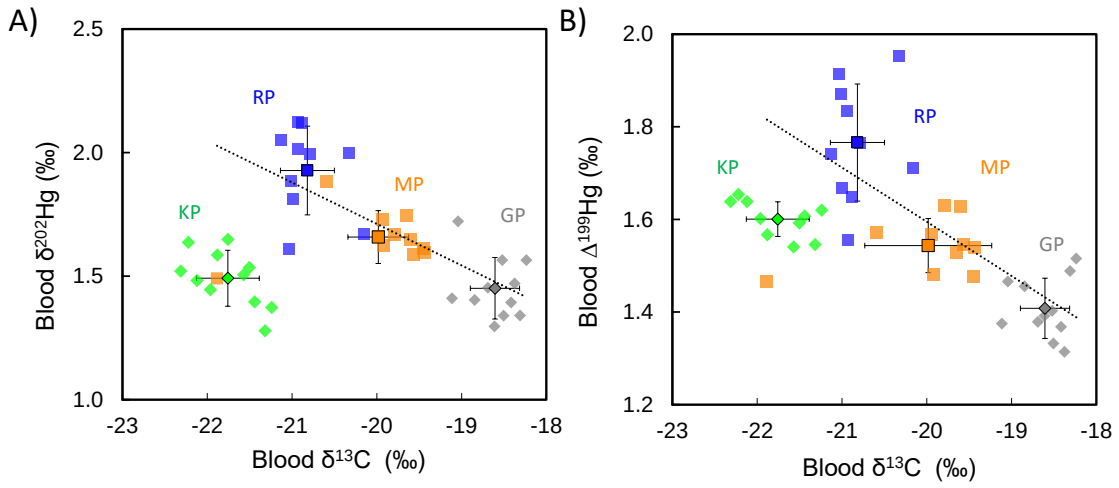

Figure 4.2. A) Blood δ^{202}Hg versus δ^{13}C values of subantarctic penguins from Possession Island, Crozet archipelago. Regression equation (excluding KP) is y=--0.17x-1.64, R^2=-0.73, p<0.0001. B) Blood Δ^{199}Hg versus δ^{13}C values. Regression equation is y=-0.12x-0.74, R^2=-0.71, p<0.0001. Abbreviations: GP, gentoo penguin; KP, king penguin; MP, macaroni penguin; RP, rockhopper penguin.

Hg isotopic values and penguin species-specific foraging habitats

MIF ratios and estimation of the extent of photochemical processes

Photochemical reactions of MeHg and iHg in the water column are recognised as the main driver of Hg MIF values and each process is characterized by a different Δ^{199}Hg/Δ^{201}Hg ratio. Since this Δ^{199}Hg/Δ^{201}Hg ratio is assumed to be preserved in the food chain after MeHg assimilation by primary producers and during bio-magnification up the food web, it is used to identify mechanisms involving MIF variations (Bergquist and Blum, 2007). Theoretical slopes

have been experimentally designed in aquatic systems (Bergquist and Blum, 2007), corresponding to 1.36±0.02 for MeHg photodemethylation and 1.00±0.02 for iHg photoreduction in freshwater with natural DOC. Although studies in freshwater fish also reported $\Delta^{199}Hg/\Delta^{201}Hg$ ratios close to 1.3 (Laffont et al., 2009; Gantner et al., 2009; Sherman et al., 2013), slightly lower $\Delta^{199}Hg/\Delta^{201}Hg$ ratios have been observed in marine organisms (Senn et al., 2010; Point et al., 2011; Gehrke et al., 2011; Day et al., 2012; Blum et al., 2013; Kwon et al., 2014). This effect may be the result of different ligands associated with Hg in aqueous solutions (such as organic matter, dissolved cations and the presence of halogens in seawater). Indeed, variable $\Delta^{199}Hg/\Delta^{201}Hg$ ratios have been recently documented for MeHg photodemethylation under different types and concentrations of DOC (Chandan et al., 2015), indicating that low concentrations of DOC relative to MeHg could involve lower $\Delta^{199}Hg/\Delta^{201}Hg$ ratios. The overall $\Delta^{199}Hg/\Delta^{201}Hg$ ratio for penguin blood samples (1.16±0.05) is consistent with those previously reported in marine fish and seabirds (Senn et al., 2010; Day et al., 2012; Blum et al., 2013). Due to the predominance of MeHg in penguin blood, and assuming a potential diminution in MIF slope due to low DOC concentrations in subantarctic waters, the obtained ratio seems to indicate an accumulation of residual MeHg that has principally undergone photochemical demethylation.

Hg MIF in marine fish has been used to estimate the relative proportion of MeHg formed in the open ocean that is photochemically degraded prior its entry into the food web (Blum et al. 2013). Thus, it has been shown to be an effective proxy of fish foraging depths (Blum et al. 2013). Assuming MeHg photodemethylation as the major photochemical process, we estimated the percentage of presumed photodemetylated MeHg before entering the food web based on experimental studies (Bergquist and Blum 2007) (detailed in Annexes). The overall difference between penguins (~3%) was surprisingly low when taking into account the range of habitats used by the penguins (from coastal benthic/pelagic feeders to mesopelagic feeders). However, considering the existence of higher amounts of DOC in benthic waters relative to the pelagic domains, more substantial differences should be found between sites, even for equivalent MeHg concentrations among the compartments. Previous studies in fish from the Gulf of Mexico estimated that MeHg in coastal fish was ~10-20% degraded in contrast to oceanic fish whose percentage of photodemethylated MeHg was ~40-65% (Senn et al., 2010). Even higher in surface waters, photodegradation appears overall limited in the southern Indian Ocean subpolar waters compared to subtropical waters as a consequence of lower sunlight extent and slighter angle of incidence. However, further investigations are needed to evaluate if photodemethylation really varies across a larger latitudinal range (Chapter 4.2).

MIF variations with penguin foraging depths

The decrease of light penetration with depth leads to the reduction of the rate of MeHg photodemethylation with the subsequent less extent of Hg MIF (Blum et al. 2013). Although Hg MIF is much more sensitive to photochemical reactions, photodemethylation also induces MDF by production of isotopically lighter MeHg and so that the remaining iHg is enriched in heavier isotopes (Bergquist and Blum 2007). In the North Pacific Ocean, Blum et al., (2013) documented a Δ^{199}Hg offset of ~5 ‰ between fish feeding at the surface mixed layer and at 600 m depth. Here, we aimed to assess the correlation between Hg MIF and penguin foraging depths in the Southern Ocean. Although MIF values of RP, MP and GP were in good agreement with the predicted relationship between Δ^{199}Hg values and foraging depth, this trend did not hold for KP since they feed at deeper depths and should show lower blood Δ^{199}Hg values than MP. Since KP adults are representative of Polar Front water masses during this time, this result is likely associated to a latitudinal effect in Hg isotopic values (Chapter 4.2). Anyway, Hg isotopic values allow visualising penguin foraging depths, which are generally complex to determine accurately due to penguin seasonal foraging changes or vertical movements of prey among other factors. Indeed, by interpretation of δ^{13}C values we can only determine different foraging habitats in a spatial scale (inshore to offshore or latitudinal movements), as well as satellite tracking that enables only horizontal monitoring. Since Hg MIF values offers efficient tracking of foraging depths, measuring Hg isotopes represents a valuable tool for complementary interpretation of avian ecological habits.

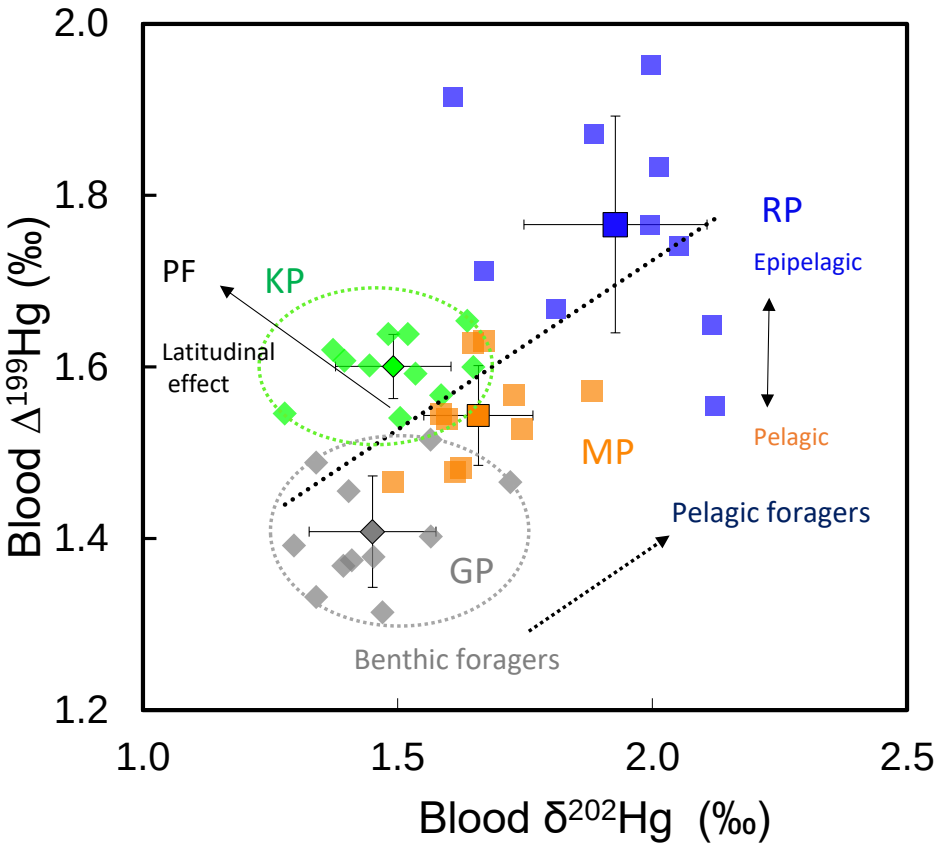

Figure 4.3 Blood Hg MIF versus MDF values (Δ^{199}Hg versus δ^{202}Hg) of subantarctic penguins from Possession Island, Crozet archipelago. Regression equation is y=-0.39x-0.93, R^2=0.60, p<0.0001. Abbreviations: PF, Polar Front; GP, gentoo penguin; KP, king penguin; MP, macaroni penguin; RP, rockhopper penguin.

Tracing distinct MeHg sources over inshore-offshore and pelagic-benthic gradients

Considering only Hg MIF values is not enough for the complete understanding of the exposure pathways to MeHg relative to specific foraging habitats in penguins. Therefore, we further explored and compared Hg isotopic values between penguins, both in a horizontal (inshore-offshore) and in a vertical (benthic-pelagic) dimension. Previous studies have documented Hg isotopic differences between coastal and oceanic marine organisms (Senn et al., 2010; Day et al., 2012; Perrot et al., 2012), indicating the existence of contrasted environmental MeHg sources with distinct Hg isotopic baseline and different extent of aquatic photochemistry. Marine sediments are characterized by negative to slightly positive MDF values and low or near-to-zero MIF values and therefore lighter Hg isotopic values are typically found in coastal biota relative to oceanic organisms. Moreover, reduced light penetration as a consequence of higher turbidity in coastal ecosystems limits Hg photochemistry. Hence, it contributes to the lower Hg MIF values of MeHg accumulated in coastal relative to open ocean food webs, excepting

mesopelagic organisms. Apart from different extent of photochemical processes, biotic methylation is known to occur in benthic sediments and in the open water column below the surface mixed layer (Blum et al. 2013). Since microbiological methylation produces MeHg enriched in lighter isotopes compared to the residual iHg pool (Rodriguez Gonzalez et al. 2009), greater methylation yields than demethylation promote the accumulation of isotopically lighter MeHg (lower δ^{202}Hg values) (Perrot et al., 2015).

For easily tracking MeHg sources between Crozet marine compartments, KP were not considered in the discussion since they are representative of Polar Front waters during the studied period. Assuming different MeHg sources between inshore-offshore Crozet areas, benthic GP were expected to accumulate Hg with a sediment origin, i.e. lower δ^{202}Hg and Δ^{199}Hg values, relative to oceanic foragers. Due to the lack of Hg isotopic data on sediments from Crozet Islands, we estimated negative δ^{202}Hg values and close to zero Δ^{199}Hg values, as commonly observed in sediments from other sites such as in the Arctic Ocean (δ^{202}Hg: -1.37±0.38 ‰; Δ^{199}Hg: -0.02±0.07 ‰) (Gleason et al. 2016) and the Antarctic coasts (δ^{202}Hg:-0.39±0.49 ‰; Δ^{199}Hg: 0.71±0.43 ‰) (Zheng et al., 2015). Indeed, Zheng et al., (2015) observed similar MIF values between historical sediment profiles and penguin and seal fresh faeces, suggesting that faeces were the dominant sources of Hg to the sediments at different time periods. Due to the representative penguin community in Crozet Islands, a significant fraction of Hg accumulated in coastal sediments of could be of ornithogenic origin and therefore display similar values as Antarctic sediments. GP presented the lowest δ^{202}Hg and Δ^{199}Hg values, indicative of their higher exposure to benthic MeHg. Greater methylation in benthic waters may also implicate the production of isotopically lighter MeHg at depth and its accumulation in the benthic food web, contributing to the lower δ^{202}Hg values and the high levels of MeHg observed in GP. The significant correlations between δ^{13}C and Hg isotopic values seem to indicate a progressive transition from terrestrial to marine values both in a horizontal foraging trend (inshore-offshore) and vertical gradient (benthic-pelagic). This suggests that the lower Hg isotopic values observed in benthic ecosystems may derive from *in situ* Hg methylation in sediment and reduced exposure to sunlight (due to depth) while a gradual increase in Δ^{199}Hg (and δ^{202}Hg) was observed through offshore shallower areas as a consequence of a higher magnitude of photochemistry. Nevertheless, the low variations in Hg isotopes values between benthic and pelagic penguins compared to previous inshore-offshore values measured in other marine ecosystems (Senn et al., 2010; Day et al., 2012) seem to indicate a higher degree of mixture between benthic and pelagic MeHg sources. The remote location of the Crozet Islands, which are surrounded by deep oceanic waters (4000-5000 m), could explain a lower impact of the sediment-derived MeHg inputs compared to continental coastal zones. Moreover, these islands have a plateau of around 150 km wide that interacts with different water masses derived from the Antarctic Circumpolar Current (Pollard et al. 2007), potentially

favouring the recirculation and mixing of MeHg from different sources. The relationship between Hg isotopes (δ^{202}Hg and Δ^{199}Hg) and MeHg concentration (Figure 4.S4) indicates that each penguin species reflects an exposure to different MeHg sources. A potentially higher productivity in the Polar Front compared to subantarctic waters would lead to greater bacterial methylation, which could then explain the lower δ^{202}Hg values and higher MeHg concentrations obtained in KP compared to the other pelagic penguins (Chapter 4.2). This indicates that KP feed on a specific food web which is potentially enriched in MeHg compared to other subantarctic penguins. Therefore, Hg isotopes in sympatric penguins of the Crozet Islands represent an ecosystem characterised by three distinct food webs exposed to different levels and sources of MeHg, clearly dominated by a pelagic-benthic gradient and a latitudinal effect (potentially linked to productivity).

Conclusions

The combination of blood isotopic values (Hg, C and N) of penguins together with the documented information about their feeding ecology allows characterizing the major factors explaining their levels of MeHg exposure in relationship with their contrasted ecological habits. The observed Hg isotopic variations from benthic to pelagic penguins suggest the existence of mixing sources deriving from MeHg production at depth and increased photochemical processes when going to shallower offshore waters. Due to the scarce data on Hg isotopic composition in the Southern Ocean, further research is needed to investigate biogeochemical sources of MeHg formation and the processes leading to accumulation of Hg in biota from these remote ecosystems.

Main **findings** of this work:

- **Penguins** with contrasted feeding ecology were used to test the **variability of Hg isotopic values** according to their known **feeding habitats and diets**.
- Hg **MIF** (Δ^{199}Hg) varied **in function of penguin foraging depths**, thus allowing estimating the **extent of MeHg photodemethylation** with depths.
- Differences in **Hg isotopic composition** (0.48 ‰ for δ^{202}Hg and 0.35 ‰ for Δ^{199}Hg) from **benthic to pelagic penguins** suggested **different MeHg biogeochemical sources** across a vertical axis.
- **Species-specific foraging habitats and latitudinal movements** of penguins determine their exposure to **distinct environmental MeHg sources**.

Acknowledgments

The authors thank M. Loubon and F. Théron who helped collecting blood samples in the field, A. Carravieri for managing the sample database, E. Tessier, S. Bérail and J. Barre (IPREM) for technical assistance during Hg speciation and Hg isotopic analyses, and M. Brault-Favrou and G. Guillou for preparing and running stable isotope samples, respectively. The present work was supported financially and logistically by the Institut Polaire Français Paul Emile Victor (IPEV, programme no. 109, H. Weimerskirch), and the Terres Australes et Antarctiques Françaises (TAAF) and by the Agence Nationale de la Recherche (program POLARTOP, O. Chastel). It was also supported financially by the Région Poitou-Charentes (now Région Nouvelle Aquitaine) through a PhD grant to MR, and by the French national program EC2CO Biohefect/Ecodyn//Dril/MicrobiEen (TIMOTAAF project, to DA). The IUF (Institut Universitaire de France) is acknowledged for its support to PB.

Part 4.2: Latitudinal variations of Hg biogeochemical pathways from Antarctic to subtropical waters in the Southern Ocean as revealed by MeHg isotopic composition in seabirds

Abstract

The magnitude of mercury (Hg) contamination in the Southern Ocean ecosystems remains still poorly unknown and determining its fate and impact in these remote areas represents a major challenge. Seabirds are exposed to large quantities of Hg (mainly methylmercury, MeHg) via the diet and have been identified as effective biomonitors of Hg marine contamination. In this study, Hg isotopic composition was measured in blood samples of two ubiquist seabird models (penguins and skua chicks) from the marine environments around the French Southern Ocean territories. These lands cover a wide latitudinal gradient from the Adélie Land (66°39′S, Antarctic) to Crozet Islands (46°25′S, subantarctic) and Amsterdam Island (37°47'S, subtropical). Mass dependent (MDF) and mass independent (MIF) Hg isotopic values obtained in both seabird models separated populations geographically. Blood samples from Antarctic seabirds displayed lower MDF (δ^{202}Hg) values (from -0.02 to 0.79 ‰) than subantarctic (from 0.88 to 2.12 ‰) and subtropical (1.44-2.37 ‰) communities along with increasing southern latitude. However, mean MIF values (Δ^{199}Hg) ranged slightly from Antarctic (1.31 to 1.73 ‰) to subtropical (1.69 to 2.04‰), hence a total mean enrichment in the order of 0.3 ‰ between sites, suggesting that MeHg photodemethylation was not the main explanatory factor of the heavier isotopic signatures (δ^{202}Hg) accumulated in seabirds when decreasing latitude. Although MDF latitudinal variations can be partially explained by photochemical processes, the existence of biogeochemical pathways (methylation/demethylation/reduction) or even biological processes (trophic effects and/or metabolic mechanisms) could induce additional MDF between Antarctic and subtropical marine environments. Overall, this work demonstrates that Hg isotopic variations recorded in seabird blood samples provide new information on the major biogeochemical processes involved in the Hg cycle in the water column of the Southern Ocean ecosystems.

Keywords: mercury, isotopes, Southern Ocean, seabirds, sources, biogeochemistry

Introduction

Although Antarctic and subantarctic environments have been usually perceived as remote areas untouched by anthropogenic pressure, they are reached by contaminants through ocean circulation and atmospheric transport (Fitzgerald et al., 2007). Mercury (Hg) is considered a globally distributed pollutant of major concern for humans and wildlife especially under its form of methylmercury (MeHg), a potent neurotoxin which is capable to accumulate in tissues of living organisms and to biomagnify within the food webs (Mason et al. 1996; Watras et al. 1998). Hg biogeochemical cycle is highly complex and comprises several chemical processes and biological transformations, such as methylation/demethylation and oxidation/reduction reactions that control its abundance and speciation in the water column. In the aquatic compartment, Hg methylation is mainly produced by anaerobic micro-organisms (Compeau and Bartha, 1985). Due to its intense biomagnification along marine food webs, top predators are exposed to high levels of MeHg through the food pathway. Such high exposure poses severe health risks and has impact on the populations (e.g. Tartu et al. 2013; Goutte et al. 2014a).

In the Southern Ocean, particularly in the Indian Ocean sector, various studies have reported worryingly increasing levels of Hg bioaccumulation in biota, especially in top predators (e.g., Bocher et al., 2003; Carravieri et al., 2014bc). Nevertheless, scarce information is available on Hg concentrations, spatial distribution and speciation in the water column from this remote area of the world ocean (Cossa et al. 2011; Lamborg et al. 2014; Canario et al. 2017). Despite its distance from industrial sources of Hg contamination, the most important pathways for Hg transport to the Southern Ocean and Antarctic zones involve a combination of atmospheric input, oceanic currents and sea ice processes that can explain the consequential concentrations of MeHg observed in these remote areas (Cossa et al., 2011). Observations on Hg species distribution in the Southern Ocean suggested distinct features of Hg cycle such as net atmospheric Hg inputs on surface water near the ice edge, Hg enrichment in brine during sea ice formation and net Hg methylation (Cossa et al., 2011). Geographical trends on MeHg in southern oceanic waters suggested more elevated concentrations in Antarctic waters (including the sea ice zone) whereas progressively decreasing MeHg amounts were observed in subantarctic and subtropical seawaters (Cossa et al., 2011). Surprisingly, this north to south increasing gradient is opposed to the observed trend in tissues of seabirds that increase from Antarctic, through subantarctic to subtropical populations (Blévin et al., 2013; Carravieri et al , 2014b; Goutte et al., 2014, Carraveri et al., 2017).

Understanding the Hg cycle in the Southern Ocean and tracing the processes that transform Hg on its various chemical forms are key in determining how it is transported to these remote areas and what is its fate and impact once it gets there. The use of Hg stable isotopes offers a new

and powerful perspective for exploring the cycle of this element and have demonstrated to be useful to depict Hg sources or quantify its reactivity within different environmental compartments (Blum et al. 2014). Hg has seven isotopes which experience mass-dependent and mass-independent isotopic fractionation (MDF and MIF, respectively). Most biogeochemical processes such as volatilisation, reduction, demethylation and methylation induce MDF (Rodriguez Gonzalez et al. 2009; Kritee et al. 2007; Kritee et al., 2009; Zheng and Hintelmann 2010a). Only photochemical demethylation and reduction processes have been identified as producing MIF on odd Hg isotopes (199, 201) at significant levels (Zheng and Hintelmann 2009a; Bergquist and Blum 2007; Sherman et al. 2010; Perrot et al. 2012; Gantner et al. 2009). Consequently, the combination of Hg MDF and MIF signatures provide interesting and complementary information for Hg potential sources and transformation pathways.

Seabirds are exposed to large quantities of Hg via the marine food webs and have been identified as effective biomonitors of Hg contamination, particularly due to ecological and practical reasons (Burger and Gochfeld, 2004; Furness and Camphuysen, 1997). Indeed, marine birds are generally colonial and philopatric, enabling to take samples during their reproduction period and to follow numerous individuals simultaneously and repeatedly over time. Moreover, they are particularly powerful samplers of ocean environments, exploiting a wide variety of prey and a great diversity of foraging habitats and thus providing access to different marine compartments otherwise difficult to sample. Numerous studies have focused on the biomonitoring of Hg using seabirds' tissues, preferentially by analyses of blood and feathers which can be non-lethally collected. Due to their ecological characteristics, chicks and penguins are the most pertinent seabird models for tracing Hg contamination. Indeed, they reflect local contamination since adult penguins are restricted to more precise areas than migratory flying seabirds, and chicks are fed with prey from waters around the colony (Blévin et al., 2013; Carravieri et al., 2014c).

In this research work, the objective was to investigate Hg dynamics over a wide latitudinal gradient across the Southern Indian Ocean, from Antarctica to the subtropics. Analyses of Hg isotopic composition were performed in blood tissues of two seabird models from the French Southern and Antarctic Territories: skua chicks (2 species) and adult penguins (6 species). Although both feathers and blood have been validated as effective tracers for Hg isotopic studies (Chapter 3.1), blood samples were chosen for this study since they provide more-specific Hg isotopic signatures and hence, a better discrimination between populations. As a consequence of different geographical and climatic parameters, we expected to observe significant variations in Hg isotopic signatures between distant southern regions that could provide new insights for tracking Hg cycle in the Southern Ocean.

Material and methods

Sampling sites

Sample collection was conducted during the austral summer 2011-2012 (from October to February) in four sites of the French Southern and Antarctic Territories, depending on the seabird species breeding colonies: Adélie Land (66°40'S, 140°10'E), Crozet Islands (46°26'S, 51°45'E), Kerguelen Islands (49°21′S, 70°18′E) and Amsterdam Island (37°50'S, 77°31'E). Chicks from two species of skua (Antarctic and subantarctic skua) and adults from five species of penguins (Adélie, king, macaroni, eastern rockhopper and northern rockhopper) were investigated. Exact dates of sample collection of each seabird species are specified in Annexes (Table 4.S9). Blood samples were collected and centrifuged as detailed elsewhere (Carravieri et al. 2017). Details of ecological characteristics of each seabird species at the different locations are specified in Annexes.

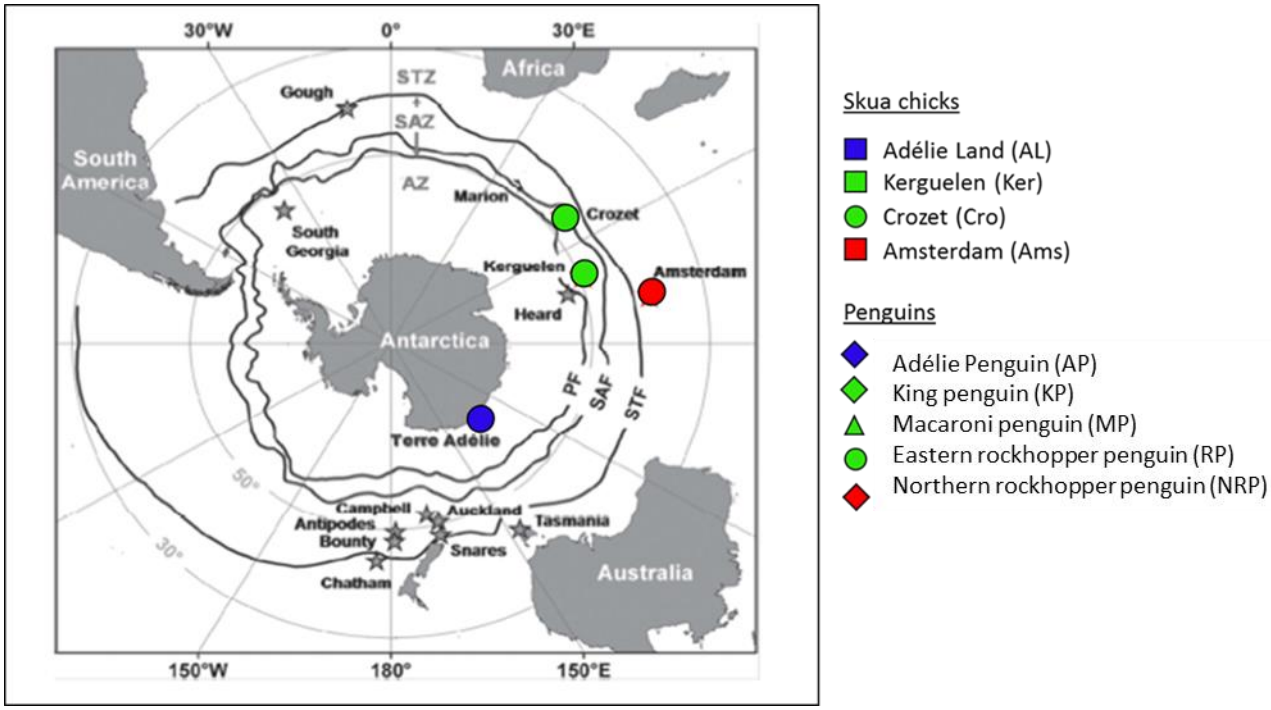

Figure 4.4 Field sampling legend of skua chick and penguin samples at colony locations over a latitudinal gradient from Antarctic (Adélie Land), subantarctic (Crozet and Kerguelen Islands) and subtropical zones (Amsterdam Island).

Reference materials, sample preparation and analytical description

For the validation of the analytical results, two certified reference material were analysed: human hair IAEA-086 and tuna fish ERM-CE-464. An internal reference sample was prepared with pool samples collected from different individuals of king penguin from Crozet Islands: RBC-KP (red blood cells) and was analysed at each analytical session.

For Hg speciation analyses, Hg was extracted from blood samples (0.10-0.15 g) by alkaline microwave digestion with 5 mL of tetramethylammonium hydroxide (25% TMAH in H_2O, Sigma Aldrich) (Rodrigues et al., 2011). Details of the extraction method, analysis and quantification of Hg species are included in (Chapter 3.1). For Hg isotopic analyses, blood samples (0.05-0.10 g) were digested with 3 or 5 mL of HNO_3 acid (65%, INSTRA quality) after a predigestion step overnight at room temperature and later extraction in Hotblock at 75ºC during 8 h (6 h in HNO_3 and 2 h more after the addition of 1/3 of the total volume of H_2O_2 (30%, ULTREX quality)). Details of Hg isotopic analyses are included in (Chapter 3.1).

Statistical tests

Statistical tests were performed using RStudio. Before analyses, data were checked for normality of distribution and homogeneity of variances using Shapiro–Wilk and Breusch-Pagan tests, respectively. According to this, parametrical (One-way ANOVA) or non-parametrical tests (Kruskal–Wallis with Conover-Iman test) were performed. Statistically significant results were set at $\alpha = 0.05$.

Results

Hg concentrations and Hg speciation trends

Hg accumulation in seabird tissues showed a latitudinal gradient with THg concentrations increasing from Antarctic through subantarctic to subtropical populations of both seabird models. MeHg was the dominant Hg form accumulated in blood tissues for all the individuals (92±7%), meaning that blood Hg isotopic composition corresponds essentially to MeHg isotopic values. Skua blood and penguin blood exhibited significantly different MeHg concentrations between sites (Kruskal-Wallis, H=31.09 and 43.05, respectively, both $p<0.0001$). Skua blood MeHg concentrations increased from 0.51 to 3.78 $\mu g \cdot g^{-1}$ (n=40), respectively for Antarctic and subtropical populations. Penguin blood MeHg also increased from Antarctic to subtropical populations (0.43 to 1.95 $\mu g \cdot g^{-1}$, respectively, n=51), in the order AP < RP < MP < KP < NRP (Table 4.2).

Table 4.2. Total and MeHg concentrations (Mean ±1SD, µg.g^{-1} dw), Hg isotopic composition (δ^{202}Hg and Δ^{199}Hg, Mean ± SD, ‰) of the skua and penguin species breeding at the different studied sites. n means the number of individuals analysed. Values not sharing the same superscript letter are statistically different.

Species	Code	Location	Sampling date	n	THg	MeHg	δ^{202}Hg	Δ^{199}Hg
					µg g^{-1}	µg g^{-1}	‰	‰
Antarctic skua	AL	Adélie Land	Dec 2011-Jan 2012	9	0.53±0.08^{A}	0.51±0.09^{A}	0.23±0.13^{A}	1.51±0.08^{A}
Subantarctic skua	Ker	Kerguelen	Dec 2011	10	2.32±0.34^{B}	2.16±0.33^{B}	1.04±0.08^{B}	1.61±0.06^{A}
Subantarctic skua	Cro	Crozet	Jan-Feb 2012	11	1.81±1.19^{B}	1.70±1.16^{B}	1.39±0.18^{C}	1.69±0.11^{B}
Subantarctic skua	Ams	Amsterdam	Dec 2011	10	4.00±0.89^{C}	3.78±0.79^{C}	1.56±0.08^{D}	1.76±0.05^{B}
Adélie penguin	AP	Adélie Land	Feb 2012	10	0.47±0.12^{A}	0.43±0.11^{A}	0.56±0.20^{A}	1.54±0.11^{A}
King penguin	KP	Crozet	Oct 2011	11	2.01±0.29^{B}	1.88±0.28^{B}	1.49±0.11^{B}	1.60±0.04^{A}
Macaroni penguin	MP	Crozet	Jan 2012	10	1.06±0.16^{C}	1.01±0.15^{C}	1.66±0.11^{C}	1.54±0.06^{A}
Eastern rockhopper penguin	RP	Crozet	Feb 2012	10	0.97±0.20^{C}	0.93±0.19^{C}	1.93±0.18^{D}	1.77±0.13^{B}
Northern rockhopper penguin	NRP	Amsterdam	Nov 2011	10	2.40±0.56^{B}	1.95±0.43^{B}	2.16±0.14^{E}	1.89±0.12^{B}

Hg isotopic composition values

Skua and penguin blood samples showed large ranges of mean δ^{202}Hg values between Antarctic and subtropical (0.23-1.56 ‰ and 0.53-2.16 ‰, respectively). Blood δ^{202}Hg differed amongst sites for skuas and penguins (H=33.82 and 44.02, respectively, both $p<0.0001$). Latitudinal mean enrichment of blood δ^{202}Hg values was 1.33±0.15 ‰ (-0.02 to 1.71 ‰) for skuas and 1.60±0.25 ‰ (0.24-2.37 ‰) for penguins.

The same latitudinal trend but lower variations were observed for mean Δ^{199}Hg values between sites in skuas (1.31-1.87 ‰) and penguins (1.54-1.89 ‰). Skua blood Δ^{199}Hg values were significantly lower for Adélie Land and Kerguelen relative to Crozet and Amsterdam populations (H=24.76, $p<0.0001$). Similarly, lower Δ^{199}Hg values were observed for AP, KP and MP comparing to RP and NRP (H=34.02, $p<0.0001$). The mean enrichment of blood Δ^{199}Hg values was 0.25±0.09 ‰ (1.31-1.85 ‰) for skua and 0.36±0.16 ‰ (1.38-2.04 ‰).

Measured blood δ^{202}Hg values followed the predicted theoretical MDF line whereas significant MIF of odd Hg isotopes (Δ^{199}Hg and Δ^{201}Hg) was observed for all the individuals (Figure 4.S5), indicating that MeHg accumulated in seabird tissues had undergone photochemical processes before its incorporation into the food web.

Correlations between Hg isotopic signatures and latitudinal trends

A strong correlation was found between Δ^{199}Hg and δ^{202}Hg values in both skuas and penguins (R^2=0.76 and 0.61, respectively, both $p<0.0001$; Figure 4.5). Δ^{199}Hg/Δ^{201}Hg slopes obtained for blood samples of penguins (1.21±0.04) and skuas (1.14±0.04) (Figure 4.6). A significant and positive relationship was observed between latitude and blood δ^{202}Hg values for both skua and penguins (R^2=0.91 and 0.85, respectively, both $p<0.0001$). Blood Δ^{199}Hg values were also correlated with latitude in skuas (R^2=0.56, $p<0.0001$) and penguins (R^2=0.19, $p=0.001$) (Figure 4.8).

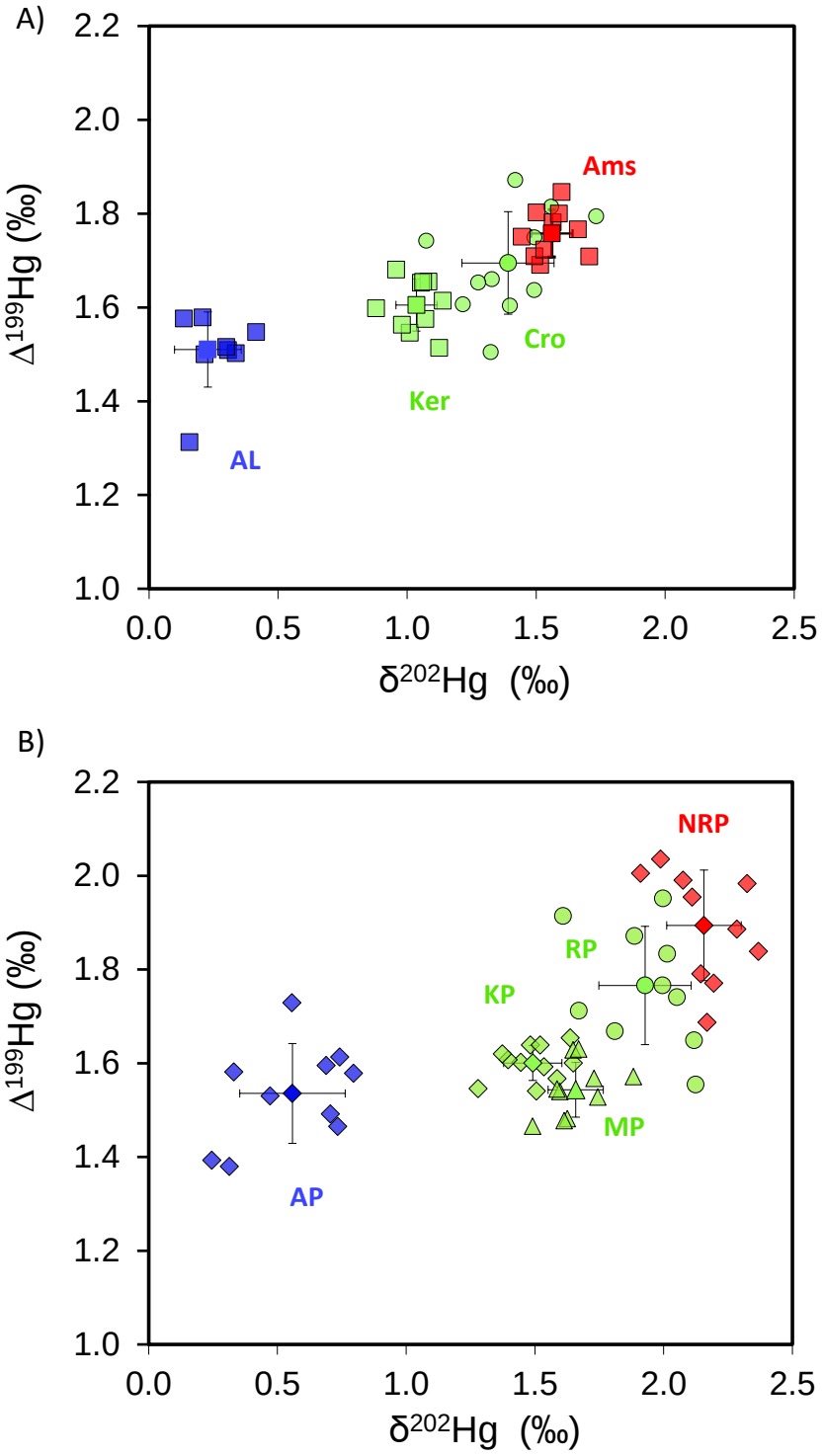

Figure 4.5 Hg MDF versus Hg MIF (expressed as δ^{202}Hg and Δ^{199}Hg, respectively) for blood samples of A) skua chicks and B) penguin adults (right) from the Southern Ocean. See Figure 4.4 for legend.

Discussion

The solid relationship of Δ^{199}Hg and δ^{202}Hg values with latitude (and between Δ^{199}Hg and δ^{202}Hg themselves) could be explained by two possible factors: i) different sources of Hg with distinct isotopic signatures (MDF and MIF) or ii) different processes before Hg incorporation and/or during uptake and bioaccumulation in the food web that produce both Hg MDF and MIF across the different sites. We expected that the most plausible explanation would be a combination of both factors, meaning that there is a different Hg isotopic baseline (due to distinct MeHg sources) and an influence of processes associated to geographically changing parameters which would induce Hg isotopic fractionation across the study sites. In the following sections, potential sources and processes explaining the observed Hg isotopic latitudinal trends were conceptually proposed, tested and discussed.

Potential Hg sources affecting MDF and MIF variations over latitude

The Southern Ocean ecosystems present a Hg cycle principally characterised by inputs from oceanic currents, net Hg atmospheric deposition to the ocean surface and substantial net Hg methylation (Pacyna et al., 2010; Cossa et al., 2011).

Different water masses of the studied area of the Southern Ocean derive from distinct origins, such as the Antarctic circumpolar current, Polar Front and subtropical waters, then present contrasted characteristics (temperature, biological productivity, etc.) and are exposed to different sunlight conditions that could affect the magnitude of Hg photochemical processes. Furthermore, assuming greater Hg reduction and volatilisation extents as a result of higher temperature, subtropical waters could exhibit heavier MeHg isotopic signatures than Antarctic waters. Nevertheless, seawater Hg isotopic information is still scarce with only one study in the Arctic Canadian coastal area that exhibited negative δ^{202}Hg values (–2.85 to –1.10 ‰) and mostly slightly positive Δ^{199}Hg values (< 0.37 ‰).

In Antarctic zones, the sequestration of atmospheric Hg in the sea ice compartment is supposed to be responsible of an additional input of Hg to the ocean (Gionfriddo et al., 2016; Cossa et al., 2011). Polar Regions are characterized by unique phenomena called atmospheric mercury depletion events (AMDEs) which consist in rapid oxidation of gaseous Hg^0 in air through reactions with halogens such as bromine (Lindberg et al. 2002; Ariya et al., 2002). Supposing that we could extrapolate Arctic AMDEs for interpreting the dynamics in Antarctic ecosystem, substantial deposition of oxidized Hg in Antarctic snowpack could have an influence in Hg MIF signatures of Antarctic seabirds. In the Arctic, snow samples impacted by AMDEs in Alaska

displayed near to zero δ^{202}Hg values (from -0.5 to 0.7 ‰) and highly negative Δ^{199}Hg values (down to -5 ‰) (Sherman et al. 2010; Obrist et al. 2017). Arctic ice cores reported negative δ^{202}Hg values (down to -2.48‰) and mostly near-to zero or positive Δ^{199}Hg (up to 2.44‰), opposite to Arctic snow during AMDEs but overlapping with Hg^0 samples (Sherman et al., 2010) and surface Arctic seawater (Štrok et al., 2015). Moreover, there are additional processes that could bring oxidized Hg to Antarctic coasts by katabatic winds (Angot et al., 2016b). Direct measurements of wet deposition (iHg) have documented slightly negative δ^{202}Hg (-0.44 to -4.27 ‰) and positive Δ^{199}Hg values (0.19 to 1.16 ‰). Significant even-MIF of ^{200}Hg has also been observed in precipitation samples, leading to slightly negative Δ^{200}Hg in the vapour Hg^0 and consistently positive Δ^{200}Hg in precipitation (Sherman et al. 2012b; Chen et al., 2012; Štrok et al., 2015; Demers et al., 2013; Gratz et al., 2010; Rolison et al., 2013; Wang et al., 2015; Yuan et al., 2015), hypothetically induced by oxidation processes of atmospheric Hg^0 (Chen et al. 2012). An influence of wet deposition could thus affect iHg isotopic baseline in a given ecosystem. However, the slight differences in Δ^{199}Hg values between Antarctic and the subantarctic seabird communities seem to indicate an absence of a high influence of Hg inputs from snow or sea ice melting in Antarctic food web. These results seems to indicate that atmospheric deposition is not substantial enough or cannot be detected in the Hg accumulated in the blood of skua and penguins and sea ice melting and wet deposition seems unlikely an important factor of Hg latitudinal trends.

Sediment erosion and its mobilization to opened areas could also contribute to Hg release into the aquatic compartment in water masses surrounding the Antarctic continent or the coastal zones in the vicinity of the subantarctic islands. Soils, sediments and vegetation from remote areas samples typically report negative δ^{202}Hg and close-to-zero Δ^{199}Hg values (Obrist et al., 2017; Gleason et al., 2016). Antarctic ornithogenic sediments showed negative δ^{202}Hg values (around -0.5 ‰) and slightly positive Δ^{199}Hg (~0.71 ‰) (Zheng et al., 2015). On the assumption that a higher interaction between coastal sediment and biota is produced in the Antarctic zone near the continent comparing to subantarctic and subtropical islands, Antarctic seabirds may exhibit lower δ^{202}Hg and Δ^{199}Hg values relative to subantarctic and subtropical communities. However, Hg sediment inputs in coastal waters of the subantarctic and subtropical islands are not negligible, since benthic penguin populations have been shown to be also influenced by sediment-derived Hg at the local scale of Crozet archipelago (Chapter 4.1). Therefore, continental influence has to be considered likely to ice melting under climate warming conditions. It is however unlikely a major factor driving the observed latitudinal trend in Hg isotopes.

MIF: effect of different photochemistry over latitude

Spatial variability in MeHg photodemethylation at a large scale

Because significantly positive Hg MIF is assumed to be the consequence of photochemical processes before incorporation into the food webs (Bergquist and Blum, 2009; Bergquist and Blum, 2007), the variability of Δ^{199}Hg values among the three geographically distant areas (Antarctic, subantarctic and subtropical waters) was considered to be mainly the consequence of distinct surface ocean photochemistry conditions. In this study, we covered a southern to northern gradient that extends from Polar Regions off the Antarctic continent to subtropical oceanic environments, through which different climatic factors may contribute to the observed latitudinal Hg MIF pattern.

Aquatic photochemical MeHg demethylation is known to induce an increase in MIF (Δ^{199}Hg and Δ^{201}Hg) and MDF values (δ^{202}Hg) in the residual MeHg pool, resulting in a Δ^{199}Hg/Δ^{201}Hg ratio of 1.36±0.04, as reported by experimental studies in freshwater with natural content of dissolved organic carbon (DOC) (Bergquist and Blum, 2007). Meanwhile, photochemical reduction of iHg originated a Δ^{199}Hg/Δ^{201}Hg ratio of 1.00±0.01 (Bergquist and Blum, 2007).Δ^{199}Hg/Δ^{201}Hg slopes obtained for blood samples of penguins (1.21±0.04) and skuas (1.14±0.04) are in good agreement with those previously obtained in marine fish and birds (Senn et al., 2010; Blum et al., 2013; Point et al., 2011; Day et al. 2012).

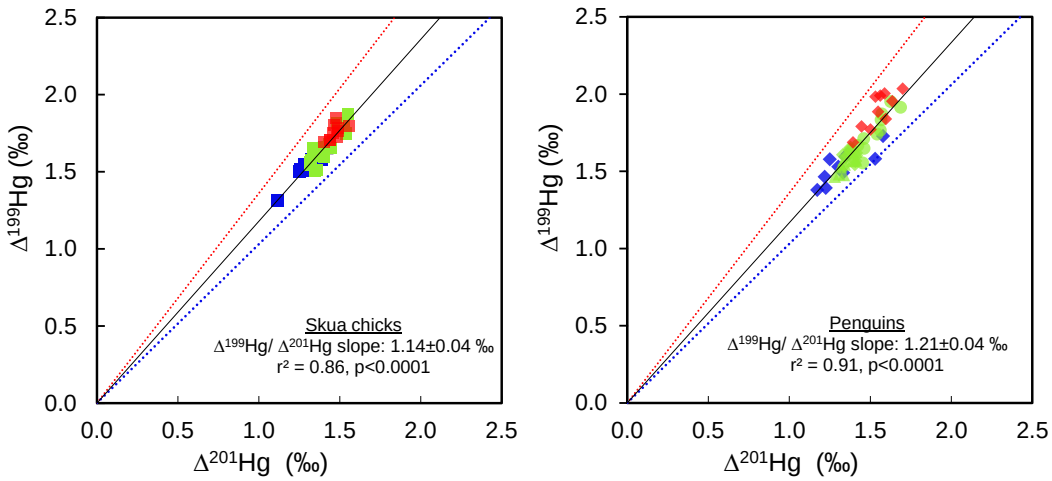

Figure 4.6. Hg MIF signatures (Δ^{199}Hg versus Δ^{201}Hg) for blood samples of skua chicks (left) and penguins (right) from the Southern Ocean. See Figure 4.4 for legend. The solid line represents the Δ^{199}Hg/Δ^{201}Hg slope of the samples. The red dashed line represents the theoretical Δ^{199}Hg/Δ^{201}Hg slope for MeHg photodemethylation in the water column and the blue dashed line represents the theoretical Δ^{199}Hg/Δ^{201}Hg slope expected for photoreduction of iHg in the water column (Bergquist and Blum 2007).

Assuming that MeHg photodegradation is the dominant photochemical process before MeHg assimilation in seabird tissues, we estimated the fraction of photodemethylated MeHg of each area based on three different experimental models (Chandan et al. 2015; Bergquist and Blum, 2007) (detailed in Annexes) and considering both different types and concentrations of DOC (MeHg:DOC ratios) and also the amount of reduced sulphur content in organic matter (MeHg:Sred-DOC ratios). Basing our estimations on the most similar conditions to our study areas, we obtained that the difference on the extent of photodemethylated MeHg from Antarctic and subantarctic to subtropical zones was in the order of 2% (based on Chandan et al., 2015 models) and 5% (based on Bergquist and Blum, 2007) (Table 4.S5). No substantial changes in latitudinal variations were observed in the calculated results when changing these parameters. Calculated photodemethylation extents in Antarctic coastal ecosystem by the same experimental approximation was similar to our findings (Zheng et al., 2015). It is noteworthy to highlight that the applied fractionation models represent more realistic environmental conditions (low MeHg: Sred-DOC ratios) than previous experimental studies so that they are more representative of the processes occurring under natural conditions in the environment. Nevertheless, these estimations are also based on laboratory experimental models so that the degree of extrapolation must be taken into account. The insignificant variations in MeHg photodemethylation extent over the studied latitudinal gradient (~ 2%) suggests that MeHg photodemethylation is, for instance, not influencing the observed increasing MeHg concentrations from Antarctic to subtropical seabird communities.

The slight MIF latitudinal variations between such distant sites of the Southern Ocean strongly suggest that the extent of photodemethylation is closely related to the distinct conditions for the photochemical processes to occur. Even if the annual mean day photoperiod is similar in the different sites (~12h, Jasmine et al., 2009), Hg isotopic signatures of penguin blood samples reflect only the summer conditions when the daily photoperiod is longer in Antarctic zones. However, the different angles of solar incidence between the different latitudes affect the UV/visible light and the transmission in surface waters that control directly the extent of the various photochemical processes (Rose et al., 2015). As it was commented above, the DOC quality and quantity is a controlling factor of the photochemical demethylation of MeHg and the resulting MIF (Chandan et al., 2015). For instance, we have shown that DOC concentrations would rather be homogenous over the different latitudes (Tremblay et al., 2015; Canario et al., 2017; Ogawa et al., 1999) but the higher biological productivity usually observed in Antarctic and the Polar Front zones compared to subtropical waters may lead to different DOM quality and photochemical reactivity. For example, we can expect higher photodemethylation efficiency in the southern latitudes which may also compensate the lack of efficient solar radiation (UV/visible light). Furthermore, it is important to consider that specific foraging habitats between seabird

species inhabiting the same latitudes could also induce variations in Hg MIF, especially when using penguins as models (Chapter 4.1).

Temporal variability in MIF values: winter and summer periods in Antarctic zone

Antarctic ecosystems are characterised by contrasted annual insolation conditions between the dark period of the austral winter, when the sun does not rise above the horizon, and summertime during which day length accounts ~16h. As previously said, the lower angle of solar incidence probably inhibits the photodegradation of dissolved MeHg in surface water. Therefore, lower MeHg photodemethylation efficiency could be expected in Antarctic waters comparing to northern latitudes. Despite the extreme sunlight conditions in Antarctic ecosystems, Antarctic seabird populations (Adélie penguins and Antarctic skua chicks) presented similar Δ^{199}Hg values compared to subantartic communities. Hg isotopic composition of seabird blood in chicks and adult penguins is representative of the recent Hg exposure before sampling, i.e., the breeding period (Chapter 3.1), in the case of Adélie penguins and Antarctic skuas during summertime. We compared blood Hg isotopic values of these two summer breeding species with a winter breeder penguins inhabiting Antarctic ecosystems, the emperor penguin that are then representative of the Antarctic winter period (Figure 4.7). Significantly lower Δ^{199}Hg values of emperor penguin relative to the other two summer breeders (~0.5 ‰) could suggest lower photodemethylation extent in winter as a result of lower solar radiation and a potentially higher influence of sea ice cover, as already demonstrated in previous studies in the Arctic (Point et al., 2011; Masbou et al., 2015). However, greater foraging depths of emperor penguins could also affect Δ^{199}Hg variations between summer and winter seabird populations (Wienecke et al. 2007).

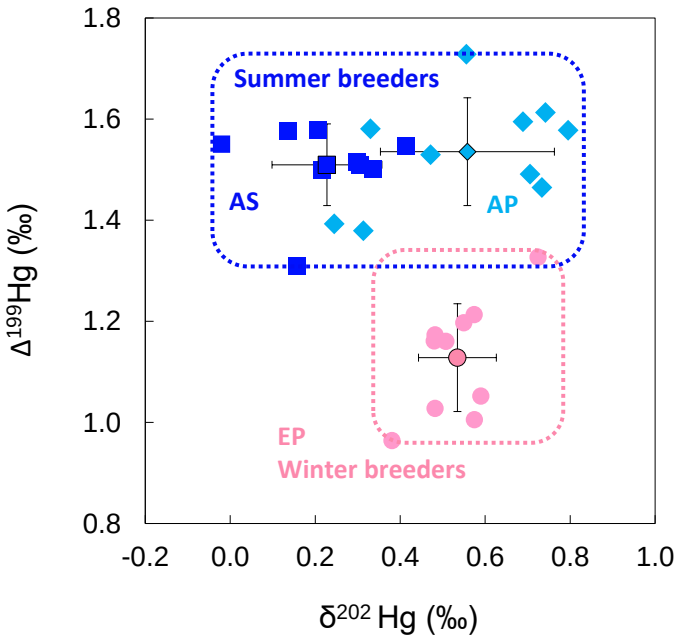

Figure 4.7. Comparison of Hg isotopic composition (δ202Hg, Δ199Hg) of Antarctic seabirds representative of the summer period (AP: Adélie penguins, AS: Antarctic skua) and winter period (EP: emperor penguins) of Adélie Land.

Potential MDF of Hg isotopes during aquatic biogeochemical pathways

Much higher mean latitudinal variations were observed for δ^{202}Hg values (skuas: 1.33±0.15 ‰ and penguins: 1.60±0.25 ‰) than for Δ^{199}Hg values (skuas 0.25±0.09 ‰ and penguins: 0.36±0.16 ‰). By deconvolution of the corresponding enrichment factors of δ^{202}Hg experimentally obtained for photochemical demethylation (Chandan et al. 2015), we estimated that around 0.3‰ of the total δ^{202}Hg enrichment may also be induced by this photochemical process (details in Annexes). This means that the remaining 1.0-1.3 ‰ of latitudinal δ^{202}Hg variation may be the consequence of different Hg trophic sources and/or biogeochemical processes inducing an enrichment in heavier isotopes when decreasing latitude.

Apart the potential sources mentioned above, kinetically process-driven fractionation have also been found to alter Hg isotopic composition. For instance, solar radiation can directly affect water surface temperatures, and the presence of ice cover can also create a thermal barrier in surface water masses on the vicinity of the Antarctic continent. There are at least three potential biogeochemical pathways that could produce an enrichment in heavier Hg isotopes (δ^{202}Hg) as a consequence of progressively increasing water temperature with latitude: i) reduction and volatilisation of inorganic Hg^0 from the aquatic compartment to the atmosphere leading to a pool of dissolved Hg^0 enriched in heavier isotopes, ii) increasing microbial methylation/demethylation ratios leading to the enrichment of the remaining MeHg in heavier Hg isotopes and/or iii) MeHg assimilation efficiency, trophic processes or metabolic responses inducing Hg MDF at different degrees.

Reduction and volatilisation

We postulate that higher temperature in subtropical water comparing to Antarctic waters would result in a higher degree of biotic reduction and greater volatilisation extent. This would thus produce a residual pool of Hg^{2+} enriched in heavier isotopes in the aqueous phase, which would be coherent with the MDF enrichment presently found with decreasing latitude. However, this fact would be contradictory with the higher MeHg concentrations at higher latitudes reported for the water column (Cossa et al. 2011). Kritee et al. (2007) demonstrated that Hg bacterial reduction result in Hg MDF leaving the remaining inorganic fraction enriched in heavy isotopes and defining a Rayleigh system for which the fractionation factor (expressed as difference of δ^{202}Hg) appeared to be between -1.3 and -2.0 ‰. A substantially higher biological reduction in subtropical ecosystems relative to Antarctic zones could therefore explain a part of latitudinal MDF variations. Hg volatilisation process of aqueous Hg^0 into gaseous Hg^0 has been found to induce MDF with a low fractionation factor of the order of 0.47 ‰ (Zheng et al. 2007). Based on water temperature recorded on the approximate latitudinal sites (Cossa et al. 2011; Canario et al.

2017), we estimated the fraction of volatilised Hg by calculation of Henry's law constant (K_H) reported by experimental studies on saline water (Andersson et al. 2008) (detailed in Annexes). We estimated that volatilisation processes could only contribute to 0.03 ‰ of MDF variation, indicating that this conceptual hypothesis is not sufficient to explain total Hg MDF differences across the investigated latitudinal gradient.

Biotic Hg methylation and demethylation

Water temperature and concentration of organic matter are two factors assumed to influence methylation activity (Fitzgerald et al., 2007). The binding of iHg to sinking organic particles facilitates its transport through depth, where it can be methylated by microorganisms with rates that will depend on the type of microbial communities associated with phytoplankton degradation (Heimbürger et al. 2010). Based on our findings, we hypothesized that higher MeHg concentrations in subtropical seabirds were possibly the result of higher net biotic methylation occurring there in the mesopelagic zone. Experimental measurements of isotopic fractionation during net MeHg methylation (i.e simultaneous methylation and demethylation) by sulphate-reducing bacteria suggested a fractionation factor in the order of -2.5 ‰ (Perrot et al., 2015), so that the theoretical magnitude of isotopic enrichment of this process could largely explain the obtained MDF latitudinal variation. Experimental abiotic methylation/demethylation by MeCo exhibited a fractionation factor of -1.6 ‰ (Jiménez-Moreno et al., 2013). However, specific enrichment factors must be extrapolated to our environmental conditions in order to estimate if the obtained latitudinal variations in δ^{202}Hg values in seabirds could be explained by different extent of methylation/demethylation pathways across the three studied areas in the Southern Ocean. An increasing methylation/demethylation ratio from Antarctic to subtropical zones would produce an enrichment in heavier isotopes of the residual pool of $MeHg^+$ (i.e. assuming steady state) with decreasing latitude. This supposition could be thus in good agreement with our isotopic latitudinal trends findings and with the higher MeHg levels found in subtropical seabirds compared to those from Antarctic zones.

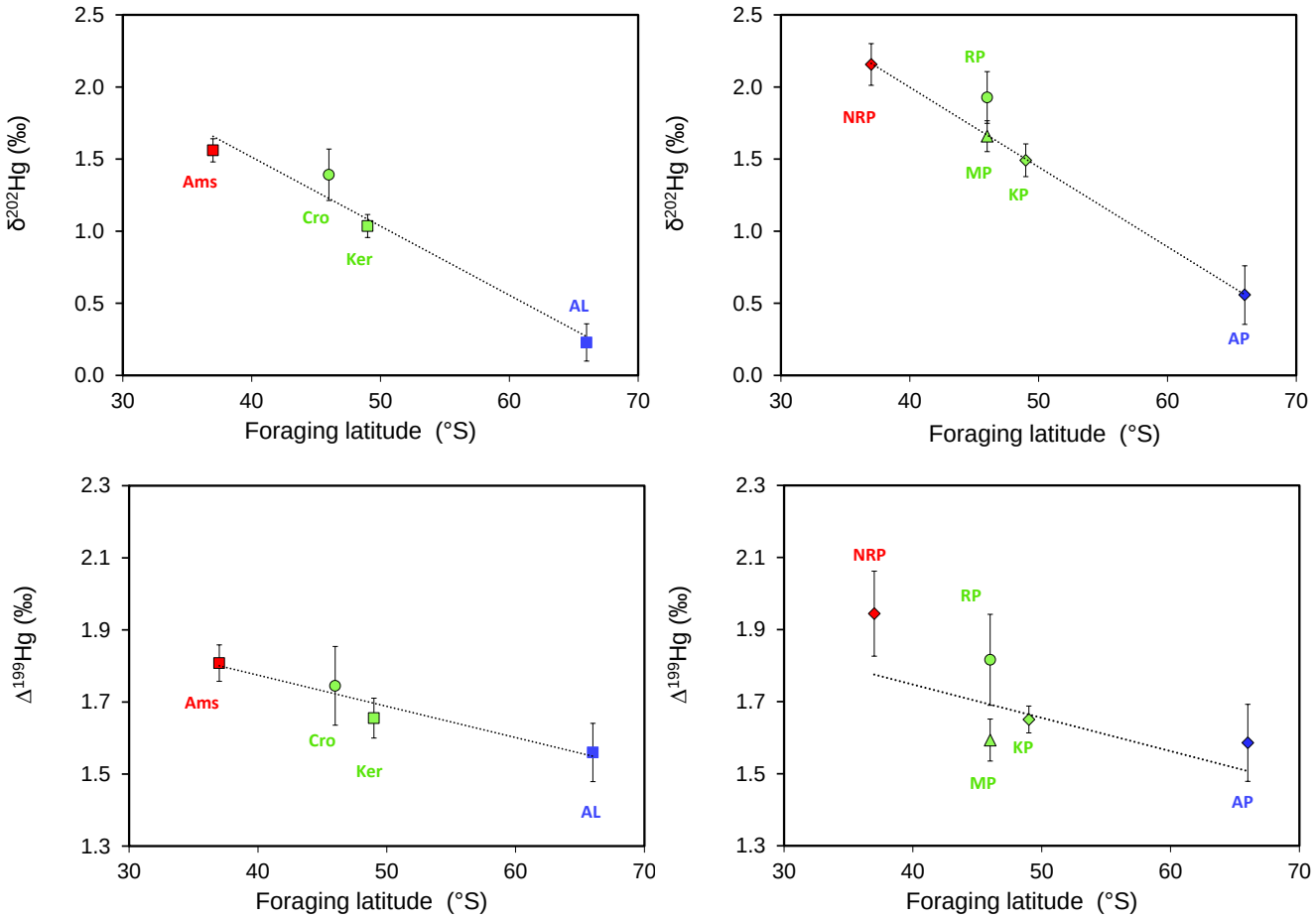

Figure 4.8. Mean Hg isotopic composition versus latitude for blood samples of skua chicks (left) and penguin adults (right) from the Southern Ocean. A) Regression equations for skua δ^{202}Hg blood-latitude (y=-0.05+3.43, R^2=0.91, p<0.0001) and for penguin δ^{202}Hg blood-latitude (y=-0.05x-4.21, R^2=0.85, p<0.0001). B) Regression equations for skua Δ^{199}Hg blood-latitude (y=-0.01+2.07, R^2=0.56, p<0.0001) and for penguin Δ^{199}Hg blood-latitude (y=-0.01x+2.07, R^2=0.19, p=0.001).

Trophic effects and metabolic processes

Physicochemical characteristics of a given marine ecosystem are known to strongly influence Hg bioavailability for primary producers. For instance, colder and low productivity systems are assumed to be more susceptible to Hg bioaccumulation due to the inhibition of growth biodilution, slow MeHg excretion rates and simpler food webs with less diversity of species (Lavoie et al. 2013). In our context, the difference in water temperature between sites are not an explanatory factor since lower MeHg concentrations were observed in Antarctic seabirds comparing to the other communities. However, this could be due to an influence of higher productivity in Antarctic and Polar Front zones as a result of seasonal release of nutrients and algal blooms during austral summer (Sullivan et al. 1993; Sokolov, 2008), which is enhanced by sea ice melting in Antarctic coastal zones (Sokolov, 2008; Riaux-Gobin et al., 2013). This phenomenon could thus reduce the uptake of MeHg at the basal food web (Pickhardt et al., 2002) inducing a biomass dilution of Hg concentrations (Karimi et al., 2007; Chen et al., 2005) and lower Hg concentrations in final predators. Moreover, this effect could potentially explain the increase of non-assimilated MeHg pool in the aquatic compartment, coherent with (Cossa et al., 2011). Additionally, a higher complexity of the food web could explain Hg increasing levels from Antarctic to subtropical ecosystems, as already hypothesized by Carravieri (2014), and also induce a higher enrichment in MDF as a consequence of higher number of trophic levels. Antarctic ecosystem is characterised by a less complex food web in which predators feed on key available species, such as the Antarctic krill *Euphausia superba* (Brasso et al. 2014; Cherel 2008). By contrast, subantarctic and subtropical ecosystems dispose of a larger diversity of prey species including four species of Euphausiids (Cherel et al. 2007; Bost et al. 2009), constituting a more complex food web.

The lower latitudinal MDF enrichment observed for skua chicks in comparison with penguins could potentially be linked to different level of Hg exposure or contrasted metabolic response. Although higher blood Hg concentrations were obtained for skua chicks relative to penguins at the different latitudes, lower δ^{202}Hg values were exhibited by skuas despite their higher trophic level. These observations could be explained by potential less efficient metabolic processes in chicks (such as hepatic demethylation) as a consequence of age, which could induce lower *in vivo* Hg isotopic fractionation leading to lower blood δ^{202}Hg values compared to adult penguins (Chapter 3.2). Apart different levels of Hg exposure or metabolic response, variations in δ^{202}Hg values between seabird species have been shown to be strongly dependent on Hg sources associated to different integration times between tissues (Chapter 3.1) or specific foraging ecologies (Chapter 4.1).

Conclusion

The investigation of latitudinal Hg isotopic composition in seabirds showed a progressive and linear increase in δ^{202}Hg and Δ^{199}Hg values from Antarctic through subantarctic to subtropical populations. Slight variations in MIF (Δ^{199}Hg values) between sites indicated that photochemical reactions are not an explanatory factor of the increased bioaccumulation trend obtained from Antarctic to subtropical marine food webs, but it is neither opposed to this trend. Moreover, geographical variations in MeHg-DOC ratios have been shown to strongly affect MeHg photodemethylation extent despite most favourable solar conditions at lower latitude. The larger degree of MDF (δ^{202}Hg) with latitude suggest the existence of additional processes between sites, such as biological reduction, methylation and/or demethylation processes. Also, trophic or metabolic processes could also contribute to the observed trend although this hypothesis seems less probable. This work includes the first Hg isotopic data of the Southern Ocean and Antarctic ecosystems over a unique latitudinal gradient, which is representative of the MeHg cycle in the different study areas. In consequence, the present exploration of MDF and MIF values in seabirds allows the elucidation and quantification of potential biogeochemical pathways of Hg in the Southern Ocean and contributes to better understanding the oceanic and global Hg cycling.

Main **findings** of this study:

- Measurement of Hg isotopic composition in seabirds exhibited an **overall latitudinal variation in the order of 0.36 ‰ (Δ^{199}Hg values) and 1.2 ‰ (δ^{202}Hg values)**, increasing from Antarctic trough subantarctic to subtropical populations.

- **Latitudinal variations of Hg MIF (Δ^{199}Hg values) reflected in seabirds** enabled to **estimate the degree of MeHg photodemethylation in surface waters of the Southern Ocean**, thus providing quantitative information about Hg photochemical processes in these still poorly understood environments.

- Slight variations in MeHg photodemethylation extent (~2%) between the distant study areas (66°S-39°S) suggests that **photodemethylation processes are not the main explanatory factor of the heavier isotopic signatures (δ^{202}Hg)**.

- **Different biogeochemical pathways inducing Hg MDF**, such as different extent of reduction, and/or methylation/demethylation processes, **could potentially explain the additional enrichment δ^{202}Hg values** observed in subtropical seabirds relative to Antarctic seabirds.

Acknowledgments

The authors thank all the fieldworkers that contributed to the collection of seabird blood and feather samples in the frame of the program no. 109 (H. Weimerskirch) supported by the Institut Polaire Français Paul Emile Victor (IPEV) and the Terres Australes et Antarctiques Françaises (TAAF) and by the Agence Nationale de la Recherche (program POLARTOP, O. Chastel). Special thanks are due to A. Carravieri who managed the sample database. The present work was supported financially by the Région Poitou-Charentes (now Région Nouvelle Aquitaine) through a Ph.D. grant to MR, and by the French national program EC2CO Biohefect/Ecodyn//Dril/MicrobiEen (TIMOTAAF project, P.I. D. Amouroux). The IUF (Institut Universitaire de France) is acknowledged for its support to PB.

Chapter 5.

Conclusions and perspectives

Chapter 5. Conclusions and perspectives

The present doctoral work includes new and valuable information about the exposure pathways of MeHg accumulated in seabirds that help identifying the processes involved in the Hg geochemical cycle in the Southern Ocean. This dissertation has been focused in the investigation, for the first time, on the origin of Hg, the production processes of MeHg and its transfer to marine ecosystems in the Southern Ocean, more precisely in the Indian Ocean sector. Based on previous investigations achieved during the doctoral work of A. Carravieri on the determination of Hg baseline in the southern Indian Ocean seabirds and on the main factors driving its accumulation in these species, this work directly focused in a precise selection of seabird species with specific ecological habits that enabled to provide key information of the main factors influencing seabird MeHg exposure and bioaccumulation pathways. By combination of total Hg isotopic composition (δ^{202}Hg, Δ^{199}Hg) and Hg speciation in this unique collection of avian samples, an important database of Hg isotopic information has been created in these poorly understood ecosystems, facilitating a better comprehension of the Hg cycle in remote areas of the Southern Ocean at different spatial .

The main **findings** concluded from this doctoral work are that:

- The investigation of **Hg isotopes** in seabirds permits to establish relationships between Hg **accumulation in the food web**, **Hg biogeochemistry** in marine coastal and oceanic environments and internal **metabolic mechanisms** in response to Hg contamination in seabirds;

- Due to the different Hg turnover, residence time and integration of Hg exposure between seabird tissues, **tissue-specific Hg isotopes give access to** distinct of sources Hg acquired in individuals at **different temporal and geographical windows**, providing information of Hg exposure in vast spatial zones and at different stages of their annual cycle;

- Blood and feathers in chicks can be effectively and indifferently used for biomonitoring of local contamination using Hg isotopes, whereas in adults each tissue provides access to different temporal exposure: blood at recent scale (i.e. exposure during the breeding period) and feathers at seasonal scale (i.e., exposure during wintery period), thus providing complementary isotopic information at different stages of seabird annual cycle;

- Seabirds effectively represent the **specific Hg environmental exposure in each marine compartments** in function of their by their foraging habitats and latitudinal movements and **Hg isotopes in their tissues can be useful to trace sources and exposure pathways of MeHg** of these areas of difficult to access.

5.1 Hg speciation in feathers of a large seabird community of the Southern Ocean

A first important contribution of this thesis is the development and adaptation of an analytical technique that allows an accurate, precise and simultaneous quantification of Hg compounds (MeHg and iHg) in feather samples (Chapter 2). Even it was already admitted that most of the Hg present in seabird's feathers is MeHg, only organic Hg had been analysed leading to estimation of MeHg content up to 130% (e.g., Bond et al., 2009a). It was therefore necessary to better evaluate the fraction of THg which is under MeHg and iHg forms. Our work on this issue was published in Talanta and comprises a detailed compilation of Hg speciation methods in feathers exposing the principal limitations of classical techniques. The optimised extraction method, the analytical technique (by GC-ICPMS) together with species-specific isotope dilution analysis allowed the achievement of very good analytical performances. The developed method was efficaciously applied to feather samples from 13 marine bird species from the Southern Ocean (penguins, albatrosses, petrels and skuas) to investigate the variability of Hg speciation across a large range of Hg exposure conditions and concentrations, including adult individuals and chicks (Figure 5.1).

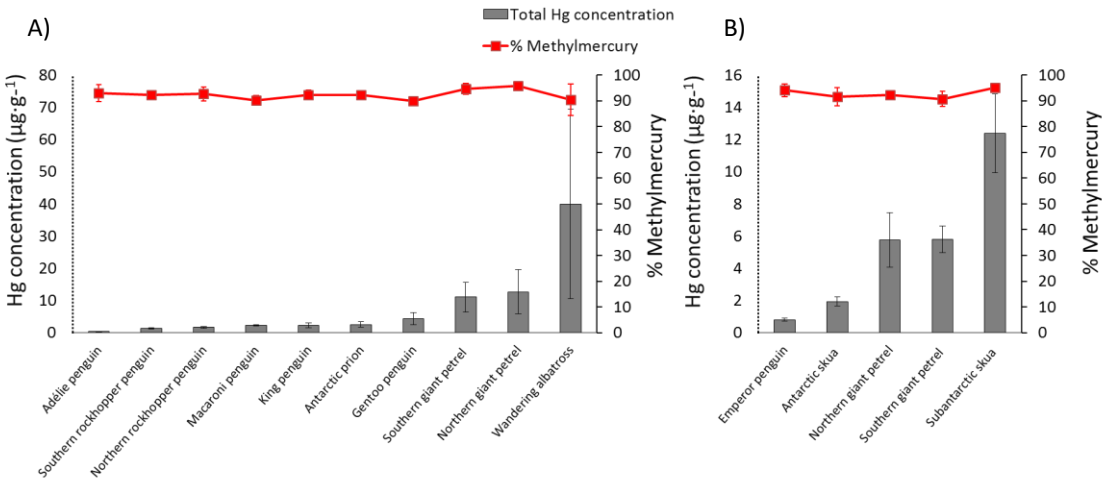

Figure 5.1. Overall results of total Hg concentrations (µg·g^{-1}, dw) and MeHg proportion (%) in feathers from adult (A) and chick (B) individuals of 13 seabird species from the Southern Ocean.

- For absolutely all the seabird individuals analysed (adults and chicks), **MeHg appeared to be the major species** independently of total Hg concentrations.
- All the single feathers displayed **more than 80%** of Hg as MeHg and represents **on average 92±2%.** This finding was in good agreement with previous observations and with the

evidence that seabirds excrete MeHg in moulting feathers which therefore represents a very efficient Hg detoxification strategy.

- However, this study also permitted to highlight that **non-negligible amounts of iHg** were present in feathers from some individuals, meaning that it cannot be considered the analysed THg in feathers equals MeHg.
- The **precise quantification of Hg species is essential when Hg isotopic analyses are performed afterwards** because Hg speciation strongly influences the measured Hg isotopic signatures.
- Moreover, the application of methods measuring both Hg compounds' concentrations in feathers is recommended in cases of accidental iHg contamination, as already detected in feather museum collections.

5.2 Blood vs feathers: which level of information is provided by Hg isotopes of each bioindicator tissue?

The choice of the best bioindicator tissue for Hg contamination is fundamental for interpreting the level of Hg environmental contamination. Since blood and feathers can be non-lethally collected, a deep investigation of Hg isotopic signatures in blood and feathers was performed in chicks using skuas and in adults using penguins (Chapter 3.1), permitting to conclude that:

- **In chicks, blood and feathers had identical Hg isotopic values,** meaning that the two tissues can be easily compared in interpretative terms without any correction factor. Since chicks present a simultaneous moult of all the feathers before fledging, **blood and feathers are both representative of a well-defined period of Hg uptake** during the breeding period when they are fed by their parents with **local prey.** Therefore **both tissues provide the same information** by Hg isotopic analyses and can be sampled indifferently in chicks during fieldwork.
- **In adult penguins, Hg isotopic composition differed between blood and feathers**, most likely as a consequence of **different tissue-specific temporal windows of Hg exposure**. Feathers of adult penguins are supposed to be representative of local conditions around the colonies year round. However, the difference between **feather and blood Hg isotopic signatures reflects** changes in foraging habitats and or prey in the inter-breeding period, as a result of **integration of Hg from diverse sources** during the whole year (between two moults).

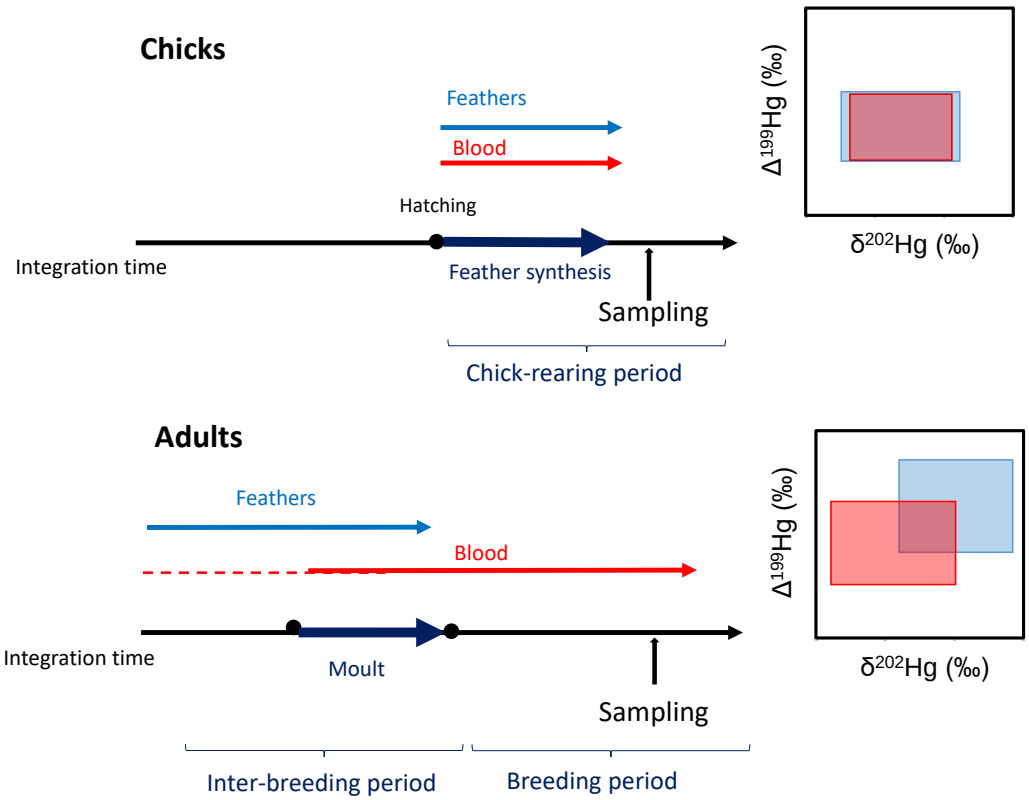

Figure 5.2. Schematic explanation of the integration windows of Hg reflected by blood and feathers in chick and adult individuals providing their consequent tissue-specific Hg isotopic signatures.

As a consequence, **chick blood and feathers are effective bioindicator tissues for local and recent contamination studies**. However, when working **on adults, blood is more appropriate** if we want information about **recent assimilation and/or local contamination**, when adult individuals stay near the colonies during the breeding period. The use of adult feathers need a very good knowledge on the biology and ecology of the seabird species to allow relevant interpretation and to avoid bias and erroneous conclusions. Indeed, the main limitation of the use of adult feathers for local contamination is the fact that they reflect Hg year-round exposure, which should be especially remarkable in flying adults that migrate over large spatial scales for many species with dramatic changes their diet. However, this **integrative effect of adult feathers could be interesting for tracking whole annual Hg contamination**. Measurements of Hg isotopic composition in **feathers of flying migratory seabirds** could open a **new horizon for exploring Hg exposure pathways in large zones** of the marine environment during the inter-breeding period.

Perspective. Hg isotopic signatures could be measured in feathers of seabird species that have molted in different areas, **permitting the access of Hg isotopic information of migratory destinations** during the inter-breeding period. The complementary interpretation of $\delta^{13}C$ signatures in feathers would allow the localization of the areas where feather have been synthetized. This same approach could also be performed within a same individual, in feathers that have been synthetized in different zones, which should be practicable in seabird species with prolonged feather moult, such as sooty and grey-headed albatrosses or giant petrels.

5.3 Hg isotopes in internal tissues: do they contribute to explore metabolic aspects in seabirds?

As detailed in Chapter 3.2, analyses of Hg speciation and Hg isotopic composition in internal tissues, in feathers and in blood of seabirds enabled the exploration of key metabolic processes, such as detoxification by MeHg demethylation in liver, tissue-specific accumulation or excretion yields into feathers. This study is the first focusing on metabolic aspects in seabirds by investigation of Hg isotopes and was assessed in three different seabird models in order to compare the metabolic response according to the level of Hg exposure, the trophic ecology, and the age. Among the key results, it was obtained that:

- The correlation between Hg speciation and $\delta^{202}Hg$ values in the studied seabird tissues is indicative of metabolic mechanisms, such as MeHg demethylation in liver, inter-organ transfer and MeHg remobilisation from internal tissues for its excretion through feathers. Therefore, **Hg isotopes in internal tissues can be thus useful for investigation of metabolic mechanisms** in response to Hg contamination.

- When comparing different seabird species, Hg concentrations and speciation together with variations in $\delta^{202}Hg$ values between tissues can **reveal distinct mechanisms or efficiency of detoxification**. For instance, Antarctic prions (low trophic level) exhibited low Hg concentrations and low fraction of iHg in the liver as well as lower variation in $\delta^{202}Hg$ values between muscles and liver in comparison with white-chinned and giant petrels (higher trophic levels). This effect suggests less extent or efficiency of the hepatic demethylation in Antarctic prion compare to the two other species, which could be related to their low level of Hg exposure, so less necessity of detoxifying MeHg, and/or to a higher efficiency of excretion by moult.

- Variable **Hg MIF ($\Delta^{199}Hg$) isotopic signatures between internal tissues** (long-term accumulation) and feathers (inter-moult period incorporation) reflect different **temporal**

windows of Hg exposure, with feathers generally showing significantly greater Δ^{199}Hg values, potentially **as a consequence of distinct Hg sources during wintery migration**. Although this pattern was not accomplished in the case of giant petrel, mostly due to a "reservoir effect", it was concluded that extrinsic factors in terms of temporal and geographical aspects of Hg exposure highly affects Hg isotopic information between feathers and internal tissues, as previously observed between feathers and blood in adult individuals (Chapter 3.1).

- The **different Hg turnover and residence time between muscles (annual scale) and liver (long-term/ life-accumulation)** could affect not only δ^{202}Hg values but also Δ^{199}Hg values, potentially providing insights of **distinct Hg sources during the life of an individual.** This is the case of white-chinned petrels, which exhibited significantly different Δ^{199}Hg values between liver and muscles. Indeed, muscles are assumed to reflect Hg acquisition since the last moult, where a high fraction of MeHg (~80%) has been remobilised into growing feathers. Consequently, Hg accumulated in muscles corresponds to Hg acquired the following year relative to Hg present in feathers (in case of annual moulting). However, Hg in liver is considered to represent long-term accumulation, probably during all their life time. Distinct sources of Hg accumulated specifically in each tissue maybe associated with variability of foraging ecology during their annual cycle or even with age could potentially affect isotopic variability between muscles and liver. However, this hypothesis needs to be further clarified.

Although some metabolic aspects were identified according to Hg speciation and isotopic variations among tissues, the **redistribution and excretion pathways of Hg in seabirds need to be further investigated** in order to clarify their metabolic responses. For example, it is still not clear if the isotopically heavier fraction of non-demethylated MeHg in the liver is later redistributed into muscle, thus enriching δ^{202}Hg values in this storage organ, or if it is directly excreted in feathers (composed of the isotopically heaviest fraction). In the first case, MeHg stored in muscles would be assumed to be a combination of non-metabolised MeHg uptaken from diet and the non-demethylated MeHg fraction redistributed from liver, indicating that muscle is an intermediate storage organ influenced by Hg demethylation in liver and MeHg excretion by feathers. In the second case, the preferential excretion of isotopically heavier MeHg through feathers would be easily explained as the excretion of MeHg remaining fraction from demethylation. Another observation that needs to be clarified in future studies is the presence of high fractions of iHg in muscles observed in giant petrels, especially in old individuals. This could suggest a redistribution of iHg from livers to muscles as a result of a high MeHg demethylation

rate (and subsequent iHg concentrations accumulated in liver during their life) or due to high amounts of iHg by dietary uptake since they feed on seabird or mammal carrion (livers).

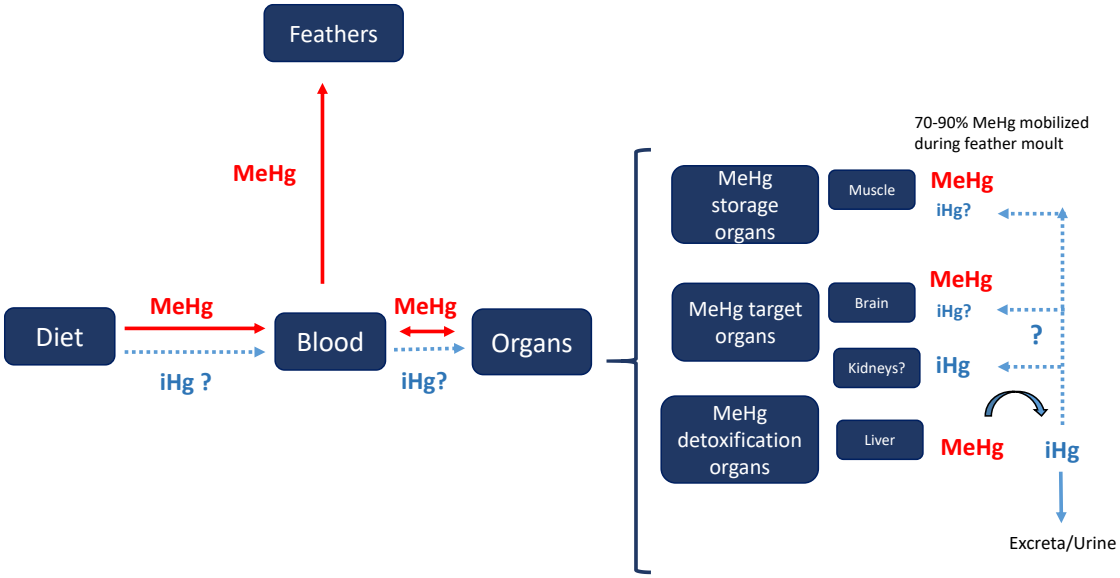

Figure 5.3. Schematic design of the metabolic processes inducing MDF in the organisms o birds and the reflect of distinct Hg sources as a result of different times of integration between internal tissues (long-term accumulation) and feathers (seasonal acquisition during inter-breeding periods).

Perspectives. MDF signatures (δ^{202}Hg) were significantly different among tissues of seabirds and mainly dependent on the fraction of MeHg and were thus assumed as a valuable tool for explore metabolic processes in response to Hg contamination (demethylation in liver, excretion by feathers, transfer among tissues, etc). As a consequence, an interesting perspective would be the performance of **Hg-Compound Specific Isotopic Analysis** (CSIA) that consists in the simultaneous determination of Hg isotopic signatures in both MeHg and iHg by the coupling GC-MC-ICPMS (objective of TIMOTAAF project, EC2CO, CNRS, 2nd year). This approach, satisfactory applied in internal tissues of marine mammals (Perrot et al., 2016), would provide information on the influence of metabolism responses on *in vivo* distribution of Hg. Indeedn this is the objective For example, similar Δ^{199}Hg isotopic signatures of MeHg and iHg accumulated in internal tissues would indicate an unique source of Hg assimilated through food, essentially in the form of MeHg, with iHg being the metabolised Hg fraction (i.e., the result of hepatic demethylation). According to this, we could also clarify if the total amount of iHg in livers derives uniquely from *in vivo* demethylation or if a fraction of this iHg could be directly come from food intake. Significant ingestion of iHg could occur in the case of white-chinned and giant petrels, as they respectively feed on offal from fish fisheries and on seabird or mammals carrion (Cipro et al. 2014; González-Solís et al., 2002), possibly influencing MIF signatures of iHg in their livers.

Moreover, the investigation of Hg species-specific δ^{202}Hg values in key organs would provide insights about *in vivo* demethylation of MeHg, which is widely assumed to occur mainly in livers, but could be observed in other tissues such as kidneys, brain or even muscles.

5.4 Can the use Hg isotopic analyses in seabirds provide a better understanding of the Hg cycle in southern marine ecosystems?

As demonstrated in Chapter 4, Hg isotopic composition in seabirds constitutes a valuable tool for the definition of MeHg sources and a potential variability of processes among the different marine compartments although, as extensively discussed, this requires a precise selection of bioindicator tissues and seabird species of well-known trophic ecology. Hg isotopic signatures in blood samples of chicks (skuas) and of adults (penguins) permitted to reveal different MeHg sources and levels of exposure depending on specific foraging behaviour variability within a same ecosystem. It also showed a latitudinal effect in Hg isotopic signatures suggesting an influence of the processes involved in the Hg biogeochemical cycle between the studied sites of the Southern Ocean. The main results of this part permitted some general conclusions:

- A progressive increase in Hg isotopic signatures from benthic to pelagic penguins (δ^{202}Hg: 1.45-1.93 ‰ and Δ^{199}Hg: 1.41-1.77 ‰) suggested an influence of **different MeHg biogeochemical characteristics across inshore-offshore marine compartments.**

- **Specific foraging habitats and latitudinal movements** of penguins highly determine their exposure to **distinct environmental MeHg sources** in the variable marine ecosystems of the Southern Ocean.

- Variations of Hg MIF signatures in function of seabird foraging depths permit an estimation of the extent of MeHg photodemethylation at different depths of the water column with a total difference of ~3% of MeH photodemethylated between pelagic and benthic ecosystems.

- Latitudinal variations in Hg MIF signatures in function of seabird breeding sites allow to estimate the extent of MeHg photodemethylation over a latitudinal gradient of the Southern Ocean from Antarctica to the subtropics (~2%), suggesting that photodemethylation is not the main explanatory factor of the latitudinal enrichment in heavier isotopic values (δ^{202}Hg) while they have no impact on the fact that higher MeHg concentrations are bioaccumulated in subtropical seabirds relative to Antarctic communities.

- High latitudinal variations in Hg MDF over the studied latitudinal gradient could partly explained by photochemistry, but also by different extent of Hg volatilisation, biotic reduction, bacterial methylation/demethylation and/or trophic and metabolic processes

associated to different climatic conditions (water temperature, presence of organic matter, pH, etc.).

In conclusion, this doctoral work demonstrates the relevance of the use of seabirds as bioindicators to understand changing dynamics and processes involved in the Hg cycle in these marine compartments and includes the first screening of Hg isotopic results in the Southern Ocean. The study and comparison of different seabird species with contrasted ecological characteristics from a same region allows to reflect the Hg contamination of different habitats and thus to obtain information about the contamination of a given ecosystem. As an example, Figure 5.4 includes mean Hg isotopic composition (δ^{202}Hg, Δ^{199}Hg) in feathers from all the seabird species analysed in the subantarctic zone (Kerguelen and Crozet Islands). This compilation permits a global view of Hg isotopic variation between seabirds in function of their foraging habitats (in terms of space and depth), trophic ecology, age or influence of latitudinal movements between migratory and resident species.

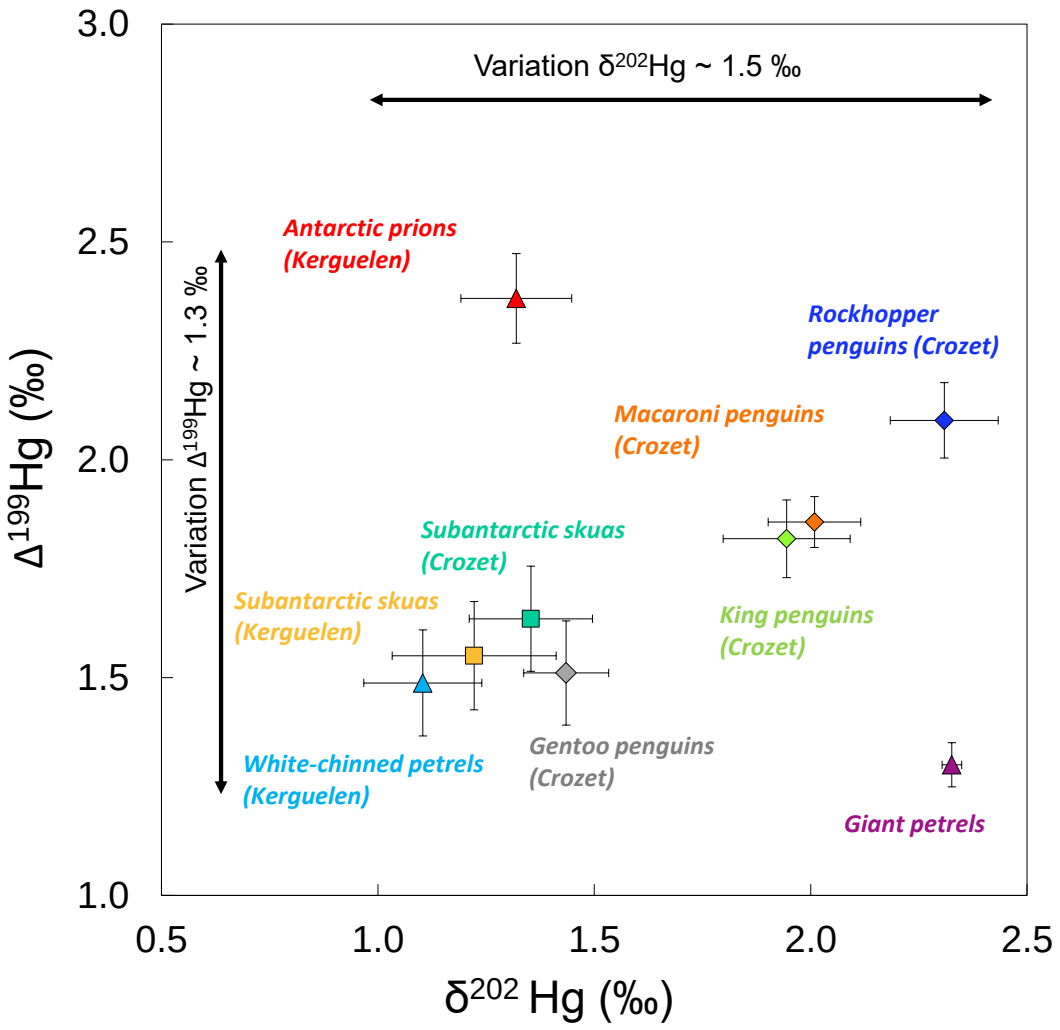

Figure 5.4. Compilation of mean MDF and MIF values of feathers of seabirds from subantarctic waters of the Southern Ocean including Antarctic prions, white-chinned petrels and southern giant petrels, subantarctic skuas and the four subantarctic penguins. PF means Polar Front.

Perspectives. Many perspectives are issued from this work mainly concerning a better characterisation of MeHg sources and a more precise estimation of processes involved in Hg cycle at different marine compartments and latitudes in the Southern Ocean:

1. For a better understanding of the Hg sources and transformation or bioaccumulation pathways of Hg in the Southern Ocean, Hg isotopic studies using seabirds as bioindicators should be combined with an **isotopic exploration of the complete marine food webs**, starting by basal trophic web organisms (phyto- or zooplankton) and fish, but also by analyses of potential

trophic Hg contributor sources such as marine sediments or sea ice cover or even seawater. The complementary analysis of Hg isotopes on these same samples should offer a wide perspective of Hg pathways, enabling a better determination of the potential origin and/or major sources of MeHg formation.

2. Preliminary estimations of photodemethylation rates in function of seabird foraging depths or latitudinal patterns across the Southern Ocean are based in photochemical fractionation factors determined in experimental freshwater conditions (Chandan et al., 2015). Although these calculations are performed at different types and concentrations of organic matter (related to sulphur content), and thus provide more fine and realistic estimations than pioneer experimental studies in freshwater (Bergquist and Blum, 2007), there is certainly a **lack of accuracy in relation to the different composition of marine waters**. Therefore, photochemical experimental studies in different seawater type matrices, under different conditions of organic matter and halogens, could be of key importance to improve the interpretations of Hg isotopic composition in marine organisms.

3. Due to the absence of Hg isotopic values in Antarctic zones, a comparison with other remote areas such as the Arctic ecosystem, which has been more widely studied, could also give an additional point of owing the similarity of climatic conditions, such as reduced extent of solar radiation and the presence of sea ice cover. For instance, in Figure 5.5 we compared Hg isotopic signatures in seabird eggs (murre) from Alaska (Day et al. 2012) with the seven penguin populations studied during this doctoral work. It can be observed that Alaskan seabirds and subantarctic and subtropical penguins are positioned in a progressive linear increase of δ^{202}Hg and Δ^{199}Hg values. Similar δ^{202}Hg and Δ^{199}Hg values were found between emperor penguins and Alaskan seabirds, although slightly higher Δ^{199}Hg values were exhibited by Adélie penguins. As commented in Chapter 4.2, emperor penguins are representative of winter periods in Antarctica, reflecting a higher influence of sea ice cover and less solar radiation extent, probably more similar with climatic conditions in the Arctic where sea ice cover remains more permanent during all year long comparing to the Antarctic continent. Higher influence of sediment-derived Hg from the continent and riverine inputs must also be considered in the Arctic system when comparing and interpreting Hg isotopic signatures of both Polar Regions. Similarly, further investigations of Hg isotopic composition in sediments, seawater and other organisms of the concerned marine food webs would be of key importance for the clarification and estimation of the impact of local sources of MeHg accumulated in seabird tissues.

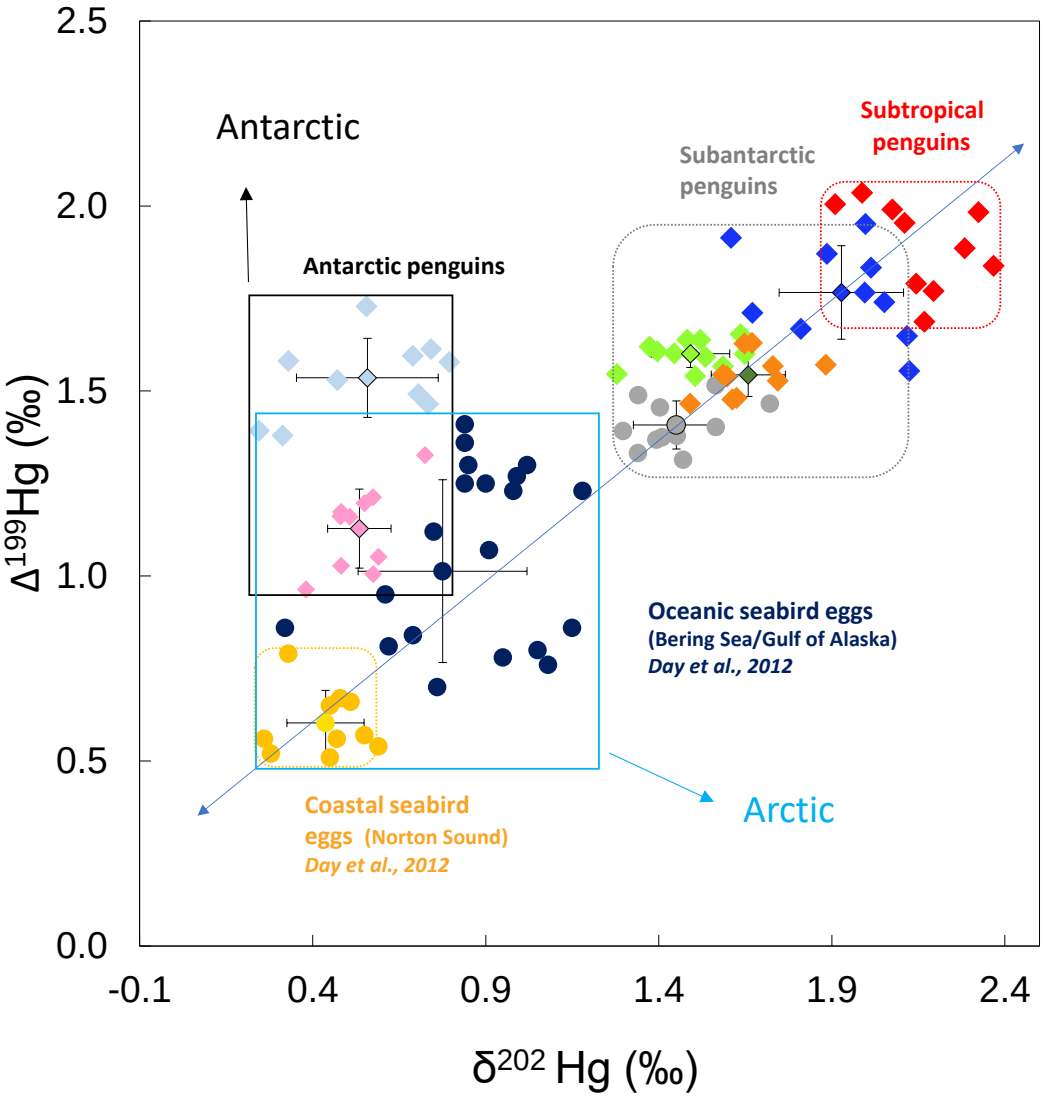

Figure 5.5. Comparison of MDF ($\delta^{202}Hg$) and MIF ($\Delta^{199}Hg$) values of penguin blood samples (diamonds) with Arctic seabird eggs from oceanic zones Bering Sea (55-65ºN, 170ºW) and Gulf of Alaska (55-60ºN, 130-160ºW) and coastal zones (Norton Sound, 64ºN, 164ºW) represented with dark blue circles (oceanic) and yellow circles (coastal) (Day et al., 2012)

References

AMAP (2011) *Arctic Monitoring and Assessment Program 2011: Mercury in the Arctic*.

Amos H. M., Jacob D. J., Holmes C. D., Fisher J. A., Wang Q., Yantosca R. M., Corbitt E. S., Galarneau E., Rutter A. P., Gustin M. S., Steffen A., Schauer J. J., Graydon J. A., St Louis V. L., Talbot R. W., Edgerton E. S., Zhang Y. and Sunderland E. M. (2012) Gas-particle partitioning of atmospheric Hg(II) and its effect on global mercury deposition. *Atmos. Chem. Phys.* **12**, 591–603.

Amos H. M., Jacob D. J., Streets D. G. and Sunderland E. M. (2013) Legacy impacts of all-time anthropogenic emissions on the global mercury cycle. *Global Biogeochem. Cycles* **27**, 410–421.

Amyot, M., Gill, G.A., Morel, F.M.M., (1997) Production and loss of dissolved gaseous mercury in coastal seawater. *Environ. Sci. Technol.* **31**, 3606–3611.

Anderson O. R. J., Phillips R. A., McDonald R. A., Shore R. F., McGill R. A. R. and Bearhop S. (2009) Influence of trophic position and foraging range on mercury levels within a seabird community. *Mar. Ecol. Prog. Ser.* **375**, 277–288.

Andersson M. E., Gårdfeldt K., Wängberg I. and Strömberg D. (2008) Determination of Henry's law constant for elemental mercury. *Chemosphere* **73**, 587–592.

Andrews G. K., Fernando L. P., Moore K. L., Dalton T. I. M. P. and Sobieskif R. J. (1996) Avian Metallothioneins : Structure , regulation and evolution. *Am. Inst. Nutr.* **3**, 1308–1316.

Angot H., Dastoor A., De Simone F., Gardfeldt K., Gencarelli C. N., Hedgecock I. M., Langer S., Magand O., Mastromonaco M. N., Nordstrom C., Pfaffhuber K. A., Pirrone N., Ryjkov A., Selin N. E., Skov H., Song S., Sprovieri F., Steffen A., Toyota K., Travnikov O., Yang X. and Dommergue A. (2016) Chemical cycling and deposition of atmospheric mercury in polar regions: Review of recent measurements and comparison with models. *Atmos. Chem. Phys.* **16**, 10735–10763.

Angot H., Dion I., Vogel N., Legrand M., Magand O. and Dommergue A. (2016) Multi-year record of atmospheric mercury at Dumont d'Urville, East Antarctic coast: Continental outflow and oceanic influences. *Atmos. Chem. Phys.* **16**, 8265–8279.

Appelquist, H.; Asbirk, S.; Drabæk, I. Mercury monitoring: Mercury stability in bird feathers. *Marine Pollution Bulletin* 1984, **15**, 22–24.

Arai T., Ikemoto T., Hokura A., Terada Y., Kunito T., Tanabe S. and Nakai I. (2004) Chemical forms of mercury and cadmium accumulated in marine mammals and seabirds as determined by XAFS analysis. *Environ. Sci. Technol.* **38**, 6468–6474.

Ariya P. A., Khalizov A. and Gidas A. (2002) Reactions of gaseous mercury with atomic and molecular halogens: Kinetics, product studies, and atmospheric implications. *J. Phys. Chem. A* **106**, 7310–7320.

Arrigo K. R. and Thomas D. N. (2004) Large scale importance of sea ice biology in the Southern Ocean. *Antarct. Sci.* **16**, 471–486.

Atwell L., Hobson K. A. and Welch H. E. (1998) Biomagnification and bioaccumulation of mercury in an arctic marine food web: insights from stable nitrogen isotope analysis. *Can. J. Fish. Aquat. Sci.* **55**, 1114–1121.

Avramescu M. L., Yumvihoze E., Hintelmann H., Ridal J., Fortin D. and R.S. Lean D. (2011) Biogeochemical factors influencing net mercury methylation in contaminated freshwater sediments from the St. Lawrence River in Cornwall, Ontario, Canada. *Sci. Total Environ.* **409**, 968–978.

Bakir F., Damluji S. F., Amin-Zaki L., Murtadha M., Khalidi A., N. Y. Al-Rawi N. ., Tikriti S., Dhahir H. I., Clarkson T. W., Smith J. C. and Doherty R. A. (1973) Methylmercury Poisoning in Iraq. *Science*, **181,** 230-241.

Bargagli R., Agnorelli C., Borghini F. and Monaci F. (2005) Enhanced deposition and bioaccumulation of mercury in Antarctic terrestrial ecosystems facing a coastal polynya. *Environ. Sci. Technol.* **39**, 8150–8155.

Bargagli R., Monaci F., Sanchez-Fernandez C. and Cateni D. (1998) Biomagnification of mercury in an Antarctic marine coastal food web. *Mar. Ecol. Prog. Ser.* **169**, 65–76.

Barkay T., Miller S. M. and Summers A. O. (2003) Bacterial mercury resistance from atoms to ecosystems. *FEMS Microbiol. Rev.* **27**, 355–384.

Barrie L. A., Bottenheim J. W., Schnell R. C., Crutzen P. J. and Rasmussen R. A. (1988) Ozone destruction and photochemical reactions at polar sunrise in the lower Arctic atmosphere. *Nature* **334**, 138–141.

Bearhop S., Ruxton G. D. and Furness R. W. (2000a) Dynamics of mercury in blood and feathers of great skuas. *Environ. Toxicol. Chem.* **19**, 1638–1643.

Bearhop S., Phillips R. A., Thompson D. R., Waldron S. and Furness R. W. (2000b) Variability in mercury concentrations of great skuas Catharacta skua: The influence of colony, diet and trophic status inferred from stable isotope signatures. *Mar. Ecol. Prog. Ser.* **195**, 261–268.

Beattie S. A., Armstrong D., Chaulk A., Comte J., Gosselin M. and Wang F. (2014) Total and methylated mercury in arctic multiyear sea ice. *Environ. Sci. Technol.* **48**, 5575–5582.

Benoit J. M., Gilmour C. C., Heyes A., Mason R. P. and Miller C. L. (2002) Geochemical and Biological Controls over Methylmercury Production and Degradation in Aquatic Ecosystems. *Biogeochem. Environ. Important Trace Elem.* **835**, 19–262.

Benoit J. M., Gilmour C. C. and Mason R. P. (2001) Aspects of bioavailability of mercury for methylation in pure cultures of Desulfobulbus propionicus (1pr3). *Appl. Environ. Microbiol.* **67**, 51–58.

Berglund M., Lind B., Björnberg K. A., Palm B., Einarsson Ö. and Vahter M. (2005) Inter-individual variations of human mercury exposure biomarkers: a cross-sectional assessment. *Environ. Heal. A Glob. Access Sci. Source* **4**, 20.

Bergquist B. a. and Blum J. D. (2009) The odds and evens of mercury isotopes: Applications of mass-dependent and mass-independent isotope fractionation. *Elements* **5**, 353–357.

Bergquist B. a and Blum J. D. (2007) Mass-dependent and -independent fractionation of Hg isotopes by photoreduction in aquatic systems. *Science* **318**, 417–20.

Bigeleisen J. (1996) Nuclear size and shape effects in chemical reactions. Isotope chemistry of the heavy elements. *J. Am. Chem. Soc.* **118**, 3676–3680.

Blain S., Queguiner B., Armand L., Belviso S., Bombled B., Bopp L., Bowie A., Brunet C., Brussaard C., Carlotti F., Christaki U., Corbiere A., Durand I., Ebersbach F., Fuda J.-L. L., Garcia N., Gerringa L., Griffiths B., Guigue C., Guillerm C., Jacquet S., Jeandel C., Laan P., Lefevre D., Lo Monaco C., Malits A., Mosseri J., Obernosterer I., Park Y.-H. H., Picheral M., Pondaven P., Remenyi T., Sandroni V., Sarthou G., Savoye N., Scouarnec L., Souhaut M., Thuiller D., Timmermans K., Trull T., Uitz J., van Beek P., Veldhuis M., Vincent D., Viollier E., Vong L., Wagener T. (2007) Effect of natural iron fertilization on carbon sequestration in the Southern Ocean. *Nature* **446**, 1070–1074.

Blain S., Tréguer P., Belviso S., Bucciarelli E., Denis M., Desabre S., Fiala M., Martin Jézéquel V., Le Fèvre J., Mayzaud P., Marty J. C. and Razouls S. (2001) A biogeochemical study of the island mass effect in the context of the iron hypothesis: Kerguelen Islands, Southern Ocean. *Deep. Res. Part I Oceanogr. Res. Pap.* **48**, 163–187.

Blévin P., Carravieri A., Jaeger A., Chastel O., Bustamante P. and Cherel Y. (2013) Wide range of mercury contamination in chicks of southern ocean seabirds. *PLoS One* **8**, e54508.

Blum J. D. and Bergquist B. a. (2007) Reporting of variations in the natural isotopic composition of mercury.

Anal. Bioanal. Chem. **388**, 353–359.

Blum J. D., Popp B. N., Drazen J. C., Anela Choy C. and Johnson M. W. (2013) Methylmercury production below the mixed layer in the North Pacific Ocean. *Nat. Geosci.* **6**, 879–884.

Blum J. D., Sherman L. S. and Johnson M. W. (2014) Mercury Isotopes in Earth and Environmental Sciences. *Annu. Rev. Earth Planet. Sci.* **42**, 249–269.

Bocher P., Caurant F., Miramand P., Cherel Y. and Bustamante P. (2003) Influence of the diet on the bioaccumulation of heavy metals in zooplankton-eating petrels at Kerguelen archipelago, Southern Indian Ocean. *Polar Biol.* **26**, 759–767.

Bon C., Della Penna A., d'Ovidio F., Y.P. Arnould J., Poupart T. and Bost C.-A. (2015) Influence of oceanographic structures on foraging strategies: Macaroni penguins at Crozet Islands. *Mov. Ecol.* **3**, 32.

Bond A. L. and Diamond Æ. A. W. (2009) Total and Methyl Mercury Concentrations in Seabird Feathers and Eggs. *Arch. Environ. Contam. Toxicol*, 286–291.

Bond A. L., Hobson K. A. and Branfireun B. A. (2015) Rapidly increasing methyl mercury in endangered ivory gull (Pagophila eburnea) feathers over a 130 year record. *Proc. R. Soc. B-Biological Sci.* **282**, 19–32.

Bost C. A., Cotté C., Terray P., Barbraud C., Bon C., Delord K., Gimenez O., Handrich Y., Naito Y., Guinet C. and Weimerskirch H. (2015) Large-scale climatic anomalies affect marine predator foraging behaviour and demography. *Nat. Commun.* **6**, 8220.

Bost C. A., Putz K. and Lage J. (1994) Maximum diving depth and diving patterns of the gentoo penguin Pygoscelis papua at the Crozet Islands. *Mar. Ornithol.* **22**, 237–244.

Bost C. A., Zorn T., Le Maho Y. and Duhamel G. (2002) Feeding of diving predators and diel vertical migration of prey: King penguins' diet versus trawl sampling at Kerguelen Islands. *Mar. Ecol. Prog. Ser.* **227**, 51–61.

Bost C. A, Thiebot J. B., Pinaud D., Cherel Y. and Trathan P. N. (2009) Where do penguins go during the inter-breeding period? Using geolocation to track the winter dispersion of the macaroni penguin. *Biol. Lett.* **5**, 473–476.

Bowman J. S., Berthiaume C. T., Armbrust E. V. and Deming J. W. (2014) The genetic potential for key biogeochemical processes in Arctic frost flowers and young sea ice revealed by metagenomic analysis. *FEMS Microbiol. Ecol.* **89**, 376–387.

Boyd P. W. (2002) The role of iron in the biogeochemistry of the Southern Ocean and equatorial Pacific: A comparison of in situ iron enrichments. *Deep. Res. Part II Top. Stud. Oceanogr.* **49**, 1803–1821.

Boyd P. W., Watson A J., Law C. S., Abraham E. R., Trull T., Murdoch R., Bakker D. C., Bowie A. R., Buesseler K. O., Chang H., Charette M., Croot P., Downing K., Frew R., Gall M., Hadfield M., Hall J., Harvey M., Jameson G., LaRoche J., Liddicoat M., Ling R., Maldonado M. T., McKay R. M., Nodder S., Pickmere S., Pridmore R., Rintoul S., Safi K., Sutton P., Strzepek R., Tanneberger K., Turner S., Waite A. and Zeldis J. (2000) A mesoscale phytoplankton bloom in the polar Southern Ocean stimulated by iron fertilization. *Nature* **407**, 695–702.

Brasso R. L., Chiaradia A., Polito M. J., Raya Rey A. and Emslie S. D. (2014) A comprehensive assessment of mercury exposure in penguin populations throughout the Southern Hemisphere: Using trophic calculations to identify sources of population-level variation. *Mar. Pollut. Bull.* **97**, 408–418.

Brasso R. L., Drummond B. E., Borrett S. R., Chiaradia A., Polito M. J. and Rey A. R. (2013) Unique pattern of molt leads to low intraindividual variation in feather mercury concentrations in penguins. *Environ. Toxicol. Chem.* **32**, 2331–2334.

Bratkic A., Vahcic M., Kotnik J., Obu Vazner K., Begu E., Woodward E. M. S. and Horvat M. (2016) Mercury presence and speciation in the South Atlantic Ocean along the 40°S transect. *Global Biogeochem. Cycles*

30, 105–119.

Braune B. M. (1987) Comparison of Total Mercury Levels in Relation to Diet and Molt for Nine Species of Marine Birds. *Arch. Environ. Contam. Toxicol* **224**, 217–224.

Bridge E. S. (2006) Influences of morphology and behavior on wing-molt strategies in seabirds. *Mar. Ornithol.* **34**, 7–19.

Bridges C. C. and Zalups R. K. (2010) Transport of inorganic mercury and methylmercury in target tissues and organs. *J. Toxicol. Environ. Health. B. Crit. Rev.* **13**, 385–410.

Bridou R., Monperrus M., Gonzalez P. R., Guyoneaud R. and Amouroux D. (2011) Simultaneous determination of mercury methylation and demethylation capacities of various sulfate-reducing bacteria using species-specific isotopic tracers. *Environ. Toxicol. Chem.* **30**, 337–344.

Brooks S., Lindberg S., Southworth G. and Arimoto R. (2008) Springtime atmospheric mercury speciation in the McMurdo, Antarctica coastal region. *Atmos. Environ.* **42**, 2885–2893.

Buchachenko A. L., Ivanov V. L., Roznyatovskii V. A., Artamkina G. A., Vorob'ev A. K. and Ustynyuk Y. A. (2007) Magnetic isotope effect for mercury nuclei in photolysis of bis(p-trifluoromethylbenzyl)mercury. *Dokl. Phys. Chem.* **413**, 39–41.

Burger J. and Gochfeld M. (2004) Marine Birds as Sentinels of Environmental Pollution. *EcoHealth J. Consort.*, 263–274.

Bustamante P., Carravieri A., Goutte A., Barbraud C., Delord K., Chastel O., Weimerskirch H. and Cherel Y. (2016) High feather mercury concentrations in the wandering albatross are related to sex, breeding status and trophic ecology with no demographic consequences. *Environ. Res.* **144**, 1–10.

Bustamante P., Lahaye V., Durnez C., Churlaud C. and Caurant F. (2006) Total and organic Hg concentrations in cephalopods from the North Eastern Atlantic waters: Influence of geographical origin and feeding ecology. *Sci. Total Environ.* **368**, 585–596.

Cai H. and Chen J. (2015) Mass-independent fractionation of even mercury isotopes. *Sci. Bull.*

Canario J., Santos-Echeandía J., Koch B. P. and Laglera L. (2017) Mercury and methylmercury in the Atlantic sector of the Southern Ocean. *Deep. Res. Part II* **138**, 52–62.

Carravieri A. (2014) Seabirds as bioindicators of Southern Ocean ecosystems: concentrations of inorganic and organic contaminants, ecological explanation and critical evaluation. Université de La Rochelle.

Carravieri A., Bustamante P., Churlaud C. and Cherel Y. (2013) Penguins as bioindicators of mercury contamination in the Southern Ocean: birds from the Kerguelen Islands as a case study. *Sci. Total Environ.* **454**–**455**, 141–148.

Carravieri A., Bustamante P., Churlaud C., Fromant A. and Cherel Y. (2014) Moulting patterns drive within-individual variations of stable isotopes and mercury in seabird body feathers: implications for monitoring of the marine environment. *Mar. Biol.* **161**, 963–968.

Carravieri A., Bustamante P., Tartu S., Meillère A., Labadie P., Budzinski H., Peluhet L., Barbraud C., Weimerskirch H., Chastel O. and Cherel Y. (2014) Wandering albatrosses document latitudinal variations in the transfer of persistent organic pollutants and mercury to southern ocean predators. *Environ. Sci. Technol.* **48**, 14746–14755.

Carravieri A., Cherel Y., Blévin P., Brault-Favrou M., Chastel O. and Bustamante P. (2014) Mercury exposure in a large subantarctic avian community. *Environ. Pollut.* **190**, 51–7.

Carravieri A., Cherel Y., Brault-favrou M., Churlaud C., Peluhet L., Labadie P. and Bustamante P. (2017) From Antarctica to the subtropics : Contrasted geographical concentrations of selenium , mercury , and persistent organic pollutants in skua chicks (Catharacta spp .). *Environ. Pollut.* **228**, 464–473.

Carravieri A., Cherel Y., Jaeger A., Churlaud C. and Bustamante P. (2016) Penguins as bioindicators of mercury contamination in the southern Indian Ocean: geographical and temporal trends. *Environ. Pollut.* **213**, 195–205.

Celo V., Lean D. R. S. and Scott S. L. (2006) Abiotic methylation of mercury in the aquatic environment. *Sci. Total Environ.* **368**, 126–37.

Chandan P., Ghosh S. and Bergquist B. A. (2015) Mercury isotope fractionation during aqueous photoreduction of monomethylmercury in the presence of dissolved organic matter. *Environ. Sci. Technol.* **49**, 259–267.

Chaulk A., Stern G. A., Armstrong D., Barber D. G. and Wang F. (2011) Mercury distribution and transport across the ocean-sea-ice-atmosphere interface in the arctic ocean. *Environ. Sci. Technol.* **45**, 1866–1872.

Chen B., Wang T., Yin Y., He B. and Jiang G. (2007) Methylation of inorganic mercury by methylcobalamin in aquatic systems. *Appl. Organomet. Chem.* **21**, 462–467.

Chen C. Y., Pickhardt P. C., Xu M. Q. and Folt C. L. (2008) Mercury and arsenic bioaccumulation and eutrophication in Baiyangdian Lake, China. *Water. Air. Soil Pollut.* **190**, 115–127.

Chen C. Y., Stemberger R. S., Kamman N. C., Mayes B. M. and Folt C. L. (2005) Patterns of Hg bioaccumulation and transfer in aquatic food webs across multi-lake studies in the northeast US. *Ecotoxicology* **14**, 135–147.

Chen J., Hintelmann H., Feng X. and Dimock B. (2012) Unusual fractionation of both odd and even mercury isotopes in precipitation from Peterborough, ON, Canada. *Geochim. Cosmochim. Acta* **90**, 33–46.

Chen J., Hintelmann H., Zheng W., Feng X., Cai H., Wang Z., Yuan S. and Wang Z. (2016) Isotopic evidence for distinct sources of mercury in lake waters and sediments. *Chem. Geol.* **426**, 33–44.

Chen J., Pehkonen S. O. and Lin C. J. (2003) Degradation of monomethylmercury chloride by hydroxyl radicals in simulated natural waters. *Water Res.* **37**, 2496–2504.

Cherel Y. (2008) Isotopic niches of emperor and Adélie penguins in Adélie Land, Antarctica. *Mar. Biol.* **154**, 813–821.

Cherel Y., Bocher P., De Broyer C. and Hobson K. A. (2002) Food and feeding ecology of the sympatric thin-billed Pachyptila belcheri and Antarctic P . desolata prions at Iles Kerguelen , Southern Indian Ocean. **228**, 263–281.

Cherel Y., Fontaine C., Richard P. and Labat J.P. (2010) Isotopic niches and trophic levels of myctophid fishes and their predators in the Southern Ocean. *Limnol. Oceanogr.* **55**, 324–332.

Cherel Y. and Hobson K. A. (2007) Geographical variation in carbon stable isotope signatures of marine predators : a tool to investigate their foraging areas in the Southern Ocean. *Mar. Ecol. Prog. Ser.* **329**, 281–287.

Cherel Y., Hobson K. A., Guinet C. and Vanpe C. (2007) Stable isotopes document seasonal changes in trophic niches and winter foraging individual specialization in diving predators from the Southern Ocean. *J. Anim. Ecol.* **76**, 826–836.

Cherel Y., Jaeger A., Alderman R., Jaquemet S., Richard P., Wanless R. M., Phillips R. A. and Thompson D. R. (2013) A comprehensive isotopic investigation of habitat preferences in nonbreeding albatrosses from the Southern Ocean. *Ecography (Cop.).* **36**, 277–286.

Cherel Y., Jaquemet S., Maglio A. and Jaeger A. (2014) Differences in δ13C and δ15N values between feathers and blood of seabird chicks: Implications for non-invasive isotopic investigations. *Mar. Biol.* **161**, 229–237.

Cherel Y., Quillfeldt P., Delord K. and Weimerskirch H. (2016) Combination of At-Sea Activity , Geolocation and Feather Stable Isotopes Documents Where and When Seabirds Molt. *Front. Ecol. Evol.* **4**.

Choi S.C., Chase T. and Bartha R. (1994) Metabolic Pathways Leading to Mercury Methylation in Desulfovibrio desulfuricans LS. *Appl. Environ. Microbiol.* **60**, 4072–4077.

Chouvelon T., Spitz J., Caurant F., Mèndez-Fernandez P., Autier J., Lassus-Débat a., Chappuis a. and Bustamante P. (2012) Enhanced bioaccumulation of mercury in deep-sea fauna from the Bay of Biscay (north-east Atlantic) in relation to trophic positions identified by analysis of carbon and nitrogen stable isotopes. *Deep. Res. Part I Oceanogr. Res. Pap.* **65**, 113–124.

Cipro C. V. Z., Cherel Y., Caurant F., Miramand P., Méndez-Fernandez P. and Bustamante P. (2014) Trace elements in tissues of white-chinned petrels (Procellaria aequinoctialis) from Kerguelen waters, Southern Indian Ocean. *Polar Biol.* **37**, 763–771.

Clarkson T. W. (2002) The Three Modern Faces of Mercury Methyl Mercury in Fish History of Human Exposure. *Environ. Health Perspect.* **110**, 11–23.

Clarkson T. W. and Magos L. (2006) The toxicology of mercury and its chemical compounds. *Crit. Rev. Toxicol.* **36**, 609–662.

Clarkson T. W., Vyas J. B. and Ballatori N. (2007) Mechanisms of mercury disposition in the body. *Am. J. Ind. Med.* **50**, 757–764.

Clémens S., Monperrus M., Donard O. F. X., Amouroux D. and Guérin T. (2011) Mercury speciation analysis in seafood by species-specific isotope dilution : method validation and occurrence data. *Anal Bioanal Chem* **401**, 2699–2711.

Clémens S., Monperrus M., Donard O. F. X., Amouroux D. and Guérin T. (2012) Mercury speciation in seafood using isotope dilution analysis: A review. *Talanta* **89**, 12–20.

Comiso J. C. (2003) Large-scale Characteristics and Variability of the Global Sea Ice Cover. *Sea Ice An Introd. to its Physics, Chem. Biol. Geol.*, 1–31.

Compeau G. C. and Bartha R. (1985) Sulfate-Reducing Bacteria: Principal Methylators of Mercury in Anoxic Estuarine Sedimentt. *Appl. Environ. Microbiol.* **50**, 498–502.

Cossa D. (2013) Marine biogeochemistry: Methylmercury manufacture. *Nat. Geosci.* **6**, 810–811.

Cossa D., Averty B. and Pirrone N. (2009) The origin of methylmercury in open Mediterranean waters. *Limnol. Oceanogr.* **54**, 837–844.

Cossa D., Heimbürger L.E., Lannuzel D., Rintoul S. R., Butler E. C. V., Bowie A. R., Averty B., Watson R. J. and Remenyi T. (2011) Mercury in the Southern Ocean. *Geochim. Cosmochim. Acta* **75**, 4037–4052.

Cransveld A. A. E., Amouroux D., Tessier E., Koutrakis E., Ozturk A. A., Bettoso N., Mieiro C. L., Berail S., Barre J. P. G., Sturaro N., Schnitzler J. G. and Das K. (2017) Mercury stable isotopes discriminate different populations of European seabass and trace potential Hg sources around Europe. *Environ. Sci. Technol.*

Cuvin-Aralar M. L. A. and Furness R. W. (1991) Mercury and selenium interaction: A review. *Ecotoxicol. Environ. Saf.* **21**, 348–364.

Das R., Bizimis M. and Wilson A. M. (2013) Tracing mercury seawater vs. atmospheric inputs in a pristine SE USA salt marsh system: Mercury isotope evidence. *Chem. Geol.* **336**, 50–61.

Day R. D., Roseneau D. G., Berail S., Hobson K. a., Donard O. F. X., Vander Pol S. S., Pugh R. S., Moors A. J., Long S. E. and Becker P. R. (2012) Mercury stable isotopes in seabird eggs reflect a gradient from terrestrial geogenic to oceanic mercury reservoirs. *Environ. Sci. Technol.* **46**, 5327–5335.

Delmont T. O., Hammar K. M., Ducklow H. W., Yager P. L. and Post A. F. (2014) Phaeocystis antarctica blooms strongly influence bacterial community structures in the Amundsen Sea polynya. *Front. Microbiol.* **5**, 1–14.

Delord K., Cotté C., Péron C., Marteau C., Pruvost P., Gasco N., Duhamel G., Cherel Y. and Weimerskirch H. (2010) At-sea distribution and diet of an endangered top predator : relationship between white-chinned petrels and commercial longline fisheries. **13**, 1–16.

Demers J. D., Blum J. D. and Zak D. R. (2013) Mercury isotopes in a forested ecosystem: Implications for air-surface exchange dynamics and the global mercury cycle. *Global Biogeochem. Cycles* **27**, 222–238.

Desrosiers M., Planas D. and Mucci A. (2006) Mercury methylation in the epilithon of boreal shield aquatic ecosystems. *Environ. Sci. Technol.* **40**, 1540–1546.

Dietz R., Nielsen C. O., Hansen M. M. and Hansen C. T. (1990) Organic mercury in Greenland birds and mammals. *Sci. Tot. Environ.* **95**, 41–51.

Dietz R., Sonne C., Basu N., Braune B., O'Hara T., Letcher R. J., Scheuhammer T., Andersen M., Andreasen C., Andriashek D., Asmund G., Aubail A., Baagøe H., Born E. W., Chan H. M., Derocher A. E., Grandjean P., Knott K., Kirkegaard M., Krey A., Lunn N., Messier F., Obbard M., Olsen M. T., Ostertag S., Peacock E., Renzoni A., Rigét F. F., Skaare J. U., Stern G., Stirling I., Taylor M., Wiig Ø., Wilson S. and Aars J. (2013) What are the toxicological effects of mercury in Arctic biota? *Sci. Total Environ.* **443**, 775–90.

Dock L., Rissanen R. and Vahter M. (1994) Mercury in the Pregnant Hamster. *Toxicology.* **94**, 134-142.

Dommergue A., Ferrari C. P., Gauchard P.A. and Boutron C. F. (2003) The fate of mercury species in a sub-arctic snowpack during snowmelt. *Geophys. Res. Lett.* **30**, 1621.

Dommergue A., Sprovieri F., Pirrone N., Ebinghaus R., Brooks S., Courteaud J. and Ferrari C. (2009) Overview of mercury measurements in the Antarctic troposphere. *Atmos. Chem. Phys. Discuss.* **9**, 26673–26695.

Donovan P. M., Blum J. D., Yee D., Gehrke G. E. and Singer M. B. (2013) An isotopic record of mercury in San Francisco Bay sediment. *Chem. Geol.* **349**–**350**, 87–98.

Douglas T. A., Sturm M., Simpson W. R., Blum J. D., Keeler G. J., Perovich D. K., Biswas A., Johnson K. and Alvarez-Aviles L. (2008) Influence of Snow and Ice Crystal Formation and Accumulation on Mercury Deposition to the Arctic. *Environ Sci Technol.* **42**, 1542–1551.

Ducklow H. W., Steinberg D. K. and Buesseler K. O. (2001) Upper ocean carbon export and the biological pump. *Oceanography* **14**, 50–58.

Ebinghaus R., Kock H. H., Temme C., Einax J. W., Löwe A. G., Richter A., Burrows J. P. and Schroeder W. H. (2002) Antarctic springtime depletion of atmospheric mercury. *Environ. Sci. Technol.* **36**, 1238–1244.

Eckley C. S. and Hintelmann H. (2006) Determination of mercury methylation potentials in the water column of lakes across Canada. *Sci. Total Environ.* **368**, 111–125.

Ekstrom E. B., Morel F. M. M. and Benoit J. M. (2003) Mercury Methylation Independent of the Acetyl-Coenzyme A Pathway in Sulfate-Reducing Bacteria Mercury Methylation Independent of the Acetyl-Coenzyme A Pathway in Sulfate-Reducing Bacteria. *Appl. Environ. Microbiol.* **69**, 5414–5422.

Elliott J. E. and Scheuhammer A. M. (1997) Heavy metal and metallothionein concentrations in seabirds from the Pacific coast of Canada. *Mar. Pollut. Bull.* **34**, 794–801.

Elliott J. E., Scheuhammer A. M., Leighton F. A. and Pearce P. A. (1992) Heavy metal and metallothionein concentrations in Atlantic Canadian seabirds. *Arch. Environ. Contam. Toxicol.* **22**, 63–73.

Enrico M., Le Roux G., Marusczak N., Heimbürger L. E., Claustres A., Fu X., Sun R. and Sonke J. E. (2016) Atmospheric Mercury Transfer to Peat Bogs Dominated by Gaseous Elemental Mercury Dry Deposition. *Environ. Sci. Technol.* **50**, 2405–2412.

Estrade N., Carignan J. and Donard O. F. X. (2010) Isotope tracing of atmospheric mercury sources in an urban area of northeastern France. *Environ. Sci. Technol.* **44**, 6062–7.

Estrade N., Carignan J. and Donard O. F. X. (2009) Measuring Hg Isotopes in Bio-Geo-Environmental Reference Materials. *Geostand. Geoanalytical Res.* **34**, 79–93.

Estrade N., Carignan J. and Donard O. F. X. (2011) Tracing and quantifying anthropogenic mercury sources in soils of northern France using isotopic signatures. *Environ. Sci. Technol.* **45**, 1235–42.

Estrade N., Carignan J., Sonke J. E. and Donard O. F. X. (2009) Mercury isotope fractionation during liquid–vapor evaporation experiments. *Geochim. Cosmochim. Acta* **73**, 2693–2711..

Evers D. C., Savoy L. J., Desorbo C. R., Yates D. E., Hanson W., Taylor K. M., Siegel L. S., Cooley J. H., Bank M. S., Major A., Munney K., Mower B. F., Vogel H. S., Schoch N., Pokras M., Goodale M. W. and Fair J. (2008) Adverse effects from environmental mercury loads on breeding common loons. *Ecotoxicology* **17**, 69–81.

Feng C., Pedrero Z., Gentès S., Barre J., Renedo M., Tessier E., Berail S., Maury-Brachet R., Mesmer-Dudons N., Baudrimont M., Legeay A., Maurice L., Gonzalez P. and Amouroux D. (2015) Specific Pathways of Dietary Methylmercury and Inorganic Mercury Determined by Mercury Speciation and Isotopic Composition in Zebrafish (*Danio rerio*). *Environ. Sci. Technol.* **49**, 12984–12993.

Feng X., Foucher D., Hintelmann H., Yan H., He T. and Qiu G. (2010) Tracing mercury contamination sources in sediments using mercury isotope compositions. *Environ. Sci. Technol.* **44**, 3363–8.

Fitzgerald W. F., Lamborg C. H. and Hammerschmidt C. R. (2007) Marine biogeochemical cycling of mercury. *Chem. Rev.* **107**, 641–62.

Fleming E. J., Mack E. E., Green P. G. and Nelson D. C. (2006) Mercury Methylation from Unexpected Sources : Molybdate-Inhibited Freshwater Sediments and an Iron-Reducing Bacterium. *Appl. Environ. Microbiol.* **72**, 457–464.

Fort J., Robertson G. J., Grémillet D., Traisnel G. and Bustamante P. (2014) Spatial Ecotoxicology: Migratory Arctic Seabirds Are Exposed to Mercury Contamination While Overwintering in the Northwest Atlantic. *Environ. Sci. Technol.* **48**, 11560-11567

Van Franeker J. A., Bathmann U. V. and Mathot S. (1997) Carbon fluxes to Antarctic top predators. *Deep. Res. Part II Top. Stud. Oceanogr.* **44**, 435–455.

Fromant A., Carravieri A., Bustamante P., Labadie P., Budzinski H., Peluhet L., Churlaud C., Chastel O. and Cherel Y. (2016) Wide range of metallic and organic contaminants in various tissues of the Antarctic prion, a planktonophagous seabird from the Southern Ocean. *Sci. Total Environ.* **544**, 754–764.

Furness R. W. and Camphuysen C. J. (1997) Seabirds as monitors of the marine environment. *ICES J. Mar. Sci.* **54**, 726–737.

Furness R. W., Muirhead S. J. and Woodburn M. (1986) Using bird feathers to measure mercury in the environment: Relationships between mercury content and moult. *Mar. Pollut. Bull.* **17**, 27–30.

Furness R. W., Thompson D. R. and Becker P. H. (1995) Spatial and temporal variation in mercury contamination of seabirds in the North Sea. *Helgolãnder Meeresuntersuchungen* **49**, 605–615.

Gantner N., Hintelmann H., Zheng W. and Muir D. C. (2009) Variations in stable isotope fractionation of Hg in food webs of Arctic lakes. *Environ. Sci. Technol.* **43**, 9148–54.

Gårdfeldt K., Munthe J., Strömberg D. and Lindqvist O. (2003) A kinetic study on the abiotic methylation of divalent mercury in the aqueous phase. *Sci. Total Environ.* **304**, 127–136.

Gehrke G. E., Blum J. D. and Marvin-DiPasquale M. (2011) Sources of mercury to San Francisco Bay surface sediment as revealed by mercury stable isotopes. *Geochim. Cosmochim. Acta* **75**, 691–705.

Ghosh S., Schauble E. A., Lacrampe Couloume G., Blum J. D. and Bergquist B. A. (2013) Estimation of nuclear volume dependent fractionation of mercury isotopes in equilibrium liquid-vapor evaporation experiments. *Chem. Geol.* **336**, 5–12.

Gilmour C. C., Elias D. A., Kucken A. M., Brown S. D., Palumbo A. V., Schadt C. W. and Wall J. D. (2011) Sulfate-reducing bacterium Desulfovibrio desulfuricans ND132 as a model for understanding bacterial mercury methylation. *Appl. Environ. Microbiol.* **77**, 3938–3951.

Gilmour C. C., Henry E. A. and Ralph M. (1992) Sulfate Stimulation of Mercury Methylation in Freshwater Sediments. *Environ. Sci. Technol.* **26**, 2281–2287.

Gionfriddo C. M., Tate M. T., Wick R. R., Schultz M. B., Zemla A., Thelen M. P., Schofield R., Krabbenhoft D. P., Holt K. E. and Moreau J. W. (2016) Microbial mercury methylation in Antarctic sea ice. *Nat. Microbiol.* **1**, 16127.

Gleason J. D., Blum J. D., Moore T. C., Polyak L., Jakobsson M., Meyers P. A. and Biswas A. (2016) Sources and cycling of mercury in the paleo Arctic Ocean from Hg stable isotope variations in Eocene and Quaternary sediments. *Geochim. Cosmochim. Acta*. **197**, 245-262

González-Solís J., Croxall J. P. and Briggs D. R. (2002) Activity patterns of giant petrels, Macronectes spp., using different foraging strategies. *Mar. Biol.* **140**, 197–204.

González-Solís J., Sanpera C. and Ruiz X. (2002) Metals and selenium as bioindicators of geographic and trophic segregation in giant petrels Macronectes spp. *Mar. Ecol. Prog. Ser.* **244**, 257–264.

Goutte A., Barbraud C., Meillere A., Carravieri A., Bustamante P., Labadie P., Budzinski H., Delord K., Cherel Y., Weimerskirch H. and Chastel O. (2014) Demographic consequences of heavy metals and persistent organic pollutants in a vulnerable long-lived bird, the wandering albatross. *Proc. R. Soc. B Biol. Sci.* **281**, 20133313.

Goutte A., Bustamante P., Barbraud C., Delord K., Weimerskirch H. and Chastel O. (2014) Demographic responses to mercury exposure in two closely related antarctic top predators. *Ecology* **95**, 1075–1086.

Grandjean P., Satoh H., Murata K. and Eto K. (2010) Adverse effects of methylmercury: Environmental health research implications. *Environ. Health Perspect.* **118**, 1137–1145.

Gratz L. E., Keeler G. J., Blum J. D. and Sherman L. S. (2010) Isotopic composition and fractionation of mercury in Great Lakes precipitation and ambient air. *Environ. Sci. Technol.* **44**, 7764–70.

Grégoire D. S. and Poulain A. J. (2014) A little bit of light goes a long way: the role of phototrophs on mercury cycling. *Metallomics* **6**, 396–407.

Hagan N., Robins N., Hsu-Kim H., Halabi S., Espinoza Gonzales R. D., Ecos E., Richter D. and Vandenberg J. (2015) Mercury hair levels and factors that influence exposure for residents of Huancavelica, Peru. *Environ. Geochem. Health* **37**, 507–514.

Hahn E., Hahn K. and Stoeppler M. (1993) Bird feathers as bioindicators in areas of the German Environmental Specimen Bank - bioaccumulation of mercury in food chains and exogenous deposition of atmospheric pollution with lead and cadmium. *Sci. Total Environ.* **139/140**, 259–270.

Hamelin S., Amyot M., Barkay T., Wang Y. and Planas D. (2011) Methanogens: Principal methylators of mercury in lake periphyton. *Environ. Sci. Technol.* **45**, 7693–7700.

Hammerschmidt C. R. and Bowman K. L. (2012) Vertical methylmercury distribution in the subtropical North Pacific Ocean. *Mar. Chem.* **132**–**133**, 77–82.

Hammerschmidt C. R. and Fitzgerald W. F. (2006) Bioaccumulation and trophic transfer of methylmercury in Long Island Sound. *Arch. Environ. Contam. Toxicol.* **51**, 416–424.

Hammerschmidt C. R. and Fitzgerald W. F. (2004) Geochemical Controls on the Production and Distribution of Methylmercury in Near-Shore Marine Sediments. *Environ. Sci. Technol.* **38**, 1487–1495.

Hammerschmidt C. R., Lamborg C. H. and Fitzgerald W. F. (2007) Aqueous phase methylation as a potential source of methylmercury in wet deposition. *Atmos. Environ.* **41**, 1663–1668.

Harada M. (1995) Minamata disease: methylmercury poisoning in Japan caused by environmental pollution. *Crit. Rev. Toxicol.* **25**, 1–24.

Harmon S. M., King J. K., Gladden J. B. and Newman L. A. (2007) Using sulfate-amended sediment slurry batch reactors to evaluate mercury methylation. *Arch. Environ. Contam. Toxicol.* **52**, 326–331.

Heimbürger L.E., Sonke J. E., Cossa D., Point D., Lagane C., Laffont L., Galfond B. T., Nicolaus M., Rabe B. and van der Loeff M. R. (2015) Shallow methylmercury production in the marginal sea ice zone of the central Arctic Ocean. *Sci. Rep.* **5**, 10318.

Heimbürger L. E., Cossa D., Marty J. C., Migon C., Averty B., Dufour A. and Ras J. (2010) Methyl mercury distributions in relation to the presence of nano- and picophytoplankton in an oceanic water column (Ligurian Sea, North-western Mediterranean). *Geochim. Cosmochim. Acta* **74**, 5549–5559.

Hines M. E., Horvat M., Faganeli J., Bonzongo J. C. J., Barkay T., Major E. B., Scott K. J., Bailey E. A., Warwick J. J. and Lyons W. B. (2000) Mercury biogeochemistry in the Idrija River, Slovenia, from above the mine into the Gulf of Trieste. *Environ. Res.* **83**, 129–139.

Hoefs J. (1997) *Stable isotope geochemistry*. Springer.,

Honda K., Nasu T. and Tatsukawa R. (1986) Seasonal changes in mercury accumulation in the black-eared kite, *Milvus migrans lineatus*. *Environ. Pollut. Ser. A, Ecol. Biol.* **42**, 325–334.

Ikemoto T., Kunito T., Tanaka H., Baba N., Miyazaki N. and Tanabe S. (2004) Environmental Contamination and Detoxification Mechanism of Heavy Metals in Marine Mammals and Seabirds : Interaction of Selenium with Mercury , Silver , Copper , Zinc , and Cadmium in Liver. *Arch. Environ. Contam. Toxicol* **413**, 402–413.

Jackson S. (1988) Diets of the white-chinned petrel and sooty shearwater in the Southern Benguela Region, South Africa. *Condor* **90**, 20–28.

Jackson T. a., Whittle D. M., Evans M. S. and Muir D. C. G. (2008) Evidence for mass-independent and mass-dependent fractionation of the stable isotopes of mercury by natural processes in aquatic ecosystems. *Appl. Geochemistry* **23**, 547–571.

Jaeger A. and Cherel Y. (2011) Isotopic investigation of contemporary and historic changes in penguin trophic niches and carrying capacity of the Southern Indian Ocean. *PLoS One* **6**.

Jaeger A., Lecomte V., Weimerskirch H., Richard P. and Cherel Y. (2010) Seabird satellite tracking validates the use of latitudinal isoscapes to depict predators' foraging areas in the Southern Ocean. *Rapid Commun. Mass Spectrom.* **24**, 3567–3577.

Janssen S. E., Schaefer J. K., Barkay T. and Reinfelder J. R. (2016) Fractionation of Mercury Stable Isotopes during Microbial Methylmercury Production by Iron- and Sulfate-Reducing Bacteria. *Environ. Sci. Technol.* **50**, 8077–8083.

Jasmine P., Muraleedharan K. R., Madhu N. V, Devi C. R. A., Alagarsamy R., Achuthankutty C. T., Jayan Z., Sanjeevan V. N. and Sahayak S. (2009) Hydrographic and productivity characteristics along 45 ° E longitude in the southwestern Indian Ocean and Southern Ocean during austral summer 2004. **389**, 97–116.

Jensen S. and Jernelöv a (1969) Biological methylation of mercury in aquatic organisms. *Nature* **223**, 753–754.

Jiménez-Moreno M., Perrot V., Epov V. N., Monperrus M. and Amouroux D. (2013) Chemical kinetic isotope fractionation of mercury during abiotic methylation of Hg(II) by methylcobalamin in aqueous chloride media. *Chem. Geol.* **336**, 26–36.

Jiskra M., Wiederhold J. G., Bourdon B. and Kretzschmar R. (2012) Solution speciation controls mercury isotope fractionation of Hg(II) sorption to goethite. *Environ. Sci. Technol.* **46**, 6654–62.

Jitaru P., Gabrielli P., Marteel A., Plane J. M. C., Planchon F. A. M., Gauchard P.A., Ferrari C. P., Boutron C. F., Adams F. C., Hong S., Cescon P. and Barbante C. (2009) Atmospheric depletion of mercury over Antarctica during glacial periods. *Nat. Geosci.* **2**, 505–508.

Karimi R., Chen C. Y., Pickhardt P. C., Fisher N. S. and Folt C. L. (2007) Stoichiometric controls of mercury dilution by growth. *Proc. Natl. Acad. Sci. U. S. A.* **104**, 7477–7482.

Kehrig H. A., Hauser-Davis R. A., Seixas T. G. and Fillmann G. (2015) Trace-elements, methylmercury and metallothionein levels in Magellanic penguin (Spheniscus magellanicus) found stranded on the Southern Brazilian coast. *Mar. Pollut. Bull.* **96**, 450–455.

Kim E. Y., Murakami T., Saeki K. and Tatsukawa R. (1996) Mercury levels and its chemical form in tissues and organs of seabirds. *Arch. Environ. Contam. Toxicol.* **30**, 259–266.

Kim E. Y., Saeki K., Tanabe S., Tanaka H. and Tatsukawa R. (1996) Specific accumulation of mercury and selenium in seabirds. *Environ. Pollut.* **94**, 261–265.

Kooyman A. G. L., Cherel Y., Le Maho, Y.; Croxall J. P., Thorson P. H., Ridoux V., Kooyman C. A. (1992) Diving Behavior and Energetics During Foraging Cycles in King Penguins. *Ecol Monogr* **62**, 143–163.

Korb R. E. and Whitehouse M. (2004) Contrasting primary production regimes around South Georgia, Southern Ocean: Large blooms versus high nutrient, low chlorophyll waters. *Deep. Res. Part I Oceanogr. Res. Pap.* **51**, 721–738.

Krishnamurthy S. (1992) Biomethylation and environmental transport of metals. *J. Chem. Educ.* **69**, 347–350.

Kritee K., Barkay T. and Blum J. D. (2009) Mass dependent stable isotope fractionation of mercury during mer mediated microbial degradation of monomethylmercury. *Geochim. Cosmochim. Acta* **73**, 1285–1296.

Kritee K., Blum J. D. and Barkay T. (2008) Mercury Stable Isotope Fractionation during Reduction of Hg(II) by Different Microbial Pathways. *Environ. Sci. Technol.* **42**, 9171–9177.

Kritee K., Blum J. D., Johnson M. W., Bergquist B. A. and Barkay T. (2007) Mercury Stable Isotope Fractionation during Reduction of Hg(II) to Hg(0) by Mercury Resistant Microorganisms. *Environ. Sci. Technol.* **41**, 1889–1895.

Ksionzek K. B., Lechtenfeld O. J., McCallister S. L., Schmitt-Kopplin P., Geuer J. K., Geibert W. and Koch B. P. (2016) Dissolved organic sulfur in the ocean: Biogeochemistry of a petagram inventory. *Science.* **354**, 456–459.

Kwon S. Y., Blum J. D., Carvan M. J., Basu N., Head J. A., Madenjian C. P. and David S. R. (2012) Absence of fractionation of mercury isotopes during trophic transfer of methylmercury to freshwater fish in captivity. *Environ. Sci. Technol.* **46**, 7527–34.

Kwon S. Y., Blum J. D., Chen C. Y., Meattey D. E. and Mason R. P. (2014) Mercury Isotope Study of Sources and Exposure Pathways of Methylmercury in Estuarine Food Webs in the Northeastern U.S. , *Environ. Sci. Technol.* 48, *10089-10097*.

Kwon S. Y., Blum J. D., Chirby M. A. and Chesney E. J. (2013) Application of mercury isotopes for tracing trophic transfer and internal distribution of mercury in marine fish feeding experiments. *Environ. Toxicol. Chem.* **32**, 2322–30.

Laffont L., Maurice L., Amouroux D., Navarro P., Monperrus M., Sonke J. E. and Behra P. (2013) Mercury speciation analysis in human hair by species-specific isotope-dilution using GC-ICP-MS. *Anal. Bioanal. Chem.* **405**, 3001–10.

Laffont L., Sonke J. E., Maurice L., Hintelmann H., Pouilly M., Bacarreza Y. S., Perez T. and Behra P. (2009) Anomalous mercury isotopic compositions of fish and human hair in the Bolivian amazon. *Environ. Sci. Technol.* **43**, 8985–8990.

Laffont L., Sonke J. E., Maurice L., Monrroy S. L., Chincheros J., Amouroux D. and Behra P. (2011) Hg

speciation and stable isotope signatures in human hair as a tracer for dietary and occupational exposure to mercury. *Environ. Sci. Technol.* **45**, 9910–9916.

Lalonde J. D., Poulain A. J. and Amyot M. (2002) The role of mercury redox reactions in snow on snow-to-air mercury transfer. *Environ. Sci. Technol.* **36**, 174–178.

Lamborg C. H., Hammerschmidt C. R., Bowman K. L., Swarr G. J., Munson K. M., Ohnemus D. C., Lam P. J., Heimbürger L.E., Rijkenberg M. J. a. and Saito M. a. (2014) A global ocean inventory of anthropogenic mercury based on water column measurements. *Nature* **512**, 65–68.

Larose C., Dommergue A., De Angelis M., Cossa D., Averty B., Marusczak N., Soumis N., Schneider D. and Ferrari C. (2010) Springtime changes in snow chemistry lead to new insights into mercury methylation in the Arctic. *Geochim. Cosmochim. Acta* **74**, 6263–6275.

Larose C., Dommergue A., Marusczak N., Coves J., Ferrari C. P. and Schneider D. (2011) Bioavailable mercury cycling in polar snowpacks. *Environ. Sci. Technol.* **45**, 2150–2156.

Lavoie R. a, Jardine T. D., Chumchal M. M., Kidd K. a and Campbell L. M. (2013) Biomagnification of Mercury in Aquatic Food Webs: A Worldwide Meta-Analysis. *Environ. Sci. Technol.* **47**, 13385-13394

Leclerc M., Planas D. and Amyot M. (2015) Relationship between Extracellular Low-Molecular-Weight Thiols and Mercury Species in Natural Lake Periphytic Biofilms. *Environ. Sci. Technol.* **49**, 7709–7716.

Legrand M., Feeley M., Tikhonov C., Schoen D. and Li-muller A. (2010) Methylmercury Blood Guidance Values for Canada. *Can. J. Public Heal.* **101**, 28–31.

Lehnherr I. and St. Louis V. L. (2009) Importance of ultraviolet radiation in the photodemethylation of methylmercury in freshwater ecosystems. *Environ. Sci. Technol.* **43**, 5692–5698.

Lehnherr I., St. Louis V. L., Hintelmann H. and Kirk J. L. (2011) Methylation of inorganic mercury in polar marine waters. *Nat. Geosci.* **4**, 298–302.

Lescroël A. and Bost C. A. (2005) Foraging under contrasting oceanographic conditions: The gentoo penguin at Kerguelen Archipelago. *Mar. Ecol. Prog. Ser.* **302**, 245–261.

Lescroël A., Ridoux V. and Bost C. A. (2004) Spatial and temporal variation in the diet of the gentoo penguin (Pygoscelis papua) at Kerguelen Islands. *Polar Biol.* **27**, 206–216.

Li M., Schartup A. T., Valberg A. P., Ewald J. D., David P., Yin R., Balcom P. H. and Sunderland E. M. (2016) Environmental Origins of Methylmercury Accumulated in Subarctic Estuarine Fish Indicated by Mercury Stable Isotopes. *Environ. Sci. Technol.* **50**, 11559-15568.

Li M., Sherman L. S., Blum J. D., Grandjean P., Weihe P., Sunderland E. M. and Shine J. P. (2014) Assessing sources of human methylmercury exposure using stable mercury isotopes. *Environ. Sci. Technol.* **48**, 8800–8806.

Lin C. J. and Pehkonen S. O. (1999) Aqueous phase reactions of mercury with free radicals and chlorine: Implications for atmospheric mercury chemistry. *Chemosphere* **38**, 1253–1263.

Lindberg S. E., Brooks S., Lin C. J., Scott K. J., Landis M. S., Stevens R. K., Goodsite M. and Richter A. (2002) Dynamic oxidation of gaseous mercury in the arctic troposphere at polar sunrise. *Environ. Sci. Technol.* **36**, 1245–1256.

Malinovsky D., Latruwe K., Moens L. and Vanhaecke F. (2010) Experimental study of mass-independence of Hg isotope fractionation during photodecomposition of dissolved methylmercury. *J. Anal. At. Spectrom.* **25**, 950.

Malinovsky D. and Vanhaecke F. (2011) Mercury isotope fractionation during abiotic transmethylation reactions. *Int. J. Mass Spectrom.* **307**, 214–224.

Mallory M. L., Braune B. M., Provencher J. F., Callaghan D. B., Gilchrist H. G., Edmonds S. T., Allard K. and

O'Driscoll N. J. (2015) Mercury concentrations in feathers of marine birds in Arctic Canada. *Mar. Pollut. Bull.* **98**, 308–313.

Mao H., Talbot R. W., Sive B. C., Youn Kim S., Blake D. R. and Weinheimer A. J. (2010) Arctic mercury depletion and its quantitative link with halogens. *J. Atmos. Chem.* **65**, 145–170.

Marshall J. and Speer K. (2012) Closure of the meridional overturning circulation through Southern Ocean upwelling. *Nat. Geosci.* **5**, 171–180.

Marvin-DiPasquale M., Agee J., McGowan C., Oremland R. S., Thomas M., Krabbenhoft D. and Gilmour C. C. (2000) Methyl-Mercury Degradation Pathways: A Comparison among Three Mercury-Impacted Ecosystems. *Environ. Sci. Technol.* **34**, 4908–4916.

Masbou J. (2014) Doctorat Université de Toulouse III Paul Sabatier: Étude des processus métaboliques, écologiques et biogéochimiques contrôlant le fractionnement isotopique de Hg chez les mammifères marins de l'Arctique. .

Masbou J., Point D., Sonke J. E., Frappart F., Perrot V., Amouroux D., Richard P. and Becker P. R. (2015) Hg Stable Isotope Time Trend in Ringed Seals Registers Decreasing Sea Ice Cover in the Alaskan Arctic. *Environ. Sci. Technol.* **49**, 8977–8985.

Mason R. P., Choi A. L., Fitzgerald W. F., Hammerschmidt C. R., Lamborg C. H., Soerensen A. L. and Sunderland E. M. (2012) Mercury biogeochemical cycling in the ocean and policy implications. *Environ. Res.* **119**, 101–117.

Mason R. P. and Fitzgerald W. F. (1990) Alkylmercury species in the equatorial Pacific. *Nature* **347**, 457.

Mason R. P. and Pirrone N. (2009) *Mercury Fate and Transport in the Global Atmosphere*. Springer.

Mason R. P., Reinfelder J. R. and Morel F. M. M. (1995) Bioaccumulation of mercury and methylmercury. *Water Air Soil Pollut* **80**, 915–921.

Mason R. P., Reinfelder J. R. and Morel F. M. M. (1996) Uptake, toxicity and trophic transfer of Hg in a coastal diatom. *Environ. Sci. Toxicol.* **30**, 1835–1845.

Mason R. P. and Sullivan K. A. (1999) The distribution and speciation of mercury in the South and equatorial Atlantic. *Deep. Res. Part II Top. Stud. Oceanogr.* **46**, 937–956.

Mead C., Lyons J. R., Johnson T. M. and Anbar A. D. (2013) Unique Hg stable isotope signatures of compact fluorescent lamp-sourced Hg. *Environ. Sci. Technol.* **47**, 2542–2547.

Meija J., Ouerdane L. and Mester Z. (2009) Isotope scrambling and error magnification in multiple-spiking isotope dilution. *Anal. Bioanal. Chem.* **394**, 199–205.

Mil-Homens M., Blum J., Canário J., Caetano M., Costa A. M., Lebreiro S. M., Trancoso M., Richter T., de Stigter H., Johnson M., Branco V., Cesário R., Mouro F., Mateus M., Boer W. and Melo Z. (2013) Tracing anthropogenic Hg and Pb input using stable Hg and Pb isotope ratios in sediments of the central Portuguese Margin. *Chem. Geol.* **336**, 62–71.

Møller A. K., Barkay T., Hansen M. A., Norman A., Hansen L. H., Soslash;rensen S. J., Boyd E. S. and Kroer N. (2014) Mercuric reductase genes (merA) and mercury resistance plasmids in High Arctic snow, freshwater and sea-ice brine. *FEMS Microbiol. Ecol.* **87**, 52–63.

Mongin M. M., Abraham E. R. and Trull T. W. (2009) Winter advection of iron can explain the summer phytoplankton bloom that extends 1000 km downstream of the Kerguelen Plateau in the Southern Ocean. *J. Mar. Res.* **67**, 225–237.

Monperrus M., Gonzalez P. R., Amouroux D., Alonso J. I. G. and Donard O. F. X. (2008) Evaluating the potential and limitations of double-spiking species-specific isotope dilution analysis for the accurate quantification of mercury species in different environmental matrices. *Anal Bioanal Chem*. **390**, 655–666.

Monperrus M., Tessier E., Amouroux D., Leynaert A., Huonnic P. and Donard O. F. X. (2007) Mercury methylation, demethylation and reduction rates in coastal and marine surface waters of the Mediterranean Sea. *Mar. Chem.* **107**, 49–63.

Monteiro L. R., Costa V., Furness R. W. and Santos R. S. (1996) Mercury concentrations in prey fish indicate enhanced bioaccumulation in mesopelagic environments. *Mar. Ecol. Prog. Ser.* **141**, 21–25.

Monteiro L. R. and Furness R. W. (1997) Accelerated increase in mercury contamination in North Atlantic mesopelagic food chains as indicated by time series of seabird feathers. *Environ. Toxicol. Chem.* **16**, 2489–2493.

Monteiro L. R. and Furness R. W. (2001) Kinetics, dose-response, and excretion of methylmercury in free-living adult Cory's shearwaters. *Environ. Sci. Technol.* **35**, 739–746.

Mopper K. and Zhou X. (1990) Hydroxyl Radical Photoproduction in the Sea as Its Potential Impact on Marine Processes. *Nature* **250**, 661–664.

Morel F. M. M., Kraepiel A. M. L. and Amyot M. (1998) The Chemical Cycle and Bioaccumulation of Mercury. *Annu. Rev. Ecol. Syst.* **29**, 543–566.

Mougeot F., Genevois F. and Bretagnolle V. (1998) Predation on burrowing petrels by the brown skua (Catharacta skua lo È nnbergi) at Mayes Island, Kerguelen. *J. Zool. London* **244**, 429–438.

Nakazawa E., Ikemoto T., Hokura A., Terada Y., Kunito T., Tanabe S. and Nakai I. (2011) The presence of mercury selenide in various tissues of the striped dolphin: evidence from l-XRF-XRD and XAFS analyseswz. *Metallomics* **3**, 719–725.

Navarro P., Clémens S., Perrot V., Bolliet V., Tabouret H., Guérin T., Monperrus M. and Amouroux D. (2013) Simultaneous determination of mercury and butyltin species using a multiple species-specific isotope dilution methodology on the European, Anguilla anguilla glass eel and yellow eel. *Int. J. Environ. Anal. Chem.* **93**, 166–182.

Nerentorp Mastromonaco M. G., Gårdfeldt K., Assmann K. M., Langer S., Delali T., Shlyapnikov Y. M., Zivkovic I. and Horvat M. (2017) Speciation of mercury in the waters of the Weddell, Amundsen and Ross Seas (Southern Ocean). *Mar. Chem.* **193**, 20–33.

Nerentorp Mastromonaco M., Gardfeldt K., Jourdain B., Abrahamsson K., Granfors A., Ahnoff M., Dommergue A., M??jean G. and Jacobi H. W. (2016) Antarctic winter mercury and ozone depletion events over sea ice. *Atmos. Environ.* **129**, 125–132.

Ngugi D. K., Blom J., Stepanauskas R. and Stingl U. (2015) Diversification and niche adaptations of Nitrospina-like bacteria in the polyextreme interfaces of Red Sea brines. *ISME J.*, 1–17.

Nigro M. and Leonzio C. (1996) Intracellular storage of mercury and selenium in different marine vertebrates. *Mar. Ecol. Prog. Ser.* **135**, 137–143.

Norheim G. and Frøslle A. (1978) The Degree of Methylation and Organ Distribution of Mercury in Some Birds of Prey in Norway. *Acta Pharmacol. Toxicol. (Copenh).* **43**, 196–204.

Obrist D., Agnan Y., Jiskra M., Olson C. L., Dominique P., Hueber J., Moore C. W., Sonke J. and Helmig D. (2017) Tundra uptake of atmospheric elemental mercury drives Arctic mercury pollution. *Nat. Publ. Gr.* **547**, 201–204.

Ogawa H., Fukuda R. and Koike I. (1999) Vertical distributions of dissolved organic carbon and nitrogen in the Southern Ocean. *Deep. Res. I* **46**, 1809-1826.

Oremland R. S., Culbertson C. W. and Winfrey M. R. (1991) Methylmercury decomposition in sediments and bacterial cultures: Involvement of methanogens and sulfate reducers in oxidative demethylation. *Appl. Environ. Microbiol.* **57**, 130–137.

Pacyna E. G., Pacyna J. M., Steenhuisen F. and Wilson S. (2006) Global anthropogenic mercury emission

inventory for 2000. *Atmos. Environ.* **40**, 4048–4063.

Pacyna E. G., Pacyna J. M., Sundseth K., Munthe J., Kindbom K., Wilson S., Steenhuisen F. and Maxson P. (2010) Global emission of mercury to the atmosphere from anthropogenic sources in 2005 and projections to 2020. *Atmos. Environ.* **44**, 2487–2499.

Palmisano F., Cardellicchio N. and Zambonin P. G. (1995) Speciation of mercury in dolphin liver: A two-stage mechanism for the demethylation accumulation process and role of selenium. *Mar. Environ. Res.* **40**, 109–121.

Parks J. M., Johs A., Podar M., Bridou R., Hurt R. A., Smith S. D., Tomanicek S. J., Qian Y., Brown S. D., Brandt C. C., Palumbo A. V, Smith J. C., Wall J. D., Dwayne A. E. and Liyuan L. (2013) The Genetic Basis for Bacterial Mercury Methylation. *Science.* **339**, 1332–1335.

Pedrero Z., Bridou R., Mounicou S., Guyoneaud R., Monperrus M. and Amouroux D. (2012) Transformation, localization, and biomolecular binding of Hg species at subcellular level in methylating and nonmethylating sulfate-reducing bacteria. *Environ. Sci. Technol.* **46**, 11744–11751.

Pedrero Z., Ouerdane L., Mounicou S., Lobinski R., Monperrus M. and Amouroux D. (2012) Identification of mercury and other metals complexes with metallothioneins in dolphin liver by hydrophilic interaction liquid chromatography with the parallel detection by ICP MS and electrospray hybrid linear/orbital trap MS/MS. *Metallomics* **4**, 473–9.

Péron C., Delord K., Phillips R. A., Charbonnier Y., Marteau C., Louzao M. and Weimerskirch H. (2010) Seasonal variation in oceanographic habitat and behaviour of white-chinned petrels Procellaria aequinoctialis from Kerguelen Island. **416**, 267–284.

Perrot V. and Bridou R. (2015) Identical Hg Isotope Mass Dependent Fractionation Signature during Methylation by Sulfate-Reducing Bacteria in Sulfate and Sulfate-Free Environment. *Environ. Sci. Technol.* **49**, 1365-1363.

Perrot V., Epov V. N., Pastukhov M. V, Grebenshchikova V. I., Zouiten C., Sonke J. E., Husted S., Donard O. F. X. and Amouroux D. (2010) Tracing sources and bioaccumulation of mercury in fish of Lake Baikal--Angara River using Hg isotopic composition. *Environ. Sci. Technol.* **44**, 8030–7.

Perrot V., Jimenez-Moreno M., Berail S., Epov V. N., Monperrus M. and Amouroux D. (2013) Successive methylation and demethylation of methylated mercury species (MeHg and DMeHg) induce mass dependent fractionation of mercury isotopes. *Chem. Geol.* **355**, 153–162.

Perrot V., Masbou J., Pastukhov M. V., Epov V. N., Point D., Bérail S., Becker P. R., Sonke J. E. and Amouroux D. (2016) Natural Hg isotopic composition of different Hg compounds in mammal tissues as a proxy for in vivo breakdown of toxic methylmercury. *Metallomics* **8**, 170–178.

Perrot V., Pastukhov M. V, Epov V. N., Husted S., Donard O. F. X. and Amouroux D. (2012) Higher mass-independent isotope fractionation of methylmercury in the pelagic food web of Lake Baikal (Russia). *Environ. Sci. Technol.* **46**, 5902–11.

Pickhardt P. C., Folt C. L., Chen C. Y., Klaue B. and Blum J. D. (2002) Algal blooms reduce the uptake of toxic methylmercury in freshwater food webs. *Proc. Natl. Acad. Sci. U. S. A.* **99**, 4419–23. A

Pirrone N., Cinnirella S., Feng X., Finkelman R. B., Friedli H. R., Leaner J., Mason R., Mukherjee A. B., Stracher G. B., Streets D. G. and Telmer K. (2010) Global mercury emissions to the atmosphere from anthropogenic and natural sources. *Atmos. Chem. Phys.* **10**, 5951–5964.

Plancke J. (1977) *Phytoplankton biomass and productivity in the Subtropical Convergence area and shelves of the western Indian subantarctic islands.* Adaptions. ed. D. Liano, GA, Smithsonian Institution, Washington.

Point D., Davis W. C., Garcia Alonso J. I., Monperrus M., Christopher S. J., Donard O. F. X., Becker P. R. and Wise S. a. (2007) Simultaneous determination of inorganic mercury, methylmercury, and total mercury

concentrations in cryogenic fresh-frozen and freeze-dried biological reference materials. *Anal. Bioanal. Chem.* **389**, 787–798.

Point D., Ignacio Garcia Alonso J., Clay Davis W., Christopher S. J., Guichard A., Donard O. F. X., Becker P. R., Turk G. C. and Wise S. a. (2008) Consideration and influence of complexed forms of mercury species on the reactivity patterns determined by speciated isotope dilution model approaches: A case for natural biological reference materials. *J. Anal. At. Spectrom.* **23**, 385.

Point D., Sonke J. E., Day R. D., Roseneau D. G., Hobson K. A., Pol S. S. Vander, Moors A. J., Pugh R. S., Donard O. F. X. and Becker P. R. (2011) Methylmercury photodegradation influenced by sea-ice cover in Arctic marine ecosystems. *Nat. Geosci.* **4**, 1–7.

Pollard R. T., Lucas M. I. and Read J. F. (2002) Physical controls on biogeochemical zonation in the Southern Ocean. *Deep. Res. Part II Top. Stud. Oceanogr.* **49**, 3289–3305.

Pollard R. T., Venables H. J., Read J. F. and Allen J. T. (2007) Large-scale circulation around the Crozet Plateau controls an annual phytoplankton bloom in the Crozet Basin. *Deep. Res. Part II Top. Stud. Oceanogr.* **54**, 1915–1929.

Pongratz R. and Heumann K. G. (1999) Production of methylated mercury, lead, and cadmium by marine bacteria as a significant natural source for atmospheric heavy metals in polar regions. *Chemosphere* **39**, 89–102.

Poulain A. J., Lalonde J. D., Amyot M., Shead J. A., Raofie F. and Ariya P. A. (2004) Redox transformations of mercury in an Arctic snowpack at springtime. *Atmos. Environ.* **38**, 6763–6774.

Pućko M., Burt a., Walkusz W., Wang F., Macdonald R. W., Rysgaard S., Barber D. G., Tremblay J. É. and Stern G. a. (2014) Transformation of mercury at the bottom of the arctic food web: An overlooked puzzle in the mercury exposure narrative. *Environ. Sci. Technol.* **48**, 7280–7288.

Pütz K. (2002) Spatial and temporal variability in the foraging areas of breeding king penguins. *Condor* **104**, 528–538.

Queipo Abad S., Rodríguez-González P. and García Alonso J. I. (2016) Evidence of the direct adsorption of mercury in human hair during occupational exposure to mercury vapour. *J. Trace Elem. Med. Biol.* **36**, 16–21.

Ratcliffe B. Y. D. A. (2012) British Birds Changes Attributable to Pesticides in Egg Breakage Frequency and Egshell Thickness in some British Birds. **7**, 67–115.

Renedo M., Bustamante P., Tessier E., Pedrero Z., Cherel Y. and Amouroux D. (2017) Assessment of mercury speciation in feathers using species-specific isotope dilution analysis. *Talanta* **174**, 100–110.

Riaux-Gobin C., Dieckmann G. S., Poulin M., Neveux J., Labrune C. and Vétion G. (2013) Environmental conditions, particle flux and sympagic microalgal succession in spring before the sea-ice break-up in Adélie Land, East Antarctica. *Polar Res.* **32**.

RiauxGobin C., Klein B. and Duchene J. C. (2000) A pigment analysis of feeding modes of Thelepus extensus (Polychaeta, Terebellidae) in relation to wave exposure at the Iles Kerguelen. *Antarct. Sci.* **12**, 52–63.

Ridley W. P., Dizikes L. J. and Wood J. M. (1977) Biomethylation of toxic elements in the environment. *Science* **197**, 329–32.

Ridoux V. (1994) Marine Ornithology: The diets and dietary segregation of seabirds at the Subantarctic Crozet Islands. Part 2. .

Rodary D., Wienecke B. C. and Bost C. a. (2000) Diving behaviour of Adelie penguins (Pygoscelis adeliae) at Dumont D'Urville, Antarctica: nocturnal patterns of diving and rapid adaptations to changes in sea-ice condition. *Polar Biol.* **23**, 113–120.

Rodrigues J. L., Rodriguez Alvarez C., Rodriguez Farinas N., Berzas Nevado J. J., Barbosa Jr. F. and Rodriguez

Martin-Doimeadios R.C. (2011) Mercury speciation in whole blood by gas chromatography coupled to ICP-MS with a fast microwave-assisted sample preparation procedure. *Journal of Analytical Atomic Spectrometry*. **26**, 436–442.

Rodríguez-González P., Marchante-Gayón J. M., García Alonso J. I. and Sanz-Medel A. (2005) Isotope dilution analysis for elemental speciation: a tutorial review. *Spectrochim. Acta Part B At. Spectrosc.* **60**, 151–207.

Rodriguez Gonzalez P., Tessier E., Guyoneaud R. and Monperrus M. (2009) Species-Specific Stable Isotope Fractionation of Mercury during Hg (II) Methylation by an Anaerobic Bacteria (Desulfobulbus propionicus) under Dark Conditions. *Environ. Sci. Technol.* **43**, 9183-9188.

Rodriguez Martin-Doimeadios R. C., Krupp K., Amouroux D., Donard O. F. X., Martin-Doimeadios R. C. R. and Krupp E. (2002) Application of Isotopically Labeled Methylmercury for Isotope Dilution Analysis of Biological Samples Using Gas Chromatography/ICMS. *Anal. Chem.* **74**, 2505–2512.

Rodríguez Martín-Doimeadios R. C., Tessier E., Amouroux D., Guyoneaud R., Duran R., Caumette P. and Donard O. F. X. (2004) Mercury methylation/demethylation and volatilization pathways in estuarine sediment slurries using species-specific enriched stable isotopes. *Mar. Chem.* **90**, 107–123.

Rolison J. M., Landing W. M., Luke W., Cohen M. and Salters V. J. M. (2013) Isotopic composition of species-specific atmospheric Hg in a coastal environment. *Chem. Geol.* **336**, 37–49.

Rose C. H., Ghosh S., Blum J. D. and Bergquist B. A. (2015) Effects of ultraviolet radiation on mercury isotope fractionation during photo-reduction for inorganic and organic mercury species. *Chem. Geol.* **405**, 102–111.

Rowland I. R. (1988) Interactions of the Gut Microflora and the Host in Toxicology *. *Toxicol. Pathol.* **16**.

Sanial V., Van Beek P., Lansard B., D'Ovidio F., Kestenare E., Souhaut M., Zhou M. and Blain S. (2014) Study of the phytoplankton plume dynamics off the Crozet Islands (Southern Ocean): A geochemical-physical coupled approach. *J. Geophys. Res. Ocean.* **119**, 2227–2237.

Schaefer J. K., Yagi J., Reinfelder J. R., Cardona T., Ellickson K. M., Tel-Or S. and Barkay T. (2004) Role of the bacterial organomercury lyase (MerB) in controlling methylmercury accumulation in mercury-contaminated natural waters. *Environ. Sci. Technol.* **38**, 4304–4311.

Schartup A. T., Balcom P. H. and Mason R. P. (2014) Sediment-Porewater Partitioning, Total Sulfur, and Methylmercury Production in Estuaries. *Environ. Sci. Technol.* **48**, 954-960

Schartup A. T., Balcom P. H., Soerensen A. L., Gosnell K. J., Calder R. S. D., Mason R. P. and Sunderland E. M. (2015) Freshwater discharges drive high levels of methylmercury in Arctic marine biota. *Proc. Natl. Acad. Sci.* **112**, 11789–11794.

Schauble E. A. (2007) Role of nuclear volume in driving equilibrium stable isotope fractionation of mercury, thallium, and other very heavy elements. *Geochim. Cosmochim. Acta* **71**, 2170–2189.

Schroeder W. H. and Munthe J. (1998) Atmospheric mercury - An overview. *Atmos. Environ.* **32**, 809–822.

Selin N. E., Javob D. J., Park R. J., Yantosca R. M., Strode S., Jaeglé L. and Jaffe D. (2007) Chemical cycling and deposition of atmospheric mercury: Global constraints from observations. *J. Geophys. Res. Atmos.* **112**, 1–14.

Senn D. B., Chesney E. J., Blum J. D., Bank M. S., Maage A. and Shine J. P. (2010) Stable isotope (N, C, Hg) study of methylmercury sources and trophic transfer in the northern gulf of Mexico. *Environ. Sci. Technol.* **44**, 1630–7.

Sheppard D. S., Deely J. M. and Edgerley W. H. L. (1997) Heavy metal content of meltwaters from the Ross Dependency , Antarctica. *New Zeal. J. Mar. Freshw. Res.* **31**, 313–325.

Sherman L. S. and Blum J. D. (2013) Mercury stable isotopes in sediments and largemouth bass from Florida lakes, USA. *Sci. Total Environ.* **448**, 163–175.

Sherman L. S., Blum J. D., Basu N., Rajaee M., Evers D. C., Buck D. G., Petrlik J. and Digangi J. (2015) Assessment of mercury exposure among small-scale gold miners using mercury stable isotopes. *Environ. Res.* **137**, 226–234.

Sherman L. S., Blum J. D., Douglas T. A. and Steffen A. (2012) Frost flowers growing in the Arctic ocean-atmosphere-sea ice-snow interface: 2. Mercury exchange between the atmosphere, snow, and frost flowers. *J. Geophys. Res. Atmos.* **117**, 1–10.

Sherman L. S., Blum J. D., Franzblau A. and Basu N. (2013) New Insight into Biomarkers of Human Mercury Exposure Using Naturally Occurring Mercury Stable Isotopes. *Environ. Sci. Technol.* **47**, 3403-3409.

Sherman L. S., Blum J. D., Johnson K. P., Keeler G. J., Barres J. a. and Douglas T. a. (2010) Mass-independent fractionation of mercury isotopes in Arctic snow driven by sunlight. *Nat. Geosci.* **3**, 173–177.

Sherman L. S., Blum J. D., Keeler G. J., Demers J. D. and Dvonch J. T. (2012) Investigation of local mercury deposition from a coal-fired power plant using mercury isotopes. *Environ. Sci. Technol.* **46**, 382–390.

Simpson W. R., von Glasow R., Riedel K., Anderson P., Ariya P., Bottenheim J., Burrows J., Carpenter L., Frieß U., Goodsite M. E., Heard D., Hutterli M., Jacobi H.-W., Kaleschke L., Neff B., Plane J., Platt U., Richter A., Roscoe H., Sander R., Shepson P., Sodeau J., Steffen A., Wagner T. and Wolff E. (2007) Halogens and their role in polar boundary-layer ozone depletion. *Atmos. Chem. Phys. Discuss.* **7**, 4285–4403.

Skyllberg U., Bloom P. R., Qian J., Lin C. M. and Bleam W. F. (2006) Complexation of mercury(II) in soil organic matter: EXAFS evidence for linear two-coordination with reduced sulfur groups. *Environ. Sci. Technol.* **40**, 4174–4180.

Slemr F., Schuster G. and Seiler W. (1985) Distribution, speciation, and budget of atmospheric mercury. *J. Atmos. Chem.* **3**, 407–434.

Smith C. N., Kesler S. E., Blum J. D. and Rytuba J. J. (2008) Isotope geochemistry of mercury in source rocks, mineral deposits and spring deposits of the California Coast Ranges, USA. *Earth Planet. Sci. Lett.* **269**, 399–407.

Smith J. C., Allen P. V, Turner M. D., Most B., Fisher H. L. and Hall L. L. (1994) The kinetics of intravenously administered methyl mercury in man. *Toxicol. Appl. Pharmacol.* **128**, 251–256.

Snyder R. . (1971) Congenital Mercury Poisoning. *N. Engl. J. Med.* **284**, 18

Soerensen A. L., Skov H., Jacob D. J., Soerensen B. T. and Johnson M. S. (2010) Global concentrations of gaseous elemental mercury and reactive gaseous mercury in the marine boundary layer. *Environ. Sci. Technol.* **44**, 7425–7430.

Sokolov S. (2008) Chlorophyll blooms in the Antarctic Zone south of Australia and New Zealand in reference to the Antarctic Circumpolar Current fronts and sea ice forcing. *J. Geophys. Res. Ocean.* **113**.

Sokolov S. and Rintoul S. R. (2007) On the relationship between fronts of the Antarctic Circumpolar Current and surface chlorophyll concentrations in the Southern Ocean. *J. Geophys. Res. Ocean.* **112**, 1–17.

Somer E. (1978) *Die Verschmutzung der Nord und Ostsee: natürlich bedingt oder von Menschen verschludet?*,

Spalding M. G., Frederick P. C., McGill H. C., Bouton S. N. and McDowell L. R. (2000) Methylmercury accumulation in tissues and its effects on growth and appetite in captive great egrets. *J. Wildl. Dis.* **36**, 411–422.

Sprovieri F., Pirrone N., Bencardino M., D'Amore F., Angot H., Barbante C., Brunke E.-G., Arcega-Cabrera F., Cairns W., Comero S., Diéguez M. del C., Dommergue A., Ebinghaus R., Feng X. Bin, Fu X., Garcia P. E., Gawlik B. M., Hageström U., Hansson K., Horvat M., Kotnik J., Labuschagne C., Magand O., Martin L., Mashyanov N., Mkololo T., Munthe J., Obolkin V., Islas M. R., Sena F., Somerset V., Spandow P., Vardè M., Walters C., Wängberg I., Weigelt A., Yang X. and Zhang H. (2016) Five-year

records of Total Mercury Deposition flux at GMOS sites in the Northern and Southern Hemispheres. *Atmos. Chem. Phys. Discuss.* **0**, 1–33.

Steffen A., Lehnherr I., Cole A., Ariya P., Dastoor A., Durnford D., Kirk J. and Pilote M. (2014) Atmospheric mercury in the Canadian Arctic. Part I: A review of recent field measurements. *Sci. Total Environ.* **509-510**, 3-15

Stein E. D., Cohen Y. and Winer A. M. (1996) Environmental Distribution and Transformation of Mercury Compounds. *Crit. Rev. Environ. Sci. Technol.* **26**, 1–43.

Stephens C. R., Shepson P. B., Steffen A., Bottenheim J. W., Liao J., Huey L. G., Apel E., Weinheimer A., Hall S. R., Cantrell C., Sive B. C., Knapp D. J., Montzka D. D. and Hornbrook R. S. (2012) The relative importance of chlorine and bromine radicals in the oxidation of atmospheric mercury at Barrow, Alaska. *J. Geophys. Res. Atmos.* **117**, 1–16.

Streets D. G., Devane M. K., Lu Z., Bond T. C., Sunderland E. M. and Jacob D. J. (2011) All-time releases of mercury to the atmosphere from human activities. *Environ. Sci. Technol.* **45**, 10485–10491.

Štrok M., Baya P. A. and Hintelmann H. (2015) The mercury isotope composition of Arctic coastal seawater. *Comptes Rendus - Geosci.* **347**, 368–376.

Sullivan C., Arrigo K. R., Mcclain C. R., Comiso J. C. and Firestone J. (1993) Dsributions of Phytoplankton Blooms in the Southern Ocean. *Science.* **262**, 1832–1837.

Sun G., Sommar J., Feng X., Lin C. J., Ge M., Wang W., Yin R., Fu X. and Shang L. (2016) Mass-dependent and -independent fractionation of mercury isotope during gas-phase oxidation of elemental mercury vapor by atomic Cl and Br. *Environ. Sci. Technol.* **50**, 9232–9241.

Sunderland E. M., Krabbenhoft D. P., Moreau J. W., Strode S. A. and Landing W. M. (2009) Mercury sources, distribution, and bioavailability in the North Pacific Ocean: Insights from data and models. *Global Biogeochem. Cycles* **23**, 1–14.

Sunderland E. M. and Schartup A. T. (2016) Biogeochemistry: Mercury methylation on ice. *Nat. Microbiol.* **1**, 16165.

Tan S. W., Meiller J. C. and Mahaffey K. R. (2009) The endocrine effects of mercury in humans and wildlife. *Crit. Rev. Toxicol.* **39**, 228–269.

Tang S., Feng X., Qiu J., Yin G. and Yang Z. (2007) Mercury speciation and emissions from coal combustion in Guiyang, southwest China. *Environ. Res.* **105**, 175–182.

Tartu S., Goutte A., Bustamante P., Angelier F., Moe B., Clément-Chastel C., Bech C., Gabrielsen G. W., Bustnes J. O. and Chastel O. (2013) To breed or not to breed: endocrine response to mercury contamination by an Arctic seabird. *Biol. Lett.* **9**, 20130317.

Temme C., Einax J. W., Ebinghaus R. and Schroeder W. H. (2003) Measurements of atmospheric mercury species at a coastal site in the antarctic and over the south atlantic ocean during polar summer. *Environ. Sci. Technol.* **37**, 22–31.

Thayer J. S. (1989) Methylation: Its role in the environmental mobility of heavy elements. *Appl. Organomet. Chem.* **3**, 123–128.

Thiebot J., Cherel Y., Acqueberge M. and Elien A. U. R. (2014) Adjustment of pre-moult foraging strategies in Macaroni Penguins Eudyptes chrysolophus according to locality, sex and breeding status. *Ibis*, **156**, 511–522.

Thiers L., Delord K., Barbraud C., Phillips R. A., Pinaud D. and Weimerskirch H. (2014) Foraging zones of the two sibling species of giant petrels in the Indian Ocean throughout the annual cycle : implication for their conservation. **499**, 233–248.

Thompson D. R., Becker P. H. and Furness R. W. (1993) Long-term changes in mercury concentrations in

herring gulls Larus argentatus and common terns Sterna hirundo from the German North Sea coast. *J. Appl. Ecol.* **30**, 316–320.

Thompson D. R., Furness R. W. and Lewis S. A. (1993) Temporal and spatial variation in mercury concentrations in some albatrosses and petrels from the sub-Antarctic. *Polar Biol.* **13**, 239–244.

Thompson D. R., Bearhop S., Speakman J. and Furness R. W. (1998) Feathers as a means of monitoring mercury in seabirds: Insights from stable isotope analysis. *Environ. Pollut.* **101**, 193–200.

Thompson D. R., Furness R. W. and Monteiro L. R. (1998) Seabirds as biomonitors of mercury inputs to epipelagic and mesopelagic marine food chains. *Sci. Total Environ.* **213**, 299–305.

Thompson D. R., Furness R. W. and Walsh P. M. (1992) Historical changes in mercury concentrations in the marine ecosystem of the north and north-east Atlantic ocean as indicated by seabird feathers. *J. Appl. Ecol.* **29**, 79–84.

Thompson D. R., Hamer K. C. and Furness R. W. (1991) Mercury Accumulation in Great Skuas Catharacta Skua of Known Age and Sex, and Its Effects Upon Breeding and Survival. *J. Appl. Ecol.* **28**, 672–684.

Thompson D. R., Stewart F. M. and Furness R. W. (1990) Using seabirds to monitor mercury in marine environments. The validity of conversion ratios for tissue comparisons. *Mar. Pollut. Bull.* **21**, 339–342.

Thompson D. R.and Furness R. W. (1989a) Comparison of the Levels of total and organic mercury in seabird feathers. *Mar. Pollut. Bull.* **20**, 577–579.

Thompson and Furness (1989b) Differences in the chemical form of mercury stored in South Atlantic seabirds. *Environ. Pollut.* **60**, 305–317.

Tremblay L., Caparros J., Leblanc K. and Obernosterer I. (2015) Origin and fate of particulate and dissolved organic matter in a naturally iron-fertilized region of the Southern Ocean. *Biogeosciences* **12**, 607–621.

Tremblay Y. and Cherel Y. (2003) Geographic variation in the foraging behaviour, diet and chick growth of rockhopper penguins. *Mar. Ecol. Prog. Ser.* **251**, 279–297.

Trull T. W. and Armand L. (2001) Insights into Southern Ocean carbon export from the δ13c of particles and dissolved inorganic carbon during the SOIREE iron release experiment. *Deep. Res. Part II Top. Stud. Oceanogr.* **48**, 2655–2680.

Tseng, C.M., De Diego, A., Martin, F.M., Amouroux, D., Donard O. F. X. (1997) Rapid determination of inorganic mercury and methylmercury in biological reference materials by hydride generation, cryofocusing, atomic absorption spectrometry after open focused microwave-assisted alkaline digestion. *J. Anal. At. Spectrom.* **12**, 743–750.

Tsubaki T. and Irukayama K. (1977) *Minamata disease. Methylmercury poisoning in Minamata and Niigata, Japan.* North-Holl.

Tsui M. T. K., Blum J. D., Kwon S. Y., Finlay J. C., Balogh S. J. and Nollet Y. H. (2012) Sources and transfers of methylmercury in adjacent river and forest food webs. *Environ. Sci. Technol.* **46**, 10957–64.

Ullrich S., Tanton T.W. and Abdrashitova S. (2001) Mercury in the aquatic environment: a review of factors affecting methylation. *Crit. Rev. Environ. Sci. Technol.* **31**, 241–293.

UNEP (2013) Global Mercury Assessment 2013: Sources, Emissions, Releases, and Environmental Transport. *UNEP*, 42.

UNEP (2012) Reducing Mercury Use in Artisanal and Small-Scale. *UNEP*

Urey H. . (1947) The Thermodynamic Properties of Isotopic Substances. *J. Chem. Soc.*, 562–580.

US EPA (2007) Mercury total (organic and 7439-97-6 inorganic). *Methods*, 1–17.

Uthe J. S. and Grift B. (1972) Rapid Semimicro Method for the Determination of Methyl Mercury in Fish Tissue.

Vahter M., Akesson A., Lind B., Björs U., Schütz A. and Berglund M. (2000) Longitudinal study of methylmercury and inorganic mercury in blood and urine of pregnant and lactating women, as well as in umbilical cord blood. *Environ. Res.* **84**, 186–94.

Vahter M., Motter N. K., Friberg L. T., Birger Lind S., Charleston J. S. and Burbacher T. (1995) Demethylation of methylmercury in different brain sites of Macaca fascicularis Monkeys during long-term subclinical methylmercury exposure. *Toxicol. Appl. Pharmacol.* **134**, 273–284.

Vo A.-T. E., Bank M. S., Shine J. P. and Edwards S. V (2011) Temporal increase in organic mercury in an endangered pelagic seabird assessed by century-old museum specimens. *Proc. Natl. Acad. Sci. U. S. A.* **108**, 7466–7471.

Wagemann R. U., Trebacz E., Boila G. and Lockhart W. L. (1998) Methylmercury and total mercury in tissues of arctic marine mammals. *Sci. Tot. Environ.* **218**, 19-31.

Walker C. H. (2003) Neurotoxic Pesticides and Behavioural Effects Upon Birds. *Ecotoxicology*. **12**, 307-316

Van Walleghen J., Blanchfield P. and Hintelmann H. (2007) Elimination of mercury by yellowperch in the wild. *Env. Sci Technol* **41**, 5895–5901.

Wang R., Feng X.-B. and Wang W.-X. (2013) In vivo mercury methylation and demethylation in freshwater tilapia quantified by mercury stable isotopes. *Environ. Sci. Technol.* **47**, 7949–57.

Wang W. X. and Wong R. S. K. (2003) Bioaccumulation kinetics and exposure pathways of inorganic mercury and methylmercury in a marine fish, the sweetlips Plectorhinchus gibbosus. *Mar. Ecol. Prog. Ser.* **261**, 257–268.

Wang Z., Chen J., Feng X., Hintelmann H., Yuan S., Cai H., Huang Q., Wang S. and Wang F. (2015) Mass-dependent and mass-independent fractionation of mercury isotopes in precipitation from Guiyang, SW China. *Comptes Rendus - Geosci.* **347**, 358–367.

Watras C. J., Back R. C., Halvorsen S., Hudson R. J. M., Morrison K. A. and Wente S. P. (1998) Bioaccumulation of mercury in pelagic freshwater food webs. *Sci. Total Environ.* **219**, 183–208.

Weimerskirch H. (1991) Sex-specific differences in molt strategy in relation to breeding in the wandering albatross. *Condor* **93**, 731–737.

Whalin L., Kim E. H. and Mason R. (2007) Factors influencing the oxidation, reduction, methylation and demethylation of mercury species in coastal waters. *Mar. Chem.* **107**, 278–294.

WHO (2007) Exposure tonMercury: A major public health concern. *WHO*, 4.

WHO (2000) Health Systems: Improving Perfomance- The World Health Report 2000. *World Heal. Organ.* **78**, 1–215.

WHO (2008) Mercury Assessing the environmental burden of disease at national and local levels. *WHO* **16**, 1–42.

Wiederhold J. G. (2015) Metal stable isotope signatures as tracers in environmental geochemistry. *Environ. Sci. Technol.* **49**, 2606–2624.

Wiederhold J. G., Cramer C. J., Daniel K., Infante I., Bourdon B. and Kretzschmar R. (2010) Equilibrium mercury isotope fractionation between dissolved Hg(II) species and thiol-bound Hg. *Environ. Sci. Technol.* **44**, 4191–7.

Wienecke B., Robertson G., Kirkwood R. and Lawton K. (2007) Extreme dives by free-ranging emperor penguins. *Polar Biol.* **30**, 133–142.

Wiener J. G., Krabbenhoft D. P., Heinz G. H. and Scheuhammer M. A. (2003) *Ecotoxicology of mercury. Handbook of Ecotoxicology*. eds. D. J. Hoffman, B. A. Rattner, G. A. Burton, and J. Cairns, Lewis Publisher.

Woehler E. J. (1995) Consumption of Southern Ocean marine resources by penguins. The penguins: ecology and management. Chipping Norton: Surrey Beatty & Sons.

Wolfe M. F., Schwarzbach S. and Sulaiman R. A. (1998) Effects of mercury on wildlife: A comprehensive review. *Environ. Toxicol. Chem.* **17**, 146–160.

Yamakawa A., Takeuchi A., Shibata Y., Berail S. and Donard O. F. X. (2016) Determination of Hg isotopic compositions in certified reference material NIES No. 13 Human Hair by cold vapor generation multi-collector inductively coupled plasma mass spectrometry. *Accredit. Qual. Assur.*

Yang L. and Sturgeon R. E. (2009) Isotopic fractionation of mercury induced by reduction and ethylation. *Anal. Bioanal. Chem.* **393**, 377–85.

Yin R., Feng X., Chen B., Zhang J., Wang W. and Li X. (2015) Identifying the sources and processes of mercury in subtropical estuarine and ocean sediments using hg isotopic composition. *Environ. Sci. Technol.* **49**, 1347–1355.

Yin Y., Li Y., Tai C., Cai Y. and Jiang G. (2014) Fumigant methyl iodide can methylate inorganic mercury species in natural waters. *Nat. Commun.* **5**, 4633.

Young E. D., Galy A. and Nagahara H. (2002) Kinetic and equilibrium mass-dependant isotope fractionation laws in nature and their geochemical and cosmochemical significance. *Geochim. Cosmochim. Acta* **66**, 1095–1104.

Yuan S., Zhang Y., Chen J., Kang S., Zhang J., Feng X., Cai H., Wang Z., Wang Z. and Huang Q. (2015) Large Variation of Mercury Isotope Composition During a Single Precipitation Event at Lhasa City, Tibetan Plateau, China. *Procedia Earth Planet. Sci.* **13**, 282–286.

Zhang H. and Lindberg S. E. (2001) Sunlight and iron(III)-induced photochemical production of dissolved gaseous mercury in freshwater. *Environ. Sci. Technol.* **35**, 928–935.

Zhang T. and Hsu-Kim H. (2010) Photolytic degradation of methylmercury enhanced by binding to natural organic ligands. *Nat. Geosci.* **3**, 473–476.

Zheng W., Foucher D. and Hintelmann H. (2007) Mercury isotope fractionation during volatilization of Hg(0) from solution into the gas phase. *J. Anal. At. Spectrom.* **22**, 1097. Available at: http://xlink.rsc.org/?DOI=b705677j.

Zheng W. and Hintelmann H. (2010a) Isotope Fractionation of Mercury during Its Photochemical Reduction by Low-Molecular-Weight Organic Compounds. *J. Phys. Chem. A* **114**, 4246–4253.

Zheng W. and Hintelmann H. (2010b) Nuclear field shift effect in isotope fractionation of mercury during abiotic reduction in the absence of light. *J. Phys. Chem. A* **114**, 4238–45.

Zheng W. and Hintelmann H. (2009) Mercury isotope fractionation during photoreduction in natural water is controlled by its Hg/DOC ratio. *Geochim. Cosmochim. Acta* **73**, 6704–6715.

Zheng W., Xie Z. and Bergquist B. A. (2015) Mercury Stable Isotopes in Ornithogenic Deposits As Tracers of Historical Cycling of Mercury in Ross Sea, Antarctica. *Environ Sci Technol*. **49**, 7623-7632

Zhu A., Zhang W., Xu Z., Huang L. and Wang W.-X. (2013) Methylmercury in fish from the South China Sea: geographical distribution and biomagnification. *Mar. Pollut. Bull.* **77**, 437–44.

Annexes

Annexes: Chapter 2. Analytical methods and techniques

Table 2.S1. Comparison of THg concentrations obtained by the developed speciation method (SSE) and AMA-254 analyses in feather samples. N for SSE method is referred to number of extractions (analysed in triplicate). N for AMA-254 is referred to number of analyses.

Sample	THg SSE (ng g $^{-1}$)				THg AMA-254 (ng g $^{-1}$)				Rec (%) as
	Mean	SD	RSD (%)		Mean	SD	RSD (%)		(AMA-254/SSE)*100
F-KP	3899	62	1.6	*(n=3 ext)*	3816	275	7.2	*(n=12)*	98
P-WCP02	724	6	0.8	*(n=3 ext)*	706	33	4.7	*(n=3)*	98
P-FA09	3711	12	0.3	*(n=3 ext)*	3589	155	4.3	*(n=3)*	97

Table 2.S2: Comparison of MeHg concentrations obtained for simultaneous species extraction (SSE) and MeHg selective extraction (MSE) methods by isotope dilution analyses with spike addition before extraction in Certified Reference Materials (NIES-13) and feather samples for the key species studied. N is referred to number of extractions

Sample		***N***	**MeHg (ng·g^{-1})**	**Recovery (%) MSE/SSE*100**
NIES-13	Human hair CRM	***Certified values***	***3800 ± 400***	
		SSE	*3*	3647 ± 46	96 ± 3
		MSE spike after	*3*	3045 ± 142	80 ± 4
		MSE spike before	*3*	3687 ± 233	97 ± 6
F-KP	King penguin feathers	SSE	*3*	2539 ± 39	
		MSE spike after	*3*	1971 ± 9	76 ± 7
		MSE spike before	*3*	2108 ± 260	82 ± 10
P-WCP02	White-chinned petrel feathers	SSE	*1*	579 ± 7	
		MSE spike after		NA	
		MSE spike before	*1*	425 ± 17	73 ± 3
P-FA09	Antarctic prion feathers	SSE	*1*	2966 ± 8	
		MSE spike after	*1*	1883 35	63 ± 1
		MSE spike before	*1*	2472 ± 64	83 ± 2
P-FSN	Pheasant feathers	SSE	*1*	4.3 ± 0.1	
		MSE spike after	*1*	4.3 ± 0.2	100 ± 4
		MSE spike before	*1*	5.3 ± 0.1	123 ± 3

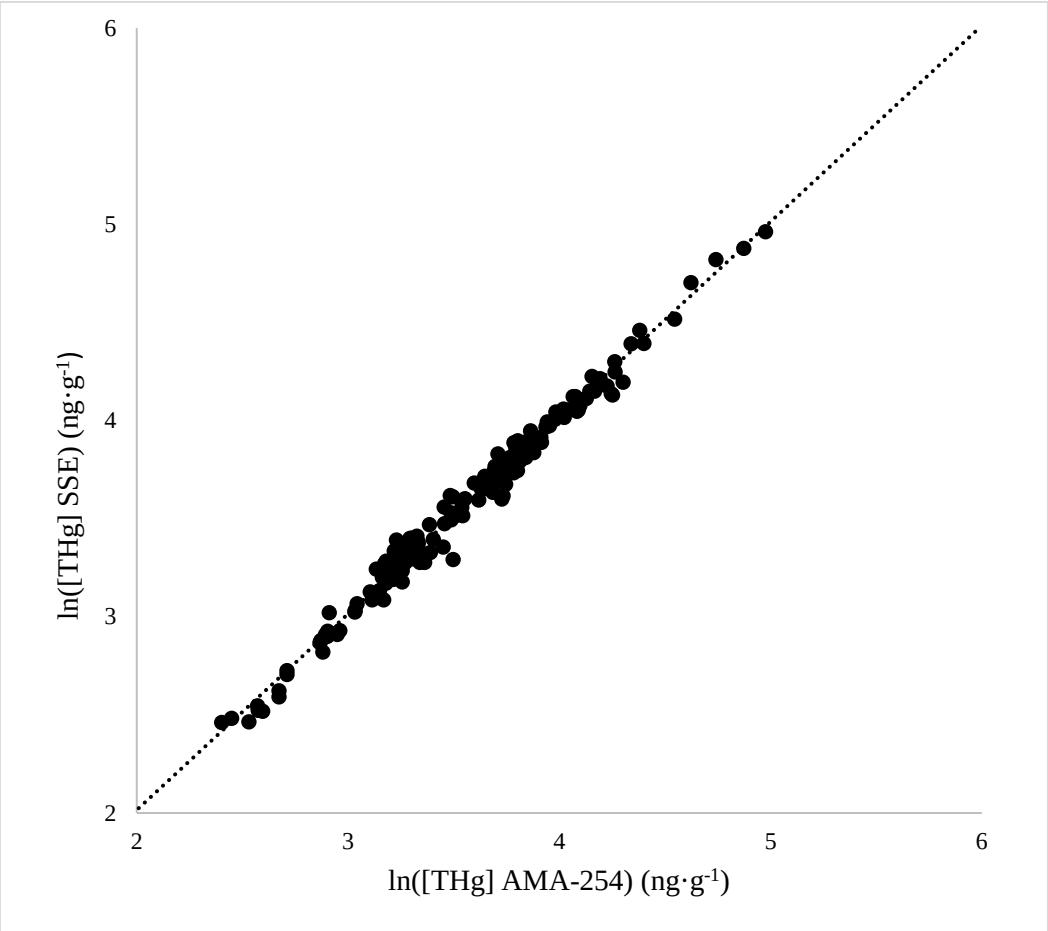

Figure 2.S1. Comparison of THg concentrations (ng·g^{-1}, logarithmic representation) obtained by simultaneous species extraction SSE (MeHg+iHg) and by AMA-254 for all feather samples of the 13 seabird species studied (n=175 individuals).

Annexes: Chapter 3. Methodological approach: Biological aspects

Feathers and blood from seabirds as efficient biomonitoring tissues for Hg isotopic studies: implications of using chicks and adults

Experimental

Hg isotopic composition analyses

Hg isotopic compositions of samples are reported using delta notation according to the following equations:

$$\delta^{xxx}\mathrm{Hg} = [(^{xxx/198}\mathrm{Hg}_{sample} / {}^{xxx/198}\mathrm{Hg}_{\ NIST\ 3133}) - 1)] \cdot 1000\ (‰) \qquad (1)$$

MIF signatures are expressed using capital delta notation, as suggested elsewhere (Bergquist and Blum 2007), according to the following equations:

$$\Delta^{204}\mathrm{Hg} = \delta^{204}\mathrm{Hg} - (1.493 \cdot \delta^{202}\mathrm{Hg}) \qquad (2)$$

$$\Delta^{201}\mathrm{Hg} = \delta^{201}\mathrm{Hg} - (0.752 \cdot \delta^{202}\mathrm{Hg}) \qquad (3)$$

$$\Delta^{200}\mathrm{Hg} = \delta^{200}\mathrm{Hg} - (0.502 \cdot \delta^{202}\mathrm{Hg}) \qquad (4)$$

$$\Delta^{199}\mathrm{Hg} = \delta^{199}\mathrm{Hg} - (0.252 \cdot \delta^{202}\mathrm{Hg}) \qquad (5)$$

Table 3.S1: Mean values of total Hg, MeHg and iHg concentrations and Hg isotopic composition for skua and penguin populations

Species	Location	Date	Tissue	n	MeHg±SD (µg g^{-1})	iHg±SD (µg g^{-1})	THg±SD (µg g^{-1})	δ^{204}Hg±2SD ‰	δ^{202}Hg±2SD ‰	δ^{201}Hg±2SD ‰	δ^{200}Hg±2SD ‰	δ^{199}Hg±2SD ‰	Δ^{204}Hg±2SD ‰	Δ^{201}Hg±2SD ‰	Δ^{200}Hg±2SD ‰	Δ^{199}Hg±2SD ‰
Antarctic skua	Adélie Land	Dec 2011-Jan 2012	Feathers	11	1.82±0.27	0.17±0.08	1.93±0.28	0.10±0.43	0.00±0.36	1.30±0.30	0.00±0.18	1.46±0.15	0.10±0.14	1.30±0.07	-0.00±0.05	1.46±0.07
			Blood	9	0.51±0.09	0.05±0.02	0.53±0.08	0.35±0.17	0.23±0.13	1.45±0.11	0.10±0.08	1.57±0.09	0.01±0.08	1.28±0.08	-0.01±0.03	1.51±0.08
Subantarctic skua	Kerguelen	Dec 2011	Feathers	10	6.49±1.08	0.50±0.19	6.98±1.16	1.77±0.22	1.22±0.19	2.28±0.16	0.65±0.12	1.86±0.16	-0.05±0.18	1.36±0.06	0.03±0.05	1.55±0.12
			Blood	10	2.16±0.33	0.16±0.05	2.32±0.34	1.55±0.11	1.04±0.08	2.16±0.07	0.52±0.05	1.87±0.06	0.00±0.06	1.38±0.05	0.00±0.04	1.61±0.06
Subantarctic skua	Crozet	Jan-Feb 2012	Feathers	11	4.64±1.51	0.27±0.17	4.91±1.62	2.08±0.27	1.35±0.14	2.40±0.16	0.67±0.11	1.98±0.13	0.06±0.08	1.39±0.11	-0.01±0.06	1.63±0.12
			Blood	11	1.70±1.16	0.11±0.08	1.81±1.19	2.06±0.24	1.39±0.18	2.49±0.18	0.72±0.10	2.05±0.13	-0.01±0.08	1.44±0.09	0.02±0.03	1.69±0.11
Subantarctic skua	Amsterdam	Dec 2011	Feathers	10	11.78±2.38	0.58±0.13	12.37±2.44	2.19±0.30	1.50±0.20	2.54±0.18	0.80±0.13	2.08±0.08	-0.06±0.06	1.41±0.06	0.04±0.04	1.70±0.05
			Blood	10	3.78±0.79	0.22±0.18	4.00±0.89	2.31±0.10	1.56±0.08	2.64±0.08	0.81±0.05	2.15±0.06	-0.02±0.08	1.47±0.04	0.03±0.05	1.76±0.05
Adélie penguin	Adélie Land	Feb 2012	Feathers	10	0.35±0.08	0.03±0.02	0.37±0.09	1.01±0.19	0.67±0.13	2.04±0.15	0.32±0.09	1.97±0.14	0.01±0.06	1.53±0.14	-0.02±0.06	1.80±0.14
			Blood	10	0.43±0.11	0.03±0.04	0.47±0.12	0.82±0.29	0.56±0.20	1.75±0.20	0.25±0.12	1.68±0.14	-0.01±0.06	1.33±0.13	-0.03±0.05	1.54±0.11
King penguin	Crozet	Oct 2011	Feathers	11	2.11±0.63	0.18±0.08	2.29±0.70	2.93±0.22	1.94±0.15	3.06±0.17	0.98±0.07	2.31±0.11	0.03±0.07	1.60±0.09	0.00±0.02	1.82±0.09
			Blood	11	1.88±0.28	0.13±0.02	2.01±0.29	2.18±0.17	1.49±0.11	2.50±0.08	0.73±0.06	1.98±0.05	-0.05±0.09	1.38±0.03	-0.02±0.03	1.60±0.04
Gentoo penguin	Crozet	Oct 2011	Feathers	11	3.90±1.69	0.27±0.17	4.33±1.85	2.16±0.15	1.43±0.10	2.37±0.16	0.71±0.04	1.87±0.13	0.02±0.06	1.28±0.11	-0.01±0.04	1.50±0.12
			Blood	11	1.89±0.93	0.14±0.07	2.04±1.00	2.20±0.18	1.45±0.12	2.29±0.12	0.72±0.07	1.77±0.08	0.03±0.03	1.20±0.04	-0.01±0.02	1.41±0.06
Macaroni penguin	Crozet	Jan 2012	Feathers	10	2.05±0.23	0.40±0.15	2.27±0.24	2.98±0.18	2.01±0.15	3.10±0.15	1.00±0.06	2.36±0.11	-0.02±0.09	1.59±0.09	-0.01±0.04	1.86±0.08
			Blood	10	1.01±0.15	0.05±0.02	1.06±0.16	2.49±0.16	1.66±0.11	2.60±0.12	0.83±0.08	1.96±0.07	0.01±0.05	1.35±0.05	0.00±0.04	1.54±0.06
Eastern rockhopper penguin	Crozet	Feb 2012	Feathers	10	1.28±0.21	0.11±0.04	1.39±0.24	3.49±0.19	2.31±0.12	3.56±0.13	1.17±0.10	2.67±0.09	0.04±0.04	1.83±0.10	0.01±0.05	2.09±0.09
			Blood	10	0.93±0.19	0.04±0.02	0.97±0.20	2.89±0.25	1.93±0.18	2.99±0.04	0.98±0.07	2.25±0.12	0.01±0.06	1.54±0.08	0.07±0.07	1.77±0.13
Northern rockhopper penguin	Crozet	Nov 2011	Feathers	10	1.57±0.24	0.12±0.04	1.69±0.24	3.62±0.20	2.42±0.13	3.72±0.11	1.24±0.09	2.83±0.10	0.00±0.05	1.90±0.08	0.02±0.06	2.22±0.10
			Blood	10	1.95±0.43	0.45±0.36	2.40±0.56	3.21±0.25	2.16±0.14	3.17±0.12	1.13±0.10	2.44±0.11	-0.01±0.08	1.55±0.09	0.05±0.06	1.89±0.12

Table 3.S2: Mean values of Hg isotopic composition obtained for reference materials: UM-Almadén, NIES-13 (CRM human hair), IAEA-086 (RM human hair), ERM-CE-464 (CRM tuna fish), F-KP (IRM penguin feathers) and RBC-KP (IRM penguin red blood cells)

Sample	Reference	n	δ^{204}Hg ‰	2SD ‰	δ^{202}Hg ‰	2SD ‰	δ^{201}Hg ‰	2SD ‰	δ^{200}Hg ‰	2SD ‰	δ^{199}Hg ‰	2SD ‰	Δ^{204}Hg ‰	2SD ‰	Δ^{201}Hg ‰	2SD ‰	Δ^{200}Hg ‰	2SD ‰	Δ^{199}Hg ‰	2SD ‰
UM Almadén	This study	77	-0.84	0.22	-0.55	0.16	-0.45	0.13	-0.27	0.15	-0.17	0.12	-0.01	0.16	-0.04	0.09	0.00	0.11	-0.03	0.11
	(Sherman, Blum, Keeler, et al. 2012)	61	-	-	-0.57	0.05	-0.46	0.05	-0.28	0.03	-0.16	0.04	-	-	-0.03	0.02	0.01	0.02	-0.02	0.03
NIES-13	This study	8	2.99	0.22	2.08	0.15	3.07	0.16	1.09	0.10	2.34	0.10	-0.12	0.28	1.51	0.06	0.04	0.04	1.81	0.09
	(Yamakawa et al. 2016)	11	2.76	0.16	1.89	0.10	2.77	0.10	0.98	0.08	2.13	0.07	-0.04	0.11	1.36	0.07	0.04	0.04	1.65	0.06
IAEA-086	This study	6	0.94	0.25	0.73	0.13	0.77	0.09	0.37	0.11	0.44	0.16	-0.14	0.26	0.22	0.08	0.00	0.09	0.26	0.15
	(Yamakawa et al. 2016)	3	0.87	0.12	0.58	0.09	0.64	0.09	0.31	0.04	0.41	0.02	0.00	0.04	0.20	0.03	0.02	0.04	0.26	0.02
ERM-CE-464	This study	2	0.91	0.13	0.64	0.04	2.37	0.03	0.40	0	2.49	0.01	-0.04	0.19	1.89	0.05	0.08	0.01	2.33	0.01
	(Li et al. 2014)	9	0.94	0.06	0.70	0.04	2.49	0.06	0.43	0.05	2.55	0.08	-	-	1.96	0.06	0.07	0.04	2.38	0.07
F-KP	This study	17	2.40	0.25	1.58	0.22	2.67	0.21	0.80	0.16	2.11	0.18	0.04	0.24	1.48	0.13	0.01	0.09	1.71	0.15
RBC-KP	This study	7	1.98	0.18	1.30	0.13	2.26	0.14	0.64	0.13	1.78	0.17	0.04	0.10	1.28	0.09	-0.01	0.09	1.46	0.14

Table 3.S3: Internal reproducibility of Hg isotopic composition obtained for internal reference materials: F-KP (IRM penguin feathers) and RBC-KP (IRM penguin red blood cells) during the performed analytical sessions. N means number of analysis for the same sample extracts, which were prepared under similar procedures for each session

Sample		**Analytical session**		**δ^{204}Hg**	**δ^{202}Hg**	**δ^{201}Hg**	**δ^{200}Hg**	**δ^{199}Hg**	**Δ^{204}Hg**	**Δ^{201}Hg**	**Δ^{200}Hg**	**Δ^{199}Hg**	**n**
King penguin feathers	F-KP	May 2015	Average (‰)	2.30	1.52	2.64	0.77	2.11	0.09	1.50	0.00	1.73	8
			2SD (‰)	0.32	0.22	0.20	0.11	0.08	0.16	0.06	0.06	0.08	
		March 2016	Average (‰)	2.40	1.58	2.68	0.80	2.11	0.04	1.49	0.00	1.71	10
			2SD (‰)	0.24	0.26	0.17	0.15	0.18	0.31	0.12	0.06	0.15	
		July 2016	Average (‰)	2.44	1.60	2.70	0.85	2.15	0.05	1.50	0.04	1.74	5
			2SD (‰)	0.26	0.15	0.16	0.18	0.15	0.11	0.07	0.12	0.12	
King penguin blood	RBC-KP	March 2016	Average (‰)	1.95	1.32	2.28	0.65	1.80	-0.01	1.28	-0.01	1.47	3
			2SD (‰)	0.10	0.10	0.04	0.03	0.04	0.15	0.11	0.03	0.02	
		April 2016	Average (‰)	1.60	0.99	2.08	0.52	1.84	0.12	1.34	0.02	1.59	3
			2SD (‰)	0.37	0.20	0.29	0.36	0.08	0.15	0.14	0.25	0.05	
		July 2016	Average (‰)	1.99	1.30	2.26	0.62	1.77	0.05	1.28	-0.03	1.44	5
			2SD (‰)	0.15	0.10	0.12	0.11	0.16	0.10	0.10	0.07	0.15	

Total Hg and Hg species concentrations

Pronounced differences in total Hg concentrations were found between sites for both skua and penguin populations. However, no variation in Hg species distribution was observed between tissues, individuals, species or sites. Both feathers and blood presented a majority of MeHg for all the individuals (skuas and penguins) independently of Hg concentration. Percentages of MeHg mean values for feathers and blood of the four skua populations were 94±2% and 94±3%, respectively. Overall penguins' individuals presented a mean percentage of MeHg of 92±2% and 92±7% respectively for feathers and blood samples. Skua chick feathers displayed higher MeHg concentrations (µg/g dry mass) compared to blood samples for all the analysed individuals (3 times higher, on average for the four populations). In the case of penguins, similar concentrations were obtained in both tissues for some penguin species (Adélie, king and both eastern and northern rockhopper penguins), whereas feathers presented higher MeHg levels than blood in all the individuals of gentoo and macaroni penguins (2 times higher on average for the two populations). As a general trend, blood and feathers MeHg concentrations were highly correlated for skuas (Pearson correlation, R^2=0.89, p<0.0001, n=40) and penguin individuals (Pearson correlation, R^2=0.74, p<0.0001, n=72), as shown in Figure 3.S1.

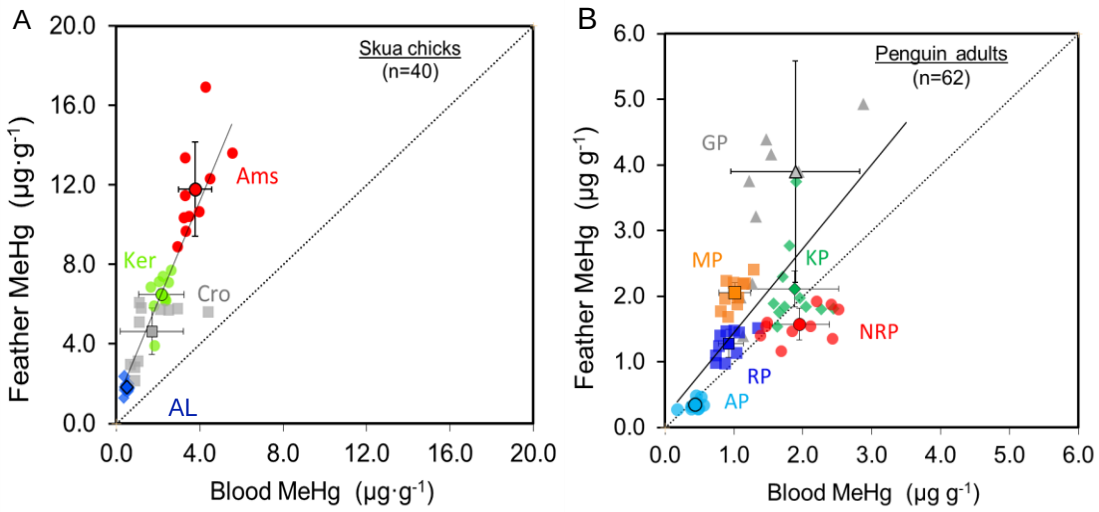

Figure 3.S1. A) Feather versus blood (red blood cells) MeHg concentrations in skua chicks. B) Feather versus blood (red blood cells) MeHg concentrations in adult penguins (individual values and mean population values). Abbreviations for the different populations are AP (Adélie penguin), GP (gentoo penguin), KP (king penguin), MP (macaroni penguin), RP (eastern rockhopper penguin) and NRP (northern rockhopper penguin).

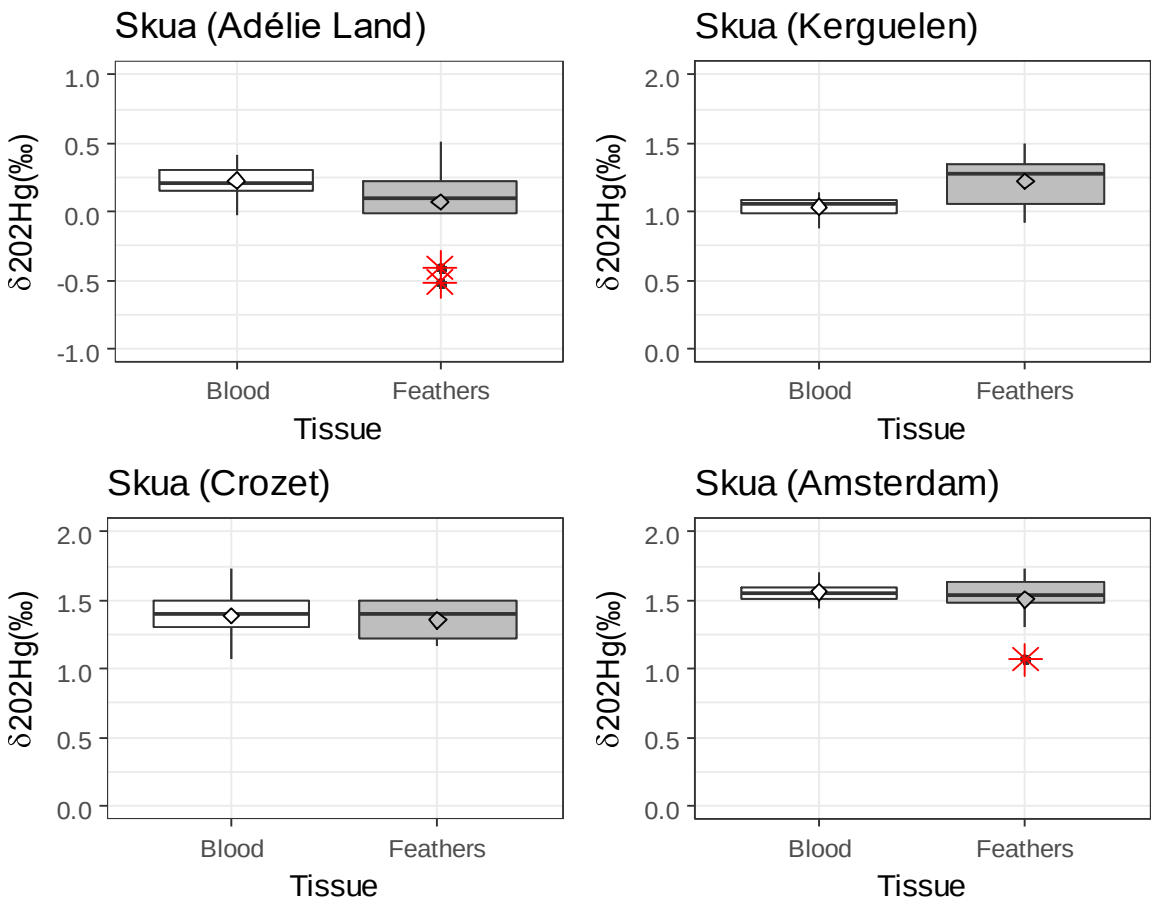

Figure 3.S2. Blood and feathers δ^{202}Hg values for the four populations of skua chicks. Diamonds indicate mean values. Black lines indicate median values. Red asterisks indicate outliers.

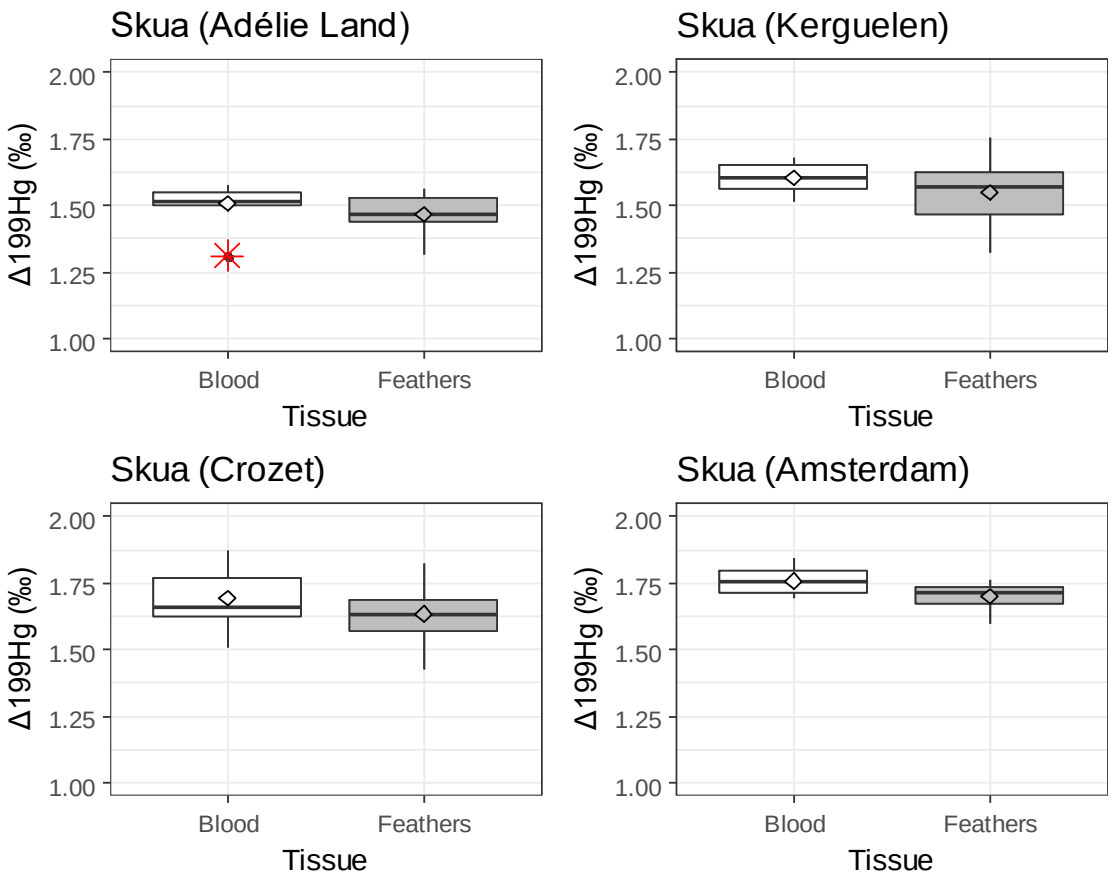

Figure 3.S3. Blood and feathers $\Delta^{199}Hg$ values for the four populations of skua chicks. Diamonds indicate mean values. Black lines indicate median values. Red asterisk indicates outlier.

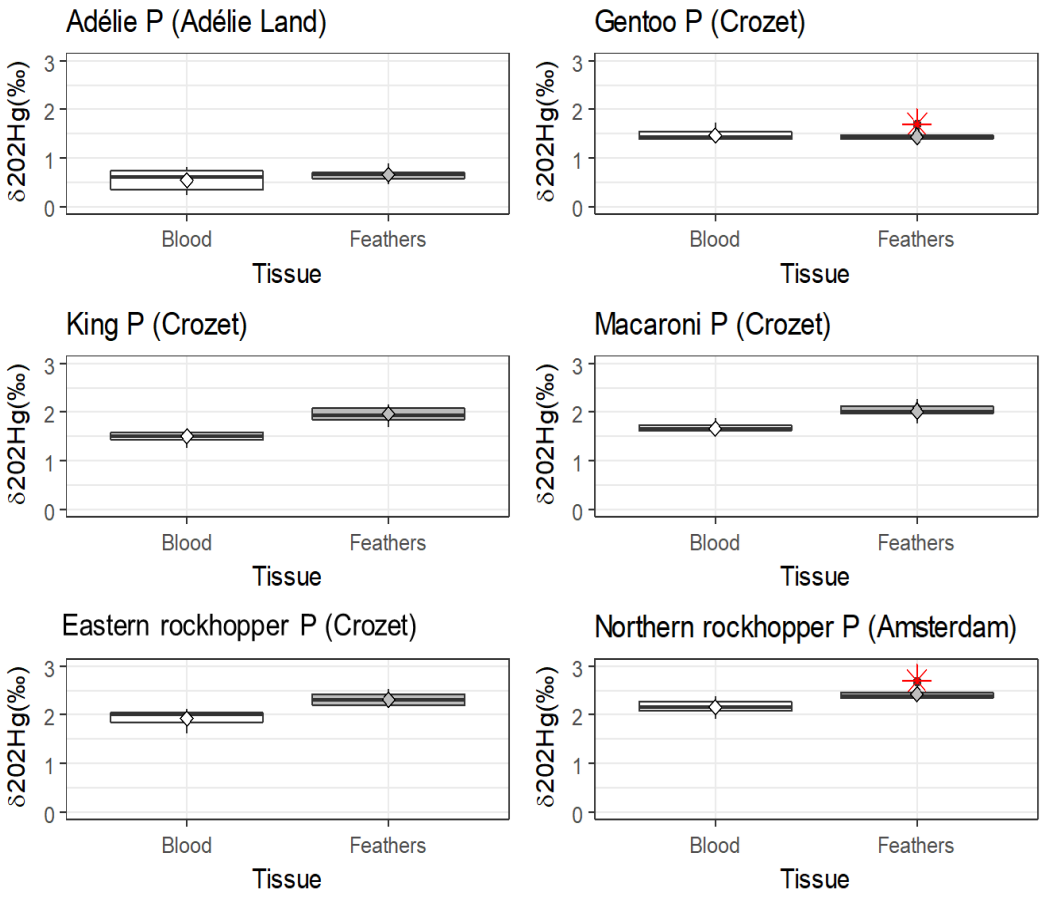

Figure 3.S4. Blood and feathers δ^{202}Hg values for the six populations of penguin adults. Diamonds indicate mean values. Black lines indicate median values. Red asterisks indicate outliers.

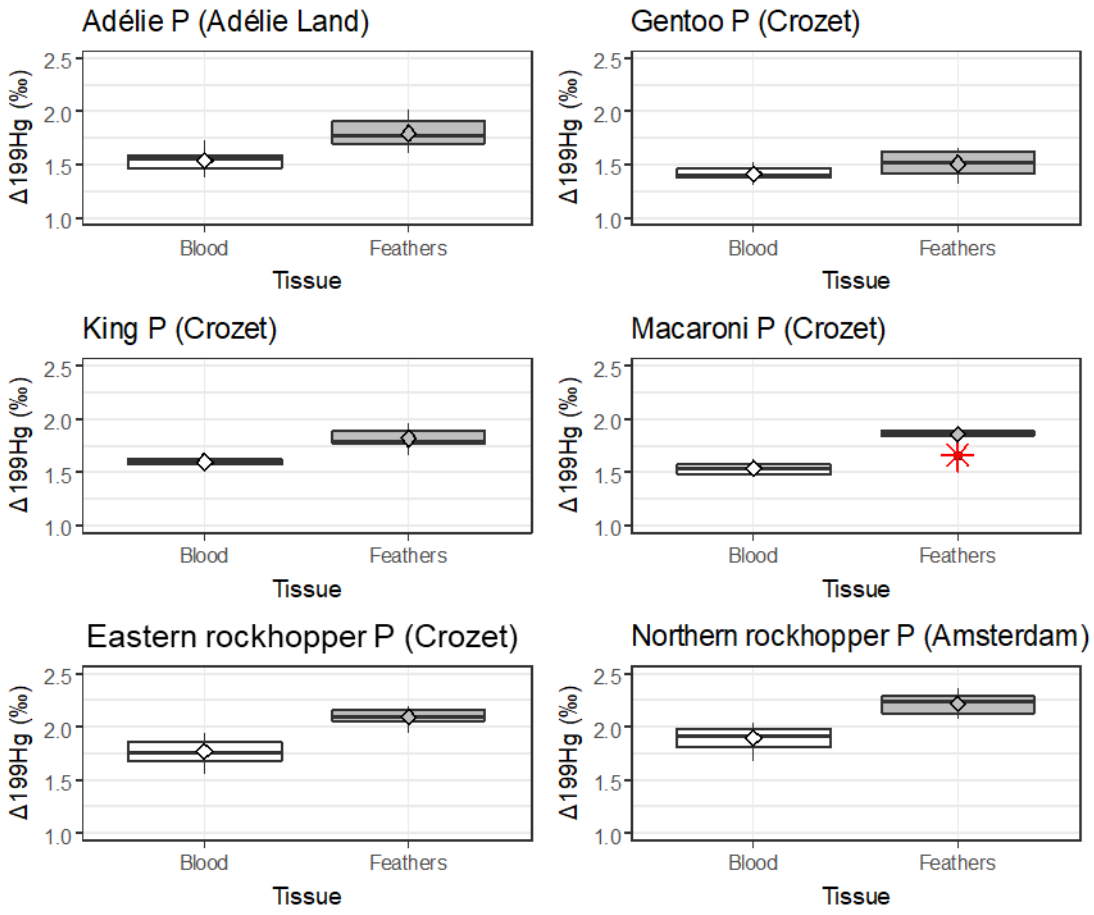

Figure 3.S5. Blood and feathers Δ^{199}Hg values for the six populations of penguin adults. Diamonds indicate mean values. Black lines indicate median values. Red asterisk indicates outliers.

Hg isotopic composition of key tissues documents Hg metabolic processes in seabirds

Hg concentrations and speciation of the three individuals of giant petrels at the individual level: influence of age

Increasing Hg concentrations were observed with age (Table 3.S8), with the oldest specimen displaying much higher Hg amounts compared to medium age adult and to the youngest one for both kidneys (50.8±0.7, 39.9±0.4 and 27.5±0.4 $\mu g \cdot g^{-1}$; respectively) and livers (405.2±6.6 and 214.2±34.2 $\mu g \cdot g^{-1}$; respectively for the oldest and youngest individual). Indeed, Hg concentrations obtained in these two organs from the oldest bird were almost twice higher comparing to the youngest one. Hg species distributions were characterized by a great predominance of iHg with livers presenting percentages of 98% (young) and 95% (old). Although kidneys also present a higher extent of iHg, its proportion was more variable between individuals with the younger birds displaying much higher fraction of iHg (more than 90%) than the old individual, whose iHg composition only achieved 66 %. Feathers also displayed increasing Hg levels with age, ranging from 8.5±0.1 through 10.3±0.1 and 21.2±0.1 $\mu g \cdot g^{-1}$, respectively for the youngest, medium age and oldest individuals. Hg concentrations in muscle were not correlated with age, since the youngest individual exhibited higher Hg content (4.1±0.1 $\mu g \cdot g^{-1}$) than the medium age giant petrel (1.7±0.1 $\mu g \cdot g^{-1}$). This could possibly be a result of more efficient remobilisation from muscle to moulting feathers for excretion of Hg in mature adults and feathers tended to accumulate mainly MeHg, Moreover, the two younger petrels presented an almost equal composition of both Hg compounds (52 and 58% of MeHg, respectively) however, the old one displayed a higher percentage of iHg (63%) which was surprising since muscles are generally considered MeHg storage organs. Blood Hg concentrations of the two younger petrels were very similar (2.97±0.01 and 3.03±0.05 $\mu g \cdot g^{-1}$), whereas the oldest presented 8 times higher blood Hg concentrations (23.9±0.1 $\mu g \cdot g^{-1}$), Much lower Hg amounts were also found in brain for the two youngest (2.8±0.2 and 1.6±0.1 $\mu g \cdot g^{-1}$) compared to the oldest individual (13.2±0.2 $\mu g \cdot g^{-1}$), however brain Hg speciation differed widely between individuals, present a similar trend for the youngest and oldest birds (around 40% of MeHg), whereas medium age individual presented much higher extent of MeHg (73%).

Table 3.S4. Mean values of Hg speciation obtained for reference materials: DOLT-4 (CRM dogfish liver), ERM-CE-464 (CRM tuna fish) and NIES-13 (CRM human hair). N means number of extractions.

Sample	**Reference**	**n**	**iHg (ng·g^{-1})**	**MeHg (ng·g^{-1})**	**Recovery MeHg**	**THg (ng·g^{-1})**	**Recovery THg**
			Mean±SD	Mean±SD	(%)	Mean±SD	(%)
DOLT-4	Certified values			1330±120		2580±220	
	Obtained values	3	1342±77	1228±60	92.4±4.5	2570±97	99.6±3.8
ERM-CE-464	Certified values			5117±158		5240±100	
	Obtained values	3	266±24	4964±44	97.0±0.9	5231±51	99.8±1.0
NIES-13	Certified values			3800±400		4420±200	
	Obtained values	3	792±78	3579±68	94.2±1.8	4319±71	97.7±1.5

Table 3.S5. Mean values of Hg isotopic composition obtained for reference materials: UM-Almadén (CRM cinnabar), DOLT-4 (CRM dogfish liver), ERM-CE-464 (CRM tuna fish), NIES-13 (CRM human hair), IAEA-086 (RM human hair), P-KP (IRM penguin feathers) and RBC-KP (IRM penguin red blood cells).

Sample	Reference	n	δ^{204}Hg ‰	2SD ‰	δ^{202}Hg ‰	2SD ‰	δ^{201}Hg ‰	2SD ‰	δ^{200}Hg ‰	2SD ‰	δ^{199}Hg ‰	2SD ‰	Δ^{204}Hg ‰	2SD ‰	Δ^{201}Hg ‰	2SD ‰	Δ^{200}Hg ‰	2SD ‰	Δ^{199}Hg ‰	2SD ‰
UM Almadén	This study	45	-0.81	0.25	-0.54	0.17	-0.44	0.14	-0.26	0.13	-0.17	0.10	-0.01	0.15	-0.04	0.07	0.01	0.08	-0.03	0.09
	(Sherman, Blum, Keeler, et al. 2012)	61	-	-	-0.57	0.05	-0.46	0.05	-0.28	0.03	-0.16	0.04	-	-	-0.03	0.02	0.01	0.02	-0.02	0.03
DOLT-4	This study	2	-0.50	0.08	-0.33	0.07	0.66	0.03	-0.13	0.10	1.01	0.04	-0.01	0.02	0.91	0.02	0.04	0.06	1.09	0.02
	(Masbou 2014)	4	-		-0.35	0.20	0.71	0.06	-0.14	0.06	1.03	0.07	-	-	0.98	0.19	0.02	0.03	1.12	0.11
ERM-CE-464	This study	2	0.91	0.13	0.64	0.04	2.37	0.03	0.40	0.00	2.49	0.01	-0.04	0.19	1.89	0.05	0.08	0.01	2.33	0.01
	(Li et al. 2014)	9	0.94	0.06	0.70	0.04	2.49	0.06	0.43	0.05	2.55	0.08	-	-	1.96	0.06	0.07	0.04	2.38	0.07
NIES-13	This study	1	2.98	-	2.07	-	3.07	-	1.10	-	2.29	-	-0.11	-	1.51	-	0.06	-	1.76	-
	(Yamakawa et al. 2016)	11	2.76	0.16	1.89	0.10	2.77	0.10	0.98	0.08	2.13	0.07	-0.04	0.11	1.36	0.07	0.04	0.04	1.65	0.06
IAEA-086	This study	1	1.23	-	0.81	-	0.76	-	0.45	-	0.50	-	0.02	-	0.15	-	0.04	-	0.29	-
	(Yamakawa et al. 2016)	3	0.87	0.12	0.58	0.09	0.64	0.09	0.31	0.04	0.41	0.02	0.00	0.04	0.20	0.03	0.02	0.04	0.26	0.02
F-KP	This study	3	2.35	0.15	1.52	0.12	2.65	0.06	0.76	0.07	2.12	0.04	0.09	0.16	1.51	0.07	0.00	0.07	1.74	0.05
RBC-KP	This study	3	1.95	0.10	1.32	0.10	2.28	0.04	0.65	0.03	1.80	0.04	-0.01	0.15	1.28	0.11	-0.01	0.03	1.47	0.02

Table 3.S6. Individual and mean values of MeHg, iHg and THg concentrations (Mean ±1SD, µg g^{-1} dw) and Hg isotopic composition ($\delta^{202}Hg$ and $\Delta^{199}Hg$, Mean ± 2SD, ‰) of tissues Antarctic prions (n=10) from Kerguelen Islands.

Sample	Tissue	MeHg	iHg	THg	$\delta^{204}Hg$	$\delta^{202}Hg$	$\delta^{201}Hg$	$\delta^{200}Hg$	$\delta^{199}Hg$	$\Delta^{204}Hg$	$\Delta^{201}Hg$	$\Delta^{200}Hg$	$\Delta^{199}Hg$
		µg g^{-1}	µg g^{-1}	µg g^{-1}	‰	‰	‰	‰	‰	‰	‰	‰	‰
FA01-LivA	Liver	1.94±0.22	1.00±0.09	2.94±0.29	NA	NA	NA	NA	NA	NA	NA	NA	NA
FA02-LivA	Liver	1.32±0.05	0.59±0.01	1.89±0.02	NA	NA	NA	NA	NA	NA	NA	NA	NA
FA03-LivA	Liver	1.22±0.04	0.66±0.01	1.87±0.05	NA	NA	NA	NA	NA	NA	NA	NA	NA
FA04-LivA	Liver	0.95±0.04	0.56±0.01	1.50±0.05	NA	NA	NA	NA	NA	NA	NA	NA	NA
FA05-LivA	Liver	1.95±0.14	0.73±0.11	2.68±0.25	NA	NA	NA	NA	NA	NA	NA	NA	NA
FA06-LivA	Liver	0.89±0.16	0.60±0.04	1.49±0.14	-0.45	-0.28	1.55	-0.20	-0.03	1.83	1.76	-0.06	1.90
FA07-LivA	Liver	1.13±0.02	0.47±0.14	1.60±0.11	0.51	0.30	1.90	0.21	0.06	1.99	1.68	0.06	1.91
FA08-LivA	Liver	1.25±0.12	1.04±0.14	2.30±0.26	-0.19	-0.10	1.56	-0.03	-0.05	1.95	1.63	0.02	1.98
FA09-LivA	Liver	1.65±0.23	0.87±0.11	2.52±0.24	-0.15	-0.09	1.50	-0.11	-0.02	1.82	1.57	-0.06	1.84
FA10-LivA	Liver	1.55±0.17	0.55±0.11	2.10±0.20	0.35	0.24	1.82	0.04	0.00	1.95	1.64	-0.08	1.89
Average	Liver	1.38±0.38	0.71±0.20	2.09±0.51	0.02±0.40	0.01±0.25	1.66±0.18	-0.02±0.16	-0.00±0.04	1.91±0.08	1.65±0.07	-0.02±0.06	1.90±0.05
FA01-MusA	Muscle	0.24±0.02	0.027±0.0003	0.28±0.02	0.47	0.15	1.92	0.13	0.26	2.13	1.81	0.06	2.09
FA02-MusA	Muscle	0.25±0.01	0.028±0.002	0.29±0.01	0.07	-0.10	1.65	-0.03	0.21	1.94	1.72	0.02	1.97
FA03-MusA	Muscle	0.18±0.00	0.077±0.004	0.26±0.01	-0.02	0.00	1.77	0.00	-0.01	2.16	1.78	0.00	2.16
FA04-MusA	Muscle	0.20±0.01	0.031±0.001	0.23±0.01	0.99	0.57	2.02	0.22	0.15	2.04	1.60	-0.07	1.90
FA05-MusA	Muscle	0.35±0.01	0.08±0.01	0.43±0.01	1.13	0.70	2.10	0.34	0.08	2.00	1.58	-0.01	1.82
FA06-MusA	Muscle	0.20±0.01	0.033±0.002	0.24±0.01	1.09	0.79	2.38	0.43	-0.08	2.30	1.79	0.04	2.10
FA07-MusA	Muscle	0.22±0.01	0.046±0.008	0.27±0.01	1.12	0.77	2.16	0.37	-0.02	1.98	1.58	-0.01	1.79
FA08-MusA	Muscle	0.27±0.01	0.042±0.003	0.31±0.01	1.34	0.89	2.32	0.44	0.02	2.06	1.65	0.00	1.83
FA09-MusA	Muscle	0.29±0.01	0.041±0.001	0.33±0.01	-0.18	-0.19	1.46	-0.13	0.10	1.73	1.60	-0.04	1.77
FA10-MusA	Muscle	0.32±0.01	0.068±0.003	0.386±0.004	0.25	0.12	1.73	0.01	0.06	1.92	1.63	-0.05	1.89
Average	Muscle	0.25±0.05	0.05±0.02	0.30±0.06	0.63±0.57	0.37±0.41	1.95±0.30	0.18±0.21	0.08±0.11	2.03±0.16	1.67±0.09	-0.01±0.04	1.93±0.14
FA01-pool-B1	Feather	1.98±0.01	0.287±0.002	2.27±0.02	1.81	1.19	2.97	0.61	2.71	0.03	2.08	0.02	2.41

FA02-pool-B1	Feather	1.91±0.05	0.15±0.01	2.06±0.05	2.27	1.55	3.22	0.77	2.77	-0.04	2.05	-0.01	2.38
FA03-pool-B1	Feather	3.09±0.04	0.185±0.005	3.28±0.04	1.76	1.22	2.89	0.64	2.57	-0.07	1.97	0.03	2.26
FA04-pool-B1	Feather	1.77±0.04	0.09±0.01	1.86±0.05	2.08	1.41	3.09	0.75	2.70	-0.02	2.03	0.04	2.34
FA05-pool-B1	Feather	1.94±0.03	0.11±0.01	2.05±0.03	1.89	1.21	2.81	0.66	2.52	0.09	1.91	0.05	2.21
FA06-pool-B1	Feather	1.84±0.03	0.11±0.01	1.96±0.03	2.22	1.51	3.33	0.80	2.90	-0.04	2.19	0.04	2.52
FA07-pool-B1	Feather	3.24±0.09	0.149±0.002	3.39±0.09	1.94	1.31	2.99	0.69	2.65	-0.01	2.00	0.04	2.32
FA08-pool-B1	Feather	1.16±0.03	0.06±0.01	1.22±0.03	1.92	1.24	3.07	0.66	2.81	0.08	2.14	0.04	2.50
FA09-pool-B1	Feather	3.84±0.05	0.14±0.01	3.98±0.06	1.98	1.27	3.11	0.62	2.78	0.09	2.16	-0.01	2.46
FA10-pool-B1	Feather	3.38±0.05	0.233±0.005	3.61±0.05	2.08	1.29	2.97	0.67	2.63	0.15	2.00	0.02	2.30
Average	Feather	2.42±0.89	0.15±0.07	2.57±0.92	2.00±0.17	1.32±0.13	3.04±0.15	0..69±0.06	2.70±0.12	0.02±0.07	2.05±0.09	0.02±0.02	2.37±0.10

Table 3.S7. Individual and mean values of MeHg, iHg and THg concentrations (Mean ±1SD, µg g^{-1} dw) and Hg isotopic composition ($\delta^{202}Hg$ and $\Delta^{199}Hg$, Mean ± 2SD, ‰) of tissues white-chinned petrels (n=10) from Kerguelen Islands.

Species	Tissue	MeHg	iHg	THg	$\delta^{204}Hg$	$\delta^{202}Hg$	$\delta^{201}Hg$	$\delta^{200}Hg$	$\delta^{199}Hg$	$\Delta^{204}Hg$	$\Delta^{201}Hg$	$\Delta^{200}Hg$	$\Delta^{199}Hg$
		µg g^{-1}	µg g^{-1}	µg g^{-1}	‰	‰	‰	‰	‰	‰	‰	‰	‰
WCP01-LivA	Liver	1.92±0.05	57.90±0.71	59.82±0.71	-1.34	-0.91	0.36	-0.45	1.00	0.03	1.05	0.01	1.23
WCP02-LivA	Liver	1.73±0.06	79.27±0.64	81.00±0.64	-1.13	-0.80	0.32	-0.43	0.92	0.07	0.92	-0.02	1.13
WCP03-LivA	Liver	5.54±0.04	69.36±0.68	74.90±0.68	-1.21	-0.80	0.42	-0.40	0.96	-0.01	1.02	0.00	1.16
WCP04-LivA	Liver	4.36±0.09	33.96±0.70	38.32±0.71	-0.20	-0.11	1.03	-0.10	1.16	-0.03	1.11	-0.04	1.19
WCP05-LivA	Liver	4.60±0.06	41.34±0.45	45.95±0.46	-0.65	-0.45	0.71	-0.27	1.05	0.02	1.05	-0.04	1.16
WCP06-LivA	Liver	7.95±0.20	69.30±0.27	77.26±0.33	-1.50	-0.99	0.17	-0.54	0.80	-0.02	0.91	-0.04	1.05
WCP07-LivA	Liver	4.97±0.05	27.98±0.54	32.94±0.54	-1.08	-0.76	0.51	-0.38	1.03	0.05	1.08	0.00	1.22
WCP08-LivA	Liver	8.15±0.06	49.46±0.24	57.62±0.25	-0.99	-0.68	0.47	-0.35	0.98	0.02	0.98	-0.01	1.15
WCP09-LivA	Liver	4.55±0.10	40.29±0.29	44.83±0.31	-0.83	-0.54	0.68	-0.26	1.09	-0.02	1.08	0.01	1.23
WCP10-LivA	Liver	5.01±0.03	25.64±0.18	30.65±0.18	-0.57	-0.35	0.79	-0.25	1.08	-0.05	1.05	-0.07	1.17
Average	Liver	4.88±2.10	49.45±18.76	54.33±18.67	-0.95±0.39	-0.64±0.27	0.54±0.26	-0.34±0.13	1.01±0.10	0.01±0.04	1.03±0.07	-0.02±0.03	1.17±0.05
WCP01-MusA	Muscle	1.67±0.13	0.60±0.02	2.27±0.13	-0.19	-0.17	0.90	-0.12	1.06	0.07	1.03	-0.04	1.10
WCP02-MusA	Muscle	1.33±0.01	0.90±0.04	2.23±0.04	-0.08	-0.14	1.08	-0.09	1.30	0.13	1.18	-0.02	1.33
WCP03-MusA	Muscle	4.27±0.02	1.07±0.03	5.34±0.03	0.83	0.60	1.60	0.33	1.52	-0.07	1.15	0.03	1.37
WCP04-MusA	Muscle	3.37±0.13	0.79±0.06	4.17±0.14	0.55	0.33	1.42	0.19	1.45	0.05	1.17	0.02	1.37
WCP05-MusA	Muscle	4.15±0.06	1.06±0.02	5.21±0.06	0.59	0.41	1.39	0.29	1.42	-0.02	1.08	0.09	1.32
WCP06-MusA	Muscle	4.75±0.11	0.82±0.04	5.57±0.12	0.58	0.40	1.37	0.17	1.29	-0.01	1.07	-0.03	1.19
WCP07-MusA	Muscle	4.07±0.09	1.01±0.03	5.08±0.10	0.69	0.48	1.54	0.20	1.46	-0.03	1.18	-0.04	1.34
WCP08-MusA	Muscle	6.15±0.06	1.66±0.04	7.81±0.07	0.38	0.21	1.22	0.10	1.31	0.06	1.06	-0.01	1.26
WCP09-MusA	Muscle	3.60±0.02	0.87±0.06	4.46±0.06	0.64	0.44	1.47	0.20	1.46	-0.02	1.13	-0.02	1.35
WCP10-MusA	Muscle	3.70±0.11	1.11±0.07	4.81±0.13	0.56	0.41	1.42	0.20	1.39	-0.05	1.11	-0.01	1.29
Average	Muscle	3.71±1.82	0.99±0.34	4.69±1.78	0.45±0.37	0.30±0.28	1.34±0.21	0.15±0.16	1.37±0.12	0.01±0.06	1.12±0.05	0.00±0.04	1.29±0.07
WCP01-pool-B1	Feathers	8.23±0.06	0.28±0.01	8.51±0.04	1.41	0.95	1.86	0.52	1.69	-0.01	1.14	0.05	1.45

WCP02-pool-B1	Feathers	3.45±0.02	0.17±0.01	3.62±0.02	1.92	1.27	2.15	0.69	1.80	0.03	1.19	0.05	1.48
WCP03-pool-B1	Feathers	4.13±0.04	0.017±0.001	4.15±0.04	1.77	1.22	2.10	0.64	1.75	-0.05	1.19	0.02	1.44
WCP04-pool-B1	Feathers	3.95±0.03	0.21±0.01	4.17±0.03	1.56	1.08	2.01	0.58	1.72	-0.05	1.20	0.04	1.45
WCP05-pool-B1	Feathers	2.77±0.02	0.24±0.02	3.01±0.03	1.30	0.91	1.97	0.48	1.86	-0.06	1.29	0.02	1.63
WCP06-pool-B1	Feathers	3.94±0.02	0.19±0.01	4.13±0.02	1.53	1.03	1.85	0.55	1.52	-0.02	1.07	0.03	1.26
WCP07-pool-B1	Feathers	8.07±0.25	0.47±0.01	8.54±0.26	1.56	1.03	2.01	0.60	1.81	0.03	1.24	0.09	1.55
WCP08-pool-B1	Feathers	6.21±0.02	0.26±0.02	6.48±0.02	1.50	1.04	1.81	0.67	1.70	-0.05	1.03	0.14	1.44
WCP09-pool-B1	Feathers	7.33±0.13	0.37±0.03	7.70±0.16	1.80	1.20	2.11	0.73	2.01	0.01	1.21	0.13	1.71
WCP10-pool-B1	Feathers	3.37±0.06	0.17±0.01	3.54±0.06	1.98	1.31	2.25	0.66	1.79	0.02	1.26	0.00	1.46
Average	Feathers	5.15±2.10	0.24±0.12	5.39±2.19	1.63±0.22	1.10±0.14	2.01±0.14	0.61±0.08	1.77±0.13	-0.01±0.03	1.18±0.08	0.06±0.05	1.49±0.21

Table 3.S8. Individual and mean values of MeHg, iHg and THg concentrations (Mean ±1SD, µg g^{-1} dw), MeHg proportion (Mean ±1SD, %) and Hg isotopic composition (δ^{202}Hg and Δ^{199}Hg, Mean ± 2SD, ‰) of tissues of southern giant petrels (n=3) from Kerguelen Islands. PGA01 is the young specimen, PGA02 a medium age individual and PGA03 the oldest individual.

Sample	Tissue	MeHg		iHg	THg	δ^{204}Hg	δ^{202}Hg	δ^{201}Hg	δ^{200}Hg	δ^{199}Hg	Δ^{204}Hg	Δ^{201}Hg	Δ^{200}Hg	Δ^{199}Hg
		µg g^{-1}	%	µg g^{-1}	µg g^{-1}	‰	‰	‰	‰	‰	‰	‰	‰	‰
PGA01-LivA	Liver	5.09±0.80	2.21±0.21	209.14±34.22	214.22±34.23	-0.44	-0.28	0.98	-0.14	1.27	-0.02	1.19	0.00	1.34
PGA03-LivA	Liver	23.50±0.10	5.80±0.11	381.69±6.56	405.19±6.57	1.06	0.68	1.64	0.32	1.40	0.05	1.13	-0.02	1.23
Average	Liver	14.29±13.02	3.89±2.15	295.41±122.01	309.71±135.03	0.31±1.06	0.20±0.68	1.31±0.47	0.09±0.33	1.34±0.09	0.01±0.05	1.16±0.04	-0.01±0.01	1.29±0.08
PGA01-KidA	Kidney	2.73±0.12	9.93±0.45	24.80±0.41	27.53±0.43	-0.48	-0.35	0.87	-0.21	1.21	0.04	1.13	-0.03	1.30
PGA02-KidA	Kidney	1.64±0.11	4.13±0.30	38.23±0.43	39.88±0.44	-1.63	-0.93	0.40	-0.44	1.13	-0.24	1.10	0.03	1.36
PGA03-KidA	Kidney	17.24±0.53	33.90±0.50	33.60±0.40	50.84±0.67	0.77	0.60	1.63	0.28	1.61	-0.12	1.18	-0.03	1.46
Average	Kidney	7.21±8.71	15.99±15.79	32.21±6.83	39.42±11.66	-0.44±1.20	-0.22±0.77	0.97±0.62	-0.12±0.36	1.14±0.04	0.11±0.14	1.14±0.04	-0.01±0.03	1.37±0.08
PGA01-PGAt	Blood	2.66±0.01	89.01±0.31	0.31±0.01	2.97±0.01	3.25	2.13	2.86	1.06	2.06	0.08	1.26	0.00	1.52
PGA02-PGAt	Blood	2.59±0.05	84.72±0.24	0.431±0.003	3.03±0.05	2.41	1.61	2.33	0.79	1.74	0.00	1.12	-0.02	1.34
PGA03-PGAt	Blood	22.89±0.12	95.52±0.12	1.04±0.03	23.93±0.13	3.43	2.30	3.05	1.14	2.15	-0.01	1.32	-0.01	1.57
Average	Blood	9.38±11.70	90.34±5.00	0.59±0.39	9.98±12.08	3.03±0.55	2.01±0.36	2.74±0.37	1.00±0.18	1.98±0.21	0.03±0.05	1.23±0.10	-0.01±0.01	1.48±0.12
PGA01-MusA	Muscle	2.09±0.01	53.15±2.12	2.03±0.14	4.11±0.14	0.49	0.38	1.54	0.17	1.50	-0.08	1.26	-0.02	1.41

PGA02-MusA	Muscle	0.97±0.10	58.23±3.45	0.69±0.02	1.66±0.10	0.53	0.43	1.51	0.18	1.51	-0.12	1.19	-0.03	1.40
PGA03-MusA	Muscle	10.71±0.24	36.72±0.66	18.46±0.21	29.18±0.32	0.93	0.55	1.52	0.20	1.42	0.11	1.10	-0.07	1.28
Average	Muscle	4.59±5.33	48.82±11.01	7.06±9.90	11.65±15.23	0.65±0.25	0.45±0.09	1.52±0.02	0.18±0.02	1.48±0.05	-0.03±0.12	1.19±0.08	-0.04±0.03	1.37±0.07
PGA01-pool-B1	Feathers	8.32±0.11	96.91±0.16	0.21±0.01	8.50±0.11	3.46	2.31	2.90	1.19	1.93	0.01	1.16	0.03	1.34
PGA02-pool-B1	Feathers	9.99±0.15	96.58±0.29	0.29±0.02	10.30±0.13	3.53	2.32	2.83	1.18	1.83	0.07	1.09	0.01	1.24
PGA03-pool-B1	Feathers	20.66±0.06	96.82±0.13	0.55±0.02	21.20±0.05	3.51	2.35	2.89	1.19	1.90	0.00	1.12	0.01	1.31
Average	Feathers	12.99±6.70	97.38±0.14	0.35±0.18	13.34±6.87	3.50±0.04	2.33±0.02	2.87±0.04	1.19±0.01	1.89±0.05	0.03±0.04	1.12±0.04	0.02±0.01	1.30±0.05
PGA01-brain-B1	Brain	1.14±0.06	40.14±2.78	1.70±0.16	2.84±0.17	1.47	0.95	1.91	0.49	1.66	0.05	1.20	0.01	1.42
PGA02-brain-B1	Brain	1.16±0.01	73.56±0.68	0.42±0.01	1.58±0.02	2.60	1.77	2.43873831	0.84	1.79	-0.05	1.10	-0.05	1.34
PGA03-brain-B1	Brain	4.44±0.10	33.54±0.95	8.79±0.20	13.23±0.22	0.15	0.10	1.35	0.02	1.43	0.01	1.28	-0.02	1.41
Average	Brain	2.25±1.90	49.08±21.45	3.64±4.51	5.88±6.39	1.41±1.22	0.94±0.84	1.90±0.54	0.45±0.41	1.62±0.18	0.00±0.05	1.19±0.09	-0.02±0.03	1.39±0.04

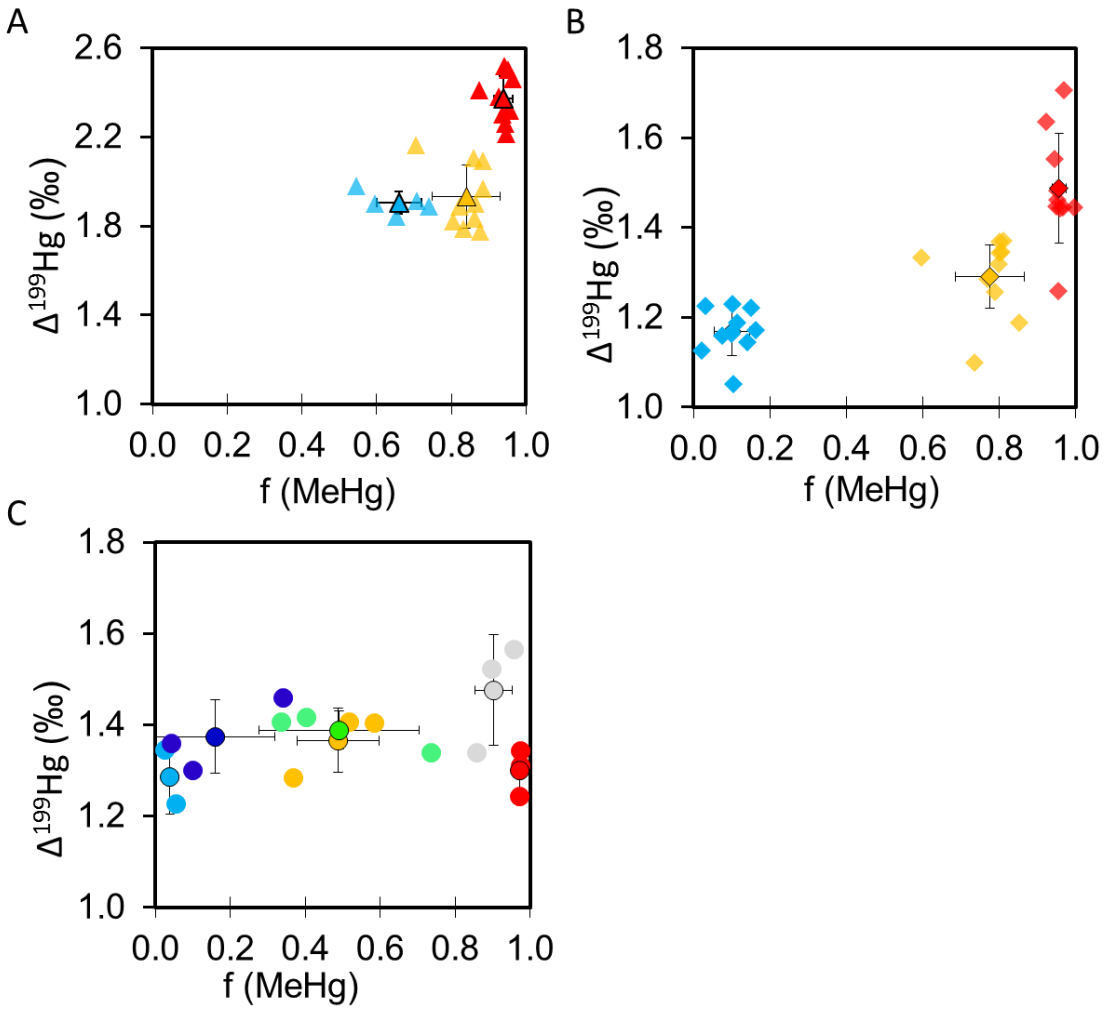

Figure 3.S6. Hg MIF relative to the fraction of MeHg A) Livers (blue), muscles (yellow) and feathers (red) of Antarctic prions (triangles). B) Livers (blue), muscles (yellow) and feathers (red) of white-chinned petrels (diamonds). C) Livers (light blue), kidneys (dark blue), muscles (yellow), feathers (red), brains (green) and blood (grey) of southern giant petrels (circles)

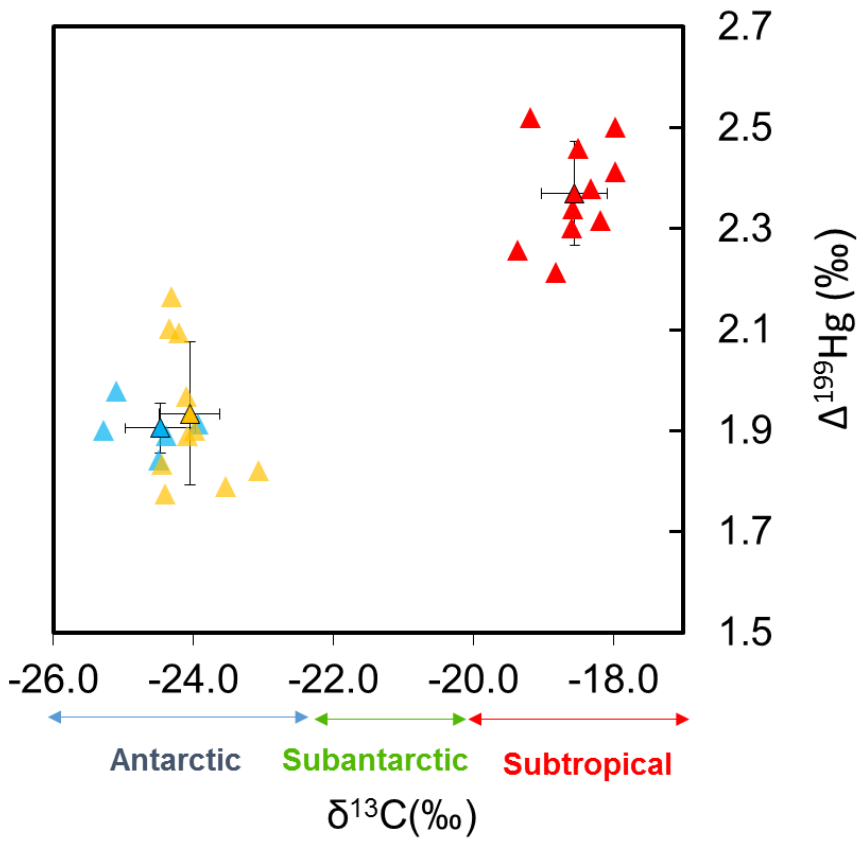

Figure 3.S7. $\Delta^{199}Hg$ (‰) relative $\delta^{13}C$ (‰) for livers (blue), muscles (yellow) and feathers (red) of Antarctic prions.

Annexes: Chapter 4. Ecological and biogeochemical aspects

Identification of sources and bioaccumulation pathways of MeHg in subantarctic penguins: a stable isotopic investigation

Estimation of the fraction of photodemethylated MeHg for each penguin population

The extent of photodemethylation undergone by MeHg before its incorporation into the aquatic food web was estimated by following Bergquist and Blum reference model (Bergquist and Blum, 2007). MIF fractionation factors ($\alpha_{\Delta 199Hg}$ and $\alpha_{\Delta 201Hg}$) were determined experimentally as a function of MeHg/DOC ratio by Rayleigh-fractionation equations in waters with the presence of 2 mg/L and 20 mg/L DOM. This same model was later extrapolated to environmental conditions in marine medium taking into account different conditions of MeHg/DOC in the Arctic Ocean (Point et al. 2011). In a more recent study by Chandan et al., (2015) photodemethylation extent was evaluated at different ratios between MeHg and reduced sulfur content in DOC (MeHg: Sred-DOC). In our study, we calculated MeHg:DOC according to previous data on the subantarctic zone of the Southern Ocean (Canario et al., 2017; Tremblay et al., 2015), MeHg amount in the pelagic zone (100-200 m depth) which is approximatively 0.48 ng per mg of dissolved organic carbon. Concentrations of DOC in surface waters were not considered since photochemical reactions are known to photodegrade organic matter and that MeHg is produced under the photic zone, where phytoplankton is degraded by bacteria. We calculated by extrapolation the MIF fractionation factors for the Crozet Islands to obtain fitting equations based on Chandan calculations (low concentrations of DOC) (Chandan et al., 2015). MeHg accumulated in GP was 13.1±0.6% photodegraded, whereas slightly greater extent of MeHg photodegradation was observed in pelagic penguins: 14.7±0.3% (KP) and 14.3±0.5% (MP) and 16.2±1.1% (RP).

Table 4.S1. Blood Hg isotopic composition of subantarctic penguins from Possession Island, Crozet archipelago (n, number of individuals). Values are means ± SD.

Species	Date	n	$\delta^{204}Hg$	$\delta^{202}Hg$	$\delta^{201}Hg$	$\delta^{200}Hg$	$\delta^{199}Hg$	$\Delta^{204}Hg$	$\Delta^{201}Hg$	$\Delta^{200}Hg$	$\Delta^{199}Hg$
			‰	‰	‰	‰	‰	‰	‰	‰	‰
King penguin	October 2011	11	2.18±0.17	1.49±0.11	2.50±0.08	0.73±0.06	1.98±0.05	-0.05±0.09	1.38±0.03	-0.02±0.03	1.60±0.04
Gentoo penguin	October 2011	11	2.20±0.18	1.45±0.12	2.29±0.12	0.72±0.07	1.77±0.08	0.03±0.03	1.20±0.04	-0.01±0.02	1.41±0.06
Macaroni penguin	January 2012	10	2.49±0.16	1.66±0.11	2.60±0.12	0.83±0.08	1.96±0.07	0.01±0.05	1.35±0.05	0.00±0.04	1.54±0.06
Eastern rockhopper penguin	February 2012	10	2.89±0.25	1.93±0.18	2.99±0.04	0.98±0.07	2.25±0.12	0.01±0.06	1.54±0.08	0.07±0.07	1.77±0.13

Table 4.S2. Mean values of Hg isotopic composition obtained for reference materials: UM-Almadén, NIES-13 (CRM human hair), hair), ERM-CE-464 (CRM tuna fish) and RBC-KP (IRM penguin red blood cells).

Sample	Reference	n	$\delta^{204}Hg$	2SD	$\delta^{202}Hg$	2SD	$\delta^{201}Hg$	2SD	$\delta^{200}Hg$	2SD	$\delta^{199}Hg$	2SD	$\Delta^{204}Hg$	2SD	$\Delta^{201}Hg$	2SD	$\Delta^{200}Hg$	2SD	$\Delta^{199}Hg$	2SD
			‰	‰	‰	‰	‰	‰	‰	‰	‰	‰	‰	‰	‰	‰	‰	‰	‰	‰
UM Almadén	This study	38	-0.84	0.23	-0.54	0.14	-0.45	0.14	-0.27	0.18	-0.17	0.14	-0.03	0.13	-0.04	0.08	0.00	0.14	-0.03	0.12
	Sherman et al., 2012a	61	-	-	-0.57	0.05	-0.46	0.05	-0.28	0.03	-0.16	0.04	-	-	-0.03	0.02	0.01	0.02	-0.02	0.03
NIES-13	This study	5	2.99	0.28	2.11	0.13	3.11	0.16	1.08	0.01	2.34	0.14	-0.14	0.24	1.52	0.05	0.05	0.07	1.80	0.08
	Yamakawa et al. 2016	11	2.76	0.16	1.89	0.10	2.77	0.10	0.98	0.08	2.13	0.07	-0.04	0.11	1.36	0.07	0.04	0.04	1.65	0.06
ERM-CE-464	This study	2	0.91	0.13	0.64	0.04	2.37	0.03	0.40	0.00	2.49	0.01	-0.04	0.19	1.89	0.05	0.08	0.01	2.33	0.01
	Li et al. 2014	9	0.94	0.06	0.70	0.04	2.49	0.06	0.43	0.05	2.55	0.08	-	-	1.96	0.06	0.07	0.04	2.38	0.07
RBC-KP	This study	5	2.00	0.15	1.32	0.12	2.28	0.14	0.64	0.14	1.79	0.18	0.04	0.10	1.29	0.09	-0.02	0.09	1.46	0.16

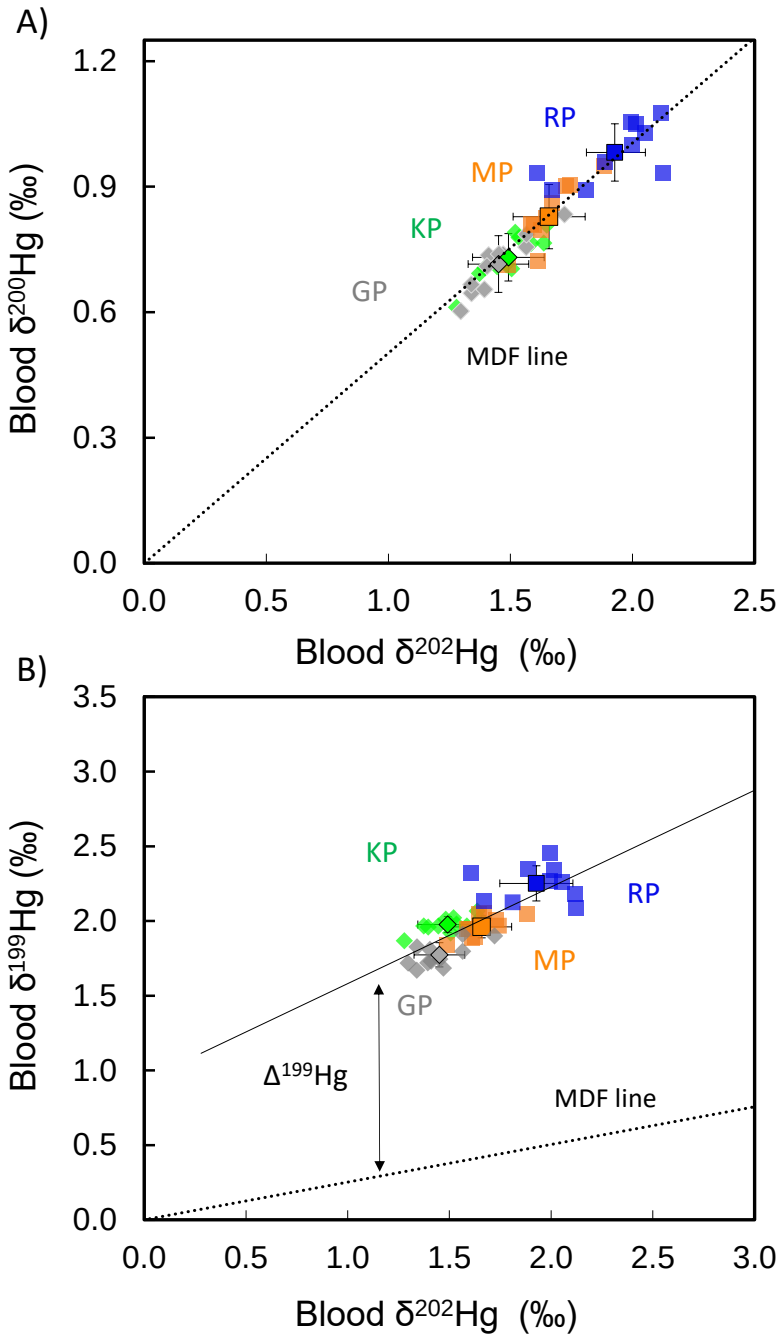

Figure 4.S1. Blood Hg MDF and MIF values of subantarctic penguins from Possession Island, Crozet Archipelago A) blood δ^{200}Hg versus δ^{202}Hg values, B) blood δ^{199}Hg versus δ^{202}Hg values. Dotted lines represent the theoretically predicted MDF based on δ^{202}Hg. Abbreviations: GP, gentoo penguin; KP, king penguin; MP, macaroni penguin; RP, rockhopper penguin.

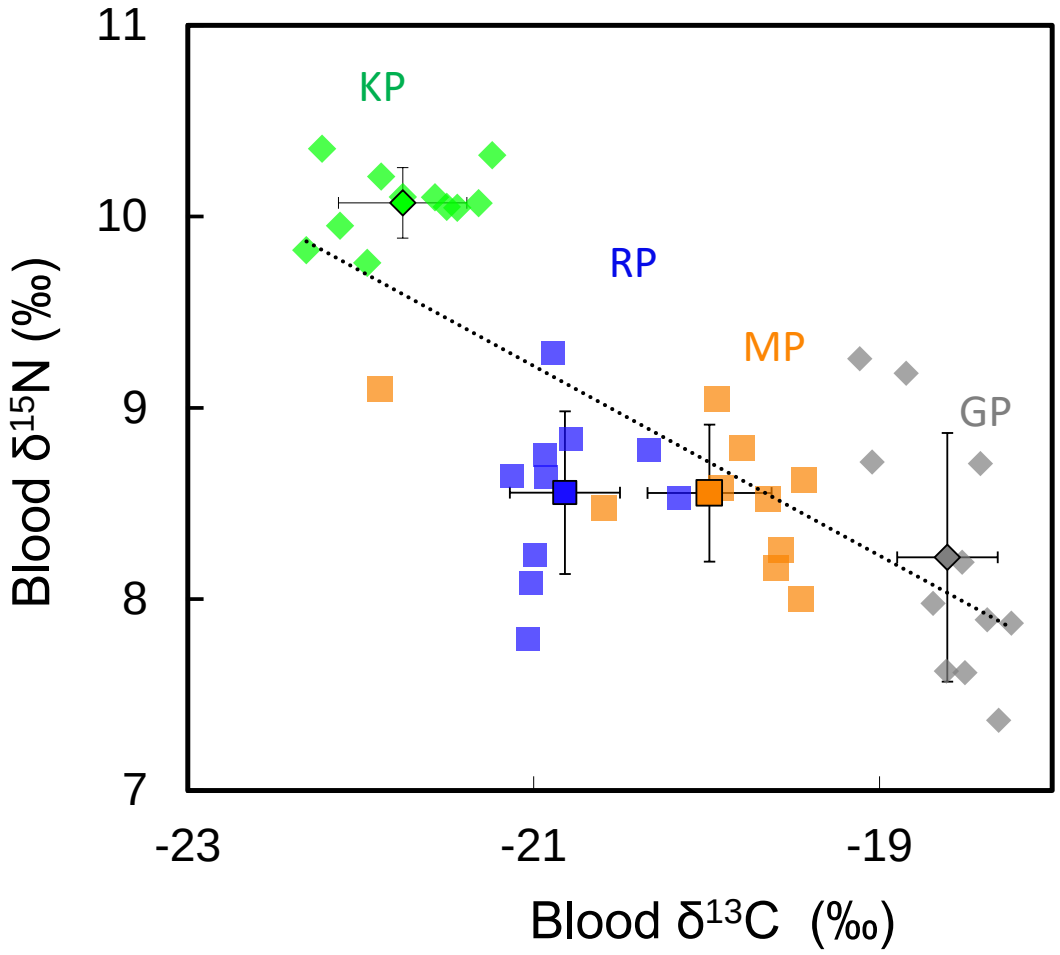

Figure 4.S2. Correlation between blood $\delta^{15}N$ and $\delta^{13}C$ values of subantarctic penguins from Possession Island, Crozet Archipelago. Regression equation is y= -0.49x - 1.19, R2= -0.74, p<0.0001. Abbreviations: GP, gentoo penguin; KP, king penguin; MP, macaroni penguin; RP, rockhopper penguin.

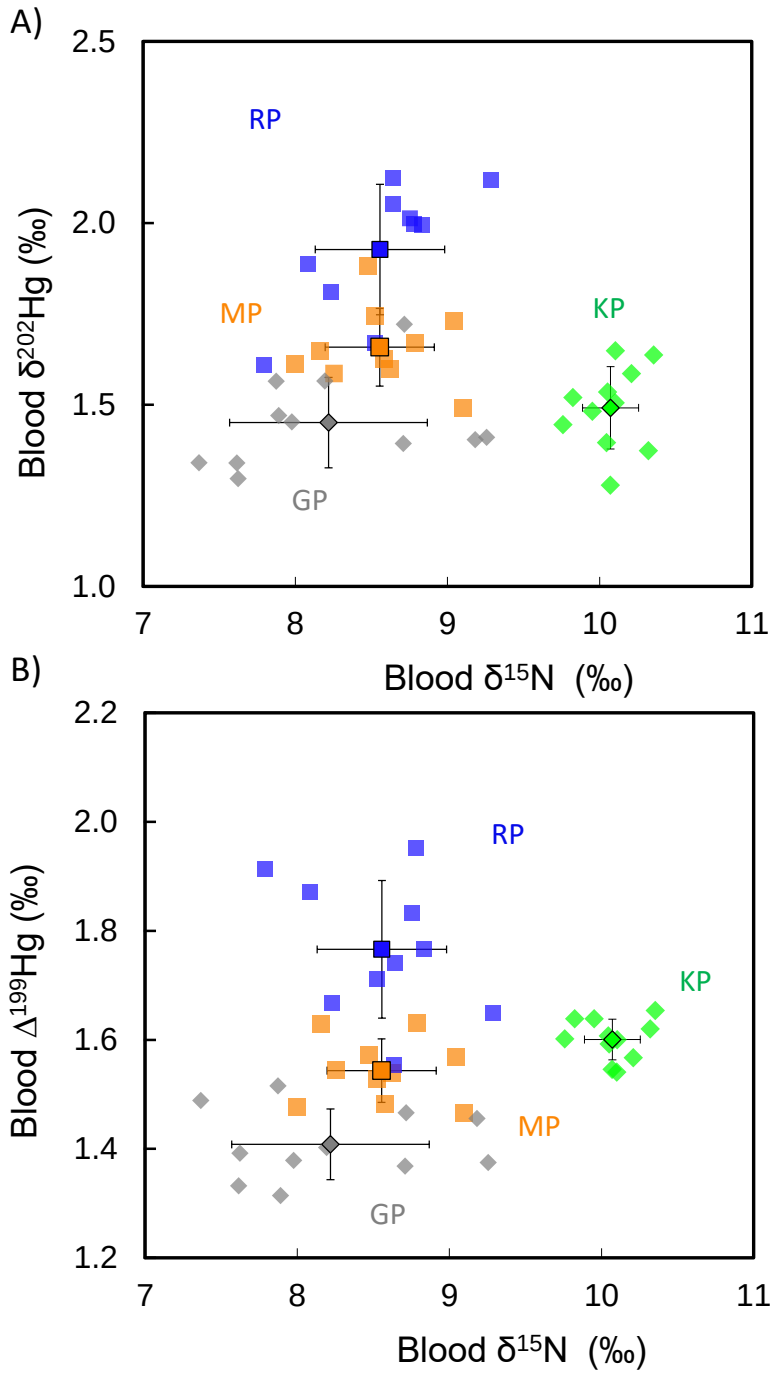

Figure 4.S3. A) Blood Hg MDF vs $\delta^{15}N$ values B) Blood Hg MIF vs $\delta^{15}N$ values of subantarctic penguins from Possession Island, Crozet Archipelago. Abbreviations: GP, gentoo penguin; KP, king penguin; MP, macaroni penguin; RP, rockhopper penguin.

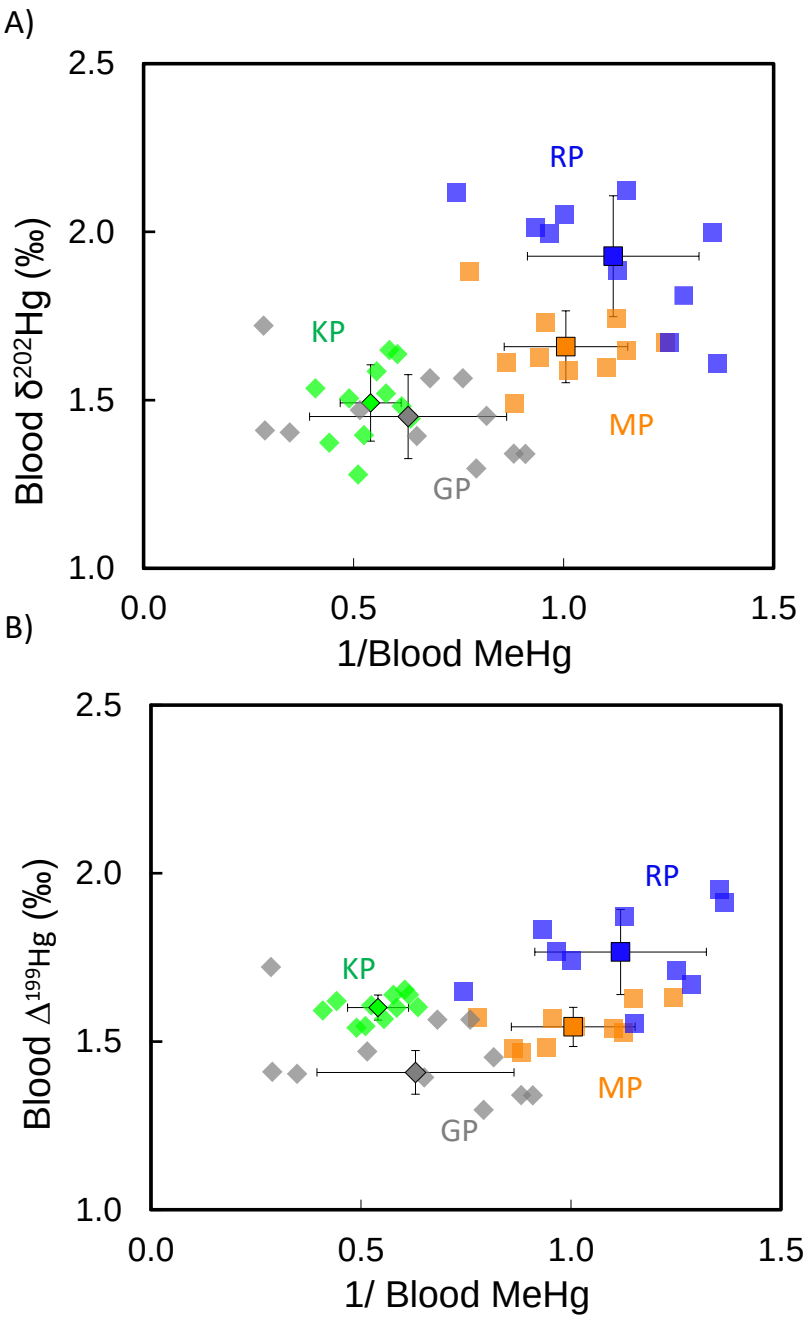

Figure 4.S4. Correlation between A) blood δ^{202}Hg and inverse of MeHg concentration B) blood Δ^{199}Hg and inverse of MeHg concentration of subantarctic penguins from Possession Island, Crozet Archipelago. Abbreviations: GP, gentoo penguin; KP, king penguin; MP, macaroni penguin; RP, rockhopper penguin.

Annexes 3.2: Identification of sources and bioaccumulation pathways of MeHg in subantarctic penguins: a stable isotopic investigation

Description of ecological characteristics of each seabird species

Skua chicks' diet is usually composed of other birds and marine mammals scavenge or seabirds eggs, and also of fish when feeding at sea. Depending on the location, skuas present different feeding ecology. Antarctic skuas from Adélie Land feed their chicks with eggs and carcasses of Adélie penguins *Pygoscelis adeliae* (Carravieri et al. 2017). In the Kerguelen Islands, their diet is particularly composed of blue petrels *Halobaena caerulea* and thin-billed prions, *Pachyptila belcheri* (Mougeot et al., 1998). Crozet skuas rely mainly on eggs and carcasses of crested penguins (*Eudyptes chrysolophus* and *E. chrysocome filholi*), but also on black rats *Rattus rattus* introduced by humans. In Amsterdam Island, skua diet is not completely recognised but, according to field observations, chicks are fed with other seabirds' eggs and carcasses and with subantarctic fur seals *Arctocephalus tropicalis* scavenge, but also with introduced brown rats *Rattus norvegicus* (Carravieri et al., 2017).

Adults from five species of penguins were studied: king penguin *Aptenodytes patagonicus*, Adélie *Pygoscelis adeliae*, macaroni *Eudyptes chrysolophus*, eastern rockhopper *E. chrysocome filholi* and northern rockhopper *E. chrysocome moseleyi* penguins. King penguins mainly feed on pelagic fish, especially myctophids such as *Krefftichthys anderssoni* (Bost et al., 2002; Cherel et al., 2010). Adélie penguins also consume fish but their diet is mostly composed of krill (especially, *Euphausia superba* and *E. crystallorophias*) (Rodary et al., 2000). Macaroni penguins primarily feed on crustaceans, such as hyperiids (e.g. *Themisto gaudichaudii*, and *Primno macropa*) and euphausiids (e.g. *E. vallentini*, *Thysanoessa* spp.), and on fish such as the myctophid *Krefftichthys anderssoni* (Cherel and Hobson 2007; Cherel et al. 2010; Thiebot et al. 2014). Eastern rockhopper penguins from Crozet Islands are known to rely upon the subantarctic krill *E. vallentini*, while northern rockhopper penguins from Amsterdam Island mainly feed on the euphasiid *Thysanoessa gregaria* and squid (Tremblay and Cherel, 2003). Chicks of emperor penguins (*Aptenodytes forsteri*) are winter breeders and were studied in order to evaluate seasonal variations (summer vs winter) in the Antarctic continent. In winter, emperor penguins mainly feed over the Antarctic continental shelf and they present excellent diving capacities foraging mainly on fish (and squids) of benthic areas between 200 and 400 m depth (Wienecke et al. 2007). Due to their seasonal mismatch relative to the other studied seabirds, they were not considered for the exploration of latitudinal trends.

Estimation of the fraction of photodemethylated MeHg in surface waters over latitude

Variations in surface ocean MeHg photodemethylation can be estimated from the MIF recorded in seabird blood based on a Rayleigh model:

$$\ln\frac{1000 + \Delta}{1000 + \Delta i} = \frac{\varepsilon(\Delta^{199}Hg)}{1000} \times \ln(f)$$

where $\Delta^{199}Hg_i$ corresponds to the initial MIF of marine MeHg before undergoing photodemethylation, which was assumed as 0 due to the negligible total Hg Δ^{199}Hg values in seawater (Štrok et al., 2015) and because MeHg is assumed to have a similar MIF as the total Hg before photodemethylation since it likely converted from inorganic Hg in the surface ocean. The $\varepsilon(\Delta^{199}Hg)$ is the enrichment factor, reported as $\varepsilon = 1000*(\alpha_{\Delta 199Hg} - 1)$ in function of the kinetic fractionation factor ($\alpha_{\Delta 199H}$) determined in laboratory experiments. f is the remaining fraction of non-photodemethylated MeHg.

Experimental estimations of enrichment factors of MeHg aquatic photodemethylation was first performed as a function of MeHg/DOC ratio by Bergquist and Blum, (2007). The relation between MIF values and the fraction of remaining MeHg was used in fish from the Lake Michigan to estimate the photodegradation extent. This reference fractionation model was later applied for estimation of the MeHg loss due to photodemethylation in marine environments (Gehrke et al., 2011; Senn et al., 2010; Point et al., 2011). Point et al. (2011) extrapolated the fractionation model to the presence of DOC in Arctic marine natural waters (lower DOC content) (Point et al., 2011). In a recent study, Chandan et al. (2015) investigated Hg isotopic fractionation factors considering changing DOC binding sites and concluded that MIF extent is strongly dependent on the amount of reduced sulphur content in organic matter (Sred-DOC). Enrichment factors were evaluated under different types and concentrations of organic matter standards: Suwanee River fulvic acid (SRFA), Pony Lake fulvic acid (PL FAR) and Nordic Lake natural organic matter (NL NOM). These two reference organic matter models present contrasted proportions of reduced sulphur organic matter (35% for SRFA, 59% for PL FAR and 50% for NL NOM). Furthermore, these models represent more realistic environmental conditions (low MeHg: Sred-DOC ratios) than previous experimental studies and can be more representative of the processes occurring under natural conditions in the environment.

In order to estimate the extent of photochemical demethylation of MeHg over the studied latitudinal gradient in the Southern Ocean we calculated the corresponding enrichment factors by application of experimental models in our own environmental conditions of MeHg:DOC and MeHg: S red-DOC. Recent published data on MeHg concentrations (Cossa et al., 2011; Nerentorp Mastromonaco et al., 2017; Canario et al., 2017), DOC concentrations (Tremblay et al., 2015;

Canario et al. 2017; Ogawa et al., 1999) and dissolved organic sulphur in organic matter 0.19±0.04 μmol L^{-1}, Ksionzek et al. 2016) in the Southern Ocean were used for this estimations. The assessment was based on three mentioned experimental studies: in mid-range MeHg: S-red-DOM ratio (SRFA) and low MeHg: S-red-DOM ratio (NL NOM) conditions (Chandan et al., 2015) and in function of MeHg:DOC ratios under high DOC conditions (Bergquist and Blum 2007). MeHg and DOC concentrations at each site were extracted from published data (Table 4.S2, 4.S3 and 4.S4). Concentrations of DOC in surface waters were not considered since photochemical reactions are known to photodegrade organic matter and that MeHg is mainly produced below the photic zone, where plankton material is undergoing bacterial degradadation and mineralization (Mason et al., 2012). We therefore extrapolated isotopic fractionation systems of these three experimental models to our conditions of MeHg: S-red-DOC ratios and MeHg:DOC ratios by fitting equations for the three sites (Antarctic, subantarctic and subtropical zones). We obtained that the difference on the extent of photodemethylated MeHg from Antarctic and subantarctic to subtropical zones was in the order of 2%, independently of the experimental model used. When considering mid-range MeHg: Sred-DOC, the extent of photodemethylated MeHg varied from ~ 9% in Antarctic to ~ 11 % in subtropical zones. Under low MeHg: Sred-DOC conditions, ~ 5% of MeHg was photodemthylated in Antarctic waters whereas ~ 6% in subtropical waters. Photodemethylated MeHg corresponding to MeHg-DOC ratios varied from ~13% in Antarctic zones to 18% in the subtropics (Table 4.S5).

Table 4.S2. Calculation of MeHg:Sred-DOC ratios for the estimation of MeHg photodemethylation based on experimental fractionation factors (Chandan et al., 2015) for mid-range MeHg:Sred-DOC, SRFA organic matter conditions, 35% S-red).

		Reference data for this study[(1)]	Other published data[(2)]	Reference data [(3)]	Reference data[(4)]				
Zone	Depth	MeHg (pmol L^{-1})	MeHg (pmol L^{-1})	DOC (mg L^{-1})	DOS min (µmol L^{-1})	S org (%)	S red (%)	S red (mg L^{-1})	MeHg/S red-DOC
Antarctic Zone	0-100	0.21	0.05	0.60	0.19	0.010	0.0035	0.0021	0.021
	100-200	0.15	0.08	0.54	0.19	0.011	0.0039	0.0023	0.014
	200-500	0.15	0.05	0.48	0.19	0.013	0.0044	0.0020	0.016
Subantarctic Zone	0-100	0.08	0.74	0.17	0.19	0.036	0.0043	0.0125	0.024
	100-200	0.11	0.33	0.48	0.19	0.013	0.0043	0.0044	0.011
	200-500	0.10	0.42	0.58	0.19	0.010	0.0043	0.0037	0.009
Subtropical Zone	0-100	0.08	0.05	0.39	0.19	0.016	0.0043	0.0055	0.013
	100-200	0.10	0.05	0.43	0.19	0.014	0.0043	0.0049	0.012
	200-500	0.10	0.05	0.52	0.19	0.012	0.0043	0.0041	0.010

[(1)]Cossa et al. 2011

[(2)]AZ: Nerentorp Mastromonaco et al. 2017; SAZ: Canario et al. 2017; STZ: Bratkic et al. 2016

[(3)] Tremblay et al. 2015; Canario et al. 2017; Ogawa et al., 1999

[(4)] Ksionzek et al. 2016

Table 4.S3. Calculation of MeHg:Sred-DOC ratios for the estimation of MeHg photodemethylation based on experimental fractionation factors (Chandan, Ghosh, and Bergquist 2015) for low-range MeHg:Sred-DOC, NL NOM organic matter conditions, 50% S-red).

		Reference data for this study[(1)]	Other published data[(2)]	Reference data [(3)]	Reference data[(4)]				
Zone	Depth	MeHg (pmol L^{-1})	MeHg (pmol L^{-1})	DOC (mg L^{-1})	DOS min (µmol L^{-1})	S org (%)	S red (%)	S red (mg L^{-1})	MeHg/S red-DOC
Antarctic Zone	0-100	0.21	0.05	0.6	0.19	0.010	0.0051	0.0030	0.014
	100-200	0.15	0.08	0.54	0.19	0.011	0.0056	0.0033	0.009
	200-500	0.15	0.05	0.48	0.19	0.013	0.0063	0.0029	0.010
Subantarctic Zone	0-100	0.08	0.74	0.17	0.19	0.036	0.0179	0.0010	0.155
	100-200	0.11	0.33	0.48	0.19	0.013	0.0063	0.0029	0.055
	200-500	0.10	0.42	0.58	0.19	0.010	0.0052	0.0035	0.045
Subtropical Zone	0-100	0.08	0.05	0.39	0.19	0.016	0.0078	0.0024	0.008
	100-200	0.10	0.05	0.43	0.19	0.014	0.0071	0.0026	0.008
	200-500	0.10	0.05	0.52	0.19	0.012	0.0058	0.0032	0.006

[(1)]Cossa et al. 2011

[(2)]AZ: Nerentorp Mastromonaco et al. 2017; SAZ: Canario et al. 2017; STZ: Bratkic et al. 2016

[(3)] Tremblay et al. 2015; Canario et al. 2017; Ogawa et al., 1999

[(4)] Ksionzek et al. 2016

Table 4.S4. Calculation of MeHg: DOC ratios for the estimation of MeHg photodemethylation based on experimental fractionation factors (Bergquist and Blum 2007) for high MeHg:DOC conditions

		Reference data for this study[(1)]	Other published data [(2)]	Reference data [(3)]	
Zone	Depth	MeHg (pmol L^{-1})	MeHg (pmol L^{-1})	DOC (mg L^{-1})	MeHg/DOC
Antarctic Zone	0-100	0.21	0.05	0.6	0.350
	100-200	0.15	0.08	0.54	0.278
	200-500	0.15	0.05	0.48	0.313
Subantarctic Zone	0-100	0.08	0.74	0.17	0.471
	100-200	0.11	0.33	0.48	0.208
	200-500	0.10	0.42	0.58	0.172
Subtropical Zone	0-100	0.08	0.05	0.39	0.256
	100-200	0.10	0.05	0.43	0.233
	200-500	0.10	0.05	0.52	0.192

[(1)]Cossa et al. 2011

[(2)]AZ: Nerentorp Mastromonaco et al. 2017; SAZ: Canario et al. 2017; STZ: Bratkic et al. 2016

[(3)] Tremblay et al. 2015; Canario et al. 2017; Ogawa et al., 1999

Table 4.S5. Estimation of MeHg photodemethylation extent reflected by each seabird population from the three studied areas based on experimental studies and considering the calculated MeHg:Sred-DOC ratios at each site.

			Mid-range MeHg:Sred-DOC ratio	Low MeHg:Sred-DOC ratio	Low MeHg:DOC ratio
			Chandan et al., 2015	Chandan et al., 2015	Bergquist and Blum, 2007
Zone	Site	Seabird species	MeHg photodemethylation (%)	MeHg photodemethylation (%)	MeHg photodemethylation (%)
Antarctic Zone	Adélie Land	Antarctic skuas	9.5±0.5	4.9±0.5	14.5±2.3
	Adélie Land	Emperor penguins	7.2±0.7	3.7±0.4	12.9±1.2
	Adélie Land	Adélie penguins	9.7±0.6	5.0±0.3	15.7±1.1
Subantarctic Zone	Kerguelen	Subantarctic skuas	9.5±0.3	4.9±0.2	17.9±0.6
	Crozet	Subantarctic skuas	9.7±0.5	5.1±0.3	18.8±1.1
	Crozet (Polar Front)	King penguins	9.4±0.2	4.9±0.1	14.7±0.3
	Crozet	Gentoo penguins	8.4±0.4	4.3±0.2	13.1±0.6
	Crozet	Macaroni penguins	9.1±0.3	4.7±0.2	14.3±0.5
	Crozet	Rockhopper penguins	9.3±0.8	4.9±0.4	16.2±1.1
Subtropical Zone	Amsterdam	Subantarctic skuas	10.6±0.3	5.5±0.1	17.2±0.4
	Amsterdam	Northern rockhopper penguin	11.3±0.7	5.9±0.4	18.4±1.1

Estimation of the MDF enrichment factor associated to MeHg photodemethylation

In order to estimate the enrichment of MDF values associated to the calculated photodemethylation extent at each site, we performed a recalculation of the fractionation factor of δ^{202}Hg values (α (δ^{202}Hg)) for our environmental conditions. We based this calculation on the enrichment factors attributed to mid-range MeHg;S red-DOC and low MeHg;S red-DOC, which seem to be the closest model to our conditions in the Southern Ocean (Tables 4.S6 and 4.S7). We could estimate a α (δ^{202}Hg)/α (Δ^{199}Hg) near 1 in both cases (and both seabird models), meaning that during photodemethylation of MeHg the same degree of fractionation is experienced by δ^{202}Hg and Δ^{199}Hg. Consequently, considering that the overall latitudinal MIF variations are attributed to MeHg photodemethylation and are in the order of 0.3 ‰ (~0.25 ‰ and ~0.32 ‰, respectively for skuas and penguins), we could explain ~0.3 ‰ of latitudinal MDF variations due to MeHg photodemethylation.

Table 4.S6. Calculation of fractionation factors of MDF (α (δ^{202}Hg)) corresponding to MeHg photodemethylation at each study area based on experimental studies under mid-range MeHg:Sred-DOC conditions (SRFA organic matter conditions, 35% S-red) (Chandan, Ghosh, and Bergquist 2015).

Conditions: mid-range MeHg;S red-DOC (35% S-red)					
Population/ Sites	ε Δ^{199}Hg (‰)	α (Δ^{199}Hg)	ε δ^{202}Hg (‰)	α (δ^{202}Hg)	Ratio α (δ^{202}Hg)/α (Δ^{199}Hg)
Skuas					
AZ	-5.23895	0.99476	-4.73312	0.99527	
SAZ	-5.24037	0.99476	-4.73440	0.99527	
STZ	-5.20641	0.99479	-4.70372	0.99530	1.00051
Penguins					
AZ	-5.30277	0.99470	-4.79078	0.99521	
SAZ	-5.26504	0.99473	-4.75669	0.99524	
STZ	-5.163113	0.99484	-4.66461	0.99534	1.00050

Table 4.S7. Calculation of fractionation factors of MDF (α (δ^{202}Hg)) corresponding to MeHg photodemethylation at each study area based on experimental studies under low MeHg:Sred-DOC conditions (NL NOM organic matter conditions, 50% S-red) (Chandan, Ghosh, and Bergquist 2015).

	Conditions: low MeHg;S red-DOC (50% S-red)				
Population/ Sites	ε Δ^{199}Hg (‰)	α (Δ^{199}Hg)	ε δ^{202}Hg (‰)	α (δ^{202}Hg)	Ratio α (δ^{202}Hg)/α (Δ^{199}Hg)
Skuas					
AZ	-1.501006	0.998499	-1.520006	0.998480	
SAZ	-1.500575	0.998499	-1.519569	0.998480	
STZ	-1.495628	0.998504	-1.514560	0.998485	0.99998
Penguins					
AZ	-1.438243	0.998562	-1.456449	0.998544	
SAZ	-1.504152	0.998496	-1.523191	0.998477	
STZ	-1.489287	0.998511	-1.508138	0.998492	0.99998

Calculation of the fraction of volatilised Hg and fractionation factor

Calculation of Henry's law constant (K_H)

The calculation of Henry's law constant permits to estimate the evasion (or volatilisation) extent of Hg from oceanic waters in function of the water surface temperature. This constant represents the fraction of gaseous Hg^0 in function of Hg^0 remaining in the aqueous phase.

$$K_{H'} = \frac{[Hg^0]_{(g)}}{[Hg^0]_{(aq)}}$$

An equation for artificial sea water (concentration conditions of 1.5 M of NaCl) was proposed by (Andersson et al. 2008).

$$K_{H'} = e\left(\frac{-1871.6}{T\,(K)}\right) + 5.28$$

Data of water temperature were taken from previous studies in austral autumn (Cossa et al. 2011) and summer (Canario et al. 2017). Based on approximate values of temperature water, we estimated yearly volatilisation extents taking place at each site. Obtained values were K_H=0.21 (T=273 K), 0.25 (T=281 K) and 0.32 (T=291 K) respectively for Antarctic, subantarctic and subtropical zones.

Calculation of kinetical fractionation factor $\alpha(^{198}Hg/^{202}Hg)$ in function of Hg remaining fraction (f_R) at each

Hg remaining fraction (f_R) was calculated from volatilisation constant K_H in order to estimate Hg fractionation magnitude during volatilisation at each location. Experimental volatilisation of aqueous Hg^0 into gaseous Hg^0 indicated MDF with a low kinetic fractionation factor $\alpha(^{198}Hg/^{202}Hg)$ obtained during experimental volatilisation process was similar for accumulative fractionation (1.00044) and instantaneous fractionation (1.00047), indicating that Hg isotopic fractionation during volatilisation is independent of initial solution volumes and volatilization rates (Zheng et al., 2007). According to this volatilization experiment, we calculated $\alpha(^{198}Hg/^{202}Hg)$ from the slope when plotting log(1000-δf/1000-δi) vs log(f_R) following this equation:

$$\log\left(\frac{1000 - \delta}{1000 - \delta i}\right) = \left(\frac{1}{\alpha} - 1\right) \times \log(f_R)$$

where δ is the isotopic composition of the remaining reactant at time t, δi is the initial isotopic composition of the reactant, fR is the fraction of the remaining reactant at time t, and α is the kinetic fractionation factor. Based on experimental calculations, we determined the Rayleigh-type fractionation slope for our model, assuming that initial $\delta^{202}Hg$ (δ_i) is 0 and taking $\alpha(^{198}Hg/^{202}Hg)$ of 1.00047 (Zheng et al., 2007) (Table 4.S8). The obtained slope represents a $\alpha(^{198}Hg/^{202}Hg)$ factor of 1.0005, meaning a total mass-dependent fractionation of 0.03 ‰ due to volatilization.

Table 4.S8. Calculation of the fraction of volatilised Hg and enrichment factor between the studied sites

Site	Water temperature (K)	Henry's constant (K_H)	Hg^0 (air)	Hg^0 (aq)	f_R (Hg^0 aq)	log (f_R)	ε $\delta^{202}Hg$ (‰)
AZ	273	0.21	0.8	3.87	0.829	-0.188	0.088
SAZ	281	0.25	0.9	3.58	0.799	-0.224	0.105
STZ	291	0.31	1.0	3.23	0.763	-0.270	0.127

Table 4.S9. Mean values of MeHg, THg and Hg isotopic composition for skua and penguin populations from the Southern Ocean.

Species	Location	Latitude	Diet	n	MeHg±SD	THg±SD	δ^{204}Hg±2SD	δ^{202}Hg±2SD	δ^{201}Hg±2SD	δ^{200}Hg±2SD	δ^{199}Hg±2SD	Δ^{204}Hg±2SD	Δ^{201}Hg±2SD	Δ^{200}Hg±2SD	Δ^{199}Hg±2SD
					(µg g^{-1})	(µg g^{-1})	‰	‰	‰	‰	‰	‰	‰	‰	‰
Antarctic skua	Adélie Land	Dec 2011-Jan 2012	penguins	9	0.51±0.09	0.53±0.08	0.35±0.17	0.23±0.13	1.45±0.11	0.10±0.08	1.57±0.09	0.01±0.08	1.28±0.08	-0.01±0.03	1.51±0.08
Subantarctic skua	Kerguelen	Dec 2011	petrels	10	2.16±0.33	2.32±0.34	1.55±0.11	1.04±0.08	2.16±0.07	0.52±0.05	1.87±0.06	0.00±0.06	1.38±0.05	0.00±0.04	1.61±0.06
Subantarctic skua	Crozet	Jan-Feb 2012	penguins & rats	11	1.70±1.16	1.81±1.19	2.06±0.24	1.39±0.18	2.49±0.18	0.72±0.10	2.05±0.13	-0.01±0.08	1.44±0.09	0.02±0.03	1.69±0.11
Subantarctic skua	Amsterdam	Dec 2011	unknown (seabirds?)	10	3.78±0.79	4.00±0.89	2.31±0.10	1.56±0.08	2.64±0.08	0.81±0.05	2.15±0.06	-0.02±0.08	1.47±0.04	0.03±0.05	1.76±0.05
Adélie penguin	Adélie Land	Feb 2012	pelagic crustaceans & fish	10	0.43±0.11	0.47±0.12	0.82±0.29	0.56±0.20	1.75±0.20	0.25±0.12	1.68±0.14	-0.01±0.06	1.33±0.13	-0.03±0.05	1.54±0.11
King penguin	Crozet	Oct 2011	pelagic fish	11	1.88±0.28	2.01±0.29	2.18±0.17	1.49±0.11	2.50±0.08	0.73±0.06	1.98±0.05	-0.05±0.09	1.38±0.03	-0.02±0.03	1.60±0.04
Macaroni penguin	Crozet	Jan 2012	pelagic crustaceans & fish	10	1.01±0.15	1.06±0.16	2.49±0.16	1.66±0.11	2.60±0.12	0.83±0.08	1.96±0.07	0.01±0.05	1.35±0.05	0.00±0.04	1.54±0.06
Eastern rockhopper penguin	Crozet	Feb 2012	pelagic crustaceans & fish	10	0.93±0.19	0.97±0.20	2.89±0.25	1.93±0.18	2.99±0.04	0.98±0.07	2.25±0.12	0.01±0.06	1.54±0.08	0.07±0.07	1.77±0.13
Northern rockhopper penguin	Amsterdam	Nov 2011	pelagic crustaceans & fish	10	1.95±0.43	2.40±0.56	3.21±0.25	2.16±0.14	3.17±0.12	1.13±0.10	2.44±0.11	-0.01±0.08	1.55±0.09	0.05±0.06	1.89±0.12

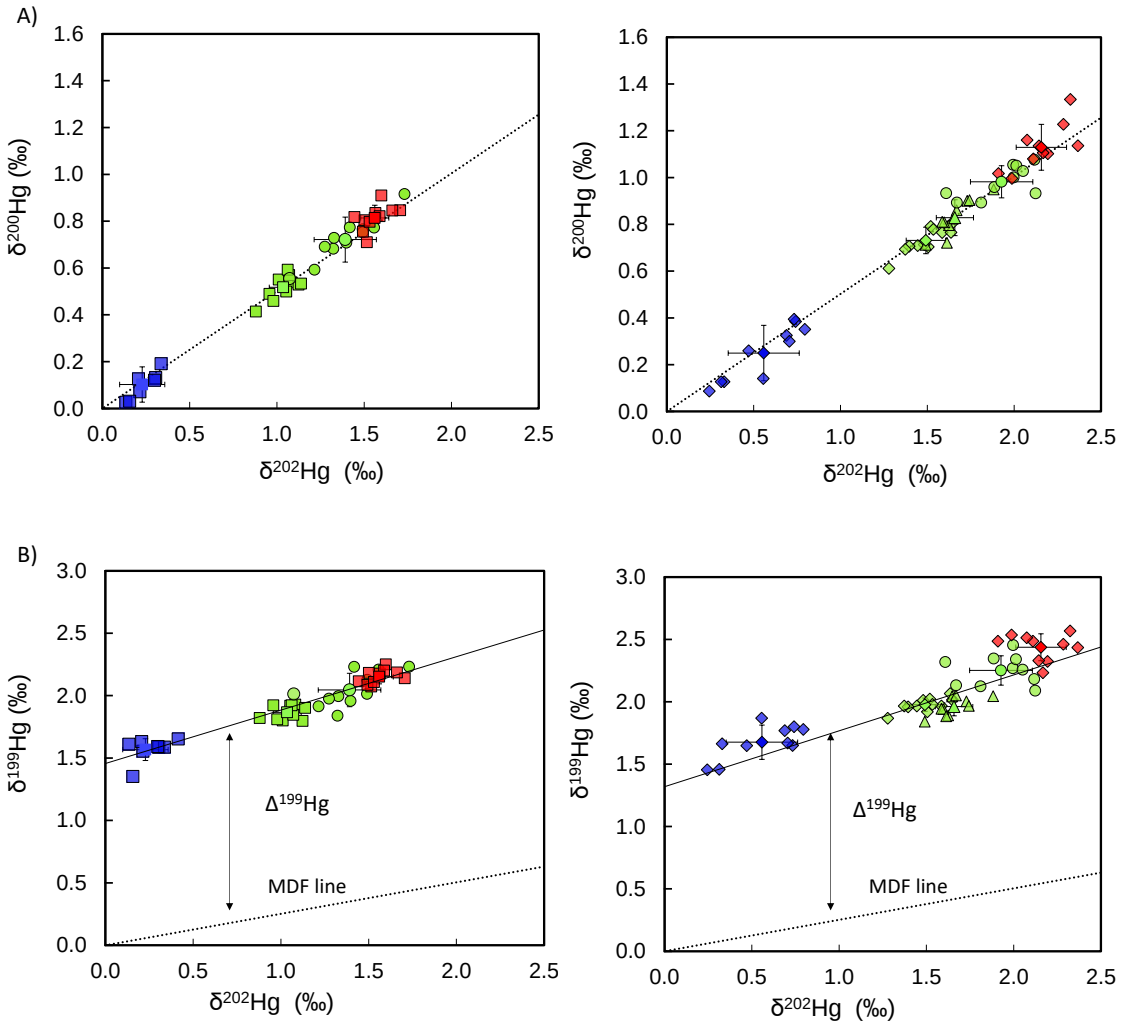

Figure 4.S5. Hg MDF and MIF signatures for blood of skua chicks (left side) and of penguins (right side) from the Southern Ocean. ***A)*** *δ^{202}Hg versus δ^{200}Hg,* ***B)*** *δ^{202}Hg versus δ^{199}Hg. Blue (Adélie Land), green (Crozet and Kerguelen) and red (Amsterdam). The dotted lines represent the theoretically predicted MDF based on δ^{202}Hg.*